Transmissible Spongiform Encephalopathy:

The relationship between PrP^{Sc} and infectivity in murine models

Susan L Campbell

A thesis submitted in partial fulfillment of the requirements of the University of Edinburgh for the degree of Doctor of Philosophy

The programme of research was carried out at the Institute for Animal Health, Neuropathogenesis Unit, Edinburgh

June 2004

Declaration

I declare that the work presented in this thesis is my own, except where otherwise stated. All experiments were designed by myself, in collaboration with my supervisors Dr Jean Manson and Dr Rona Barron. No part of this work has been, or will be, submitted for any other degree diploma or qualification.

Susan L Campbell

June 2004

Acknowledgements

I would like to thank my supervisors, Jean Manson, Rona Barron and Karen Chapman for their support and belief in me and for providing invaluable discussions, all of which has helped me to complete my studies. In particular I would like to thank Jean for giving me the opportunity to work in her research group and enabling my career to move from research assistant to postdoctoral scientist, and Rona for all of her advice and support in times of crisis!

I would also like to thank all of the staff at the Neuropathogenesis Unit without whom this research could not have been carried out. Particular acknowledgement goes to Declan King for DELFIA analysis, Anne Suttie and Sandra Mack for preparing and cutting paraffin-embedded tissues and to Aileen Boyle and Winggee Liu for performing the vacuolation score analysis. Additionally, I would like to thank all barrier staff involved in the care of experimental animals, in particular, Simon Cumming, Stuart Dunlop and Emma Murdoch who were closely associated with this research. I am also very grateful to Irene McConnell and Val Thomson, for providing invaluable advice. I would also like to thank Jill Sales from the Biological Statistic Service, Scotland (BioSS) for her help and advice.

In particular, I would like to take this opportunity to thank Glenn Telling for initially encouraging me to take up these studies and from whom I am extremely pleased to receive continued support.

In this final flurry of acknowledgements, I would like to thank the Tartan Army for providing much needed entertainment on away trips to help keep me sane! I would like to thank my parents, Anne and Bill, who offer unending support of my chosen career. Thanks for putting me through University first time round and allowing me to choose this path. Lastly, I would like to thank James for being there at the end of every day and for making this all worth while. I look forward to spending a lot more time with you after this thesis is submitted.

TABLE OF CONTENTS

Abbreviations

101LL	129/Ola mice homozygous for *Prnp* containing a proline to leucine mutation at amino acid residue 101
101PP	129/Ola mice homozygous for wild type *Prnp*
BSA	Bovine Serum Albumin
BSE	Bovine Spongiform Encephalopathy
CD	Circular Dichroism
CDI	Conformational Dependent Immunoassay
CJD	Creutzfeldt-Jacob Disease
vCJD	New variant of CJD
CNS	Central Nervous System
CSF	Cerebrospinal Fluid
CWD	Chronic Wasting Disease
Da	Dalton
DAB	Diaminobenzidine
DPX	Distyrene/tricresyl/xylene mountant
DTT	Dithiothreitol
DELFIA	Differential Extraction Lanthanide Fluorometric Immunoassay
dH_2O	Distilled Water (high quality)
DMSO	Dimethylsulphoxide
DNA	Deoxyribonucleic Acid
Dpl	Doppel
EDRF	Erythroid differentiation-related factor
EDTA	Ethylenediaminetetracetic Acid
ELISA	Enzyme Linked Immunosorbent Assay
ER	Endoplasmic Reticulum
FDC	Follicular Dendritic Cell
FFI	Fatal Familial Insomnia
FSE	Feline Spongiform Encephalopathy
GAPDH	Glyceraldehyde-3-Phosphate Dehydrogenase
Gnd HCl	Guanidine Hydrochloride
GSS	Gerstmann-Straussler Syndrome
GSS/A117V	GSS caused by an arganine to valine mutation at PrP amino acid residue 117 in humans

GSS/A116V	GSS mutation corresponding to the appropriate amino acid in mice
GSS/P102L	GSS caused by a proline to leucine mutation at PrP amino acid residue 101 in humans
GSS/P101L	GSS mutation corresponding to the appropriate amino acid in mice
GFAP	Glial Fibrial Associated Protein
GPI	Glycophosphoinositol
H&E	Haemotoxylin and Eosin staining
HFIP	1,1,1,3,3,3-hexafluoro-2-propanol
HRP	Horseraddish Peroxidase
IAH	Institute for Animal Health
ifu	infectious unit
ID_{50}	infectious dose of TSE agent that affects 50% of animals in a dilution group
kb	kilobase
LD_{50}	Lethal dose of infectious agent that affects 50% of animals in an experimental group
mRMA	Messenger RNA
NaPTA	Sodium phosphotungstic acid
Neo	Neomycin cassette construct
NMR	Nuclear Magnetic Resonance
NPU	Neuropathogenesis Unit
ORF	Open reading frame
PAGE	Polyacrylamide Gel Electrophoresis
PBS	Phosphate buffered saline
PCR	Polymerase Chain Reaction
PET	Paraffin-embedded Tissue
PIPLC	Phoshatidylinositol phospholipase C
PK	Proteinase K
PMCA	Protein Misfolding Cyclic Amplification
PMSF	Phenylmethylsulforylfluoride
POD	Peroxidase substrate
Prnp	PrP gene encoding murine PrP^{C}
PRNP	PrP gene encoding human PrP^{C}
PrP^{C}	PrP-Cellular; normal, uninfectious form of PrP
PrP^{Sc}	PrP-Scrapie; infectious form of PrP

PrP 27-30	Protease-resistant core of PrP^{Sc}
$PrP^{0/0}$	PrP null
PrP-sen	PK-sensitive forms of PrP (not necessarily PrP^{C})
PrP-res	PK-resistant forms of PrP (not necessarily PrP^{Sc})
cyPrP	Cytosolic PrP
^{Ctm}PrP	Transmembrane PrP; C-terminus in lumen
^{Ntm}PrP	Transmembrane PrP; N-terminus in lumen
rPrP	recombinant PrP
$sPrP^{Sc}$	PK-sensitive PrP^{Sc}
PVDF	Polyvinylidine fluoride
RNA	Ribonucleic Acid
SAF	Scrapie-associated Fibril
SCID	Severe Combined Immunodeficiency
SDS	Sodium Dodecyl Sulphate
A, C, G or TTP	Adenine, Cytosine, Guanine or Thymine Triphosphate
TAE	Tris acetate/EDTA buffer
TBS	Tris buffered saline
TFIP	1,1,1-trifluoro-2-propanol
TSE	Transmissible Spongiform Encephalopathy
UTR	Untranslated Region
UV	Ultraviolet light

Abstract

Transmissible Spongiform Encephalopathy (TSE) are fatal, neurodegenerative disease of humans and animals, primarily affecting the Central Nervous System. These diseases can be transmitted between individuals within the same species (sheep scrapie) and between species (BSE from cattle to human). The true nature of the infectious agent has not been fully elucidated, however the prion hypothesis suggests that a protein alone is responsible. The disease-associated protein, PrP^{Sc}, is found in infectious tissues and it is thought that this protein propagates by converting the normal, non-infectious host protein, PrP^{C}, into the infectious PrP^{Sc} form. In diseased tissue, high levels of PrP^{Sc} appear to correlate with high titres of infectivity and disease can be transmitted in short incubation times.

A murine model of TSE has been produced in which the brains of infected animals, at disease end-point, exhibit very low levels of PrP^{Sc}, and from which infectivity can be further transmitted in short incubation times. This is contradictory to the prion hypothesis. Using bioassay, the titre of infectivity was measured in the brain from three animals of this model. Other murine TSE models exhibiting high and intermediate levels of PrP^{Sc}, in brain at disease end-point were compared to the low PrP^{Sc} model. The low PrP^{Sc} model displayed infectivity titres similar to those of the high and intermediate PrP^{Sc} models. Furthermore, disease was transmitted from the low PrP^{Sc} model with shorter incubation times than from models with high and intermediate PrP^{Sc} levels.

PK-resistant PrP^{Sc} levels, in protease-treated brain homogenate, were semi-quantatively measured using immunoblot. PrP^{Sc} levels in the low model were at least eight times lower than found in the high PrP^{Sc} model, and surprisingly, levels of total PrP (PrP^{C} and PrP^{Sc}) were the same in all models. Therefore low PrP^{Sc} levels in the low model were not due to a reduced amount of PrP produced during disease in these animals. This suggested that infectivity in brain tissue of the low PrP^{Sc} model could possibly be

associated with another form of PrP, not PrP^{Sc}. Investigation of alternative forms of PrP that might be responsible for infectivity in the low PrP^{Sc} model was therefore undertaken.

No evidence of increased amounts of transmembrane PrP was found in infected animals from the low PrP^{Sc} model. Further biochemical examination of the protease resistance and detergent solubility of PrP in infected animals, using proteinase-K (PK) treatment and solublisation with sarkosyl, revealed the presence of protease-resistant, detergent insoluble PrP^{Sc}. In the low PrP^{Sc} model where infectivity was transmitted, one animal possessed protease-resistant, detergent insoluble PrP^{Sc} and two revealed only the protease-sensitive, detergent-soluble PrP^{C} normally found in uninfected animals.

In conclusion, contrary to the prion hypothesis, murine TSE models can transmit infectivity from brain tissue in which PrP^{Sc} levels are extremely low or non-detectable. Furthermore, this tissue can contain a high titre of infectivity. Alternative forms of PrP have been implicated in TSE disease, however no evidence of alternative PrP was found in the models investigated. Given that some infectious brain tissue only contained PrP with PrP^{C}-like characteristics, PrP^{Sc} may not be the infectious agent of TSE. It may be possible that a form of PrP^{C} is infectious, but it is also conceivable that a PrP-associated molecule, not studied here, is the infectious agent.

1. An Introduction to Transmissible Spongiform Encephalopathy (TSE)

1.1. Introduction

Transmissible Spongiform Encephalopathies (TSE) are a group of slow, inevitably fatal, neurodegenerative diseases affecting tissues of the Central Nervous System (CNS). These diseases have extremely long incubation times although the time from onset of illness to death of a human or animal host can be short. TSE symptoms include behavioural changes, cognitive impairment and insomnia, leading to ataxia, dementia and eventually death. These diseases are found in animals as scrapie in sheep, Bovine Spongiform Encephalopathy (BSE) in cattle, Feline SE (FSE) in domestic and captured cats and as Chronic Wasting Disease (CWD) in mule deer and elk. In humans several diseases have been described, Creutzfeldt-Jacob Disease (CJD), Gerstmann-Straussler Syndrome (GSS), Fatal Familial Insomnia (FFI), Kuru and the newly emerged variant CJD (vCJD). These diseases are transmissible both within a host species, such as scrapie from sheep to sheep and Kuru from man to man, and across species, such as cattle BSE to humans, occurring as vCJD. TSE has also been transmitted experimentally from humans and cattle to primates (Gajdusek, Gibbs & Alpers, 1967; Herzog et al., 2004) and from sheep, cattle and humans to rodents (Bruce, 1985a; Bruce et al., 2002; Tateishi & Kitamoto, 1995). The production of rodent TSE models in particular has allowed a greater understanding of the molecular and pathological mechanisms involved in these diseases.

During the disease process, it is postulated that the normal cellular form of the host protein PrP (PrP^{C}), alters conformation to become the disease-associated form of PrP (PrP^{Sc}) which itself is proposed to be the infectious agent (Bolton, McKinley & Prusiner, 1982; Prusiner, 1982). The gene encoding PrP has been found in all mammals looked at so far thus indicating a wide range of potential hosts to transmit the infectious agent.

Due to the variety of strains of TSE agent, that cause different clinical and pathological characteristics in different animals, the infectious agent was proposed to contain a nucleic acid component, but, despite repeated attempts, no disease-specific nucleic acid has been isolated along with infectivity. However, several studies have separated infectivity from aggregated PrP isolated from TSE-infected animals (Manuelidis, Sklaviadis & Manuelidis, 1987; Somerville & Dunn, 1996; Wille et al., 1996), prompting fierce debate about whether PrP is the infectious agent, or merely a component of infectious agent.

1.2. The host encoded protein, PrP^C

PrP^C is encoded by the host PrP gene, *Prnp,* in mice and *PRNP* in humans (figure 1.1). Full length PrP^C (figure 1.2) is 30-35 kDa and is expressed on the surface of most cell types including liver, kidney, spleen, heart, testes, bone marrow and blood platelets (Liu et al., 2001; MacGregor, 2001), but expression levels are highest in neurons. (Bendheim et al., 1992). PrP^C is synthesised in the rough endoplasmic reticulum and is trafficked through the golgi *en route* to the cell surface. It is modified via cleavage of

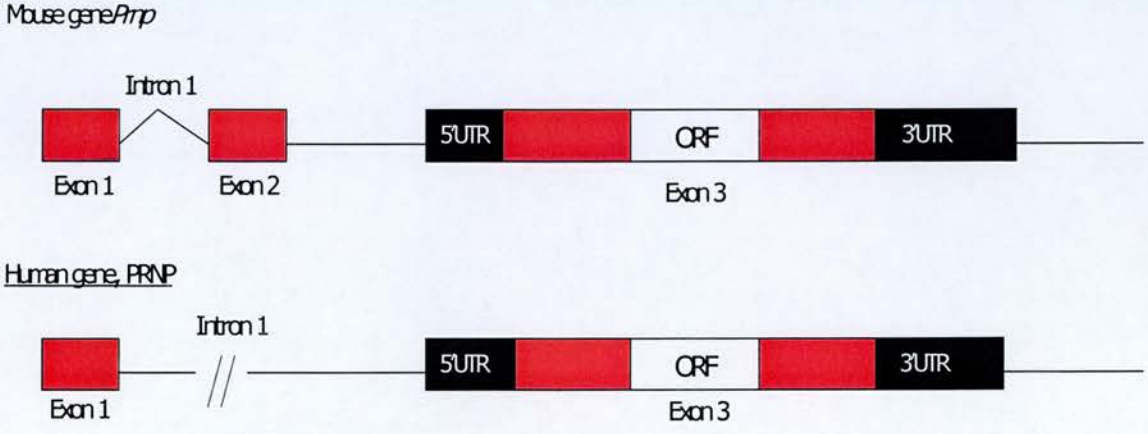

Figure 1.1 Schematic representation of the PrP gene

Prnp has three distinct exons, exon 3 containing the open reading frame (ORF).
PRNP has two distinct exons although there may as yet be an undiscovered second exon and intron within intron 1.
Adapted from (Fischer et al., 1996) and (Moore et al., 1999)

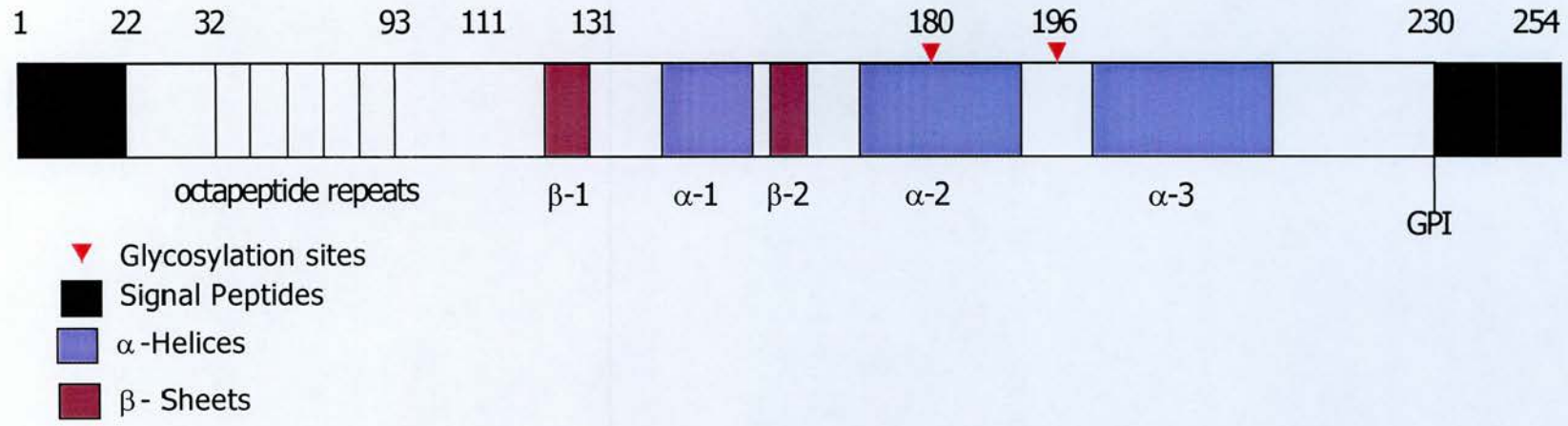

Figure 1.2 Schematic diagram of PrP

Adapted from (Fischer et al., 1996) and (Gill et al., 2000)

the N-terminal signal peptide, addition of oligosaccharide sidechains via two asparagine linked gylcosylation sites at amino acids 180 and 196, formation of the disulphide bond between cysteine residues at amino acids 179 and 214 and attachment of the glycophosphoinositol (GPI) anchor to produce the mature protein. PrP^C is then transported to the cell surface where attachment occurs via the GPI anchor, which can be cleaved by glycolipases such as phosphatidylinositol phospholipase C (PIPLC) to release it from the membrane. Recycling of PrP^C occurs via an endocytic pathway, where PrP^C is transported by endosomes back into the cell. The production and recycling process has been shown to take one hour in neuroblastoma cells (Harris, 1999).

1.2.1. PrP^C Structure

Recombinant PrP (rPrP) produced in *Esherichia coli* has been used in many studies to investigate the structure of PrP. Although rPrP lacks the post-translational modifications of eukaryotic PrP (it is not glycosylated and lacks the glycophosphoinositol (GPI) anchor), circular dichromism (CD) found the structure of this protein to be similar to that of normal hamster PrP^C (Wurthrich & Riek, 2001). Nuclear Magnetic Resonance (NMR) techniques have identified the 3D structure of human, bovine, murine and hamster PrP^C (Wurthrich & Riek, 2001) but it must be borne in mind that these structures are experimental because of the non-physiological conditions used during NMR and the recombinant nature of the protein. However, comparison of the structure of hamster, murine and bovine PrP indicate that PrP from the different sources are remarkably similar in structure. NMR studies revealed the structured nature of PrP^C residues 120-231, containing three α-helices at PrP amino acid residues 144-157, 172-193 and 200-227, and two β-sheets at residues 128-131 and 161-164 (Billeter et al., 1997; Zahn et al., 2000) (figures 1.2 & 1.3). The crystallographic structure of ovine PrP^C has recently been resolved and has been shown to exhibit a similar secondary structure to human PrP^C (Haire et al., 2004).

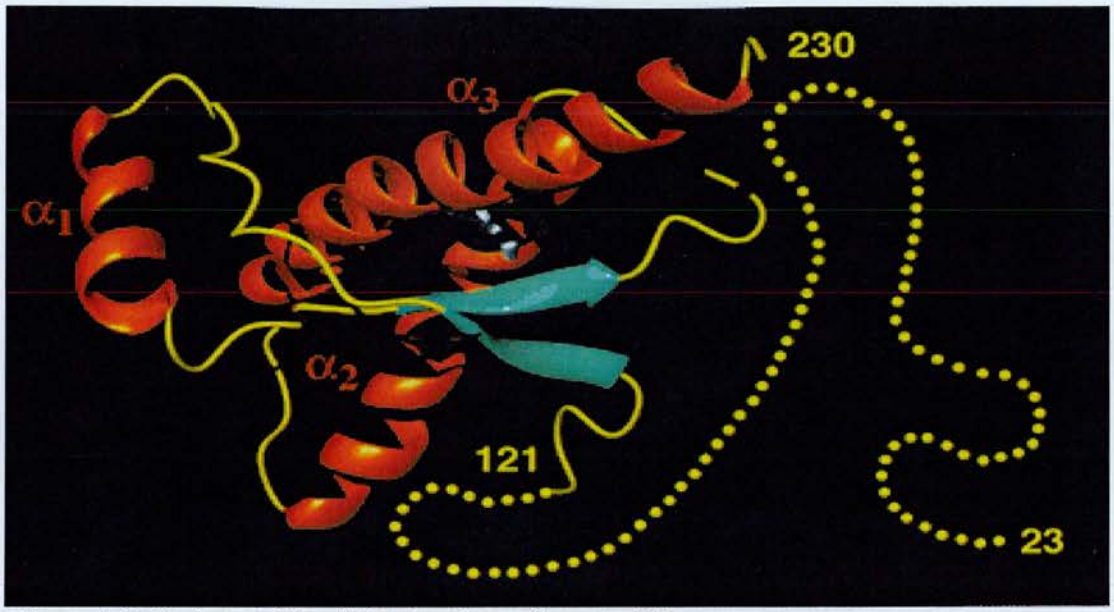

Figure 1.3 Cartoon of the NMR structure of human PrP

Sourced from (Zahn et al., 2000)

1.2.2. PrP^C Function

The normal function(s) of PrP^C has not yet been resolved. Potential roles for PrP include the determination of neuron fate during embryogenesis (Manson et al., 1992). PrP has been demonstrated to have a copper binding ability, thought to take place at the N-terminal octapeptide repeat region (figure 1.2) (Brown et al., 2000; Viles et al., 1999; Wong et al., 2000). PrP may be associated with superoxide dismutase (Brown et al., 1999), involved in normal synaptic function (Collinge et al., 1994), and play a role in the peripheral nervous and lymphoreticular systems (Bruce et al., 2000; McBride et al., 1992; Raeber et al., 1999). The rapid production and recycling of PrP^C from the cell surface back into the cell suggests that PrP^C may act as a receptor that can rapidly internalise its bound substrate (Harris, 1999). It is not known whether PrP^C binds a particular substrate, however several potential molecules have been identified, including the lamanin receptor protein (Rieger, Lasmezas & Weiss, 1999), Grb2 (Spielhaupter & Schatzl, 2001), Bcl2 (Kurschner & Morgan, 1995) and RNA aptamers (Weiss et al., 1997). It is also feasible that if the infectious agent of TSE is a virus or virus-like particle, PrP^C may act as a viral receptor (Rohwer, 1991). Elucidating the function of PrP^C may help to ascertain

whether the symptoms of TSE disease are caused by a loss of PrP^C function, rather than caused by the accumulation or PrP^{Sc} or by an intrinsic neurotoxic property of PrP^{Sc}.

1.2.3. PrP null mice

It was thought that the creation of PrP null mice would indicate a function for PrP^C, however PrP null mice (Bueler et al., 1992; Manson et al., 1994a) appear to develop normally except that they show altered sleep patterns (Tobler et al., 1996). Given the lack of obvious phenotype in PrP null mice in the absence of PrP^C it is possible that the function of PrP^C is compensated for by another protein in these mice, however as yet, no compensatory protein has been found. It has been demonstrated that PrP^C is required to support TSE infection since PrP null mice with a disrupted murine PrP gene, *Prnp*, do not express PrP^C and do not succumb to infection when inoculated (Bueler et al., 1993; Manson et al., 1994a). There is a dose-dependant effect of *Prnp* expression where disease incubation time decreases with increasing (Manson et al., 1994b). Whilst *Prnp* copy number affected the disease incubation time it did not alter the distribution or the final intensity of vacuolation and PrP deposition (Manson et al., 1994b). It has also been demonstrated that neuronal expression of PrP^C is required to support infectivity. PrP^C-expressing cells were introduced into PrP null mouse brain and upon TSE-infection only those cells expressing PrP^C displayed TSE-associated pathology (Brandner et al., 1996). These experiments have demonstrated that the expression of host PrP^C is critical in supporting TSE.

1.2.4. PrP^C and TSE

In order to further understand how PrP^C is involved in TSE, transgenic mice containing truncated PrP forms were created. Various lines of transgenic mice that expressing PrP^C with specific deletion regions have been created. PrP^C with deletions of the N-terminal 32-80 region of PrP^C (cleaved in PrP^{Sc} to produce PrP27-30), the C-terminal 144-231 region of PrP^C, and a combined deletion of both N and C-terminal regions 32-80 and 144-231

(Fischer et al., 1996) were produced. Only mice with the N-terminal deletion succumbed to TSE when infected with the mouse-passaged RML strain, suggesting that the C-terminal, globular domain of PrP must be present for TSE to occur. Furthermore, the susceptibility of PrP null mice to TSE was restored upon the introduction of a PrP construct devoid of the octapeptide repeat region. Null mice expressing a PrP gene in which region 32-93 was deleted succumbed to TSE upon infection with RML (Flechsig et al., 2000). Rescue appeared dose-dependant since mice hemizygous for the introduced gene had a longer incubation time than homozygous mice. Interestingly, in the rescued mice, PrP^{Sc} levels and titres of infectivity in brain were lower than found in wild type mice and the authors suggest this is because of the octapeptide region deletion. It may be that the presence of this region allows TSE to develop more efficiently and PrP^{Sc} to accumulate faster in wild type mice. This region may also play a role in interacting with the infectious agent of TSE. Interestingly in the rescued brain PrP^{Sc} levels were extremely low, whilst the titre of infectivity was found to be 10^7 ID_{50} units/ml (Flechsig et al., 2000). This may indicate that infectivity in the brain of rescued mice was not conferred by PrP^{Sc}. PrP^{Sc} was detected in the spinal cord however, and was transmissible to Tg20 indicator mice.

Whilst experiments using PrP null mice models indicate that the presence of PrP^{C} is clearly required for TSE, the above experiments indicate that the N-terminus of PrP^{C} is not necessarily required to support TSE. However the N-terminus can adopt a structure (Gill et al., 2000) and it may be that when the globular domain of PrP^{C} interacts with its ligand, the N-terminus may become structured and may itself form another binding site. The interaction of the N-terminus with another ligand could act as an enhancer signal for further PrP^{C}-ligand interaction and allow TSE to rapidly develop. Thus the N-terminus of PrP^{C} may not be critical for the development of TSE, however it could be rate-limiting.

1.3. The Prion hypothesis

1.3.1. PrP^{Sc} and infectivity

The discovery of an abnormal form of PrP, PrP27-30 (PrP^{Sc}), in scrapie-infected hamster and sheep brain but not from uninfected brain, lead to the initial proposal that a small proteinaceous particle, called a prion, could be responsible for conferring infectivity in TSE disease (Prusiner, 1982). This hypothesis was based on initial experiments using hamster TSE agent, 263K, in which the protease resistant PrP^{Sc} fragment was found to be the major component of TSE-infected tissues and appeared to correlate with infectivity (Bolton et al., 1982; Prusiner et al., 1982a). When applied to a sucrose gradient and separated into different fractions, most PrP^{Sc} was found in fractions with the highest infectivity titre and less PrP^{Sc} was found where infectivity was low (McKinley, Bolton & Prusiner, 1983). When fractions containing infectivity and PrP^{Sc} were investigated using electron microscopy, aggregates, or prion rods were identified (Prusiner et al., 1982a). Furthermore, scrapie-associated fibrils (SAF) identified from murine and hamster TSE models (Hilmert & Diringer, 1984; Merz et al., 1981) were found to be associated with infectivity (Diringer et al., 1983). Infectivity had previously been shown to be associated with membrane fractions from TSE-infected animals, and subsequently PrP^{Sc} was identified from membrane fractions of 263K-infected hamsters (Meyer et al., 1986). These studies suggested that PrP^{Sc} was perhaps the infectious agent of TSE since no nucleic acid was found in the preparations studied (Prusiner, 1982; Prusiner et al., 1982a). Furthermore, the addition of an anti-PrP27-30 antibody to 263K-infected hamster brain homogenate reduced the infectivity of that homogenate, indicating neutralisation of infectivity via binding of the antibody to PrP^{Sc} (Gabizon et al., 1988). Moreover, at post-mortem, the accumulation of disease-associated PrP in brain of infected animals was identified using anti-SAF antibodies (Farquhar, Somerville & Ritchie, 1989; Kascsak et al., 1987; McBride, Bruce & Fraser, 1988).

PrP27-30, SAF or prion rods have only been identified from TSE-infected brain (Kascsak et al., 1985; McKinley et al., 1983; Merz et al., 1981).

Proteinase K (PK) treatment of TSE-infected tissue homogenate reveals a protease-resistant core of PrP^{Sc} at 27-30kDa. This core is cleaved from the full length 30-35kDa protein seen before PK-treatment. In comparison, homogenate from uninfected tissues contains full-length PrP^{C} at 30-35kDa, which is completely degraded by PK-treatment (figure 1.1). In the TSE-affected host, high levels of PrP^{Sc} are usually found in brain, spinal column and other CNS tissues, and correspondingly high infectivity titres are usually found in these tissues. Lower levels of PrP^{Sc} have been reported in peripheral tissues such as spleen, lymph node, Peyers patches and tonsil as well as in peripheral nerves, and in other non-CNS tissues such as pancreas, thymus and placenta (Farquhar et al., 1996; Fraser, 1996; Groschup et al., 1996), and infectivity titres are generally lower in these tissues.

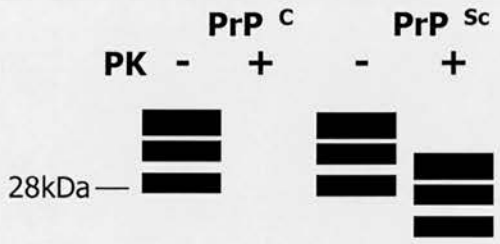

Figure 1.4 Schematic diagram of immunoblotted, proteinase K-treated PrP^{C} and PrP^{Sc}

Complete PK degradation of normal PrP^{C} from uninfected tissues compared with the PK-resistant core of infectious PrP^{Sc} from infected tissues.

Different amounts of PrP^{Sc} have been found in different brain areas (DeArmond, 1988; Kuczius & Groschup, 1999) however, the relative levels of PrP^{Sc} and titre of infectivity in specific brain areas have not been measured to truly assess the correlation between these parameters.

1.3.2. PrP^{Sc} template

Studies indicated that the primary amino acid sequence of PrP^{Sc} and of the normal, cellular form, PrP^{C}, were the same (Turk et al., 1988). The prion hypothesis radically proposed that PrP^{Sc} could convert PrP^{C} into further molecules of PrP^{Sc}, thus propagate the infectious agent. It is known that

PrP^C and PrP^{Sc} have different secondary and tertiary structure in that PrP^C mainly consists of α-helices and PrP^{Sc} has a high β-sheet content (Pan et al., 1993). It is postulated that these differences occur via a conformational change. Processes of $PrP^C \rightarrow PrP^{Sc}$ conversion are thought to occur via either (i) heterodimer conversion or (ii) seeded polymerisation (Caughey & Chesebro, 1997) (figure 1.5). The monomeric conversion model indicates that when one molecule of PrP^C and one molecule of PrP^{Sc} come together as a heterodimer, PrP^C is converted to PrP^{Sc}, creating a homodimer, which can split into two separate, infective PrP^{Sc} molecules. The seeded polymerisation model states that PrP^{Sc} exists as a polymer that can recruit PrP^C monomers, convert them to PrP^{Sc} and add them to the polymer structure. Fragmentation of the infectious polymer then facilitates multiple recruitment of PrP^C and allows the build up of PrP^{Sc} in fibrils or amyloid. Although the mechanism of $PrP^C \rightarrow PrP^{Sc}$ conversion has not been fully resolved, the seeded polymerisation method is currently favoured. *In vitro* and cyclic amplification of PrP^C using a PrP^{Sc} 'seed' has been experimentally demonstrated and is further discussed in chapter 1.3.5.

NMR also revealed the unstructured nature of N-terminal residues 23-120, however further studies have indicated the N-terminal region may be structured to some degree (Gill et al., 2000). In addition the octapeptide region of PrP^C (residues 32-93) has been shown to have copper-binding ability (Viles et al., 1999; Wong et al., 2000) thus this region of PrP may be functionally essential. It has also been suggested that the N-terminus may be capable of interaction with other proteins or the structured portion of PrP and indeed, *in vitro* conversion assays have suggested that the N-terminus of PrP may have a role in defining the conformation of converted PrP (Lawson et al., 2001).

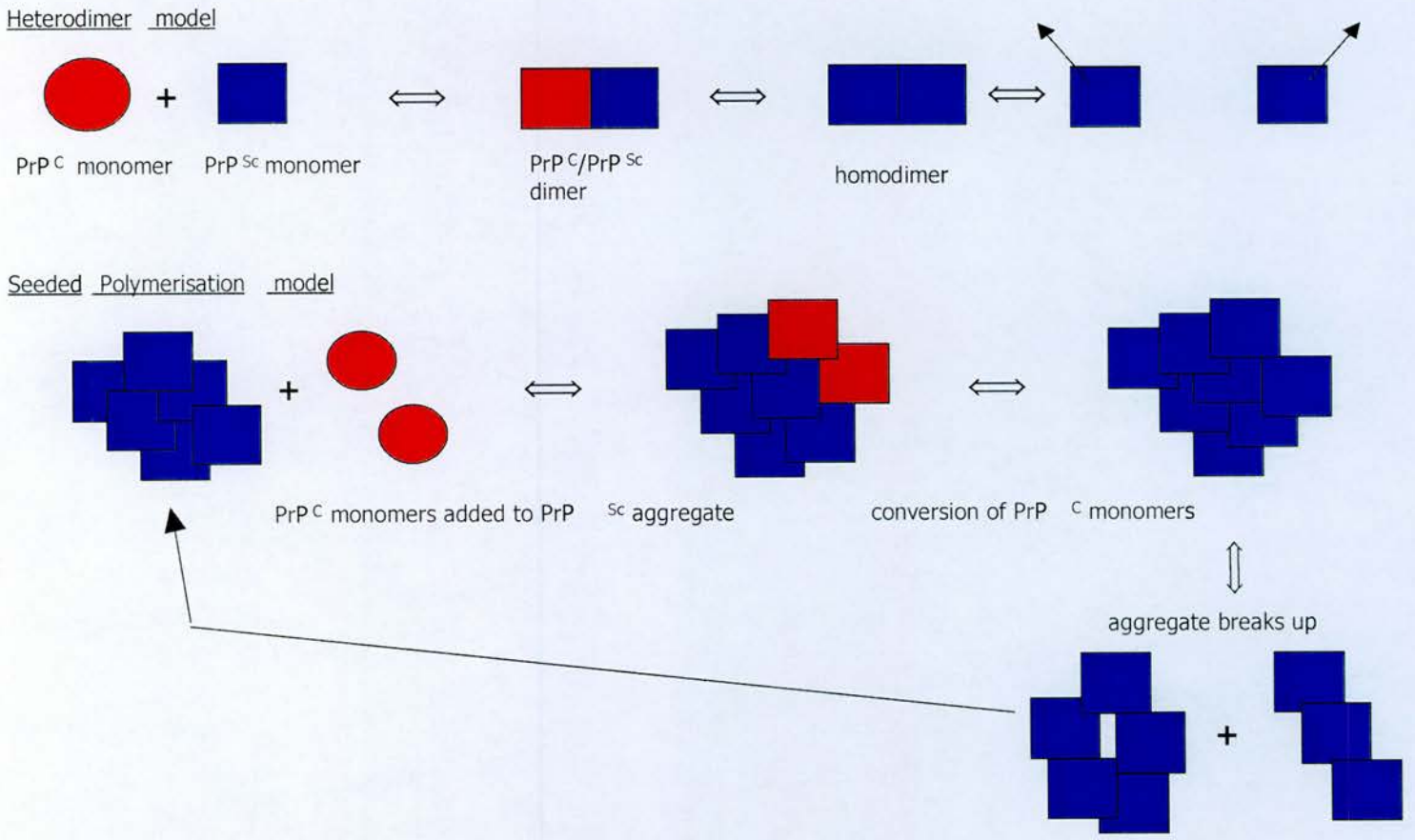

Figure 1.5 Hypothesised PrP conversion models
Adapted from (Caughey & Chesebro, 1997)

1.3.3. Alpha- and beta-folded PrP

Circular Dichroism (CD) has been used to assess the α-helical or β-sheet nature of recombinant PrP, typically of the postulated structured region at residues 120-231, producing a specific curve according to the degree of protein folding. Using physiologically relevant conditions recombinant PrP can be manipulated into the α- and β-forms to mimic PrP^{C} and PrP^{Sc} conformation in sub-cellular compartments (Jackson et al., 1999). Such experiments demonstrate that α-folded PrP is capable of conversion to a β-folded form. Furthermore, experiments have demonstrated that PrP is capable of finding different conformations and folding-intermediates suggesting that intermediate forms of PrP may exist (Baskakov et al., 2002). However, intermediate forms of PrP generated in such experiments have not been demonstrated to be infectious. The conversion of $PrP^{C} \rightarrow PrP^{Sc}$ may allow PrP^{C} to exhibit different characteristics from PrP^{Sc} thus TSE may result from a gain of function of PrP^{Sc}.

1.3.4. Yeast Prions

The rapid conversion of a protein from one conformation to another has been demonstrated in yeast. Normal soluble URE 3 and PSI proteins were shown to convert to abnormal, insoluble ure2 and sup35 aggregates in *Saccharomyces cerevisiae* (Tuite, 2000). These abnormal proteins altered the biochemical characteristics of the yeast and allowed growth under previously undesirable conditions. Such characteristics were passed on to daughter cells via transfer of the abnormal protein during replication. These experiments show proof of principal that rapid conversion can change the biochemical property of that protein, and may indicate that prion conversion is an evolutionary mechanism to deal with a rapidly changing environment. Indeed, the growth of the fungi *Podospera* can be determined by the presence of the abnormal HET-s protein, where the abnormal protein only allowed mycelia to grow in the presence of compatible protein in the cell cytoplasm (Liebman, 2002). This is an example of how *podospera* avoids the spread of viruses, where mycelia containing genetically different

material are not allowed to fuse. Thus, the conversion of PrP^{C} to PrP^{Sc} may be an evolutionary process that remains in mammals as a rare occurrence as exhibited in spontaneous TSE cases. However, it has been demonstrated that the induction, but not propagation of ure2 to URE3 in yeast requires the involvement of Mks1 protein (part of the nitrogen regulation cascade) (Edskes & Wickner, 2000). This indicates that other proteins are likely to be involved in the formation of abnormal protein. Furthermore, the prion hypothesis has proposed that different structural conformations of PrP^{Sc} could determine specific TSE strain characteristics (Aguzzi, 1998; Safar, 1996). Recent experiments have not only confirmed the transferable characteristics of yeast prion proteins, but have also indicated that these characteristics may be conferred in the structure of the yeast prion protein (King & Diaz-Avalos, 2004; Tanaka et al., 2004). Such experiments support the hypothesis that strain-specific characteristics of TSE can be determined by the conformation of PrP.

1.3.5. Cell-free conversion

Cell-free conversion experiments were devised to further investigate the interaction of PrP^{C} and PrP^{Sc} during the conversion process (Horiuchi et al., 2001; Horiuchi & Caughey, 1999; Horiuchi et al., 2000; Kocisko et al., 1994), and to examine the molecular mechanisms of the species barrier (Priola, 1999; Priola, Chabry & Chan, 2001) and of TSE strains (Bessen et al., 1995; Vorberg & Priola, 2002). Cell free conversion of purified PrP^{Sc} isolated from TSE-infected brain (as SAF or PrP 27-30) can induce PrP^{C} conversion when mixed with an excess of PrP^{C} (Caughey & Chesebro, 1997). In these experiments, radiolabelled, PK-sensitive PrP (PrP-sen) produced *in vitro* was mixed with PrP^{Sc} isolated from TSE-infected rodents. An increased concentration of radiolabelled PrP that was PK-resistant (PrP-res) indicated the conversion of PK-sensitive PrP to a PK-resistant form. This was thought to mimic the conversion of PrP^{C} to PrP^{Sc}. It appeared that homology between PrP^{C} and PrP^{Sc} was critical for the conversion of PrP since hamster PrP^{Sc} added to mouse PrP-sen (or vice verca) did not drive PrP conversion (Kocisko et al., 1995). Further studies showed that compatibility at specific residues was required for efficient conversion (Priola et al., 2001), and

seemed to fit in with the prion hypothesis where PrP^{Sc} acts as a template for PrP^{C} conversion. Subsequently, these studies indicated a critical binding event at amino acids 109-141, which only allows conversion of compatible PrP-sen and PrP-res (Horiuchi et al., 2000). Peptides corresponding to amino acids 166-179 and 200-223 of hamster PrP can block the formation of PrP-res, and since these peptides are thought to form β-sheet structures, these areas of PrP may be involved in the formation of PrP–res via a conformational change. Multiple regions of PrP are therefore thought to be involved in the formation of PrP-res (Horiuchi et al., 2001). Recently, the eukaryotic cell-derived PrP^{C} in these cell-free reactions has been replaced with recombinant PrP^{C}. This is produced from *E. coli* thus suggests that eukaryotic cellular factors are not necessary for the conversion process (Kirby et al., 2003). Moreover, glycosylation is not required for effective conversion of $PrP^{C} \rightarrow PrP^{Sc}$ (Kocisko et al., 1995), however the specific glycoform pattern of a TSE strain has been proposed to be dictated by the glycoform pattern of the PrP^{Sc} template (Vorberg & Priola, 2002).

The cell-free conversion process has been exploited in the PMCA assay (protein misfolding cyclic amplification) where small concentrations of PrP^{Sc} can be amplified using successive rounds of sonication and incubation with PrP^{C} (Saborio, Permanne & Soto, 2001; Soto, Saborio & Anderes, 2002). PrP^{Sc} from an infected sample was mixed with an excess of PrP^{C} from uninfected brain, incubation encouraged the PrP^{C} to PrP^{Sc} conversion and sonication broke up PrP^{Sc} aggregates to seed further conversion. Increased amounts of PrP-res were produced using this assay and conversion reactions were only viable in the presence of infectious brain homogenate (Saborio et al., 1999) suggesting that PrP alone is not sufficient for conversion. It is known that PrP can bind to various other proteins but it is unclear whether these play a role in aiding the conversion process.

1.4. Newly converted PrP^{Sc} and infectivity

According to the prion hypothesis, the presence of PrP^{Sc} directly correlates with the appearance of infectivity, however during cell-free conversion

experiments or PMCA the increased production of PrP-res has not been reported to associate with a concurrent increase in infectivity.

Bioassay of PrP-res produced by the cell-free conversion of chimeric mouse/hamster PrP-sen with PrP^{Sc} purified from 263K-infected hamster brain found no infectivity when transmitted to chimeric mice (Hill, Antoniou & Collinge, 1999a). This infers that the acquisition of PK-resistance by PrP is not enough to make it infectious. Such data may indicate that the PrP formed in these experiments may not have adopted an infectious conformation. Data may also suggest that there is another as yet unidentified component required for infectivity. Indeed, a recent report has shown that RNA increases PrP^{Sc} production when added to *in vitro* conversion reactions, suggesting that RNA may facilitate the $PrP^{C} \rightarrow PrP^{Sc}$ conversion process (Deleault, Lucassen & Supattapone, 2003). Moreover, the presence of non-infectious but PK-resistant forms of PrP may also suggest the existence of intermediate forms of PrP between PrP^{C} and infectious PrP^{Sc}.

It is possible to surmise, from these *in vitro* experiments, that PrP^{Sc} alone is not the infectious agent. The conversion of $PrP^{C} \rightarrow PrP^{Sc}$ may indeed occur, and there may be an increased accumulation of PrP^{Sc} in the affected host, in common with other amyloidogenic diseases where misfolded protein accumulates. However it is possible that PrP^{Sc} associates with other as yet unidentified proteins or nucleic acids within these accumulations, which when together, become infectious.

1.5. The virus hypothesis

Due to the long incubation time of TSE and the inevitable fate of animals showing clinical symptoms of TSE, investigators suggested that the scrapie agent was a slow virus, which affected the CNS (Kimberlin, 1976b). Filtration experiments initially identified the scrapie agent as a small particle of approximately 20-40nm, which was heat stable. Subsequent denaturation experiments found that the scrapie agent had a heat denaturation curve similar to that of double-stranded DNA (Millson, Hunter

& Kimberlin, 1976) and there was a reported increase in DNA synthesis rates in brains of mice clinically affected by TSE (Hunter, 1972), suggesting that the agent was a DNA virus. Experiments to isolate the scrapie agent indicated that the majority of infectivity was found in membrane fractions and suggested that the agent may be a larger component, which may have been an integral part of the host cell membrane (Millson et al., 1976). Further experiments found that UV irradiation did not destroy scrapie infectivity (Bellinger-Kawahara et al., 1987; Hunter, 1972) suggesting that either, in common with some viruses, the scrapie agent was UV-resistant or if the agent did contain nucleic acid this component would be extremely small, around 20-30 bases. Indeed, a direct comparison of the UV-resistance of scrapie and other viruses placed the scrapie agent alongside small viruses (Rohwer, 1991) indicating that the agent could be viral. Due to the small nature of the nucleic acid component, it was also considered that the infectious agent could be a viroid, a small, naked nucleic acid. However, infectivity transmitted by the scrapie agent was shown to be unaffected by treatment of brain homogenate with ribonuclease and deoxyribonuclease (Hunter, 1972; Millson et al., 1976), arguing against the presence of a naked nucleic acid component. However virologists argue that the demonstration that the scrapie agent is unaffected by nuclease yet affected by protease degradation can also be characteristic of viruses (Rohwer, 1991). Viruses composed of a nucleic acid core surrounded by a proteinaceous envelope and/or capsid would be affected by proteases, however nuclease treatment would not affect the protected nucleic acid. Such findings therefore, cannot rule out a viral component to TSE.

1.5.1. The Virino hypothesis

The Virino hypothesis arose from the observations that no host immune response was mounted during TSE infection. This hypothesis proposed a two-component model where a protective protein coat consisting of host protein surrounds, or is associated with, the infective agent. The protein itself was proposed not to be infectious but may be closely associated to the agent which may be a host independent, informational molecule such as a small replicable nucleic acid. It was proposed that the informational

molecule would be capable of providing heritable strain-specific information such as the unique vacuolation targeting, incubation time and glycoform ratio of each strain of TSE agent (Bruce & Dickinson, 1987; Kimberlin, 1982; Somerville, 1991). It was proposed that the virino agent could interact with the product of the host gene to ensure replication of the agent. Moreover, if the informational molecule was a nucleic acid that could bind to the host protein, perhaps this could explain the lack of inactivation of the agent by irradiation and the lack of host immune response (Dickinson & Outram, 1988).

Although no disease-associated nucleic acid has been found, the virus hypothesis of TSE has not become obsolete. Recent data has shown that TSE disease incubation time can be dramatically extended by inoculating two distinct strains of agent into the same mouse (Bartz, Aiken & Bessen, 2004; Manuelidis & Lu, 2003), similar to the blocking of a virulent virus infection with a slowly replicating virus. These data corroborate earlier findings (Dickinson et al., 1972) and indicate that the virus hypothesis has not been disproved.

1.6. Biochemical evidence against the prion hypothesis

If the prion hypothesis is correct and PrP^{Sc} is the infectious agent, PrP^{Sc} should correlate with infectivity. However some studies which have separated PrP^{Sc} from infectivity have questioned this hypothesis. Using organic solvents to dissociate aggregates of PrP^{Sc}, the PK-resistance of PrP^{Sc} was partially separated from the amyloid property and infectivity (Wille et al., 1996). Treatment using 2.5% HFIP (1,1,1,3,3,3-hexafluoro-2-propanol) lowered infectivity titre, but not the PK-resistance of hamster 263K, however using 10% TFIP (1,1,1-trifluoro-2-propanol), scrapie rod morphology was altered yet infectivity remained constant. Since the hamster 263K model was used to correlate PrP^{Sc} and infectivity, separation of the amyloid and PK-resistant characteristics of PrP^{Sc} from infectivity was significant.

PrP^{Sc} has been further dissociated from infectivity using detergent, pH, heat and dimethyl sulphoxide treatments. PK-treatment of detergent solubilised hamster 263K brain reduced infectivity by 97%, indicating that the infectious agent was not protease resistant (Manuelidis et al., 1987). Furthermore, treatment of brain from TSE-infected mice using high pH buffers (pH9 or pH9.6) separated PrP^{Sc} from infectivity in sucrose gradient centrifugation fractions of membrane preparations (Somerville & Dunn, 1996). In one experiment measurement of PrP content and infectivity from each fraction found 60% of infectivity in one fraction containing less than 10% PrP^{Sc}. In another experiment one fraction containing 80% PrP^{Sc} exhibited no infectivity. Moreover, heat treatment of murine TSE was shown to reduce infectivity titre but not to affect the PK-resistance of different strains of agent (Somerville et al., 2002). This indicated that infectivity was independent of the PK-resistant property of PrP. Were the infectious agent a protein alone, heat would degrade the protein, and affect its PK-resistance. The authors suggest that their findings indicate an infectious agent with an informational molecule that is protected by a heat-resistant component, consistent with the virino hypothesis (chapter 1.5.1). A further experiment examined microsomes prepared from 263K-infected hamster brain treated with dimethyl sulphoxide (DMSO) before centrifuging in a sucrose gradient (Shaked et al., 1999). Fractions of the gradient were analysed and more PrP was found at the top of the gradient, in the light fractions of DMSO-treated brain, compared to untreated brain. This PrP was shown to be PK-resistant but was not found to be any more infectious than PrP found in the equivalent gradient fraction from DMSO-untreated brain. The authors concluded that PK-resistance was not necessary for infectivity. It is possible that during $PrP^{C} \rightarrow PrP^{Sc}$ conversion, there are populations of PrP which have PK-resistant characteristics yet have not associated with infectivity. This may suggest that PrP conversion and the acquisition of infectivity are separate events, furthermore, this may indicate that rather than being the infectious agent itself, PrP^{Sc} associates with an infectious agent during disease.

1.7. Strains of Agent

The existence of different strains of infectious agent is a common concept in conventional virology. However the presence of different strains of TSE has proved a conundrum to the prion hypothesis – how can the many strains of agent with different disease characteristics be encoded for by one protein alone?

1.7.1. Strain characteristics

Scrapie from sheep and goats and BSE from cattle have been experimentally inoculated and passaged in laboratory strains of mice. After many passages in mice or hamsters, a range of stable scrapie strains emerged (Bruce, 1985a; Bruce & Dickinson, 1987). These strains can be distinguished by their specific disease incubation times when passaged through a panel of different wild type mice (table 1.1) and unique

TSE Origin	TSE Agent	Incubation Time (days)		
		C57BL Mouse	VM mouse	Hamster
Murine TSE Agent				
Natural Scrapie	ME7	180	320	n/a
	87A	350	600	n/a
	87V	n/a	290	n/a
	111A	n/a	>700	n/a
Experimental Sheep Scrapie	22C	190	470	n/a
	22L	170	210	n/a
	22A	205	460	n/a
Experimental Goat Scrapie	139A	170	210	n/a
	79A	170	310	n/a
	79V	250	280	n/a
	22H	210	350	n/a
Natural BSE	301C	210	260	n/a
	301V	280	115	n/a
Hamster TSE Agent				
Experimental Goat Scrapie	263K	n/a	n/a	70

Table 1.1 Source and disease incubation time of TSE agents in different strains of mouse
Adapted from (Bruce, 1985a), n/a: not applicable.

pathological characteristics. Indeed, strains are classically defined by disease incubation time, targeting of vacuolation via the vacuolation profile

and targeting of PrP deposition, since these characteristics remain constant upon subsequent passage through specific mouse strains. More recently, the glycosylation profile of PrP (the three-band pattern produced upon immunoblot of infected tissues – figure 1.1) and PrP conformational assays have been used to classify TSE strains.

1.7.2. Classical strain typing

1.7.2.1. Vacuolation Profile

Strain identification can be performed on the basis of vacuolar targeting in brain (Bruce, 1985a; Kimberlin, Walker & Fraser, 1989). Severity of vacuolation is scored on a scale of 0→ 5 from at least six mice and average values are then graphed to show the degree and pattern of vacuolation in twelve different areas of the brain, consisting of nine grey matter and three white matter areas (figure 1.6). The degree and pattern of vacuolation for specific strains stays constant throughout passage, therefore new strains of agent are readily identified.

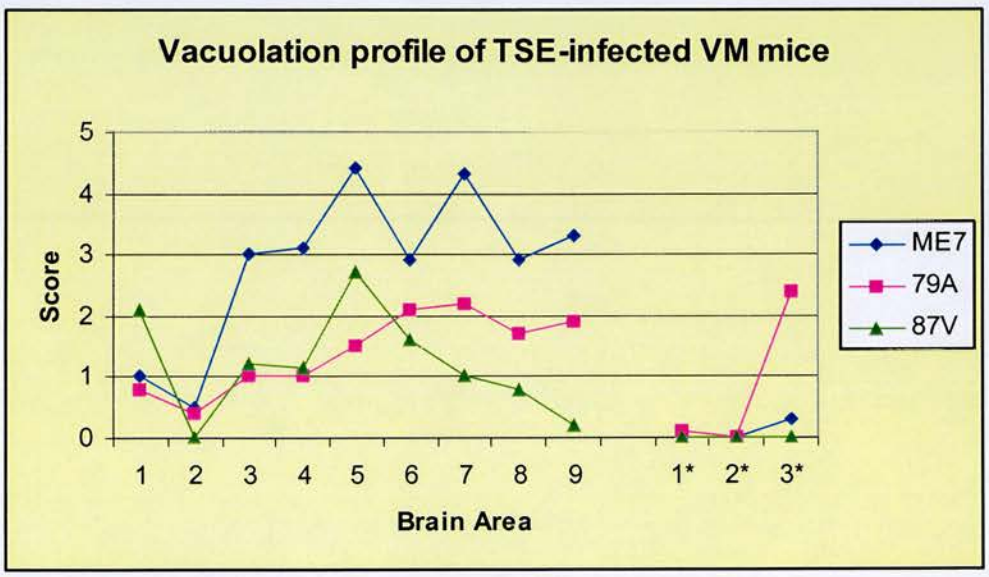

Figure 1.6 Vacuolation profiles from different murine TSE models.
Sourced from (Bruce, 1985a).

More recently these procedures have been used to characterise different experimental BSE and scrapie derived profiles (Bruce et al., 2002) and have been used to show that the strain of TSE agent responsible for new variant of CJD (vCJD) and BSE are identical (Bruce et al., 1997)

1.7.2.2. PrP deposition

Different strains of TSE agent can be characterised on the basis that each displays a different pattern of PrP deposition. Paraffin-embedded brain sections can be immunostained using PrP-specific antibodies to determine the specific brain areas in which PrP accumulation occurs during disease. Different rodent models exhibit distinct patterns of PrP deposition. For example, ME7-infected C57BL mice have a widespread pattern of PrP deposition and in 87V-infected VM mice PrP deposition is specifically targeted to the CA2 region of the hippocampus (Bruce et al., 1994; Jeffrey et al., 1997). Different targeting of PrP deposition has been seen in brain from sheep and goats orally and intracerebrally infected with BSE and natural scrapie (Foster et al., 2001a). In human TSE, different degrees and patterns of PrP deposition in infected brain are associated with different diseases (table 1.2).

Disease	Allele	age at onset	Duration	Pathology
Sporadic CJD	None	30 – 89	4.5 years	Severe grey matter vacuolation Punctate PrP deposition
Familial CJD	D178N (129V), E200K, V210I	26-70 years	3 months- 4 years	Severe vacuolation Little PrP deposition
GSS	P102L, P105L, A117V, Q217R	22-66 years	1-12 years	Vacuolation Multicentric PrP aggregates
FFI	D178N (129M)	20-71 years	6 months- 3 years	Mainly thalamic vacuolation Very little PrP deposition
Acquired/ Iatrogenic	None	25-55 years	1-25 years	As source
Kuru	None	4.5-40 years	3-18 months	No vacuolation Spiked ball PrP aggregates
vCJD	MM129	15-35 years	14 months	Severe vacuolation Florid PrP aggregation

Table 1.2 Characteristics of Human TSE Disease

The specific targeting of vacuolation and PrP deposition are the main criteria via which a TSE strain is characterised. It is not clear how the strain of agent can direct vacuolation and PrP deposition to different brain

areas. It has been suggested that it is this targeting that ultimately controls disease incubation time by specifically targeting critical areas of the brain or perhaps critical cell types. It is controversial whether PrP^{Sc} alone can account for all of the strain characteristics described above. If a protein were to confer strain characteristics it would be required to form a different conformation for each strain of agent. This would require many differently folded forms of PrP^{Sc} to exist in stable conformations (chapter 1.7.3.2).

1.7.3. Alternative methods of TSE strain classification

1.7.3.1. Glycosylation

It has been proposed that the different physiochemical properties exhibited by each strain of TSE agent can be accounted for by glycosylation. Evidence supporting this theory was demonstrated in TME (transmissible mink encephalopathy)-infected hamsters that produced two distinct TSE strains called hyper (HY) and drowsy (DY). These strains of TSE produced different disease incubation times and disease-associated pathology in hamsters (Bessen & Marsh, 1992). Upon PK-treatment the two strains produced distinct PrP^{Sc} banding patterns caused by PK cleavage at different residues at the N-terminal portion of PrP^{Sc} (Bessen & Marsh, 1992). *In vitro* conversion of PrP^{C} by HY and DY PrP^{Sc} propagated PK-resistant PrP with distinct banding patterns (Bessen et al., 1995). It was therefore implied that the HY and DY strains of TSE agent have PrP^{Sc} of different conformations and that these conformational differences may account for the different strain characteristics.

Glycosylation adds glycan chains at 2 different sites on PrP (figure 1.2). The protein can be glycosylated at either of these sites, both of these sites or not at all, producing a banding pattern of 3 different sizes of protein (figure 1.4). TSE strains isolated from human tissues have been catagorised using relative sizes and ratio of the different glycosylated bands when PrP is electrophorised on an SDS-PAGE denaturing gel (Parchi et al., 1998; Wadsworth et al., 1999b). Different banding patterns are thought to be unique to different TSE strains, however comparison of samples using this

approach has proved controversial. Samples that have different glycoform ratios may have bands that are very similar in size, and it has been shown that the use of metal chelating agents in the buffers used to prepare brain homogenates for electrophoresis can alter the band sizes in a sample (Wadsworth et al., 1999a). Moreover different laboratories have developed different classification of human disease. One lab uses a type 1 & 2 system based on the electrophoretic mobility of the unglycosylated band found after PK-treatment of PrP^{Sc} from human brain (Parchi et al., 2000). Unglycosylated bands of 21kD (type 1) and 19kDa (type 2) are produced depending upon the location of the PK cleavage site within the PrP molecule (Parchi et al., 2000). The other uses more complex typing system based upon the electrophoretic mobility and the ratio of the mono-, di-, and un-glycosylated bands after PK-treatment of a TSE-infected sample (Collinge et al., 1996). The use of two different classification systems based on glycosylation alone indicates that this method of strain identification can be complex.

Although glycotyping has been used to classify specific TSE disease in infected humans (Hill et al., 1999b; Parchi et al., 2000), cattle and sheep (Baron et al., 2000; Hope et al., 1999), this system is less useful in distinguishing different mouse-passaged strains of TSE agent since these produce similar glycosylation patterns upon immunoblot. Distinct glycoform patterns have been found in different brain areas of TSE-infected mice (Somerville, 1999) and humans (Head et al., 2001), suggesting that different cell types can produce different PrP glycoform patterns even when infected with the same TSE agent. Furthermore, different PrP isotypes have been described within the same sCJD brain (Head et al., 2004), suggesting that TSE-infected brain may contain a mix of TSE strains. Thus strain typing using glycoform ratio and protein mobility can produce complex results that are difficult to interpret.

1.7.3.2. PrP^{Sc} conformation

The conformational dependant immunoassay (CDI) can identify different structural forms of PrP^{Sc} (Safar et al., 1998). In this assay, PrP^{Sc} is unfolded

in increasing concentrations of guanidine hydrochloride (GndHCl) solution and the gradual exposure of an antibody epitope buried in the native PrP^{Sc} conformation is measured. The ratio of native/denatured protein is then plotted on a graph with each sample occupying a unique point, distinct from an uninfected control. Different mouse passaged strains of TSE were distinguished using this assay, where they could not be separated by glycoform analysis (Safar et al., 1998). This suggests that each strain of TSE agent may indeed display distinct conformations. However, since crude brain homogenate was investigated, this does not rule out the possibility that the assay also measures a molecule or complex of molecules, which may be the infectious agent and may be associated with PrP^{Sc}. This molecule or complex may itself encourage the unfolding of PrP^{Sc} as GndHCl concentrations increase.

1.8. Disease Diagnosis.

All TSE cases have common pathological hallmarks. Affected brain tissue reveals a characteristic brain spongiosis, or vacuolation (figure 1.7A) and staining using anti-PrP antibodies may reveal areas of deposition of the host-encoded, disease-associated protein, PrP (figure 1.7B). mmunostaining studies have been useful in separating BSE-infected from scrapie-infected sheep, where PrP deposition is associated with different cell types in brain, according to the host sheep breed and the TSE agent (Gonzalez, Martin & Jeffrey, 2003). Specific immunostaining can identify deposition and aggregation of PrP as large deposits and in some cases amyloid plaques. The presence of these amyloidogenic deposits links TSE to other amyloidogenic diseases such as Alzheimer's and Huntington's. In common with Alzheimer's, Huntington's, Parkinson's and Down's syndrome, astrocytic activation, or astrocytic gliosis, occurs in TSE-affected brain (Eng, Ghirnikar & Lee, 2000). Different human diseases present varying but characteristic pathology exhibiting differing degrees and distribution of vacuolation as well as different deposition characteristics (table 1.2). As discussed previously (chapter 1.2) PrP^{Sc} can be isolated along with infectivity in CNS tissues (Diringer, Beekes & Oberdieck, 1994; Kascsak et

al., 1985; McKinley et al., 1983; Prusiner et al., 1982b) thus is often used as a marker for the presence of TSE disease.

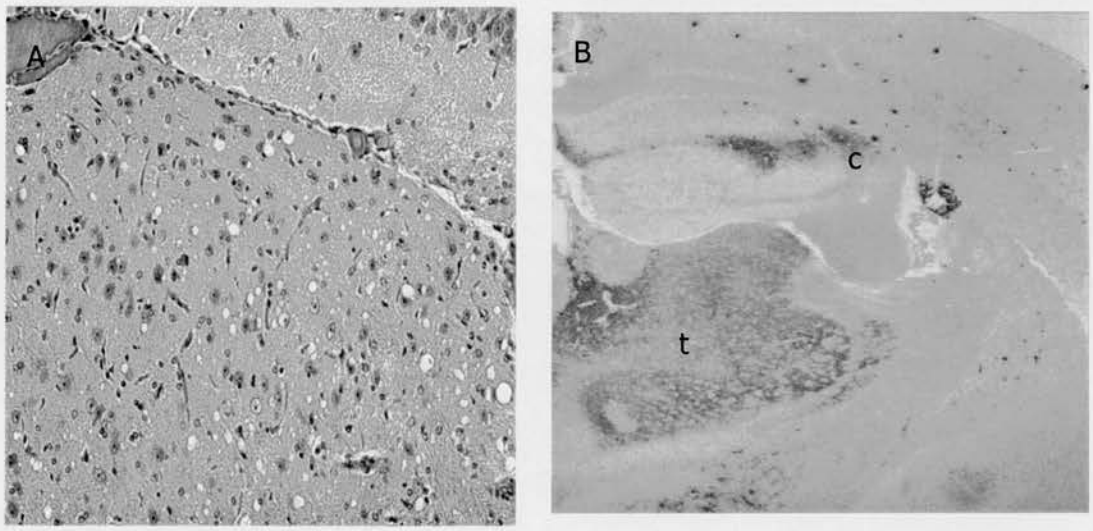

Figure 1.7 TSE-associated pathology

Vacuolar pathology in a TSE-infected mouse (A) gives the brain a spongy appearance due to holes in the tissue (sourced from H&E tissue archive, NPU, IAH). PrP deposition in the 87V/VM TSE model (B) identified using anti-PrP antibodies, seen as a brown staining, note intense staining in the thalamus (t) and CA2 region of the hippocampus (c) (image courtesy of P McBride, NPU, Edinburgh, as published in (Bruce et al., 1994)).

1.8.1. Post-mortem diagnosis

PrP^{Sc} can be experimentally distinguished from PrP^{C} due to differences in protease resistance and solubility in detergent (Meyer et al., 1986). PrP^{C} is detergent soluble and completely degraded by PK, whilst PrP^{Sc} is insoluble in detergent and PK treatment reveals a 27-30 kDa protease resistant core (figure 1.1). The close association of PK-resistant PrP^{Sc} with infectivity has lead to PrP^{Sc} increasingly being used as the marker for TSE in assays based on gel electrophoresis (SDS-PAGE) or enzyme-linked immunosorbent assay (ELISA). These systems are being used throughout Europe with the European Commission (EC) having approved three different tests for the diagnosis of BSE. These are the Enfer Test, a sandwich ELISA produced by Abbott Diagnostics, Bio-Rad's ELISA-based test Platelia™ BSE, and Prionics®-Check tests (Check-WESTERN, an immunoblot and Check-LIA, an ELISA). These assays are performed on brain tissue taken at post-mortem and all use PK-treated tissue to specifically detect PrP^{Sc}. Although these assays are primarily used to diagnose BSE in cattle, they are also

used to diagnose scrapie and chronic wasting disease (Deslys et al., 2001; Grassi, 2003; MacGregor, 2001). All the assays described commonly use brainstem material for diagnosis and rely on the detection of PK-resistant PrP^{Sc}. However recently, atypical scrapie cases were not detected using these assays even though SAF could be isolated from infected brain (Buschmann et al., 2004). Additionally, were PrP^{Sc} not present in the brainstem, but present elsewhere in the brain of infected animals, these assays would not identify PrP^{Sc} in the sample taken. Whilst the use of EC-approved assays do identify positive TSE cases, it is also possible that some cases may not be identified. These assays may not be sensitive enough to detect small amounts of PrP^{Sc} present in infected brain. Consequently the true number of positive TSE cases may be under-reported and there may be a risk of TSE-infected tissues entering and contaminating the food chain. However, if PrP^{Sc} is not the infectious agent of TSE then PrP^{Sc} may not be the best diagnostic marker for these diseases.

Additional diagnostic assays have been developed that do not rely on the detection of the PK-resistant core of PrP^{Sc}. The DELFIA assay (differential extraction lanthanide fluorometric immunoassay)(Barnard et al., 2000; MacGregor et al., 1999) separates PrP^{C} and PrP^{Sc} isoforms according to their differential solubility in 1M Guanidine Hydrochloride (GndHCl) solution, then measures the relative amounts of soluble and insoluble PrP using a sandwich ELISA. DELFIA has been reported to detect 50pg PrP (Barnard et al., 2000) and has been used to analyse the PrP^{C} content in blood and blood components, as well as measuring the amount of PrP^{Sc} in BSE-infected cattle (Barnard et al., 2000; MacGregor et al., 1999). The CDI assay (chapter 1.7.3.2) has also been used to diagnose BSE (Safar et al., 2002) and human GSS (Tremblay et al., 2004). Again this assay uses GndHCl, but rather than separating different PrP isoforms by solubility, the assay measures the ratio of antibody binding to native and GndHCl-denatured PrP in infected brain. This assay therefore does not distinguish PrP by PK-resistance rather it detects all PrP isoforms present in the tissue investigated. This assay has the advantage of detecting any PK-sensitive forms of PrP that may be infectious, however it is possible it may also

measure a PrP-associated but non-PrP component or complex which may comprise the infectious agent.

1.8.2. Pre-mortem diagnosis

As yet there is no pre-mortem test that can identify TSE prior to the occurrence of clinical symptoms. Confirmation of TSE occurs upon post-mortem examination of brain taken from the affected host. The emergence of BSE and vCJD have caused concern over potentially infected tissues entering the food chain, and the potential infectivity of human tissues and bodily fluids. Effective pre-mortem diagnosis of TSE could ensure the identification of potentially infectious tissues and enable their removal from the food chain or, in the case of human disease, allow the disposal or stringent cleansing of surgical instruments to reduce the potential risk of iatrogenic TSE.

The need to identify TSE before clinical symptoms appear has prompted a major upsurge in the development of diagnostic assays, with particular interest in those that can be performed on easily obtained fluids or tissues. The disease associated protein, PrP^{Sc}, has been detected in urine of TSE infected patients and cattle (Shaked et al., 2001) and has also been identified in blood platelet and plasma fractions (MacGregor et al., 1999). These findings suggest the potential for infectivity to be found in body fluids such as blood, and indeed BSE has been transmitted from sheep to sheep via blood transfusion (Houston et al., 2000; Hunter et al., 2002). Given the additional report of suspected transmission of CJD in humans via blood transfusion (Llewelyn et al., 2004), it is essential that rapid but sensitive diagnostic assays be developed to detect PrP^{Sc} in bodily fluids. Cerebrospinal fluid (CSF), which is easily obtained by biopsy, has also been investigated for diagnostic use. One study found an increased concentration of gamma-14-3-3 (a CSF protein marker associated with neurological disease) in TSE-infected mice (Baxter et al., 2002) using immunoblot and ELISA, whilst another study used a sensitive confocal scanning apparatus to detect extremely small amounts of PrP^{Sc} in CSF from CJD-infected patients (Bieschke et al., 2000). As yet, the CSF assays have

not been developed for human or animal diagnosis. PrP^{Sc} was found to accumulate in lymphoid tissue in human and animal TSE cases (Joiner et al., 2002; Kimberlin & Walker, 1979; Rubenstein et al., 1987; Wadsworth et al., 2001) therefore studies have been undertaken to assess the usefulness of tonsilar tissue in the pre-mortem diagnosis of human vCJD and scrapie disease (Baylis et al., 2002; Hill et al., 1999b). These studies are controversial since tonsil biopsy is an invasive surgical procedure and instruments that may become infected during surgery have the potential to further spread TSE if subsequently used on healthy individuals.

It is important to stress that the detection of PrP^{Sc} as a marker for TSE relies heavily upon the strong correlation between PrP^{Sc} and infectivity. However, these parameters have been separated and PrP^{Sc} may not be the infectious agent of TSE. It has therefore been suggested that alternative, surrogate markers should be found with definitive links to disease. One such marker is EDRF (erythroid differenciation-related factor). The expression of EDRF has been shown to reduce with increasing TSE in infected mice, hamsters, cattle and sheep brain thus the severity of TSE can be correlated with level of EDRF depletion (Miele, Manson & Clinton, 2001). However, a full evaluation of this surrogate marker for TSE diagnosis has yet to be undertaken.

1.8.3. Antibodies for PrP detection

All detection assays have in common the need for good antibodies. In SDS-PAGE systems PrP is denatured for detection thus no antibody can distinguish PrP^{Sc} from PrP^{C}. ELISA-based assay detection of PrP will depend upon the recognition of specific conformations of PrP, however antibodies produced against linear peptide sequences will not distinguish conformation. If different strains of agent have different conformations it is important that these different conformations can be detected. It is therefore essential that TSE diagnosis based upon the presence of PrP^{Sc} is confirmed using a range of conformational and non-conformational antibodies.

Polyclonal and monoclonal anti-PrP antibodies are produced by immunising mice and rabbits with purified scrapie preparations, recombinant PrP or PrP peptides (Farquhar et al., 1989; Korth et al., 1997; Li et al., 2000; Zanusso et al., 1998). Although each antibody recognises a specific linear portion of PrP, these mono- and polyclonal antibodies cannot distinguish PrP^{C} from PrP^{Sc} when protein is denatured during immunoblot or immunohistochemical analysis thus infected samples must always be compared to an uninfected control.

Antibodies that specifically recognise PrP in the PrP^{Sc} conformation have also been described (Korth et al., 1997; Polymenidou et al., 2002). These specifically recognise structural epitopes thus have been used in immunoprecipitation experiments rather than immunoblot to identify PrP^{Sc}. The 15B3 antibody recognises PrP^{Sc} from human CJD, BSE and murine scrapie (Korth et al., 1997). PrP^{Sc}-specificity may lie in the recognition of three epitopes of PrP, at 142-148, 162-170 and 214-226, which must all be exposed in the PrP^{Sc} but not PrP^{C} conformation. Despite the initial identification of this PrP^{Sc}-specific antibody, 15B3 has not been widely used. Exposure of tyrosine-tyrosine-arginine (YYR) residues is thought to be PrP^{Sc}-specific. YYR is present in the 15B3 epitope (Korth et al., 1997) and several other antibodies have been raised against peptides containing the YYR motif (Paramithiotis et al., 2003). These antibodies have been shown to be PrP^{Sc}-specific. PrP^{Sc} has been immunoprecipitated from infected mouse, hamster, cattle and ovine brain and mouse spleen using YYR antibodies, as has a misfolded, PK-sensitive form of PrP. Recently, a further antibody has been reported to selectively immunoprecipitate PrP^{Sc} from CJD-infected human brain (Zou et al., 2004). This antibody was raised against nuclear DNA extracted from Raji Burkitts lymphoma cells and may indicate the presence of DNA associating with PrP^{Sc} during disease. However this antibody may recognise the conformation of an epitope rather than PrP^{Sc} *per se*. However, antibodies that specifically identify PrP^{Sc} may provide useful tools to investigate the presence of other forms of PrP or indeed, other molecules that may be responsible for infectivity.

1.9. TSE in the absence of PrP^{Sc}

As discussed at length, PrP^{Sc} has been associated with infectivity in TSE and is widely used as a marker for the disease. However, there are cases of natural TSE in humans and experimental TSE in ruminants in which PrP^{Sc} cannot be detected in post-mortem tissue. In human FFI, no PrP^{Sc} was detected, however the associated TSE-pathology of microglial activation and pro-apoptotic neurons were found in brain from eight affected patients (Dorandeu et al., 1998). Furthermore, GSS-infected brain has been reported to contain very little if any PrP^{Sc} (Tateishi & Kitamoto, 1995; Telling et al., 1995). In GSS caused by the insertion of extra octapeptide repeat regions, extremely low levels of PrP^{Sc} were reported alongside spongiosis and gliosis (Young, 1999). In animals, atypical goat scrapie was reported with the absence of PrP^{Sc} when detected by immuostaining and immunoblotting methods, however the same brain exhibited high levels of vacuolation (Foster et al., 2001b). Another case of goat scrapie with PrP^{Sc} absent in brain was also described by the same authors (Foster et al., 2001a). Additionally, placental tissue taken from a sheep scrapie case transmitted TSE to mice, yet no PrP^{Sc} was detected in this tissue (Onodera et al., 1993).

A murine model of BSE-infected C57BL/6 mice was reported to lack PrP^{Sc} in TSE end-point brain in 58% of primary pass animals that were affected by TSE (Lasmezas et al., 1997). When brain material was further passaged 39% of TSE-affected secondary pass and 13% of tertiary pass animals did not contain PrP^{Sc}, yet brain was transmissible. Despite the demonstration of transmissibility in the absence of detectable PrP^{Sc}, the titre of infectivity was not examined in mice with and without PrP^{Sc} thus it is not known in this model whether PrP^{Sc} level affected titre of infectivity.

Gerstmann-Straussler Syndrome (GSS) can develop as a spontaneous disease in humans that have a proline to leucine mutation at PrP amino acid 102 (P102L). Murine transgenic models of GSS have been produced in which mice over-expressed a murine PrP construct containing the 101 proline to leucine mutation. Extremely low levels or the absence of PrP^{Sc} was described in brain tissue taken from these mice. Tg174 mice expressed

a high copy number of the PrP transgene, produced 8x more PrP than wild type mice and became spontaneously ill. Tg196 mice expressed fewer copies of the transgene than Tg174 mice, produced 2x wild type PrP levels and were originally reported to remain healthy (Hsiao et al., 1990). Brain tissue from spontaneously ill Tg174 mice was transmitted to Tg196 mice and caused disease. However no PrP^{Sc} was detectable in spontaneously ill Tg174 or Tg196 mice that became ill after transmission (Hsiao et al., 1990). The lack of PrP^{Sc} was also described in disease end-point brain from other lines of GSS transgenic mice (containing the P101L mutation) that became spontaneously ill, Tg(MoPrP-P101L) mice (Telling et al., 1995) and Tg(MHu2M-P101L) mice (Telling et al., 1996). Transmission of the spontaneous murine GSS from Tg174 to Tg196 mice is often taken as proof of the prion hypothesis (Hsiao et al., 1994). However, it is unclear in these experiments whether infectivity was conferred by PrP^{Sc} since very little PrP^{Sc} (if any) was found in brains of spontaneously sick mice. It has been reported that 20% of Tg194 mice become spontaneously sick (Kaneko et al., 2000), thus the transfer of brain material into these mice may accelerate a spontaneous disease already present. Furthermore, it is possible that in all of the aforementioned GSS models, the spontaneous neurodegenerative disease was due to the overexpression of the transgene and not the mutation itself or the presence of PrP^{Sc} (Westaway et al., 1994). Bioassay titration to confirm the amount of infectivity in these models was not performed.

In another murine model of GSS/P102L, gene targeted transgenic 101LL mice (129/Ola mice, which also contain a P→L mutation at amino acid 101 in the endogenous PrP gene) do not succumb to spontaneous disease but were more susceptible than wild type mice to human GSS/P102L inoculum (Manson et al., 1999). Human GSS was transmitted to mutant 101LL mice with an average incubation time of 360 days, but only transmitted to one wild type 129/Ola mouse (101PP) in 456 days. Although both wild type and mutant mice expressed similar levels of PrP^{C} in the brain, 101LL mice produced very little PK-resistant PrP when inoculated with GSS/P102L. Moreover, when the 101LL mice were infected with hamster 263K (374 days), endpoint brain also exhibited extremely low levels of PrP^{Sc} (Barron et

al., 2001). Again, 263K only transmitted to one wild type mouse (>700 days). It was not clear whether the low levels of PrP^{Sc} found in the infected 101LL mice corresponded to low titres of infectivity in the brain since bioassay was not performed on these animals. However, subsequent studies showed that despite the lack of PrP^{Sc} in GSS-infected and 263K-infected 101LL mice, TSE was transmitted from brain of infected mice in short incubation times. Given that short incubation times are thought to be indicative of high titres of infectivity (Kimberlin & Walker, 1978; Prusiner et al., 1982b), this appeared contradictory with the low PrP^{Sc} levels found in infected 101LL mouse brain.

The natural and experimental cases discussed here indicate that the use of PrP^{Sc} as a marker for TSE is not always appropriate. The presence of PrP^{Sc} does not always correlate with infectivity, which may indicate that PrP^{Sc} is not the infectious agent. It is clear that cases of TSE may be missed because of the reliance on detecting a single pathological characteristic, which may not be present in all cases. In addition to the detection of PrP^{Sc}, post mortem diagnosis of atypical cases of TSE using other pathological characteristics of TSE such as vacuolation, gliosis and neuronal loss is critical for effective diagnosis. Therefore transmission and bioassay are the only reliable methods to detect the presence of infectivity in tissues, particularly where PrP^{Sc} is not evident.

1.10. Infectivity studies

The definitive method of identifying and measuring the amount of infectivity, or titre of infectivity, in TSE infected tissues is bioassay. The titration of infectivity in large animals such as scrapie in sheep or BSE in cattle is highly expensive therefore mice are routinely used. Infectivity transmitted to mice from TSE-infected tissues has been demonstrated from various animal models (Bruce, 1985b; Kimberlin & Walker, 1979; Onodera et al., 1993; Tateishi & Kitamoto, 1995) however, the incubation time of disease transmission can be long. Infectivity titres differ according to the strain of TSE agent and the experimental model used. Mouse passaged BSE for example has high infectivity titres of 10^9 infectious units per gram

brain (Taylor et al., 2002), whilst BSE in cattle has been titrated at 10^4 infectious units per gram brain (Taylor et al., 1997). Mouse passaged TSE agents can have different infectivity titres according to the strain of mouse (Carp & Callahan, 1986). In infected animals, different organs can exhibit different titres of infectivity. The route of injection also determines the final titre of infectivity in brain, with the intracerebral route usually the most efficient (Kimberlin & Walker, 1979; Kimberlin & Walker, 1988). TSE infectivity titres are inversely related to disease incubation times with short incubation times indicative of high titres of infectivity (Kimberlin & Walker, 1978; Prusiner et al., 1982b).

1.10.1. Measurement of Infectivity titre

End-point titration in animal or cell culture is a standard method of determining the lethal dose of an agent. The dilution of agent that causes half of the animals within an experiment to die is known as an infectious dose (ID_{50}) and is similar to the lethal dose (LD_{50}) which is often investigated in the fields of virology and toxicology.

Figure 1.8 Titration of TSE infectivity

Titration in large groups of animals to assess ID_{50}, the infectious dose of agent that kills half the animals in a group.

The ID_{50} figure is calculated using statistical analysis following the method of Karber (Karber, 1931) (figure1.8). This bioassay procedure can measure one infectious unit of TSE agent which is thought to contain 10^4 to 10^5 molecules of PrP^{Sc} (McKinley et al., 1983).

This level of sensitivity is rarely matched by *in vitro* assay. Recently, two assays have been described that claim to have a similar sensitivity to bioassay (Klohn et al., 2003; Safar et al., 2002).The first assay used CDI (chapter 1.7.3.2) to quantify PrP^{Sc} present in BSE infected cattle (Safar et al., 2002). CDI proposes that different conformations of PrP^{Sc} may cause infectivity thus forms of PrP other than PK-resistant PrP^{Sc} are investigated. Using CDI PrP^{Sc} was detected from a 10^7 dilution of BSE-infected cow brain. Cattle BSE was passaged to Tg(BoPrP) mice (over-expressing bovine PrP) for bioassay and was titrated with an ID_{50} of 10^7. This indicated that CDI is capable of detecting one infectious unit of infectivity in BSE-infected brain, however this level of sensitivity has only been demonstrated for one TSE agent. The second assay assumes that PrP^{Sc} is the infectious agent of TSE and measured the amount of PrP^{Sc} taken up from TSE-infected homogenate by neuroblastoma cells (Klohn et al., 2003). PrP^{Sc} from RML-infected brain homogenate was taken up by a clone of particularly susceptible cells, which were then passaged to ensure PrP^{Sc} propagation. Cells were harvested, serially diluted, fixed onto filter paper, then PK-treated and probed using anti-PrP antibodies to identify PrP^{Sc}. PrP^{Sc} was measured in a 10^{-7} dilution of the cells therefore the titre of infectivity was measured at 10^7 infectious units, the same titre of infectivity found by bioassay of RML. The assay was not sensitive for the murine TSE agents ME7 and 22A, or for hamster 263K, and it may be that individual clones of cells must be identified for each strain of TSE agent according to their ability to uptake each agent. The application of this assay to all strains of TSE agent is not yet possible.

1.11. Alternative pathogenic forms of PrP

Particularly in human GSS cases, a lack of PrP^{Sc} has been described in affected brain (chapter 1.9) therefore forms of PrP other than PK-resistant PrP were proposed to exist in infected brain. PrP^{C} is encoded by *Prnp,* in

mice and *PRNP* in humans (figure 1.1), and it has been demonstrated that inherited cases of TSE disease are associated with different mutations within the host gene, or with insertional mutations of the octapeptide region (Young, 1999) (table 1.2). Rodent models have therefore been produced in which the *Prnp* gene contains disease-associated mutations or insertions in order to mimic human TSE and to further understand the pathological events that lead to death. Several of these diseases are thought to be due to the production of alternative forms of PrP.

1.11.1. PK-sensitive PrP

An octapeptide repeat insertional model of TSE was produced to mimic an inherited disease. Mice in this model produced PrP containing fourteen octapeptide repeats (PG14 mice) (Chiesa et al., 1998). In one human case, containing an inserted nine repeat region, PrP immunoreactive plaques were found alongside Alzheimer-associated pathology (Duchen, Poulter & Harding, 1993), however when the brain of PG14 mice was examined no conventional PrP^{Sc} was detected. These animals had suffered a neurological disease consistent with TSE, however PrP in affected brain was found to be detergent insoluble (a PrP^{Sc}-like characteristic) but less PK-resistant than PrP^{Sc}. PrP^{Sc} is usually detected using high concentrations of PK e.g. above 20μg/ml, but here, PK resistant populations at 2μg/ml PK were identified. Although the PrP found by Chiesa *et al* did not contain infectivity, this supports the existence of intermediate conformations of PrP. Such PK-sensitive forms of PrP may explain the lack of PrP^{Sc} found in the human disease. Differences in PK-resistance of PrP^{C} or PrP^{Sc} may be brought about by different conformations of alternative forms exposing or concealing PK-cleavage sites. These different structural forms of PrP may have different biochemical properties from PrP^{C} or PrP^{Sc} with differential PK-sensitivities and/or detergent solubility and therefore may have to be detected by immunoprecipitation, using a panel of different polyclonal and monoclonal antibodies. Moreover, these forms of PrP may not be the infectious agent of TSE but may be responsible for the pathology. More recently, PK-sensitive forms of PrP^{Sc} have been found in brain from a transgenic mouse model of GSS using an alternative PK-incubation temperature of $4^{0}C$ instead of $37^{0}C$

for one hour (Tremblay et al., 2004), and in human CJD-infected brain using a PrP^{Sc}-specific antibody (chapter 1.8.3) (Zou et al., 2004). It has not been shown that the PrP found in these cases was infectious therefore it is difficult to say whether PK-sensitive PrP in this model is associated with infectivity.

1.11.2. Transmembrane PrP

An *in vitro* experiment to study the translocation of PrP indicated the presence of secretory and membrane-spanning forms within microsomal membranes (Hay et al., 1987). Two different forms were identified, ^{Ctm}PrP and ^{Ntm}PrP, where the C- or N-terminus projects into the lumen of the cell (figure 1.9). A highly hydrophobic region was found between amino acids 111-134 (figure 1.2) and it is hypothesised that this region of PrP may span the lipid bi-layer of the cell causing PrP to exist in a transmembrane rather than cell surface orientation. Given the absence of PrP^{Sc} in some GSS cases, brain from human GSS caused by the associated A117V mutation (lying within the hydrophobic domain) was analysed for the presence of transmembrane PrP. Such brain was found to contain an increased amount of ^{Ctm}PrP, therefore it was proposed that the alternative transmembrane forms of PrP could be responsible for disease (Hegde et al., 1998). Transgenic mouse models were therefore produced to mimic GSS caused by the A117V mutation and other mutations were created within the proposed transmembrane domain. In each case, increasing amounts of ^{Ctm}PrP were found in brain from animals affected by neurological dysfunction. No PrP^{Sc} was found in affected brain from these models using conventional PK-treatment, however a mild PK-treatment on ice did reveal ^{Ctm}PrP (Hegde et al., 1998). Subsequent experiments have confirmed that disease-associated mutations within the hydrophobic domain of PrP increase the formation of ^{Ctm}PrP (Stewart & Harris, 2001). It is interesting to note that transmembrane forms of PrP have not been described in transgenic models with PrP mutations outside of the membrane-spanning domain (Stewart & Harris, 2001), although they have been reported in mouse neuroblastoma cells transfected with the GSS-associated P→L mutation at amino acid 101 (Mishra et al., 2002).

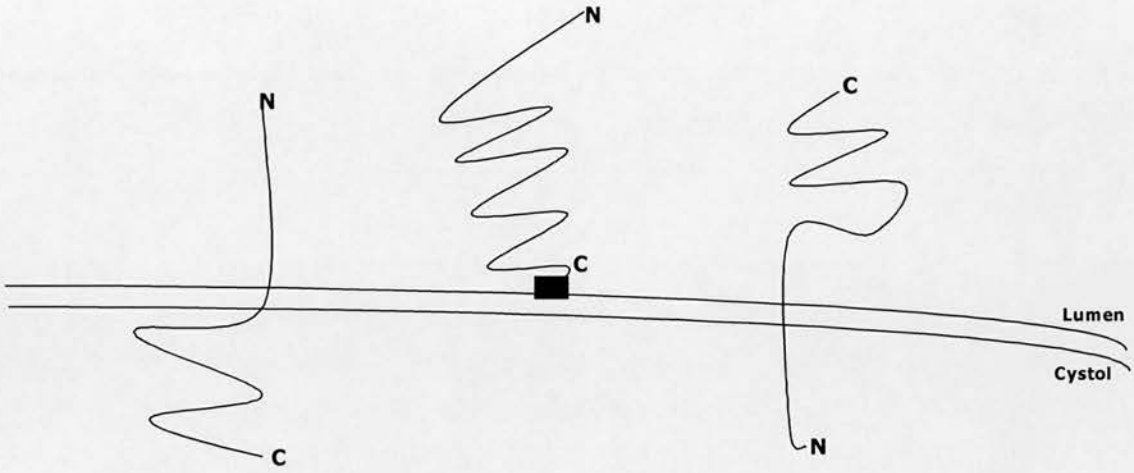

Figure 1.9 Transmembrane and secretory forms of PrP

GPI-anchored surface-bound PrP is flanked by ^{Ntm}PrP with n-terminus in the lumen (left) and ^{Ctm}PrP with c-terminus in lumen (right). Adapted from (Hegde et al., 1998) and (Stewart & Harris, 2001).

The transmembrane form of PrP has not been shown to be infectious however the presence of this in brain without PrP^{Sc} may indicate that this form is associated with TSE pathology rather than infectivity. However, extremely low levels of ^{Ctm}PrP may be present in human cases and the murine models of GSS/P101L and may be the reason for the lack of PrP^{Sc} detected in affected individuals.

1.11.3. Cytosolic PrP

The most recent form of PrP that has been alluded to *in vitro* and *in vivo* is cytosolic PrP (cyPrP) (Ma, Wollmann & Lindquist, 2002; Stewart & Harris, 2003). When the proteosome was inhibited, cyPrP accumulated in the cytoplasm of cells, and rendered cells, specifically neurons, more susceptible to the apoptotic cascades that cause cell death. It is not clear whether cyPrP originates from a breakdown in the normal PrP cycling process, however the proteosome is likely to be involved in removing improperly modified PrP. Transgenic mice expressing a cyPrP construct (PrP amino acids 23-230 but no signal sequences) produce cyPrP, which is not trafficked through the ER/golgi. The accumulation of cyPrP leads to a

neurodegenerative disease characterised by extreme neuronal loss in the cerebellum, indicating that this form of PrP is neurotoxic (Ma & Lindquist, 2002). It has not yet been demonstrated whether cyPrP is transmissible. Controversy surrounds this issue, as it remains inconclusive whether cyPrP is a true form of PrP within the cell or an artifact of experimental processes. Studies have suggested that inhibition of the proteosome itself causes an increase in PrP mRNA production and protein synthesis and it is this, not the *de novo* production of PrP that is responsible for PrP accumulation (Drisaldi et al., 2003). Moreover, it has been demonstrated that primary cultures of human neurones are not affected by cyPrP (Roucou et al., 2003), thus this form of PrP may not be applicable to human disease.

1.12. PrP neurotoxicity

Extreme pathological changes occur in the TSE-infected host. The appearance of vacuoles in brain, the deposition of the disease-associated protein, and neuronal loss are all characteristic of TSE, however not all of these characteristics appear in all TSE cases. It is not clear what causes the death of the host, however it has been proposed that there are critical brain areas to which pathology is targeted and the early targeting of pathology to these areas induces a rapid death of the host. It is not clear whether the presence of PrP^{Sc} itself is the cause of other pathology, however, a correlation has been shown between areas of PrP deposition and vacuolation (De Armond et al., 1989; Jeffrey et al., 1997) and between PrP deposition and neuronal loss (Jeffrey et al., 2000).

The exact cause of neurodegeneration is not known, however it has been surmised that the PrP^{Sc} itself could be the neurotoxic agent of TSE. A PrP peptide encompassing residues 106-126 has been demonstrated to be toxic *in vitro*, the toxic effect enhanced by the presence of microglia (Chiesa & Harris, 2001). It is not clear whether microglia release substances, as yet unidentified, that contribute to the neurotoxicity of TSE. PrP106-126 has been described as the putative neurotoxic region of PrP, however other PrP peptides, PrP147-220 and PrP 121-231, have also been found to be neurotoxic (Brown, 2002). Interestingly, PrP106-126 has been reported to

inhibit the neurotoxicity of PrP121-231 suggesting that the full-length PrP molecule may contain neurotoxic sections, which become neutralised (Brown, 2002). Endogenous cleavage of PrP^{Sc} in the TSE-affected brain may release the individual fragments, which may then be able to exert their neurotoxic effects. A recent report has found small PK-resistant fragments of PrP of 7-8kDa, in brain from patients affected by sporadic CJD (Zou et al., 2003). It is surmised that these fragments are a sub-population of the PrP27-30kDa PK-resistant fragment and it is possible that they may be the neurotoxic forms of PrP.

The lack of PrP^{Sc} in some models of TSE caused investigation into the neurotoxicity of alternative forms of PrP. The increase of ^{Ctm}PrP in human and rodent models of GSS/A117V caused speculation that ^{Ctm}PrP was neurotoxic. The neurodegenerative ability of ^{Ctm}PrP has not been clearly defined despite the *in vitro* demonstration of the neurotoxicity of the putative transmembrane region using peptide fragments that span the hydrophobic region (Haik et al., 2000). However it has been demonstrated that ^{Ctm}PrP is retained in the endoplasmic reticulum (ER), where it may trigger apoptotic or other stress-induced pathways that cause cell death.

PrP^{C} is produced in the ER, where it is post-translationally modified and folded before being trafficked through the golgi *en route* to the cell surface. It may be that misfolded forms of PrP, including ^{Ctm}PrP are identified whilst in the ER and are normally removed from the cell via proteosomal degradation, however if this degradation pathway is blocked in some way, increased concentrations of abnormal forms of PrP may accumulate. In GSS/A117V, this may contribute to the increase of ^{Ctm}PrP, however this is unlikely to occur for other familial diseases since no ^{Ctm}PrP has been found in other murine models (Stewart & Harris, 2001). However, it may be that a more general mechanism of the accumulation of misfolded forms of PrP is responsible for neurodegeneration. Recent studies have shown that that increased concentrations of PrP in the cytosol (cyPrP) is neurotoxic and causes neurodegeneration in a transgenic model (chapter 1.12.3), and indicate that this may indeed be the general mechanism responsible for neurodegeneration. Mutations in the host genome may result in the altered

capability of the proteosome to remove improperly folded forms. If this altered capability allowed the slow build up of cyPrP over time, this may explain why familial TSE occurs in aging individuals. However, the neurotoxic and neurodegenerative characteristics of the different forms of PrP have not been elucidated.

The relationship between the newly identified forms of PrP that may be responsible for neurodegeneration in familial forms of disease, and infectivity has not been thoroughly studied. TSE did not transmit from PG14 mice, which contained PK-sensitive PrP, nor from murine models of GSS/A117V, or from human cases. This indicates that PK-sensitive PrP and ^{Ctm}PrP are not infectious or do not interact with the infectious agent. No infectivity studies have yet been performed using the transgenic cyPrP model therefore it is not known if cyPrP is capable of supporting infectivity. It therefore appears that only PrP^{Sc} is the infectious agent, or that only PrP^{Sc} can associate with the infectious agent. It is possible that PK-sensitive and ^{Ctm}PrP forms of PrP are formed in the diseased animal in the $PrP^{C} \rightarrow PrP^{Sc}$ conversion pathway, but that these forms have not yet become infectious or not come into contact with the infectious agent. Further study of the formation of alternative forms of PrP may indicate how PrP becomes infectious, or where PrP interacts with the infectious agent.

1.13. Aims of this thesis

The prion hypothesis states that the disease-associated, PK-resistant protein, PrP^{Sc}, is the infectious agent of TSE. Studies in rodent TSE models have demonstrated a correlation between the amount of PrP^{Sc} and the titre of infectivity, however, such disease models contained abundant PrP^{Sc} (Bolton et al., 1982; Diringer et al., 1983; Hilmert & Diringer, 1984; McKinley et al., 1983; Prusiner, 1982). In natural and experimental cases of TSE there may be a lack of demonstrable PrP^{Sc} in the brain where infectivity is present. PrP^{Sc} is widely used as a marker for TSE disease, but clearly the absence of PrP^{Sc} cannot be guaranteed to indicate the absence of infectivity. It is therefore important to determine whether PrP^{Sc} is an

appropriate disease marker and whether PrP^{Sc} correlates with infectivity in all cases of TSE.

When inoculated with human GSS/P101L brain or the hamster 263K agent, 101LL mice developed TSE, however little PK-resistant PrP was detected in brain tissue (chapter 1.10). Moreover, infectivity was further transmitted in short incubation times from GSS/101LL and 263K/101LL brain tissue suggesting a high titre of infectivity, inconsistent with the low PrP^{Sc} levels exhibited.

The aims of this thesis were to use the 101LL rodent model to:

- investigate the relationship between PrP^{Sc} level and titre of infectivity in the apparent absence of detectable PrP^{Sc}, and,

- examine the nature of infectivity in a "low PrP^{Sc}" model.

It was hypothesised that if PrP^{Sc} masked the true nature of the infectious agent in abundant PrP^{Sc} models, the lack of PrP^{Sc} in the 101LL model may assist in identifying the infectious agent.

2. Materials and methods

2.1 Biological Definitions

For the purpose of this thesis, the term "model" refers to a combination of a mouse strain infected with a particular strain of TSE agent (C57Bl mouse infected with the murine TSE agent, ME7). Chapter 1.9 provides further details of murine TSE agents.

Transgenic mice homozygous for the GSS-associated P101L mutation are designated "101LL" and 129Ola mice homozygous for the wild type PrP gene are designated "101PP".

In all studies brain was examined from TSE-infected mice that became clinically sick. These animals were humanly culled upon identification of clinical symptoms and the brain tissue excised. This is termed " disease end-point brain".

Previous characterisation indicated that PrP^{C} is detergent-soluble and completely degraded by protease, whereas PrP^{Sc} is detergent insoluble and contains a protease resistant core (Meyer et al., 1986). These biochemical parameters are used here to define PrP^{C} and PrP^{Sc}.

2.2 Primary antibodies

Antibody	Mono/Polyclonal	WB diltuion[a]	ICC dilution[a]	PrP Epitope(s)
3F4[3]	Monoclonal	n/a	$^1/_{1000}$	108-111
5B2[1]	Monoclonal	$^1/_{10,000}$	n/a	34-45
6H4[4]	Monoclonal	n/a	$^1/_{1000}$	144-152
8H4[1]	Monoclonal	$^1/_{20,000}$	$^1/_{1000}$	175-190
8B4[1]	Monoclonal	$^1/_{20,000}$	n/a	35-40
7A12[1]	Monoclonal	$^1/_{20,000}$	n/a	90-145
1A8[2]	Polyclonal	n/a	$^1/_{1000}$	3 distinct
1B3[2]	Polyclonal	$^1/_{20,000}$	$^1/_{1000}$	4 distinct
Calnexin[b]	Polyclonal	$^1/_{2,000 - 3,000}$	n/a	n/a
GAPDH[c]	monoclonal	$^1/_{20,000}$	n/a	n/a

[a] Diluted from 1mg/ml stock solution
[b] α-calnexin supplied by Stressgen Biotechnologies Corp.
[c] α-GAPDH supplied by Chemicon Incorporated
[1] (Li et al., 2000)
[2] (Farquhar et al., 1989; Langeveld et al., 1993)
[3] (Kascsak et al., 1987)
[4] (Korth et al., 1997)

Table 2.1 Primary antibodies used in TSE research

2.3 Secondary antibodies

Antibody	WB dilution[a] (HRP-conjugated)	ICC dilution (Biotinylated)
rabbit α-mouse[b]	$^1/_{20,000}$ or $^1/_{60,000}$	$^1/_{400}$
Goat α –rabbit[c]	$^1/_{20,000}$	$^1/_{400}$
Donkey α –rabbit[c]	n/a	$^1/_{400}$

[a] secondary antibody dilution dependant on western blot chemilluminescent substrate; 1/20,000 for POD, 1/60,000 for West Dura (chapter 2.12)
[b] 0.9mg/ml stock solution
[c] 1mg/ml stock solution
HRP conjugated and biotinylated antibodies sourced from Jackson laboratories, USA.

Table 2.2 Secondary antibodies used in TSE research

2.4 Brain tissue sources

ME7/101PP: sourced from NPU experiment 522D-1A, primary passage of TSE agent ME7 in 101PP mice.

ME7/101LL: sourced from experiment 522D-1A, primary passage of TSE agent ME7 in 101LL mice.

263K/101LL: sourced from experiment 522L-1A, primary passage of hamster 263K TSE agent into 101LL mice.

GSS/101LL: sourced from experiment 522P-1A, primary passage of human GSS isolate (containing P101L mutation) into 101LL mice.

SV mice (*Prnp*-a genotype) infected with TSE agents 139A and 79V and VM mice (*Prnp*-b genotype) infected with TSE agents 79V, 22A and 301C were sourced from the NPU catalogue of archive experiments, brain tissue stored at -70°C.

Uninfected 101PP: wild type 129/Ola mice (Manson et al., 1999) (homozygous for the proline amino acid at PrP residue 101) sourced from breeding stock maintained at NPU, Edinburgh.

Uninfected 101LL: gene targetted 129/Ola mice homozygous for the leucine amino acid at PrP residue 101 (Manson et al., 1999), sourced from breeding stock maintained at NPU, Edinburgh.

2.5 Mouse brain excision

Mice were culled by cervical dislocation and the whole brain was removed. Using sterile instruments, the skin was removed from the head and the skull carefully cut open to expose the brain.

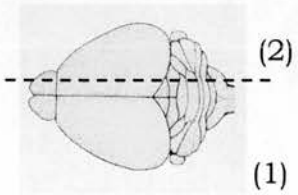

Figure 2.1 Brain tissue excised from infected animals taken for pathological (1) and biochemical (2) examination.

Whole brain was removed and cut sagitally to the right of the midline into two pieces for (1) pathological examination and (2) biochemical analysis (figure 2.1). Tissue for histopatholgy was fixed in 10% formal saline for 2-5 days. Brain for biochemical analysis was placed into a cryovial, flash frozen in liquid N_2 and stored at –70°C.

2.6 Brain homogenate preparation

All chemicals were sourced from Sigma unless stated. Brain homogenates were prepared on ice, under Category 2 or Category 3 conditions where required.

2.6.1 10% Homogenate

Tissue for homogenisation was weighed in a sterile petri-dish or freezing vial, then transferred to a clean, pre-cooled Dounce Homogeniser:

PBS Homogenate; nine volumes of cold PBS solution (minus calcium or magnesium) (Gibco) were added and the brain homogenised using 20-30 strokes of the pestle. Homogenate was stored in 50–200µl volumes in 1.5ml screw-top centrifuge tubes (Starstead), at –70°C, after flash freezing in liquid N_2.

Detergent homogenate; nine volumes of cold detergent solution (1% NP40, 1% Sodium deoxycholate, 150mM NaCl, 50mM Tris HCl pH 7.5) were added and the brain homogenised as above. Supernate was collected in 50–200µl volumes in 1.5ml screw-top centrifuge tubes after centrifugation at 16,000g for five minutes at room temperature. After flash freezing in liquid N_2, samples were stored at –70°C.

2.6.2 5% detergent homogenate

An equal volume of 2x homogenate buffer (2% NP40, 1% Sodium Deoxycholate, 300mM NaCl, 100mM Tris HCl pH7.5) was added to 10% brain homogenate in PBS or 10% brain homogenate prepared as sterile inoculum (chapter 2.22.2). Further homogenisation was performed in a

screw-top centrifuge tube using 20-30 strokes with a pre-cooled centrifuge-tube pestle (Anachem). The homogenate centrifuged at 16,000g at 10°C for one minute to remove cellular debris. Supernate was aliquoted in 20-100µl volumes in 1.5ml screw-top centrifuge tubes, flash-frozen in liquid N_2 and stored at –70°C.

2.7 Proteinase K treatment of brain homogenate

This process distinguishes PrP^{C} from PrP^{Sc} by revealing the presence of the protease resistant 27-30 kDa core of PrP^{Sc} (Prusiner ref 1982). Unless otherwise stated, the final concentration of Proteinase K (PK) was 20µg/ml. Samples were incubated at 37°C for one hour and the reaction stopped by the addition of PMSF (Sigma) to 1mM final concentration.

2.7.1 Lyophilised Proteinase K

Lyophilised PK (Sigma) was reconstituted in 10mM Tris pH 7.5 containing 1mM as $CaCl_2$ (see appendix J) to produce a 25mg/ml stock solution for long-term storage at –20°C.

2.7.2 Proteinase K Solution

PK solution (Roche) was supplied at a concentration of 19-25mg/ml. This stock was kept refrigerated for up to one year.

2.8 Deglycosylation of PrP

The enzyme N-Glycosidase F (PNGase F) removes N-linked glycan side-chains added to PrP during post-translational modification. For complete deglycosylation each reaction was incubated overnight with shaking.

2.8.1 Deglycosylation reaction

Solutions provided as a kit from New England Biolabs (UK) were 10x denaturant (5% SDS, 10% ß-mercaptoethanol), 10x G7 buffer (0.5M Sodium Phosphate pH7.5), 10% NP40 and PNGase F enzyme (500U/ml). Reactions were denatured in 1x denaturant solution at 95°C for 10 minutes, before

incubating the reaction in final concentrations of 1x G7 buffer, 1% NP40 and 1-5 units of PNGase (pre-diluting in dH_2O if required) to each reaction, at 37°C, shaking, for at least 6 hours. Protein was methanol precipitated in four volumes of ice cold methonol (Fisher), incubating at -70°C for at least 2 hours or –20°C overnight. Samples were centrifuged at 5,000-16,000g for 15 minutes, at 10°C, the methanol discarded and pellet dried before resuspending in appropriate buffer.

2.8.2 Preparation for loading onto SDS-PAGE gel

Ethanol precipitated pellets were resuspended in 120mM Tris HCl (pH 6.8) (Sigma), 1x loading buffer (Invitrogen), 1x sample reducing agent (Invitrogen) and dH_2O in a total volume of 45µl. The addition of the Tris solution was essential for efficient solublisation of the protein for electrophoresis. After denaturing at 95°C for 30 minutes, 20µl of each sample was loaded per well.

2.9 Detergent solubility of PrP

Brain prepared as 10% homogenate in PBS (chapter 2.22.2) was further homogenised with 20% (w/v) sarkosyl solution to produce a 5% homogenate. To reduce the viscosity caused by nuclear DNA contamination 1µl of Benzonase solution was added to each sample. Samples were incubated at 37°C, shaking, for 30 minutes then centrifuged at 16,000g for 10 minutes at 10°C. The pellet and supernate were carefully separated and the pellet resuspended in 10% (w/v) sarkosyl solution. On ice, the supernate was placed into a 4ml polycarbonate ultracentrifuge tube and filled with cold PBS before centrifuging at 150,000g for 2.5 hours at 10°C. Supernate and pellet were carefully separated and the tube (containing the pellet) carefully dried before resuspending the pellet in 10% sarkosyl. The volume of recovered supernate was measured and placed into 4 volumes of ice-cold methanol at -70°C for 2 hours to overnight, to precipitate protein. The precipitate was pelleted at 2,000g for 15 minutes at 10°C and the supernate discarded. All methanol was allowed to evaporate before resuspending the protein pellet in 10% sarkosyl. All pellets were

resuspended in a volume equivalent to the 10% homogenate used to start the preparation, usually 100µl. Where concentration of the samples was required, all pellets were resuspended in $^1/_5$ of the original starting volume, usually 20µl. Resuspended samples were stored at -70°C after flash freezing in liquid nitrogen.

2.10 SDS-PAGE

Polyacrylamide gel electrophoresis (PAGE) separates protein according to size. All reagents and apparatus from Invitrogen except where indicated.

Pre-cast Novex® Tris-Glycine SDS-PAGE gels with acrylamide content of 12% or 16% were purchased. Protein samples were pre-prepared in Novex® 2x sample buffer and NuPage® 10x sample reducing agent, to give 1x final concentrations of each. Samples were denatured at 95°C for 30 minutes before loading onto the gel using elongated gel loading pipette tips (Costar). Prestained standard markers (SeeBlue® or BIORAD Broad Range) were loaded into appropriate wells according to manufacturers instructions. The electrophoresis tank was connected to a BIORAD PowerPac 200, and run at 125V for 110-120 minutes until the dye-front reached the foot of the gel. Gels were removed from the cassettes and trimmed of excess acrylamide ready for protein transfer to membrane, or Coomassie Blue staining (chapter 2.15.2).

2.11 Western blot

Proteins were transferred to polyvinylidene difluoride (PVDF) membrane (Millipore, UK) using the BIORAD Trans-Blot® SD Cell. PVDF was immersed in methanol (Fisher) for 10 seconds, washed in dH_2O for two minutes and then 1x transfer buffer (39mM Glycine, 48mM Tris, 0.0375% SDS, 20% methanol [v/v]) for at least two minutes before use. The Whatman paper was thoroughly soaked in transfer buffer before making up the "transfer sandwich" of (bottom to top) 6 pieces 3MM paper, PVDF, gel, 6 pieces 3MM paper (figure 2.2). Transfer was complete after 90 minutes at 120mA per gel, with the voltage not exceeding 26V using a BIORAD PowerPac 200. Upon completion, the "sandwich" was carefully deconstucted and the PVDF

rinsed in dH_2O, ready for immunoblotting (chapter 2.12) or Ponceau Red staining (chapter 2.15.1).

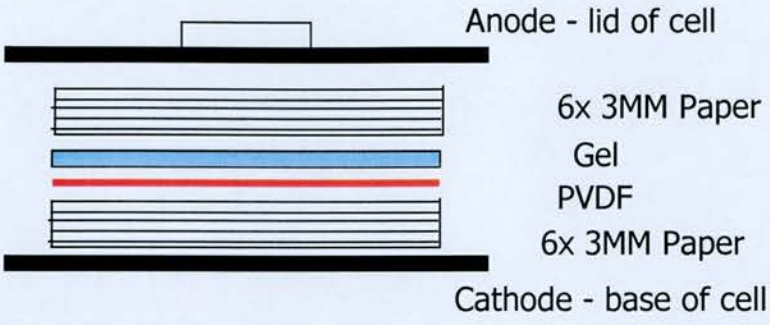

Figure 2.2 Transfer of SDS-PAGE separated protein to PVDF membrane

Electrical current runs from anode (positive) to cathode (negative) thus transferring proteins from gel to the membrane.

2.12 Immunoblot

PVDF membranes were incubated at room temperature, shaking, in the following solutions: 1x block diluted from 10x Western Blocking Reagent (Roche) using TBS (TBS (50mM Tris, 150mM NaCl, pH 7.5). Blots were probed with primary monoclonal antibody diluted in 0.5x block overnight, or primary polyclonal antibody diluted appropriately for 4 hours (chapter 2.2). Blots were washed 3x 10 minutes with TBS-tween (TBS plus 0.05% Tween 20 (Sigma)), then 2x 5 minutes with 0.5x block. Add horseradish-peroxidase conjugated secondary antibody diluted appropriately (chapter 2.3) in 0.5x block solution for 30 minutes. Wash 10x 5 minutes with TBS-tween.

2.12.1 Protein detection

Protein was visualised by non quantitative chemilluminescence after incubation with BM Chemilluminscent Blotting substrate (POD- peroxidase) (Roche). POD substrate was added directly onto the membrane and incubated for 1 minute before being exposed to Lumi-film (Roche) for up to 10 minutes to capture the luminescence.

Quantitative chemilluminescence could be achieved using Supersignal ® West Dura extended duration substrate (Pierce). Substrate was placed directly onto the Kodak Image Station 440CF, and the membrane placed into the solution. The resulting image was captured for up to one hour, and stored for later analysis using the image analysis software.

2.13 Recombinant PrP

Recombinant wild type PrP (rPrP), containing proline at amino acid 101, was kindly gifted by Dr I. Sylvester, IAH, Compton, UK. Recombinant PrP (containing 1.734mg/ml total protein) was diluted to give 10ng/µl stock concentration and stored at –70^{0}C. For immunoblot control samples, 5µl of the stock was added to the loading reaction (10µl 2x loading buffer, 2µl 10x reducing agent and 3µl dH_2O to give 20µl total) and 20µl per well was loaded after denaturing. This allowed blot to blot variation to be controlled and PrP detected by immunoblot to be quantified

2.14 Kodak Image Analysis

Using a Kodak Image Station 440CF, PrP was identified from immunoblots scanned during substrate development (chapter 2.12.1). The chemiluminescent image produced was saved as a '.bip' file using the Kodak Image analysis software. Each lane to be examined was selected, and the bands to be analysed were highlighted using specific markers. The width of the marker was adjusted to allow the marker to cover the whole band-width. The selection of bands was carried out automatically, and occasionally produced extra bands where no image was detected, or did not highlight bands that could clearly be seen by eye. Unwanted extra bands were deleted and bands required for analysis were marked manually. For each lane, a profile of the band pattern could be viewed and the bands were fitted to a Gaussian Model. The software automatically fitted each band to a symmetrical or asymmetrical Gaussian Model. The number of darkened pixels making up the image was counted and data was expressed as a pixel count or intensity. The background image across the whole lane was taken into account when applying the Gaussian model. The data generated was

exported to an Excel file to allow further analysis. The pixel intensity for each sample was compared to that of 50ng recombinant 101PP PrP (rPrP). This allowed the amount of PrP in each brain homogenate to be calculated, equivalent to rPrP to control for blot-to-blot variation.

2.15 Protein visualisation without antibodies

2.15.1 Ponceau Red Staining

To confirm protein transfer to PVDF, membrane was incubated at room temperature, shaking, with ready-made Ponceau stain (Sigma) for 2-5 minutes. Excess stain was discarded and the PVDF rinsed 2-3 times with distilled water to visualise the bands. Complete destaining was achieved by rinsing 2 times 5 minutes with TBS-tween before immunoblotting.

2.15.2 Coomassie Blue Staining

Gels were immersed in Coomassie Blue stain (0.25% Coomassie Brilliant Blue R-250 (Sigma) (w/v), 10% acetic acid (Fisher) (v/v) in 50% methanol (v/v), filtered through a Whatman No.1 filter. Incubation was at room temperature, shaking, for 30 minutes. Excess stain was removed and the gel destained (20% Acetic Acid (v/v), 10% Methanol (v/v), in dH_2O) until protein bands were clearly visible. The gel was dried (chapter 2.15.3) or photographed using the Kodak Image Station 440CF (chapter 2.15.4).

2.15.3 Drying Coomassie Gels

Coomassie stained SDS-PAGE gels were dried using a Hoefer Drygel Slab Gel Drier. The gels were assembled on top of 2 pieces of 3MM paper (larger than the gel) pre-soaked in dH_2O, covered with saran wrap and then placed in the drier. The gel was dried at 70^0 C for 1-2 hours under vacuum then allowed to cool under vacuum to ensure it remained flat.

2.15.4 Photographing coomassie stained gels

Stained SDS-PAGE gels were placed on the glass plate of the Kodak Image Station 440CF and illuminated from above. Using the Kodak Digital Science™ 1D Image Analysis Software package, the gel image was captured using a 1-5 second exposure and the image saved. Images were then directly printed or exported to Microsoft PowerPoint for labelling.

2.16 Total Protein Assay

Protein content of brain homogenate and recombinant PrP preparations were assessed using the Pierce Microwell Plate protocol and Pierce reagents. BSA standard protein and samples were diluted appropriately in PBS (Gibco) or dH_2O and applied to a microtitration plate (Linbro® EIA). 300µl of Coomassie® Plus Reagent was added to each blank well, 290µl added to sample/standard wells. After 5 seconds shaking at room temperature, absorbance was measured at 595nm using Wallac plate-reader (Victor^2 1420 Multilabel Counter). A Standard Curve of 'concentration of BSA v absorbance' was plotted and sample concentrations calculated using the equation of the standard curve. Samples were adequately diluted to lie within the linear range of absorbance detected for the standards.

2.17 Microsomal membrane preparation from brain tissue

All preparations were performed on ice. Freshly collected or frozen brain tissue (thawed before use) were homogenised in twenty volumes of microsome buffer (0.25M Sucrose, 100mM KCl, 5mM Mg Acetate, 50mM Hepes (pH7.5)) containing 0.5mM PMSF, using at least 20 strokes of the glass pestle in a Dounce homogeniser. The homogenate was transferred to screw-top centrifuge-tubes for centrifugation at 16,000g for 10 minutes at 10^{0}C. Supernate was transferred into a Beckman polycarbonate centrifuge tube and further centrifuged at 130,000g for 30 minutes at 4^{0}C to pellet microsomes. The pellet was resuspended in microsome buffer minus PMSF at 500µl per gram of starting tissue. The microsomes were flash-frozen and stored at –70^{0}C in 30µl volumes.

2.18 Microsomal PK-protection assay

Circularised microsomal membranes will possess full-length transmembrane proteins (figure 2.3). Protein external to the membrane will be cleaved upon the addition of PK whilst protein inside the membrane is protected (figure 2.3). Immunoblot detection of the protein of interest detects a size shift to a smaller protein size in PK treated compared to untreated samples. Microsomes (10µl) were incubated with 3µl 1M Tris HCl pH7.5, 1.5µl PK (from 1mg/ml stock), 1.5µl Triton X-100 in a 30µl reaction, at 37°C for 30 minutes.

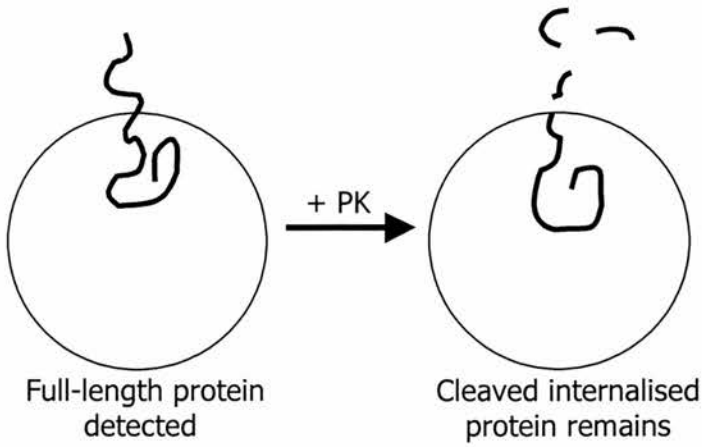

Figure 2.3 Transmembrane protein protected from PK-cleavage by microsomal membrane

Full length protein spans the microsomal membrane but only that inside the circularised membrane is protected from PK-cleavage. Full length protein is larger than cleaved protein when identified using immunoblot.

Reactions were stopped by adding 1µl of 100mM PMSF and incubating on ice for 5 minutes. Reactions were deglycosylated before methanol precipitation (chapter 2.8). They were then diluted in SDS-PAGE loading buffer and sample reducing agent for gel electrophoresis on 16% Tris/glycine gels (chapter 2.10). Control reactions, without PK treatment or detergent, Triton X-100, were also included. Samples were immunoblotted and protein detected using appropriate antibodies.

2.19 Preparation of brain for pathological examination

2.19.1 Brain tissue fixation

Formal saline-fixed brain (chapter 2.5) was immersed in 98% formic acid (BDH) for 90 minutes. Formic Acid was replaced with fresh 10% formal saline in preparation for tissue embedding.

2.19.2 Brain tissue processing and cutting

Tissues were transferred to an automated processor and processed for different times according to brain size (table 2.3). Tissue was removed and kept on hot blocks whilst trimmed coronally at each cutting level (figure 2.4A) and embedded in blocks of hot wax (figure 2.4B). Cooled blocks were trimmed of excess wax ready for cutting in 6µm microtome sections. The sections were floated into a water-bath (42-45^{0}C), then floated onto labelled Superfrost-plus glass slides for staining. Slides were dried at 37^{0}C overnight and boxed until required.

Mouse Tissues		Hamster Tissues	
Solution	Time in solution[t]	Solution	Time in solution[t]
70% alcohol	40 minutes	70% alcohol	1.5 hours
80% alcohol	40 minutes	80% alcohol	1.5 hours
95% alcohol	40 minutes	95% alcohol	1.5 hours
99% alcohol	40 minutes	99% alcohol	1.5 hours
99% alcohol	40 minutes	99% alcohol	1.5 hours
99%/xylene	30 minutes	99%/xylene	45 minutes
99%/xylene	30 minutes	99%/xylene	45 minutes
Xylene	30 minutes	Xylene	45 minutes
Xylene	30 minutes	Xylene	45 minutes
Paraffin wax	25 minutes	Paraffin wax	45 minutes
Paraffin wax	25 minutes	Paraffin wax	45 minutes
Paraffin wax	25 minutes	Paraffin wax	45 minutes

Table 2.3 Automated tissue processing

Mouse or hamster brain processed and embedded in paraffin wax using different protocols according to size of brain.

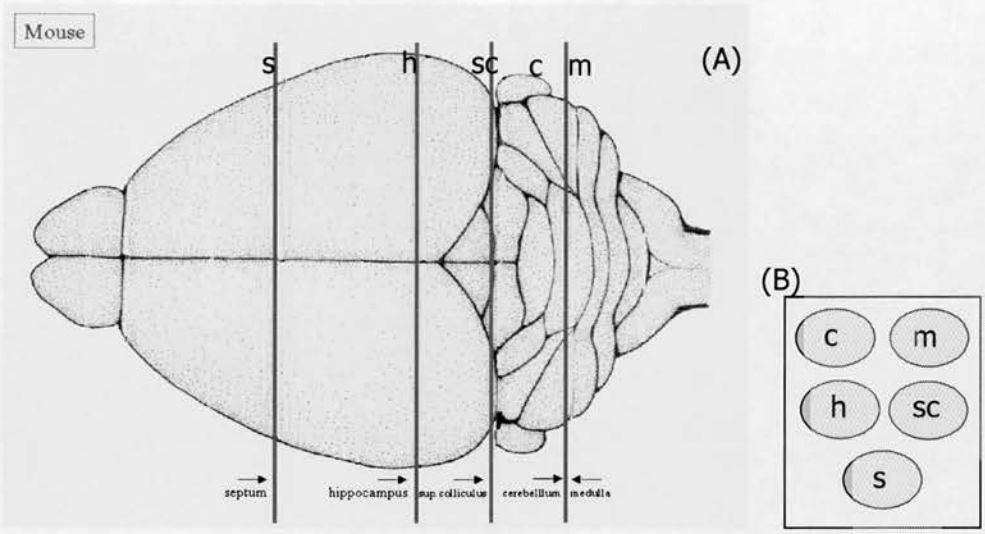

Figure 2.4 Brain sectioning for H&E and immunocytochemical staining

Half brain taken for pathological analysis (chapter 2.3). (A) Coronal sections cut at septum (s); hippocampus (h); superior colliculus (sc); cerebellum (c); medulla (m) (Fraser & Dickinson, 1968) and (B) brain segments laid out in wax blocks as indicated.

2.20 Haemotoxylin and Eosin Staining

Tissue sections were stained using an automated process (table 2.4) before mounting a coverslip (22 x 22mm) using Pertex mounting medium (BDH):

Solution	Time in solution[t]
Xylene	2x 5 minutes
90% IMS*	2x 2 minutes
95% IMS	1 minute
	3 minutes
Haematoxylin Z stain	3 minutes
	3 minutes
Scott's Tap Water[$]	2 minutes
	3 minutes
Putts Eosin	0.5 minutes
	2.5 minutes
70/% IMS	1.5 minutes
95% IMS	2x 0.5 minutes
99% IMS	2x 0.5 minutes
99% IMS/Xylene	1 minute
Xylene	3x 1 minute

Table 2.4 Haemotoxylin and Eosin automated staining process

*IMS - Industrial Methylated Spirits (supplied by Anderson, Gibb and Wilson, UK)
[$]Scott's Tap Water Substitute (0.35% sodium hydrogen carbonate, 2% magnesium sulphate in dH_2O)
Haemotoxylin and Eosin stains supplied by Thermo Shandon, UK

2.21 Immunocytochemistry

Slides of brain sections were hydrated (xylene, 99%, 94% then 70% alcohol for 5 minutes each (BDH)) before being placed into dH_2O and autoclaved at 121°C/15 minutes to help expose PrP epitopes to allow antibody detection. Sections were also treated in 98% formic acid (BDH) for 5 minutes to aid the epitope exposure process before being blocked of excess endogenous peroxidases, in 1% or 2% hydrogen peroxidase (Sigma) in methanol for 10 minutes. Sections were placed in 99-70% alcohol then washed 3x 5 minutes in PBS-BSA (1x Phosphate buffered saline plus 0.1% BSA (Sigma)). Each section was treated with 100µl of each solution as follows: 1/20 dilution of normal rabbit serum (Dako, UK) to block for 20 minutes (if using goat or donkey secondary antibodies, use goat or donkey serum (respectively) to block). Wash 3x 5 minutes in PBS-BSA. Add primary antibody overnight, 6H4, 8H4, 3F4, 1B3 and 1A8 (chapter 2.2) at 2.5µg/ml in antibody diluent (1% BSA solution in 1x PBS). Wash 3x 5 minutes in PBS-BSA. Add biotinylated secondary antibody for one hour (rabbit α-mouse for monoclonal primary antibody and goat or donkey α-rabbit for polyclonal primary antibody –chapter 2.3). Wash as before. Use ABC streptaviadin kit solutions (Dako, UK) to amplify signal, add equal volumes of solutions A and B then dilute at 1/50 in antibody diluent. Visualise PrP using diaminobenzodine (DAB) substrate (Sigma) (0.05% final concentration, activated using 0.025% final concentration hydrogen peroxide). Sections were stained for one minute in haemotoxylin then counterstained in Scott's tap-water substitute for one minute. Sections were then dehydrated (70%, 94%, 99% alcohol, 1:1 xylene:alcohol, three times xylene for 2 mins each) and coverslip mounted using DPX (distyrene/tricresyl/xylene solution (BDH). PrP staining was assessed by light microscopy. 87V-infected VM mouse brain sections were included as positive controls. To control for antibody staining, duplicate sections were probed with 1/1500 dilution of normal mouse serum and processed as above.

2.22 Bioassay measurement of infectivity titre

These methods have been described previously (Kimberlin & Walker, 1979) (chapter 1.10). All procedures were performed in a sterile environment using sterile techniques, at the appropriate containment level. Each titration experiment was approved by the Neuropathogenesis Unit, Local Ethical Review Committee (LERC).

2.22.1 Preparation of sterile brain homogenate

Brain tissue was carefully weighed, placed into a Dounce homogeniser with nine volumes of saline solution (0.9% w/v) (Martindale Pharmaceuticals, UK) and homogenised using at least 30 strokes of the pestle to prepare a 10% homogenate. The homogenate was transferred to screw-top centrifuge tubes via a 1ml syringe fitted with 26 gauge needle and aliquoted in 100µl or 200µl volumes before flash freezing in liquid N_2 and undergoing storage at -70°C, for up to nine months.

2.22.2 Preparation of inoculum

For each brain, ten-fold dilutions of homogenate were prepared for inoculum. Unopened, sterile aliquots of 10% homogenate (chapter 2.22.1) were quickly defrosted and the homogenate drawn into a 1ml syringe fitted with 26 gauge needle. 0.2ml homogenate was added to 1.8ml saline to give 10^{-2} dilution. This serial dilution was repeated until a 10^{-11} dilution was reached (figure 2.5). Each diluted inoculum was prepared using a new 1ml syringe with 26 gauge needle in preparation for inoculation.

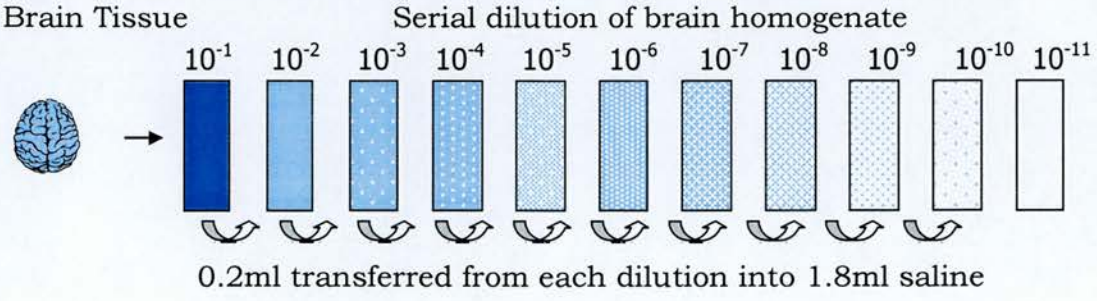

Figure 2.5 Preparation of titration inoculum

Any inoculm not used for injection was placed into sterile cryotubes (Costar), flash frozen and stored at -70^{0}C.

2.22.3 Inoculation of mice

Mice were anaesthesitised with 3% fluothane gas (delivered in oxygen) before inoculation. Twenty microlitres of inoculum was delivered into the right hemisphere of the brain using a 1ml syringe fitted with 26G $^{3}/_{8}$" needle. The needle was sheathed to expose a 2mm length to ensure that inoculum was delivered into the right mid temporal cortex. Injected animals were placed in revival cages and carefully monitored for adverse reaction to the injection procedure. Any animal showing immediate adverse reaction to the anaesthetic or injection procedures was humanely culled using a Home Office approved Schedule 1 procedure. Where possible the culled animal was replaced with another inoculated animal appropriate for that group, so that group numbers remained constant. Subsequently, animals found to be clinically TSE affected (scoring regime detailed in appendix C) or suffering inter-current illness were immediately culled in accordance with the Animals (Scientific Procedures) Act 1986, using a Schedule 1 method and brain excised (chapter 2.5).

2.22.4 Karber calculation

The dilution of TSE agent that causes half of the animals within an experiment to die is known as the infectious dose (ID_{50}). This is calculated from the number of animals exhibiting clinical and pathological signs of TSE and rarely falls within a single group therefore statistical analysis is employed, following the method of Karber (Karber, 1931). The proportion of animals exhibiting clinical signs of TSE and confirmed TSE pathology is calculated for each group and applied to the following equation:

ID_{50} = last dilution group with 100% TSE diagnosis –

($\sum$proportion of animals from 100% positive groups downwards – 0.5)

The 0.5 value is a constant applied since the final calculation is to find the dilution at which 50% of animals are affected. The calculation for the experiment illustration in chapter 1.10 would therefore be:

$ID_{50} = -2 - [(1+ 0.75+ 0.5+ 0.25+ 0)-0.5] = -2 - [2.5 - 0.5] = -4$

Therefore the dilution at which 50% of animals die is 10^{-4}, thus the original 20µl inoculum contains and ID_{50} of 10^{-4}, or 10^4 infectious units.

2.23 Preparation of murine genomic DNA from tail tissue

Mice required for breeding and experimental animals were evaluated to confirm genotype was homozygous 101PP or 101LL. Tails of live animals were taken after induced anaethesia using 3% fluothane delivered in oxygen. For each animal, two 1-2cm sections were removed from the tail tip using a fresh, sterile, flamed scalpel (to cauterise the tail), and placed into a clean microcentrifuge tube and stored at -20°C. One section of tail was treated using the following solutions to extract DNA: 800µl of tail lysis solution (15mM sodium acetate, 1% SDS, 1mM Tris (pH8), 1mM EDTA) plus PK at 200µg/ml incubated overnight at 37°C or for 2-3 hours at 64°C, shaking; lysate was mixed with 600µl of phenol (Qbiogene)/chloroform (BDH) (1 part AquaPhenol (pH 8) : 1 part chloroform) for 1 minute and centifuged at 16,000g for 5 minutes at room temperature.

600µl of the aqueous top layer was placed into a clean microcentrifuge tube, mixed with 20µl of 3M sodium acetate plus 600µl isopropanol (Fisher) and incubated at room temperature for 10 minutes.

DNA was collected by centrifugation at 16,000g for 2 minutes. The pellet was washed in 500µl ice cold 70% ethanol (v/v in dH_2O) and re-pelleted (as before). DNA was resuspended in 100µl dH_2O and stored at +4°C.

2.24 PrP genotyping of experimental animals

Genotype of experimental animals was confirmed by polymerase chain reaction (PCR) amplification of the PrP open reading frame (ORF) and enzymatic digest of the product. Mice were also screened for the PrP null allelle using PCR amplification only.

2.24.1 PrP ORF amplification

All reagents sourced from Invitrogen unless otherwise stated. Mouse genomic DNA (1µl per reaction) was amplified using oligonucleotides I (5'-gtg gct ggg gac aac ccc-3') situated in the ORF and II (5'-gcc tag acc acg aga atg cg-3') situated in the 3'UTR, to produce a 756bp product. Each reaction contained 1x PCR buffer, 0.03mM MgCl, 0.2mM di-nucletide triphosphates (Promega - ready mixed solution of ATP, CTP, GTP and TTP), 50pmol oligonucleotide (MWG Biotech AG) and 2 units Taq DNA polymerase (recombinant). Each reaction was cycled using a Biometra T3 Thermocyler, 94°C for 3 minutes (1 cycle), 94°C for 30 seconds/62°C for 30 seconds/72°C for 30 seconds (30 cycles), 72°C for 10 minutes (1 cycle), hold at 4°C.

2.24.2 Restriction digest identification of proline/leucine alleles

Restriction digest reagents sourced from Promega. The leucine allele was identified by the presence of an extra *Dde1* restriction site in the PrP ORF. The amplified PCR products were incubated with *Dde1* restriction enzyme, which recognised the restriction site: 5' C▼TNA G 3'

3' G ANT▼C 5'

DNA carrying the 101P allele was cleaved producing two fragments of 152 and 613 bp, DNA carrying the 101L allele produced three fragments of 152, 49 and 564 bp (figure 2.6). Each reaction was incubated in 1x buffer D (supplied as 10x solution 60mM Tris HCl pH 7.9, 1.5M NaCl, 60mM $MgCl_2$, 10mM DTT), 0.1mg/ml BSA and 1-10 units of enzyme (100µl final volume) at 37°C for at least 2 hours. Reactions were mixed with 4x loading buffer (0.25% bromophenol blue in 15% ficoll) and run on a 1% agarose gel in 0.5x

TAE buffer (0.2M Tris, 5.71% acetic acid (v/v), 50mM EDTA (pH8)) containing 0.6mM ethidium bromide (10mM stock tablet dissolved in dH_2O).

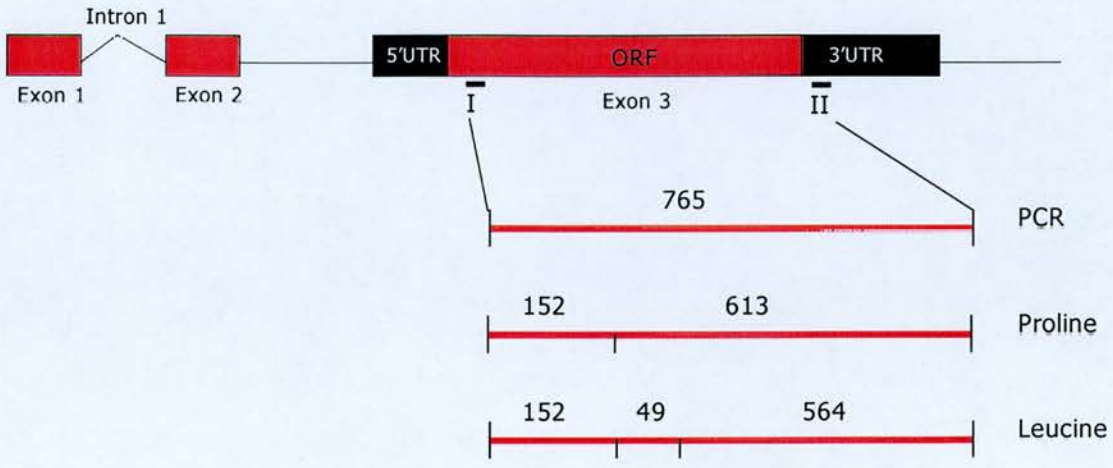

Figure 2.6 Identification of proline and leucine alleles in PrP open reading frame

2.24.3 Null allele identification

The null allele consists of a neomycin cassette inserted into *Prnp* at the unique *Kpn1* site to disrupt PrP production (Manson et al., 1994a). The null allele was identified by amplifying the neomycin cassette using oligonucleotides III (5'-ttg agc ctg gcg aac agt tc-3') and IV (5'-gat gga ttg cac gca ggt tc-3') (figure 2.7). Each PCR reaction contained PCR buffer, dinucletide triphosphates, and oligonucleotides as previously described (chapter 2.24.2). Taq polymerase was added at 1 unit per reaction. Each reaction was cycled at, 94°C for 3 minutes (1 cycle), 94°C for 30 seconds/62°C for 30 seconds/72°C for 1 minute (30 cycles), 72°C for 10 minutes (1 cycle), hold at 4°C. This reaction did not require restriction digest. The 1.2kb PCR product was visualised using 1% agarose gel as before (chapter 2.24.2).

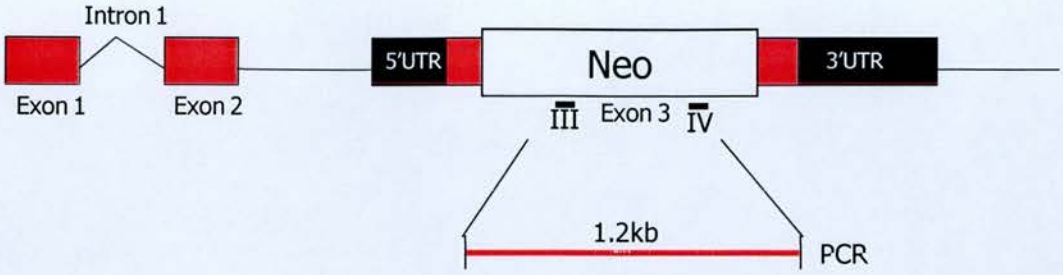

Figure 2.7 PCR amplification of murine null allelle

2.25 Measurement of PrP using DELFIA

DELFIA (Dissociation Enhanced Lanthanide Fluorometric ImmunoAssay) separates PrP according to solubility in two different concentrations of Guanidine hydorchloride. In 1M Guanidine HCl PrP^{C} is soluble and PrP^{Sc} insoluble thus can be separated using differential centrifugation. The amount of PrP in each fraction is measured using an ELISA-based technique. PrP^{Sc} is solublised in 6M Guanidine HCl to allow measurement. The percentage of insoluble PrP^{Sc} is then calculated for each sample. This method was performed by D. King (NPU, Edinburgh) and was adapted from the method shown to detect picogram amounts PrP^{Sc} in BSE-infected cattle (Barnard et al., 2000). All reagents and equipment were sourced from Perkin-Elmer unless otherwise stated.

2.25.1 Separation of soluble and insoluble PrP

One volume of 10% brain homogenate in sterile PBS (chapters 2.6.1 & 2.22.2) was added to an equal volume of 2M Guanadine HCl (Fluka Biochemicals) then tris buffer and Triton X-100 were added to give 50mM and 1% final concentrations, respectively. This mixture was homogenised on ice using 20-30 strokes of a pre-cooled centrifuge-tube pestle. One volume of NP40 buffer was added (1% NP40, 0.5% sodium deoxycholate, 150mM NaCl, 50mM Tris HCl [pH7.5]) and the mixture further homogenised using the centrifuge-tube pestle. Assay buffer was added to give 1ml final volume and the mixture thoroughly vortexed for 2 minutes. Centrifuging at

16,000g for 10, separated PrP into detergent soluble (supernate 1) and insoluble (pellet 1) fractions. The pellet was resuspended in two volumes of 6M Guanidine HCl and assay buffer added to give 1ml final volume. Centrifugation at 16,000g for 5 minutes in a bench-top centrifuge allowed the previously insoluble PrP to be collected in supernate 2.

2.25.2 Measurement of detegent soluble and insoluble PrP

All incubations were performed at room temperature, under constant agitation and all wells were filled with 200µl solution, unless otherwise stated. The ELISA procedure outlined below is depicted in figure 2.8. Capture antibody, FH11 (appendix B – sourced from IAH resource centre, Compton, UK) at 1µg/ml in PBS was used to coat a 96-well DELFIA microtitration plate, the plate refrigerated (+4°C) overnight. Unbound antibody was removed using an automated programme for DELFIA Platewasher 1296-026, then washed once with 1x wash buffer (diluted from 25x stock). (Waste brain homogenate and wash solutions were captured in a sealed bottle and treated with chlorine solution at 20,000 parts per million before disposal.) Non-specific antibody binding sites were blocked using sterile 2% BSA solution (Sigma) (in PBS plus a few grains of sodium azide – store at +4°C) for 1 hour. Wash as before.

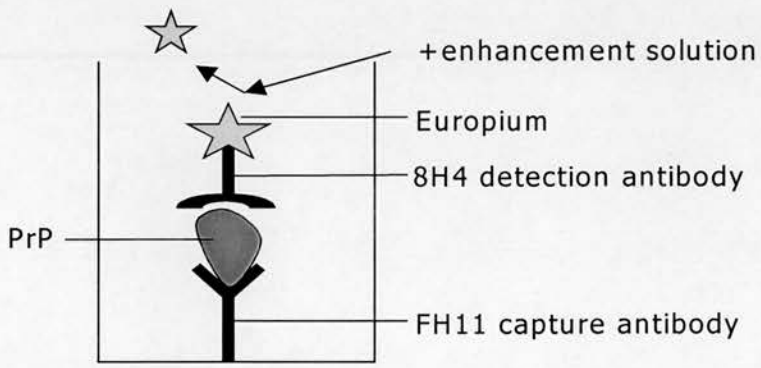

Figure 2.8 Capture and detection of PrP using DELFIA

As a blank, assay buffer was placed in the first two wells of each plate to normalise background signal. Recombinant PrP (provided by Dr I Sylvestre, IAH; Compton, UK) was diluted ten-fold in assay buffer (2000ng/ml down to

0.2ng/ml, or 400ng to 40pg rPrP per well) to produce a standard curve. Soluble and insoluble PrP fractions were loaded as neat solution in duplicate. Each plate was then incubated for one hour. Plates were washed in automated platewasher and europium-labelled 8H4 antibody (chapter 2.2) was added and incubated for exactly one hour. Unbound antibody was removed by washing six times in 1x wash buffer in platewashwer. Enhancement solution was added and the plate was incubated for 5 minutes. This allowed europium to dissociate from the 8H4 antibody, the luminescence of free europium was then measured using a Perkin-Elmer plate-reader (Victor^2 1420 Multilabel Counter) fitted with appropriate filter. WorkOut software was used to subtract background signal from each sample and standard. Sample concentrations were calculated from the resultant stantard curves. The percentage of insoluble PrP was calculated as;

$$\frac{\text{(PrP Concentration in supernate 2) x 100}}{\text{(PrP concentration in supernate 2) + (PrP concentration in supernate 1)}}$$

3. Identification of differing brain PrP^{Sc} levels in murine TSE models

3.1. Introduction

It has been demonstrated that in TSE-infected brain PrP^{Sc} correlates with infectivity (Bolton et al., 1982; McKinley et al., 1983; Prusiner, 1982), however this relationship is not straightforward and is not clearly understood. In certain tissues, the presence of PK-resistant PrP^{Sc} does not correlate with infectivity. In brain, PrP^{Sc} is detected before infectivity increases however in spleen, PrP^{Sc} was reportedly detected after the increase of infectivity titre (Farquhar et al., 1994) and infectivity has been detected in the absence of PrP^{Sc} in spleen (Czub et al., 1986a). Moreover, TSE models have been described where clinical disease occurs in animals yet PK-resistant PrP^{Sc} is not readily detectable in brain (Foster et al., 2001a) and disease transmission has been reported in the absence of PK-resistant PrP^{Sc} (Lasmezas et al., 1997; Manson et al., 1999; Onodera et al., 1993)(chapter 1.9).

The murine P101L model exhibits low levels of PK-resistant PrP^{Sc} in the brain at disease end-point when infected with human GSS (Manson et al., 1999) or hamster 263K inoculum (Barron et al., 2001). The titre of infectivity is unknown in these animals however TSE disease can be transmitted from brain in short incubation times (chapter 1.9). While short incubation times would indicate a high titre of infectivity, low PrP^{Sc} levels suggest that titre of infectivity may be low. The correlation between PrP^{Sc} and infectivity in brain has not been defined in these models.

Host *Prnp* genotype and route of inoculation are known to influence TSE disease. Depending on the *Prnp* genotype of the murine host (*Prnp*-a, *Prnp*-b or *Prnp*-a/b alleles), each TSE agent produces disease with different incubation times (Bruce et al., 1994; Carlson et al., 1986; Dickinson, Meikle & Fraser,

1968; Moore et al., 1998) (table 1.1). Moreover in brain, the degree and targeting of vacuolar pathology and PrP deposition differ depending upon *Prnp* genotype (Moore et al., 1998) and the titre of infectivity varies (Carp & Callahan, 1986; Kimberlin & Walker, 1979). The route of inoculation also affects the degree and targeting of disease-associated pathology (Carp & Callahan, 1986; Kimberlin & Walker, 1978)(chapter 1.7). In order to study the relationship between PK-resistant PrP^{Sc} and infectivity it is therefore necessary to control for PrP genotype and the route of inoculation.

The studies in this thesis aimed to define the correlation between infectivity and PK-resistant PrP^{Sc} by comparing the P101L model of TSE disease that exhibited low levels of PrP^{Sc} in brain, with TSE models that exhibited high and intermediate levels of PrP^{Sc}. The studies performed in this chapter therefore identified murine models of TSE, with similar genetic backgrounds, that exhibit high, intermediate and low PrP^{Sc} levels in brain at disease end-point. A range of TSE strains passaged in mice homozygous for *Prnp*-a or *Prnp*-b, were examined to assess the differing amounts of PrP^{Sc} produced at disease end-point in infected mice. Only models with TSE delivered via the intracerebral route were investigated.

3.2. Methodology

3.2.1. Immunoblot of PrP^{Sc} in infected animals

Brain was flash frozen in liquid nitrogen and stored at -70°C prior to analysis. Homogenate was prepared as 10% detergent homogenate (chapter 2.6.1), or as 5% detergent homogenate (chapter 2.6.2) from 10% sterile inoculum (chapter 2.22.2). One aliquot of detergent homogenate was proteinase-K (PK) treated (chapter 2.7.2). PK-treated and untreated brain was diluted to 1% homogenate in 2x SDS-PAGE loading buffer and 10x sample reducing agent (Invitrogen), electrophoresed and immunoblotted as described (chapter 2.12). PrP was probed using monoclonal antibody 8H4 (chapter 2.2 & (Zanusso et al., 1998)) and visualised using horseradish-peroxidase (HRP) conjugated rabbit α-mouse secondary antibody and POD (peroxidase) substrate (Roche) or West Dura substrate (Pierce) (chapter 2.12.1).

The infected murine models that were chosen as likely candidates for further study in this thesis, were re-examined using the polyclonal antibody, 1B3 (chapter 2.2 & (Langeveld et al., 1993)) and visualised using goat α-rabbit secondary antibody (HRP-conjugated) and POD substrate.

In order to relatively measure PrP^{Sc} levels in the different models investigated, an arbitrary scale of the level of PrP^{Sc} found in PK-treated end-point brain from each model was assigned. Scores ranged from zero to three, three indicating a high level of PrP^{Sc}.

3.2.2. Immunoblot of PrP^{C} in uninfected animals

5% detergent homogenate was prepared as detailed previously (chapter 3.2.1). Uninfected 101PP and 101LL brain homogenate was serially diluted in PBS then diluted in SDS-PAGE loading buffer and sample reducing agent (chapter 3.2.1) for immunoblot. Homogenate was loaded at either $^{1}/_{10}$ to $^{1}/_{320}$, or at $^{1}/_{5}$, $^{1}/_{7.5}$, $^{1}/_{10}$ and $^{1}/_{20}$ of the original 5% homogenate. Recombinant PrP (rPrP) was loaded at 50ng per well (chapter 3.2.4). PrP

was probed using monoclonal antibodies 8H4 or 7A12 (chapter 2.2 & (Zanusso et al., 1998)) then visualised as before (chapter 3.2.1).

3.2.3. GAPDH detection

One blot was stripped after PrP visualisation (25mM Glycine, 1% SDS (pH2), membranes washed 2x 10 minutes then 2x 5 minutes with TBS-tween) and re-probed using α-GAPDH antibody (chapter 2.2) to detect glyceraldehyde 3-phosphate dehydrogenase. GAPDH is a ubiquitious protein thus was used as a control to assess the loading of equivalent amounts of protein from each sample. Visualisation of GAPDH was achieved using secondary antibody and substrate as before (chapter 3.2.1),

3.2.4. Recombinant PrP loading control

In order to quantify PrP^C in each sample and to normalise each immunoblot, recombinant PrP was loaded into one well of each immunoblot. Recominant PrP (gift from Dr I Sylvester, IAH, Compton, UK) was diluted to give 10ng/μl stock concentration (in dH_2O) and was stored at –70°C. Five microlitres of the stock was added to the loading reaction (10μl 2x loading buffer, 2μl 10x reducing agent and 3μl dH_2O to give 20μl total) and 20μl per well was loaded after denaturing.

3.3. Results

3.3.1. PrP^{Sc} levels in different rodent models vary at end-point

PrP^{Sc} levels were assessed from different murine models, expressing different *Prnp* alleles, in order to assess the variability of PK-resistant PrP^{Sc} between models. Using the monoclonal antibody 8H4, a range of PrP^{Sc} levels was found in PK-treated brain homogenate from the murine ME7, 139A, 79V, 22A, 301C and hamster 263K models investigated. Murine TSE agents 79V and 22A were propagated in the VM strain of mice expressing the *Prnp*-b allele, whist the others were propagated in SV mice, which express the *Prnp*-a allele. Although PrP^{Sc} levels were not quantified in absolute amounts, relatively high PrP^{Sc} levels were found in hamster 263K and in murine ME7, 139A and 22A models, and intermediate PrP^{Sc} levels were found in 79V and 301V strains (figure 3.1). The amount of PrP^{Sc} in brain was not found to differ in models expressing *Prnp*-a or *Prnp*-b alleles suggesting that these genetic differences do not affect the accumulation of PrP^{Sc} during disease.

Importantly for these studies 263K or GSS-infected 101LL mice had previously demonstrated low PrP^{Sc} levels in brain (Barron et al., 2001; Manson et al., 1999). 101LL mice contain a gene targeted single point mutation within the *Prnp* gene. This proline to leucine change is present at amino acid residue 101. To minimise mouse *Prnp* background differences, TSE-infected 101LL mice were compared to wild type 129/Ola mice. These mice contain the same *Prnp*-a allele as 101LL mice except they contain the proline amino acid at residue 101.

Not all of the TSE agents previously investigated were available for study in 129/Ola mice. ME7 and 139A-infected SV mice had produced high PrP^{Sc} levels and were found to produce high levels of PrP^{Sc} in 129/Ola mice (figure 3.2A&B). Intermediate PrP^{Sc} levels had been found in 301C-infected *Prnp*-a mice, however this agent was not passaged in 129/Ola mice at the time of investigation. Intermediate PrP^{Sc} levels had also been found in 79V-infected *Prnp*-b mice, however this agent was not available in 129/Ola mice.

Instead, 79A, which has the same drowsy goat origin as 79V (Kimberlin et al., 1989), was available therefore the PrP^{Sc} level in 79A-infected 129/Ola mice was assessed (figure 3.2B).

3.3.2. 129/Ola mice exhibiting high PrP^{Sc} levels

ME7-infected 129/Ola mice were previously shown to have high PrP^{Sc} levels in brain, and developed disease with a mean incubation time of 161 days, around the same incubation time as reported for other ME7-infected *Prnp*-a mice (Manson et al., 1999). When investigated here, ME7-infected 129/Ola mice expressing the 101PP allele (ME7/101PP) were also found to have high PrP^{Sc} levels in brain when detected using monoclonal antibody 8H4 (figure 3.2A). In 139A-infected 129/Ola mice, also detected using 8H4, PrP^{Sc} levels were found to be high in brain (figure 3.2B), corresponding to the high PrP^{Sc} levels found in 139A-infected SV mice (figure 3.1).

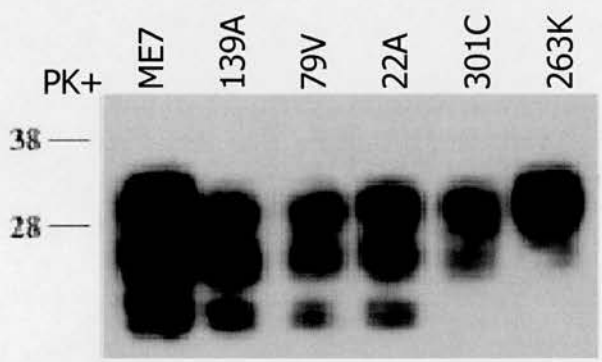

Figure 3.1 PK-resistant PrP^{Sc} levels in end-point brain from various rodent TSE models
Immunoblot of PrP^{Sc} levels found in PK treated (20µg/ml final concentration) end-point brain homogenate from infected models of TSE. PrP^{Sc} levels in PK-treated brain from SV mice (ME7, 139A, 301C), VM mice (22A & 79V) and 263K infected hamster. Brain homogenate loaded as 1% homogenate for electrophoresis and PrP^{Sc} detected using monoclonal antibody 8H4 (chapter 2.2). Visualised using rabbit α-mouse secondary antibody (chapter 2.3) and POD substrate (chapter 2.9). Chemiluminescence was captured on X-ray film after 5 minutes exposure.

The mean disease incubation times of 139A/101PP mice were similar to that of other *Prnp*-a mice, at 147 days (table 3.1 & (Barron et al., 2003)). Brain homogenate from only one animal per model was investigated for PrP^{Sc} level since ME7 and 139A TSE agents have been shown to be stable and to exhibit consistent PrP^{Sc} deposition and pathology over many passages through *Prnp*-a mice (Bruce, 1985a). The infectivity titres of

ME7/101PP and 139A/101PP mice were not known but would be expected to give high titres of infectivity 10^8 – 10^9 ifu (infectious units)/g (Carp & Callahan, 1986; Taylor et al., 2002). If PrP^{Sc} is the infectious agent of TSE, then high PrP^{Sc} levels in these models should equate to high infectivity titres.

3.3.3. 129/Ola mice exhibiting low PrP^{Sc} levels

129/Ola mice expressing the 101LL allele had been reported to contain low PrP^{Sc} levels in brain, when infected with human GSS and hamster 263K inoculum (Barron et al., 2001; Manson et al., 1999). These models have not been well characterised therefore PrP^{Sc} levels in three individual 263K-infected 101LL mice (263K/101LL) were examined using monoclonal antibody 8H4. PrP^{Sc} levels differed in individual animals. In 263K/101LL (1), a distinct band could be detected at around 30kDa (figure 3.2C, lane 2) whereas in 263K/101LL (2) and (3), no PrP^{Sc} could be detected (figure 3.2C lanes 4 and 6). The failure to detect PrP^{Sc} in 263K-infected mice is not a reflection on the ability of the antibody to recognise the TSE agent, since PrP^{Sc} from 263K-infected hamsters was detected using 8H4 (figure 3.2C lane 8).

PrP^{Sc} levels in brain homogenate from two individual GSS-infected 101LL animals (GSS/101LL) were also investigated using 8H4. Both animals were found to contain no detectable PrP^{Sc} however the result from only one animal is shown here (figure 3.2D). This data confirms that little or no detectable PrP^{Sc} is found in GSS/101LL and 263K/101LL mice at disease end-point as previously described (Barron et al., 2001; Manson et al., 1999).

3.3.4. 129/Ola mice exhibiting intermediate PrP^{Sc} levels

79A-infected 129/Ola mice (101PP) were assessed for PrP^{Sc} level and were found to contain less PrP^{Sc} compared to ME7 and 139A-infected 101PP mice (figure 3.2B). The infectivity titre of this model was not known but if PrP^{Sc} is the infectious agent, infectivity titre would be expected to be lower than that

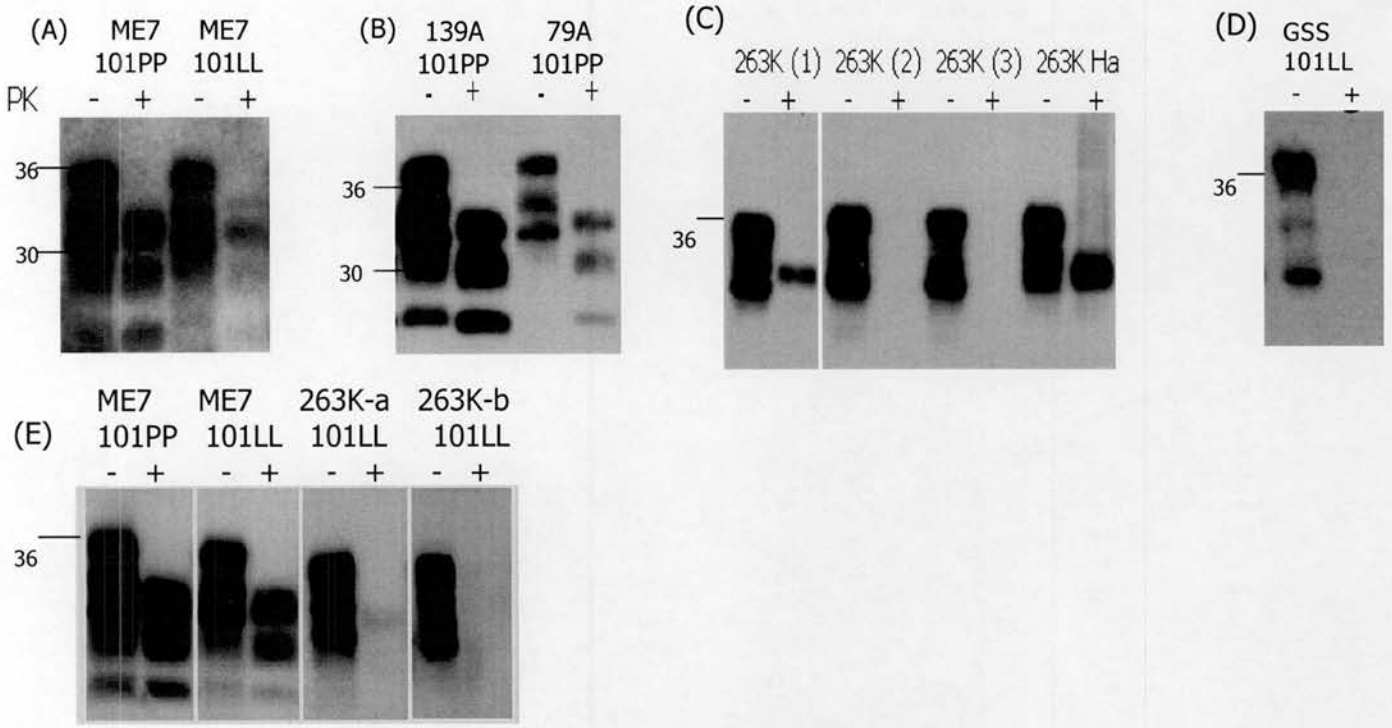

Figure 3.2 PrP^{Sc} levels in 129/Ola mice infected with different strains of TSE agent

Identification of high, intermediate and low PrP^{Sc} levels in PK-treated brain (20µg/ml final concentration) from infected 129/Ola mice. 1% brain homogenate loaded from (A) ME7-infected 101PP and 101LL mice, (B) 139A and 79A-infected 101PP mice, (C) three separate 263K-infected 101LL mice (263K) compared with 263K-infected hamster (Ha), (D) GSS-infected 101LL (courtesy of D King), detected using monoclonal antibody 8H4 (chapter 2.2). (E) verification of PrP^{Sc} levels in ME7-infected 101PP and 101LL mice and two separate 263K-infected 101LL mice, detected with polyclonal antibody 1B3 (chapter 2.2). PK untreated brain in lanes marked '-', PK-treated brain in lanes marked '+'. (A) to (C) & (E) PrP was visualised using HRP-conjugated secondary antibody (goat α-rabbit with 1B3 and rabbit α-mouse with 8H4) and POD substrate (Roche), chemiluminescent signal was detected on X-ray film (Roche) after 3-10 minutes exposure. (D) PrP was visualised using rabbit α-mouse secondary antibody (chapter 2.3) and West Dura substrate (Roche), chemilluminescence was captured using Kodak Imager.

of ME7 in 101PP mice but higher than those of GSS or 263K-infected 101LL mice. ME7-infected 101LL mice (ME7/101LL) had been reported to exhibit less PrP^{Sc} than found in ME7/101PP mice (Manson et al., 1999). Due to the reported stability of the ME7 agent in *Prnp*-a mice (Bruce, 1985a) the amount of PrP^{Sc} was investigated in one ME7-infected 101LL mouse brain using 8H4 monoclonal antibody. An intermediate PrP^{Sc} level was found in this model (figure 3.2A), confirming the previously published data. The titre of infectivity in ME7/101LL mice was not known, however, given that PrP^{Sc} levels were less than found in 101PP mice infectivity titres may be lower in ME7/101LL mice than in 101PP mice, if PrP^{Sc} is the infectious agent.

3.3.5. PrP^{Sc} level may not correlate with infectivity or short incubation time

Infectivity titres in brain taken from hamster 263K, murine ME7 and 139A models are reported to be 10^8 to 10^9 infectious units per gram (ifu/g) (table 3.1) and this appears to correlate to the high levels of PrP^{Sc} detected in these models. However, 301C, 22A and 79V have reported titres of $10^{5.5}$ to 10^6 ifu/g (table 3.1) and although 301C and 79V PrP^{Sc} levels are lower, 22A PrP^{Sc} levels appear to be as high as 139A. Although a detailed quantitative assessment was not performed here, this discrepancy appears contradictory to the hypothesis that high PrP^{Sc} levels correlate with high infectivity titres.

Another feature of TSE disease is that there is an inverse relationship between infectivity titre and disease incubation time (Kimberlin & Walker, 1978; McKinley et al., 1983). By definition if PrP^{Sc} level correlates with infectivity titre, high PrP^{Sc} levels should correlate with short incubation times. Studies here demonstrate that this relationship is generally followed, where models exhibiting highest PrP^{Sc} levels have shortest incubation times. However, 301C and 22A models have similar incubation times yet 301C-infected mice exhibit less PrP^{Sc} than 22A-infected mice (table 3.1, data above line). In the P101L models, the general trend of high PrP^{Sc} levels associating with short incubation times is also followed however there are two exceptions (table 3.1, data below line). 79A-infected 101PP mice exhibit intermediate PrP^{Sc} levels yet have the shortest incubation times of the 129/Ola mice studied here and GSS-infected 101LL mice have a shorter

TSE strain	Mouse genotype	Infectivity (ifu/g)[a]	Incubation time (days)[b]	Arbitrary PrP^{Sc} level[c]
ME7	Prnp-a	10^8	160[$]	+++
139A	Prnp-a	$10^{8.6}$ *	150[$]	+++
301C	Prnp-a	10^6 *	210[$]	++
22A	Prnp-b	$10^{5.5}$ *	200[$]	+++
79V	Prnp-b	$10^{5.5}$ *	280[$]	++
263K	hamster	10^9	65[$]	+++
ME7	Prnp-a^{101PP}	nd	161[§]	+++
139A	Prnp-a^{101PP}	nd	147[¶]	+++
79A	Prnp-a^{101PP}	nd	139[¶]	++
ME7	Prnp-a^{101LL}	nd	338[§]	++
GSS	Prnp-a^{101LL}	nd	288[ʃ]	+/-
263K	Prnp-a^{101LL}	nd	374[ʃ]	+/-

Table 3.1 Western Blot of PrP^{Sc} levels in murine models of TSE

[c] Measured by immunoblot using 8H4 monoclonal antibody (figures 3.1 & 3.2).
[a] Published infectivity titres, ME7 (Taylor, McConnell & Ferguson, 2000); 139A (Carp & Callahan, 1986), 87V and 301V (Taylor et al., 1997), Hamster 263K (Czub, Braig & Diringer, 1988). * Neuropathogenesis unit, unpublished data.
[b] Published incubation times [$] (Bruce, 1985a), [§] (Manson et al., 1999), [¶] (Barron et al., 2003), [ʃ] (Barron et al., 2001)
Note: PrP^{Sc} level and infectivity titres are representative of each model and were not measured from the same brain

disease incubation time than ME7-infected 101LL mice even though the former model exhibits less PrP^{Sc}. Therefore, while shorter incubation times are indicative of high PrP^{Sc} levels and high infectivity titers, data here indicates that the relationship between these parameters does not occur in every TSE model.

3.3.6. PrP^{C} expression in uninfected 101PP and 101LL mice

Different levels of PrP^{C} expression affect disease incubation time and the rate of PrP^{Sc} accumulation during the disease process (Manson et al., 1994b). The possibility therefore arises that lower PrP^{Sc} levels found in infected 101LL mice may be an intrinsic property of these animals if PrP^{C} is not expressed at wild-type levels. Previous investigation of PrP^{C} levels in 101PP and 101LL mice had detected less PrP^{C} in 101LL than in 101PP mice (Manson et al., 1999) therefore PrP^{C} levels in brain of uninfected 101PP and 101LL mice were re-examined. Brain homogenate was serially diluted to assess whether the limit of detection of PrP^{C} was the same from both models. Using the monoclonal antibody, 8H4, equivalent amounts of PrP^{C} were detected in brain homogenate from both lines of mice (figure 3.3A). PrP^{C} from 101LL and 101PP mice was detected at an equivalent limiting dilution of 0.03125% of brain homogenate, or 6.25µg brain equivalent (figure 3.3A). An anti-GAPDH antibody, detecting ubiquitous glyceraldehyde 3-phosphate dehydrogenase, indicated equivalent protein was loaded in each lane (figure 3.3 B). (GAPDH is a multifunctional, house-keeping enzyme involved in DNA repair and replication, mRNA regulation, tRNA export, neuronal apoptosis and in glycolysis and gluconeogenesis. It is constitutively expressed at high levels in most tissues therefore was considered to be a good loading control).

In contrast to the findings of equivalent levels of PrP^{C} in 101PP and 101LL mice it was previously demonstrated, using the 8H4 antibody, that 101LL mice expressed lower PrP^{C} levels than 101PP mice (Manson et al., 1999). Moreover, differences in secondary structure have been seen between recombinant 101LL

and recombinant wild type 101PP protein (Cappai et al., 1999). If the conformation of 101LL and 101PP PrP^C differs *in vivo*, the epitopes recognised by monoclonal antibodies may be differentially exposed in these different proteins. A more detailed study was therefore performed to futher investigate the level of PrP^C expression in 101PP and 101LL mice. PrP^C levels were assessed using two monoclonal antibodies that recognised different epitopes, 8H4 and 7A12 (appendix B & (Li et al., 2000)).

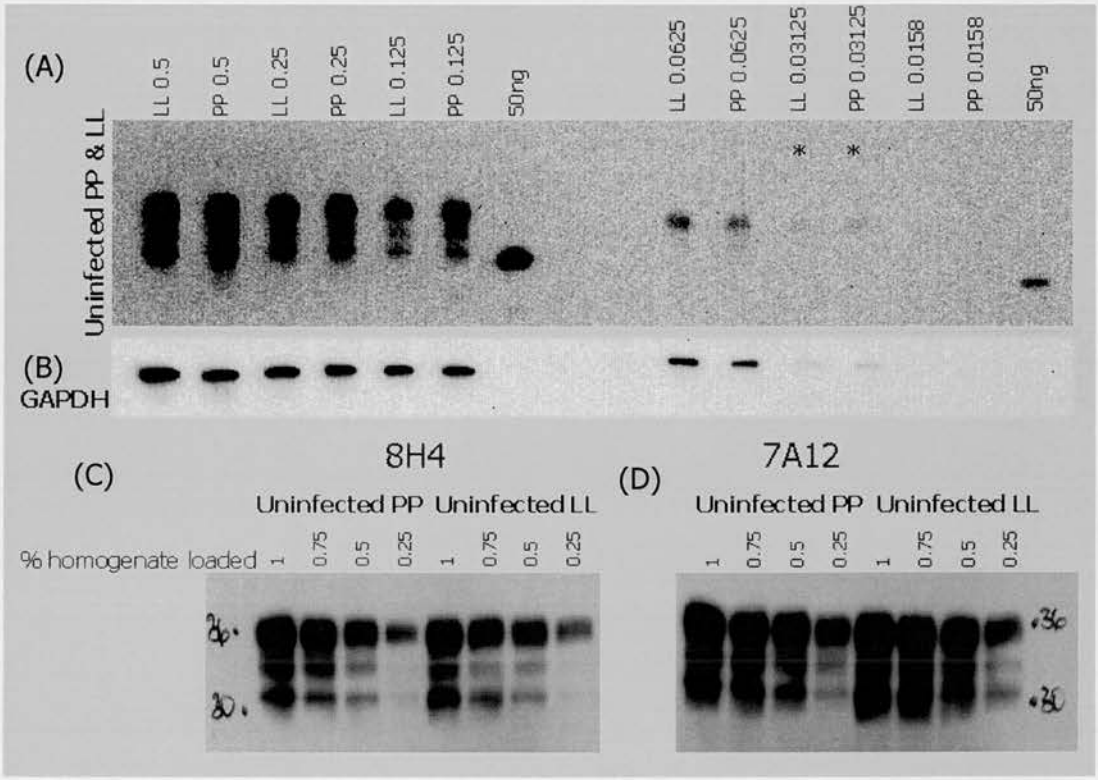

Figure 3.3 PrP^C expression is similar in 101PP and 101LL mice

PrP^C in uninfected 101PP (wild type) and 101LL mice (A) 101LL and 101PP brain homogenate loaded in doubling dilutions from a 5% detergent homogenate starting material, ranging from 0.5% to 0.0158% homogenate loaded per well. Recombinant PrP loaded into each well at a final concentration of 50ng. Probed using 8H4 monoclonal antibody (chapter 2.2). (B) Loading control glyceraldehyde 3-phosphate dehydrogenase (GAPDH) probed using α-GAPDH monoclonal antibody (chapter 2.2). PrP and GAPDH visualised using rabbit α-mouse secondary antibody and West Dura substrate (Pierce). Images were captured using Kodak imager after 15 minute exposure. (C) & (D) 5% detergent homogenate of brain diluted to load at 1% to 0.25% homogenate per well detected using 8H4 (C) and 7A12 (D) monoclonal antibodies (chapter 2.2), Markers are at 36 kDa and 30 kDa. Visualised using rabbit α-mouse secondary antibody and POD substrate (Roche). Image was captured on X-ray film (Roche) after 3 minutes exposure.

At each dilution of brain homogenate, both101LL and 101PP samples had the same affinity to the 8H4 and 7A12 antibodies (figure 3.3 C & D). This indicates that residues 90-145 (recognised by 7A12), which includes the first β-sheet and residues 175-190 (recognises by 8H4), the second α-helix, were equivalently exposed in PrP^C from both models.

(A)

% homog. loaded	Dilution from 10% homog	Intensity of detection 101PP	101LL	ng equivalent 101PP	101LL	ng equivalent in 10% homog 101PP	101LL
0.5	1/20	305850	227654	195	145	3901	2903
0.25	1/40	134803	126094	86	80	3438	3216
0.125	1/80	76623	34877	49	22	3909	1779
0.0625	1/160	65421	104721	42	67	6675	10684
0.0313	1/320	50615	43709	32	28	10328	8919
50ng recombinant PrP		78413	78413	50	50		
Mean						5650	5500
SD						2912	4011
SE						1302	1794

(B)

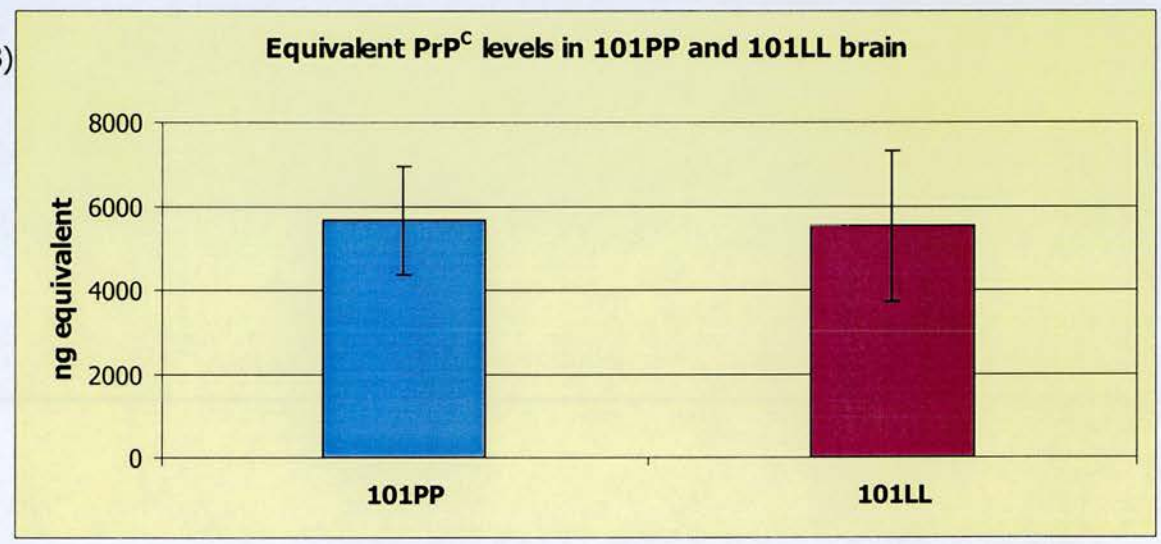

Figure 3.4 Measurement of PrP^C expressed in 101PP and 101LL mice

Densitometric analysis of PrP^C in uninfected 101PP and 101LL brain as represented in figure 3.3A. (A) Intensity of detection of each protein band by Kodak image analysis (chapter 2.10) expressed as number of pixels. At each dilution loaded, the pixel intensity is converted to ng of PrP using a known 50ng recombinant PrP (figure 3.3A lanes 7 & 14). The amount of PrP is calculated for 10% homogenate loaded at each dilution. Each sample loaded will have a margin of error due to dilution or loading errors during the experimental process therefore the mean and standard error for the samples on the immunoblot is calculated. (B) Graphical representation of mean ng PrP in each brain homogenate loaded.

Differences in PrP^{Sc} levels in 101LL-infected animals would therefore not be caused by inefficient disease propagation due to reduced levels of PrP^{C}. No gross differences in PrP^{C} level between 101PP and 101LL mice was seen after visual assessment of the immunoblot (figure 3.3A) and this was confirmed by densitometric analysis of the data (figure 3.4A&B).

3.3.7. Confirmation of PrP^{Sc} levels in murine TSE models

Each model investigated here was placed into a high, intermediate or low PrP^{Sc} category by assigning an arbitrary score ranging from one to three based on 8H4 immunoblotting of PrP^{Sc} levels. Three indicated a high PrP^{Sc} level, two an intermediate PrP^{Sc} level and one indicated low PrP^{Sc} levels. This ranking provided a relative assessment of PrP^{Sc} level in each model and was particularly appropriate for the TSE-infected 129/Ola mice that were considered for further study (table 3.1). 8H4 detection ranked ME7-infected 101PP mice (ME7/101PP) with high PrP^{Sc} levels (+++), ME7-infected 101LL mice (ME7/101LL) with intermediate PrP^{Sc} levels (++) and 101LL mice infected with hamster 263K (263K/101LL) or human GSS (GSS/101LL) inoculum with low, or non-detectable PrP^{Sc} levels (+/-). The prion hypothesis suggests that the PrP^{Sc} associated with each strain of TSE must exist in different conformations (Aguzzi, 1998; Safar, 1996). It is thought that these conformational differences account for the different strain characteristics (disease incubation time, distribution and intensity of TSE-associated pathology and infectivity titre) of each strain of agent. To take into account possible conformational differences of PrP^{Sc} in the particular models investigated here, PrP^{Sc} levels were confirmed in brain homogenate using the polyclonal antibody, 1B3 (appendix B & (Langeveld et al., 1993)). One animal from the high and intermediate models and two animals from the 263K low PrP^{Sc} model were assessed (ME7/101PP, ME7/101LL, 263K/101LL (a) and (b)) and were shown to exhibit the same levels of PrP^{Sc} as seen with 8H4 (figure 3.2E). These are the models chosen for further study and are indicated in the shaded boxes of table 3.1.

3.4. Discussion

Previous studies showed that PrP^{Sc} correlated with infectivity in brain and this correlation appears strongest in models of TSE where PrP^{Sc} is found in abundance (Bolton et al., 1982; Czub, Braig & Diringer, 1986b; De Armond et al., 1989). However, several *in vivo* studies appear to contradict the correlation of PrP^{Sc} and infectivity. These studies describe transmission of TSE disease from brain in the absence of detectable PrP^{Sc} (Barron et al., 2001; Hsiao et al., 1994; Lasmezas et al., 1997; Manson et al., 1999; Telling et al., 1996) (chapter 1.9). Transmission of infectivity from ovine placenta to mice has also been described in the absence of detectable PrP^{Sc} (Onodera et al., 1993). Therefore in order to further study the relationship between infectivity and PrP^{Sc} level, murine TSE models were identified that exhibited different amounts of PrP^{Sc} in brain at the end-point of disease, including the models of low PrP^{Sc} described previously (Barron et al., 2001; Manson et al., 1999).

3.4.1. Relative PrP^{Sc} levels in different TSE models

Different amounts of PrP^{Sc} have been described in different TSE models depending on the strain of agent and mouse strain used. A previous study (Kuczius & Groschup, 1999) reported low PrP^{Sc} levels in a 22A (*Prnp*-b) model and in 263K-infected hamsters, and high PrP^{Sc} levels in ME7 (*Prnp*-a) mice. Intermediate PrP^{Sc} levels were found in 79A (*Prnp*-a), BSE-infected (*Prnp*-a) mice (301C source (Bruce et al., 2002)) and in Chandler-infected *Prnp*-a mice (similar passage history to 139A (Kimberlin et al., 1989; Peretz et al., 2001)). This differed to the studies performed in this chapter, which assigned a different ranking to the models. High PrP^{Sc} levels were found in ME7 and 139A (*Prnp*-a) models as well as in 22A (*Prnp*-b) and hamster 263K models, intermediate PrP^{Sc} levels were found in 79A and ME7/101LL (*Prnp*-a) models, and low PrP^{Sc} levels were found in GSS and 263K-infected 101LL (*Prnp*-a) mice. Kuczius *et al* used C57BL/6 and VM95 mice, which express *Prnp*-a and *Prnp*-b alleles, however these mouse strains have different genetic backgrounds to the

SV and VM mice studied here. The differences in mouse genetic background may explain the discordant results between these two studies. TSE agents RML and 139A are of the same origin but the difference in ranking may indicate that these strains have diverged through different passage histories in the different laboratories. This is probably due to the influence of different mouse genetic background upon the selection of TSE strains (Dickinson & Meikle, 1969). The alternative ranking of the TSE agents between these two studies may also be a reflection of the different antibodies used in each study, polyclonal Ra5/7 and monoclonal 3F4 (Kuczius *et al*) compared with 8H4 monoclonal and 1B3 polyclonal antibodies. These may have differential affinities to the strains of agent used therefore may detect different amounts of PrP^{Sc}.

A comparative level of PrP^{Sc} in brain from different TSE models was required at this stage of these studies to identify potential models with high, low and intermediate PrP^{Sc} levels. The exact quantification of PrP^{Sc} levels in the TSE models chosen for further study is discussed in chapter 6. To minimise the genetic background differences and TSE agent differences, four different murine models were chosen for further study. These comprised of a single TSE agent in two lines of mice (ME7 in 101PP and 101LL mice) and three different TSE agents in a single line of mice (ME7, 263K and GSS in 101LL mice). The ideal situation of three TSE agents in a single line of mice was not available for this study. Ideally, the five different TSE agents, ME7, 139A, 79A, GSS and 263K, initially studied in *Prnp*-a mice would have been investigated, however due to time and space constrains it was not possible to assess the titre of infectivity in all of these models.

It may have been difficult to tell whether differences in infectivity titre or a lack of correlation with PrP^{Sc} in the chosen high and low models was due to the effect of strain of TSE agent or the effect of genetic background. The ME7/101LL model therefore provided a link between the different lines of mice,

101PP and 101LL, and additionally exhibited intermediate PrP^{Sc} levels when compared to the high and low PrP^{Sc} models.

3.4.2. Effect of different genetic background on disease

Different genetic background is a major factor affecting TSE disease (Lloyd et al., 2001; Manolakou et al., 2001). Even in mice with the same *Prnp* genotype, the titre of infectivity and pathological characteristics of a strain of agent can differ (Bruce & Dickinson, 1985; Carp & Callahan, 1986), therefore it was important that the genetic background of the models to be compared was kept as consistent as possible. By studying the ME7 strain of agent in 101PP and 101LL models, the effect of a single amino acid change in 129/Ola mice was assessed the upon titre of infectivity and the targeting of pathology. Due to the gene targeting method employed to introduce the leucine amino acid into endogenous murine PrP, the specific effect of this amino acid change can be directly compared in ME7-infected 101PP and 101LL models. This amino acid change has already been shown to affect disease incubation times (Barron et al., 2001), and disease pathology may differ intrinsically in 101LL mice causing lower PrP^{Sc} levels to develop in infected 101LL mice.

Different levels of PrP^{C} expression in 101PP and 101LL mice may also explain why different PrP^{Sc} levels are found in infected 101PP and 101LL mice at disease end-point. Due to the gene targeting method used to alter endogenous murine PrP, the mutant PrP gene remains under the control of endogenous murine promoter therefore the PrP^{C} levels in each model should be the same. Densitometric analysis of brain homogenate from uninfected 101PP and 101LL mice found that there was no difference in PrP^{C} level in this study. These results differ from those described previously where PrP^{C} levels in 101LL appeared lower than in 101PP (Manson et al., 1999). Manson *et al* used the same 8H4 monoclonal antibody as used here, therefore the different results are not due to the use of different antibodies. Manson *et al* used a polyclonal antibody (1A8) to confirm their findings and suggested that differential antibody affinity may be responsible for the difference in PrP^{C} detection

between the mice. However a second monoclonal antibody (7A12) used in this study did not identify any differences between 101PP and 101LL antibody affinity and confirmed the 8H4 result found here. There were differences in the preparation and loading of brain homogenate for immunoblot, which may account for the differences seen between the results here and those of Manson *et al.* Unlike the experiments here, Manson *et al* did not demonstrate equivalent protein loading on their blots. If the expression of PrP^{C} is equivalent in 101PP and 101LL mice, the reported differences in PrP^{Sc} levels between each line of mice could be due to differences in the stability of PrP^{C} in 101LL and 101PP mice, or differences in cellular trafficking of PrP^{C} in each line of mice.

The models chosen here for further study were designated, ME7/101PP (high PrP^{Sc}), ME7/101LL (intermediate PrP^{Sc}), 263K/101LL and GSS/101LL (low PrP^{Sc}). Further discussion in this thesis includes the measurements of titre of infectivity and PrP^{Sc} levels in the murine models and the correlation of these parameters. The number of PrP^{Sc} molecules per infectious unit for each particular model has been addressed and will be discussed in relation to the correlation of PrP^{Sc} level and infectivity. The possibility that the models contain alternative forms of infectious PrP, other than PrP^{Sc}, was also investigated.

4. Primary pathological characteristics of high, intermediate and low PrP^{Sc} models

4.1 Introduction

The degree of disease-associated pathology in murine models differs according to the strain of the TSE agent and the animal host infected (Bruce, McBride & Farquhar, 1989) (chapter 1.7). Different models display specific brain pathology that differ in degree and targeting of neuronal loss, targeting and severity of vacuolation and in type, targeting and severity of PrP deposition (Bruce et al., 2002; Bruce & Fraser, 1981; Fraser et al., 1989; Jeffrey et al., 1997; McBride et al., 2001). The specific targeting of the different pathologies can be investigated at disease end-point (Bruce et al., 1994; Wells & McGill, 1992). Moreover, by culling animals at specific time-points throughout an experiment the targeting and progression of pathology during disease can be investigated, providing an insight into the spread of pathology during TSE disease and how the different pathological events may be linked (Beekes, McBride & Baldauf, 1998; Jeffrey et al., 2001). The use of rodent models has allowed a better understanding of the nature and sequence of pathology during disease, however, it is still not clear what pathological event(s) actually kill the TSE-infected host.

It has been suggested that PrP^{Sc} is the infectious agent of TSE (Prusiner, 1982), however it is not clear whether the PrP^{Sc} protein is the cause of the vacuolation, neuronal loss and astrocytic pathologies associated with TSE. PrP deposition has been found in association with neuronal loss, and vacuolar change, and has been found to precede these pathologies (Jeffrey et al., 2000; Jeffrey et al., 2001). Astrocytic gliosis has been correlated with diffuse PrP deposition in 263K-infected hamsters (DeArmond et al., 1987) therefore strongly linking brain damage to the accumulation of PrP. In ME7-infected SV mice (*Prnp*-a genotype), gross neuronal loss can be detected under light microscopy (Scott & Fraser, 1984). Examination of the hippocampus, reveals a 50% loss of the hippocampal CA1 pyramidal cell

layer as well a shrunken hippocampus in comparison to that of uninfected animals (Jeffrey et al., 2001; Scott & Fraser, 1984). Neuronal loss was found to correlate with PrP deposition and with vacuolation in the ME7 model (Jeffrey et al., 2000).

The correlation of PrP deposition with areas of vacuolation has been described in the thalamus and hippocampus of 263K-infected hamsters at disease end-point (DeArmond et al., 1987), and in the CA2 region of the hippocampus and the ventral thalamic nucleus of 87V-infected mice (Bruce et al., 1989). Post-mortem analysis of BSE-affected cattle also indicated a correlation between vacuolation and PrP deposition (detected as scrapie-associated fibrils) (Wells et al., 1994), and in sCJD brain, areas of PrP deposition are found to correlate with vacuolation only in areas where large amounts of gross pathology was observed (Armstrong, Lantos & Cairns, 2001). At disease end-point, areas of PrP deposition and vacuolation correlated, however, PrP deposition was found to precede vacuolation at early stages of disease (Bruce, 1981). This may suggest that areas of PrP deposition determine areas of vacuolation. Taken together, these experiments provide evidence arguing that the presence of PrP^{Sc} can determine whether vacuolar pathology, neuronal loss and gliosis occurs in infected animals.

However, contradictory to the above studies, one study of human sCJD brain demonstrated that neuronal loss did not correlate with PrP deposition (Armstrong et al., 2001). This suggests that deposition of PrP may not be the cause of neuronal degeneration. Moreover, the correlation between PrP deposition and vacuolation is not always as consistent as described above. Some natural scrapie, BSE and experimental transmissible mink encephalopathy (TME) cases have been described where vacuolation is not abundant at disease end-point yet PrP deposition is detected either by immunoblot or immunostaining (Wells & McGill, 1992). This has also been seen in human FFI cases associated with the D178N/129M mutation (Monari et al., 1994). Conversely, vacuolation but not PrP^{Sc} deposition has been reported in one human GSS case and in transgenic animals subsequently infected with brain from this case (Telling et al., 1995). This

has also been observed in goats challenged with natural scrapie (Foster et al., 2001a). Extensive vacuolation, yet sparse PrP deposition was also seen in the P101L transgenic model after infection with human GSS (Manson et al., 1999) and hamster 263K (Barron et al., 2001). It is therefore not clear whether the disease-associated accumulation of PrP seen in some models is the true cause of other TSE-associated pathologies such as vacuolation.

The studies detailed in this chapter aimed to investigate whether there was a correlation between PrP^{Sc} deposition and vacuolar pathology in the GSS/101LL and 263K/101LL models that displayed low levels of PrP^{Sc} in the brain. The lack of PK-resistant PrP^{Sc} detected by immunoblot (chapter 3) would suggest that disease-associated PrP is not heavily deposited in the brains of GSS/101LL and 263K/101LL mice thus a high degree of vacuolation would not be expected in these mice. However, previous data indicated that brain from 263K/101LL mice is highly vacuolated, despite the lack of PK-resistant PrP^{Sc} (Barron et al., 2001). This appears to contradict the suggestion that PrP^{Sc} is the cause of TSE-associated vacuolar pathology. Furthermore, it has been shown that the majority of disease-associated PrP is PK-resistant PrP^{Sc} (McBride et al., 2001), thus immunoblot levels of PrP^{Sc} for each model should reflect the amount of disease-associated PrP detected by immunostaining. Thus, the studies performed here also aimed to investigate the amount of disease-associated PrP detected by immunostaining and immunoblot in models exhibiting high, low and intermediate levels of PrP^{Sc}. For each model (ME7/101PP, ME7/101LL, GSS/101LL and 263K/101LL), disease-associated PrP deposition was examined in brain from representative animals, using immunohistochemistry, and the specific targeting of PrP deposition was identified. The targeting and intensity of vacuolation was also identified in each model. If PK-resistant PrP^{Sc} was the cause of vacuolar pathology, the models exhibiting low levels of should not exhibit a high degree of vacuolation.

4.2 Methodology

4.2.1 Brain tissue examined

129/Ola mice chosen for study are fully described in chapter 3. Whole brain was excised from terminally ill, clinically positive ME7-infected 101PP mice and from ME7, 263K and GSS-infected 101LL mice. Tissue was fixed and 6μm sections cut as described in chapter 2.19.

4.2.2 PrP deposition

4.2.2.1 Identification of disease-associated PrP

Mouse brain sections (6μm) were immunostained using either polyclonal antibody 1B3 and biotinylated secondary donkey or goat α-rabbit antibody or immunostained with monoclonal antibodies 6H4 or 8H4 and biotinylated secondary rabbit α-mouse antibody (chapters 2.2 & 2.3). Hamster brain sections were also immunostained, using monoclonal antibody 3F4 and visualised using biotinylated rabbit α-mouse secondary antibody. Antibody epitopes are described in appendix B. Diaminobenzine (DAB) substrate was used for final visualisation in all cases (chapter 2.21). Sections were examined under light microscopy for PrP deposition seen as a brown stain against a blue counterstain for neuronal cell bodies.

4.2.2.2 Scoring PrP deposition

In order to compare the targeting of disease-associated PrP deposition between models, seven different grey matter areas were scored for severity of PrP deposition. Hippocampus, thalamus, hypothalamus, raphe of midbrain, vestibular nuclei, cortex and cerebellum were chosen here because they represented areas of high and low vacuolation therefore deposition and vacuolation could also be correlated in these areas. The amount of PrP deposited was scored on a scale of one to four for each animal examined, four indicating most deposition. The mean score for each brain area was indicated alongside the vacuolation profile, by a star.

4.2.3 Vacoulation

Brain sections were haematoxylin and eosin stained (chapter 2.20) to visualise vacuoles. Sections were examined under light microscopy at x10 magnification. Vacuolation was scored according to the methodology of Fraser (Fraser & Dickinson, 1968). Briefly, nine specific grey matter areas throughout the cerebellum, midbrain and forebrain (detailed in figure 4.1)

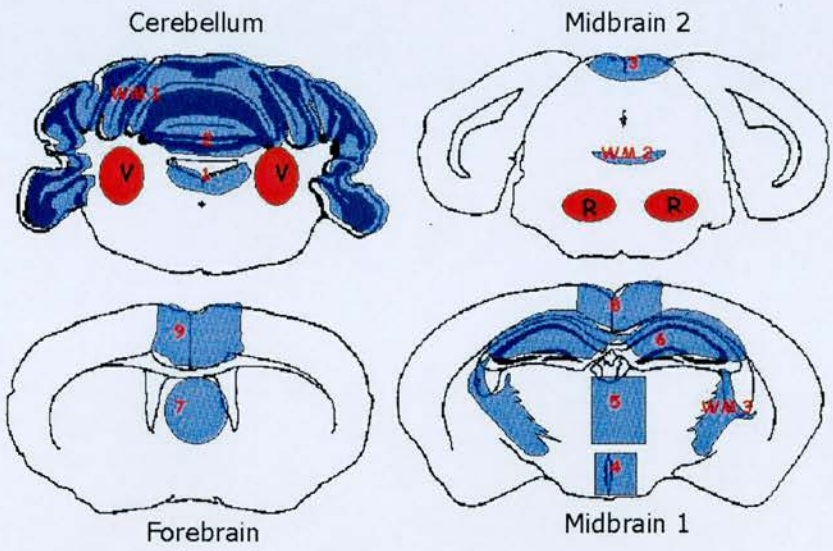

Score	Grey matter criteria
1	A few vacuoles unevenly scattered
2	A few vacuoles evenly scattered
3	Moderate vacuoles evenly scattered
4	Many vacuoles with some confluence
5	Dense vacuolation, confluent
	White matter criteria
1	Moderate vacuoles unevenly scattered
2	Moderate vacuoles evenly scattered
3	Dense vacuolation, confluent

Figure 4.1 Brain areas scored for vacuolation and vacuolation scoring regime
Nine grey matter areas scored for vacuolation, 1-Medulla of cerebellum, 2-forth ventricle of cerebellum, 3-superior colliculus, 4-hypothalamus, 5-thalamus, 6-hippocampus, 7-paraterminal body, 8-cingulate cortex, 9-anterior cingulate cortex and three white matter areas; 1*-cerebellum, 2*-tegmentum, 3*-pyramidal tract are scored. V-vestibular nuclei. R-raphe.

were scored on a scale from one to five according to the severity of vacuolation, five being the most severe and zero or one indicating normal or non-TSE vacuolation (figure 4.1). Three white matter areas in the

cerebellum and midbrain were also scored (figure 4.1). White matter is naturally more vacuolated than grey matter therefore is scored slightly differently, on a scale from one to three with three indicating most severe vacuolation and one indicating normal vacuolation (figure 4.1). For statistical significance, at least six animals per group were scored. The mean score of each group was plotted and the groups compared.

Brain tissue was removed and fixed by personnel within the animal facility at the Neuropathogenesis Unit including V Thomson, E Murdoch and S Dunlop. Further processing, wax embedding and cutting of brain sections were carried out by S Mack and A Suttie. Vacuolation was assessed and scored by experienced personnel, A Boyle and W-G Lui.

4.3 Results

4.3.1 Primary pattern of vacuolation in all models

Vacuolation is a hallmark of TSE and a vacuolation profile is unique and reproducible for each strain of TSE agent (chapter 1.7). It is thought that the presence of PrP^{Sc} causes vacuolation thus the correlation between these two parameters was investigated. The targeting and intensity of vacuolation was therefore investigated in each of the models chosen for further study in this thesis. Vacuolation profiles were plotted for each model according to the protocol of Fraser and Dickinson, 1968.

In all the models studied here, ME7/101PP exhibited the most severe vacuolation. Vacuolation was most severe in grey matter areas, particularly the thalamus (figure 4.2 A to C). The vacuolation profile for the ME7/101PP model was the same as that previously seen in other strains of mice infected with ME7 (Bruce, 1985a; Bruce et al., 2002). ME7/101LL vacuolation (figure 4.2D to F) was less intense than in ME7/101PP (figure 4.2 A to C and figure 4.3) with most vacuolation seen in the hypothalamus rather than the thalamus. This indicated that the targeting of ME7 vacuolation in 101LL mice was different to that found in 101PP mice. In white matter, vacuolar targeting in ME7/101PP and ME7/101LL brain was similar but 101LL mice exhibited lower amounts of vacuolation (figure 4.3).

Despite the lack of detectable PrP^{Sc}, GSS/101LL and 263K/101LL models display the vacuolar pathology associated with TSE (figure 4.2 G to L). In grey and white matter brain areas 263K/101LL and GSS/101LL mice had similar intensity and targeting of vacuolation except at the superior colliculus and hippocampus, where vacuolation was most severe in GSS/101LL mice (figure 4.3). The intensity of vacuolation was similar in ME7/101LL, 263K/101LL and GSS/101LL models in grey matter, however in white matter vacuolation was more intense in the 263K/101LL and GSS/101LL models in comparison to the ME7/101LL model (figure 4.3). The severity of vacuolation in brain from each model could therefore be ranked ME7/101PP > GSS/101LL > ME7/101LL ≥ 263K/101LL.

In addition, each vacuolation profile was unique to the model studied indicating that each model contained a different strain of TSE agent (chapter 1.7).

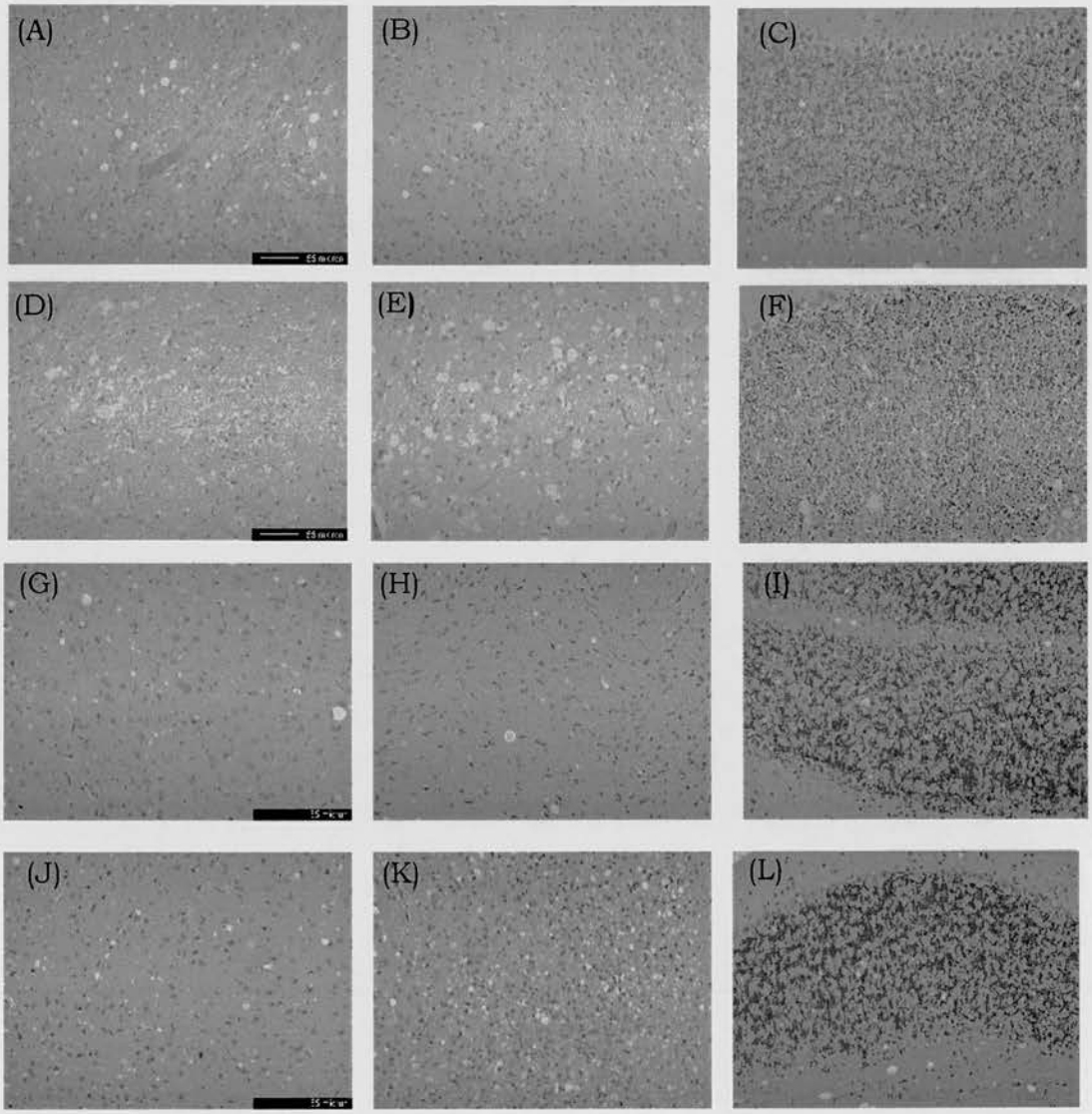

Figure 4.2 Vacuolation in TSE models

Vacuolation in brain from representative animals of each TSE model (A) to (C) ME7/101PP, (D) to (F) ME7/101LL, (G) to (I) 263K/101LL, (J) to (L) GSS/101LL. Haemotoxylin and eosin (H&E) stained coronal brain sections of 5-thalamus (left column), 6-hypothalamus (middle column), 2-granular layer of cerebellum (right column) (see figure 4.1 for brain area location). x20 magnification, bar represents 55µm.

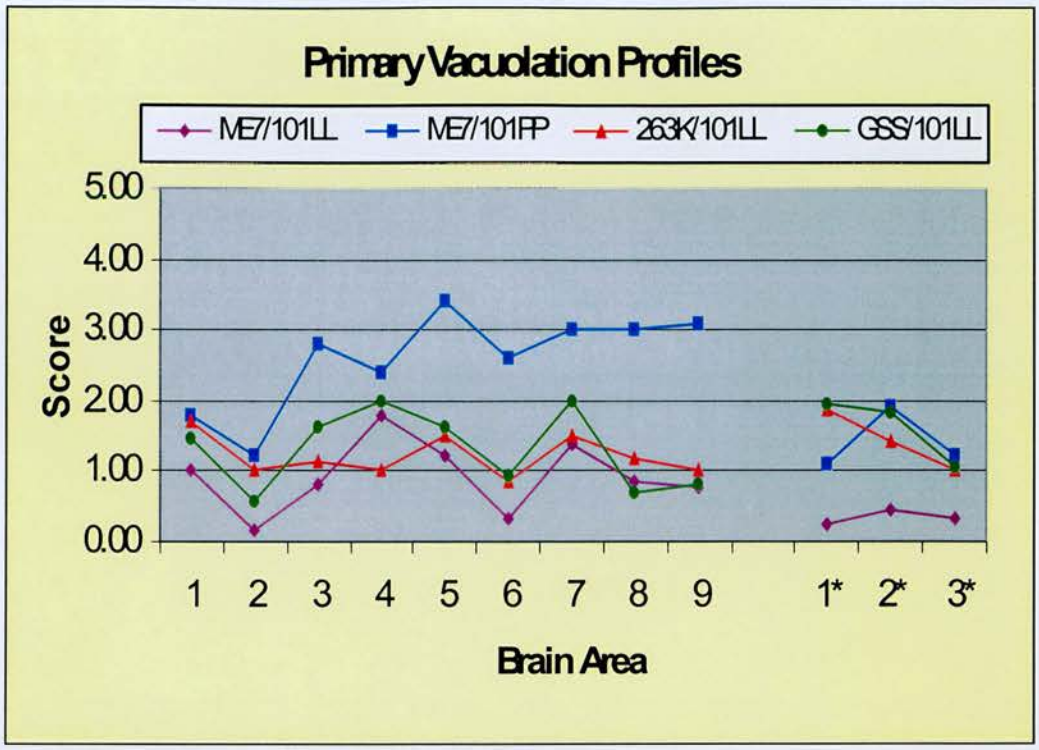

Figure 4.3 Primary vacuolation profiles

Vacuolation profile for each model. (A) Profiles consist of the mean scores of at least 6 individual animals per group. Nine grey matter areas scored for vacuolation, 1-Medulla of cerebellum, 2-forth ventricle of cerebellum, 3-superior colliculus, 4-hypothalamus, 5-thalamus, 6-hippocampus, 7-paraterminal body, 8-cingulate cortex, 9-anterior cingulate cortex and three white matter areas; 1*-cerebellum, 2*-tegmentum, 3*-pyramidal tract were scored.

4.3.2 PrP deposition pattern in ME7-infected mice

To investigate the relationship between disease-associated PrP deposition and vacuolation the intensity and pattern of PrP deposition was investigated in each model. The immunohistochemical technique used to detect the deposition of disease-associated PrP detects partially denatured PrP, which may retain some conformation. Different conformations of PrP may not be detected using a single monoclonal antibody therefore brain sections from representative animals were probed for PrP deposition using two monoclonal antibodies, 8H4 and 6H4, and the polyclonal antibody 1B3.

When ME7/101PP and ME7/101LL brain sections were stained using monoclonal antibodies 8H4 and 6H4 the tissue was found to be extremely fragile and difficult to retain on the slide. Cortex, thalamus, midbrain and

medulla of the hindbrain were often the only areas remaining after staining. Where tissue was retained on the slides staining was observed in thalamus (figure 4.4G to J), however this lacked the diffuse staining usually seen with ME7-infected brain (Bruce et al., 1994). This suggested that the immunostaining technique was not optimal.

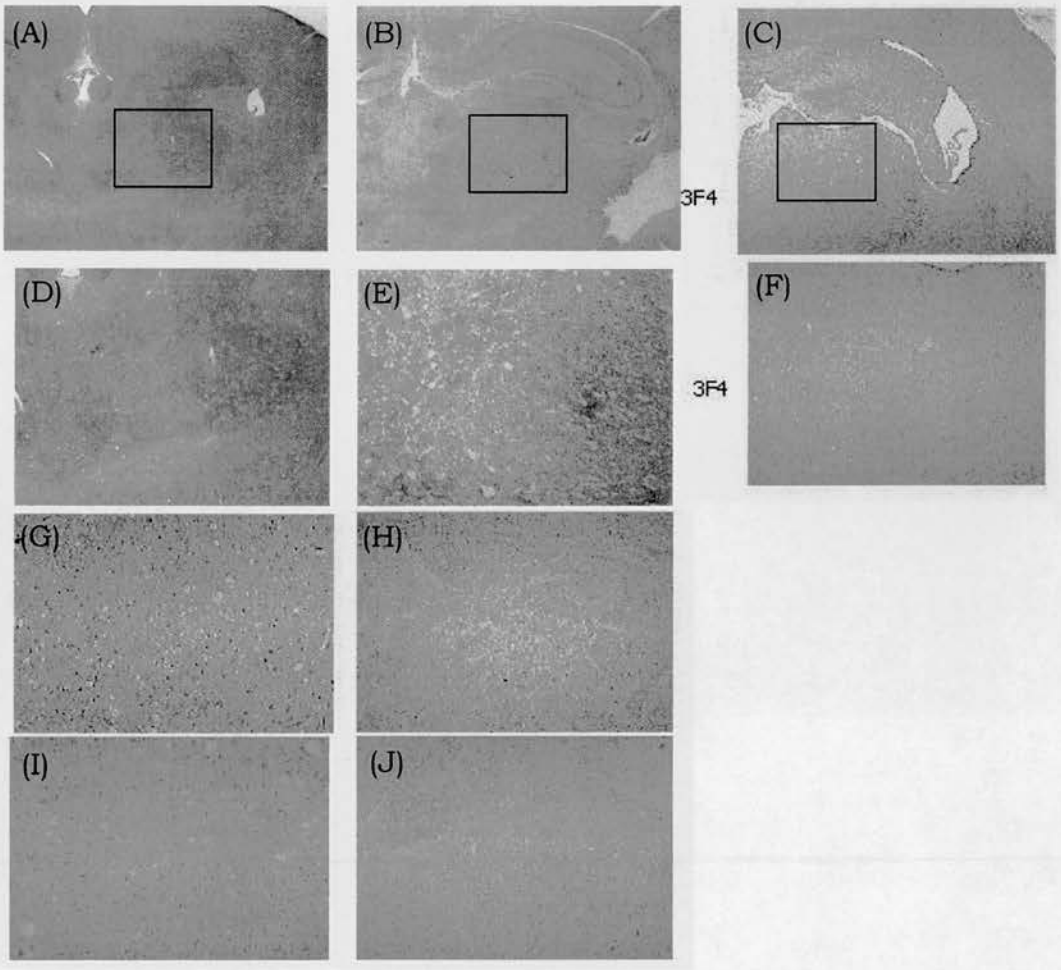

Figure 4.4 PrP deposition in ME7/101PP, ME7/101LL and hamster 263K models

Immunostaining of disease-associated PrP in TSE-infected mouse and hamster brain. Paraffin-embedded tissue cut at the hippocampal/thalamic level (figure 4.1 – midbrain 1). (A), (D), (G) & (I) ME7-infected 101PP; (B), (E), (H) & (J) ME7-infected 101LL mice detected using polyclonal antibody 1A8 (A), (B), (D) & (E), and monoclonal antibodies 8H4 (G) & (H) and 6H4 (I) & (J). (C) & (F) 263K-infected hamster brain detected with monoclonal antibody 3F4. (A) to (C) hippocampus/thalamus x 40 magnification; (D) thalamus x20 magnification; (E) to (J) thalamus x 100 magnification.

Due to the difficulty in retaining ME7/101PP and ME7/101LL tissue sections on slides during staining and due to the scarcity of 1B3 these tissues were not stained using 1B3.

ME7-infected brain had previously been stained using polyclonal antibody 1A8 (Manson et al., 1999). A retrospective investigation of these stained tissues showed the typical ME7 pattern of widespread, diffuse staining throughout ME7/101PP and ME7/101LL brain, as previously described (figure 4.4A, B, D & E). Plaque-like PrP depositions were previously described in the corpus callosum of ME7/101LL after 1A8 staining (Manson et al., 1999) and these were evident after 6H4 and 8H4 detection (data not shown). This suggested that 6H4, 8H4 and 1A8 antibodies were similarly detecting PrP in ME7/101PP and ME7/101LL models. Furthermore, 6H4, 8H4 and 1A8 staining of brain indicated that high levels of PrP were deposited in ME7/101PP brain and intermediate levels of PrP were deposited in ME7/101LL brain. Moreover, higher levels of PrP deposition in ME7/101PP mouse brain compared to ME7/101LL brain mirrored the detection by immunoblot of higher PrP^{Sc} levels in ME7/101PP than in ME7/101LL brain homogenate.

4.3.3 Primary pattern of PrP deposition in 263K-infected mice

263K/101LL deposition was examined using monoclonal antibodies 8H4 and 6H4 and polyclonal antibody 1B3, in seven separate animals. The amount of PrP deposition was less than found in ME7-infected brain and varied between individual animals, ranging from easily visible to undetectable at high magnification (figure 4.5A, E & I). PrP deposition in three animals was easily detected at x10 magnification, but in four animals PrP was only visible at x40 magnification. Where PrP deposition was present there was no difference in the distribution, type or intensity of PrP deposition detected by the 1B3, 8H4 and 6H4 antibodies (compare figure 4.5 B to D with F to H & J to L). Where PrP accumulated in 263K/101LL brain, a punctate deposition was visible (figure 4.5 A to D) similar to that previously described for 263K-infected hamsters (figure 4.4 C & F). Punctate PrP was most intense in the thalamic nuclei, hypothalamus, cortex, raphe of the midbrain and medulla of the hindbrain, as well as in the vestibular nuclei of the hindbrain (figure 4.6 A to E). However, in some 263K/101LL animals, PrP deposition was not immediately evident therefore stained tissue was investigated at high magnification. Extremely low levels

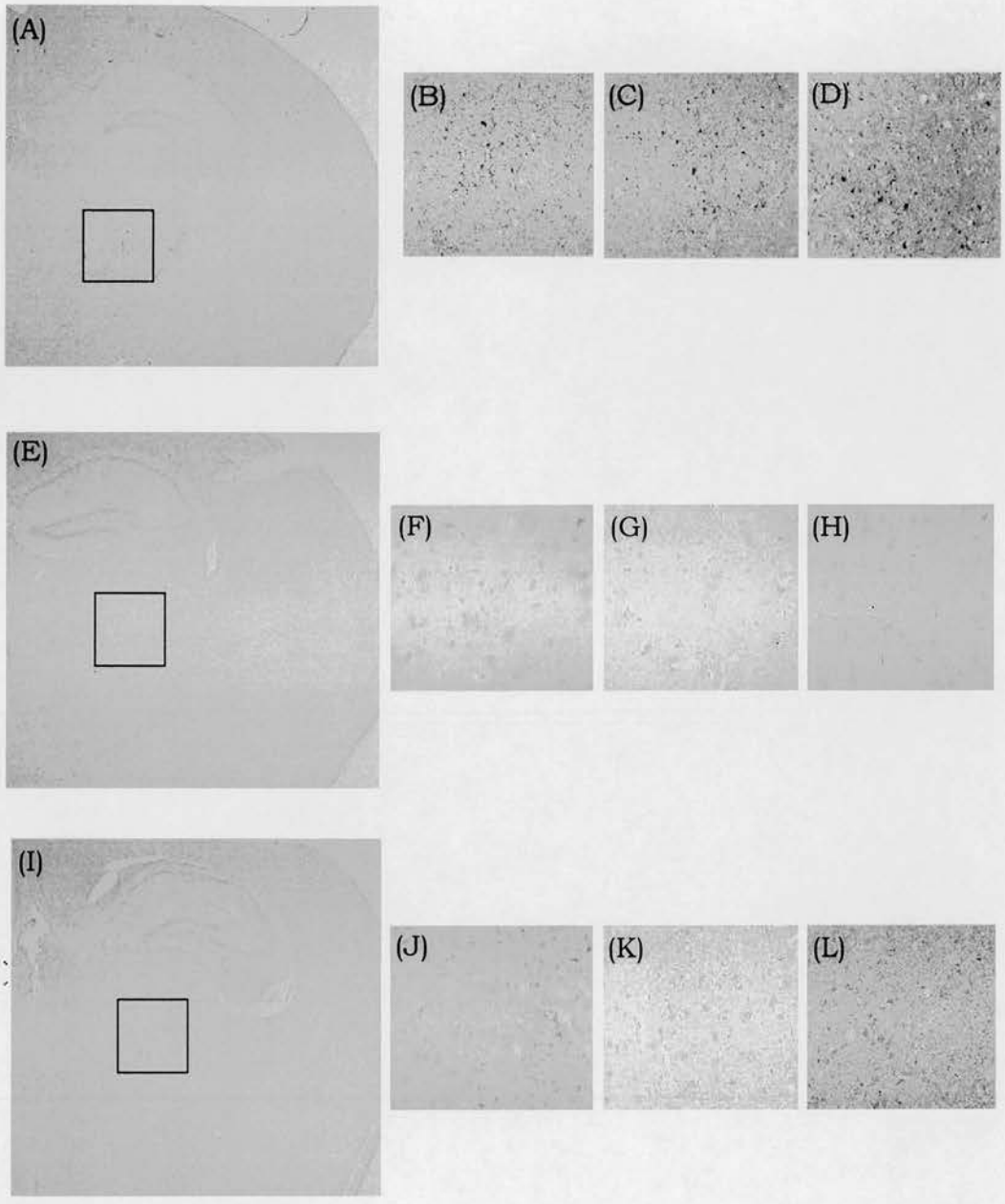

Figure 4.5 PrP deposition in 263K/101LL model

Immunostaining of three individual 263K infected 101LL brains cut at hippocampus/thalamus level (figure 4.1). (A) to (D) 263K /101LL – brain 1; (E) to (H) 263K /101LL brain 2; (I) to (L) 263K /101LL brain 3. (A), (B), (E), (F), (I) & (J) stained with monoclonal antibody 8H4; (C), (G) & (K) stained using monoclonal antibody 6H4; (D), (H) & (L) stained with polyclonal antibody 1B3. All antibodies used at 1/1000 concentration. (A), (E), & (I) Hippocampus and thalamus x40 magnification; (B) to (D), (F) to (H) & (J) to (L) thalamus x200 magnification.

of PrP deposition were seen in the thalamus, raphe and vestibular nuclei of three animals (figure 4.6 F to H), however another four animals exhibited no PrP deposition (figure 4.6 I to L). In brain areas where PrP levels were highest, staining appeared to associate with microglia and with astrocytes. PrP staining was also seen around blood vessels but was probably associated with astrocytes surrounding the vessels.

The deposition of 263K in 101LL mice was reminiscent of that seen in hamsters, except that the golden, diffuse staining seen in 263K-infected hamsters was not present. 3F4 detection of 263K in hamsters (6H4, 8H4 and 1B3 antibodies are mouse-derived and do not recognise hamster 263K. Monoclonal antibody 3F4 recognises the M108/M111 epitope in hamsters (Kanyo et al., 1999; Kascsak et al., 1987) revealed a golden brown, diffuse deposition throughout the brain, particularly in thalamus, hypothalamus (figure 4.4C & F), raphe of the midbrain and medulla of the hindbrain. PrP deposition was visible in association with microglia and astrocytes as well as neurons, as was characteristic of 263K-infected hamsters (Beekes et al., 1998)(P. McBride, personal communication). Diffuse staining is a characteristic of 263K-infected hamsters, however the lack of this staining in 263K/101LL brain may not be characteristic of the 263K/101LL model. The variability of PrP deposition identified using immunocytochemistry mirrored the variability of PrP^{Sc} detection by immunoblot. Moreover, PrP deposition levels were lower in 263K/101LL mouse brain compared to ME7-infected mouse brain, correlating with lower levels of PrP^{Sc} detected in 263K/101LL brain homogenate detected by immunoblot.

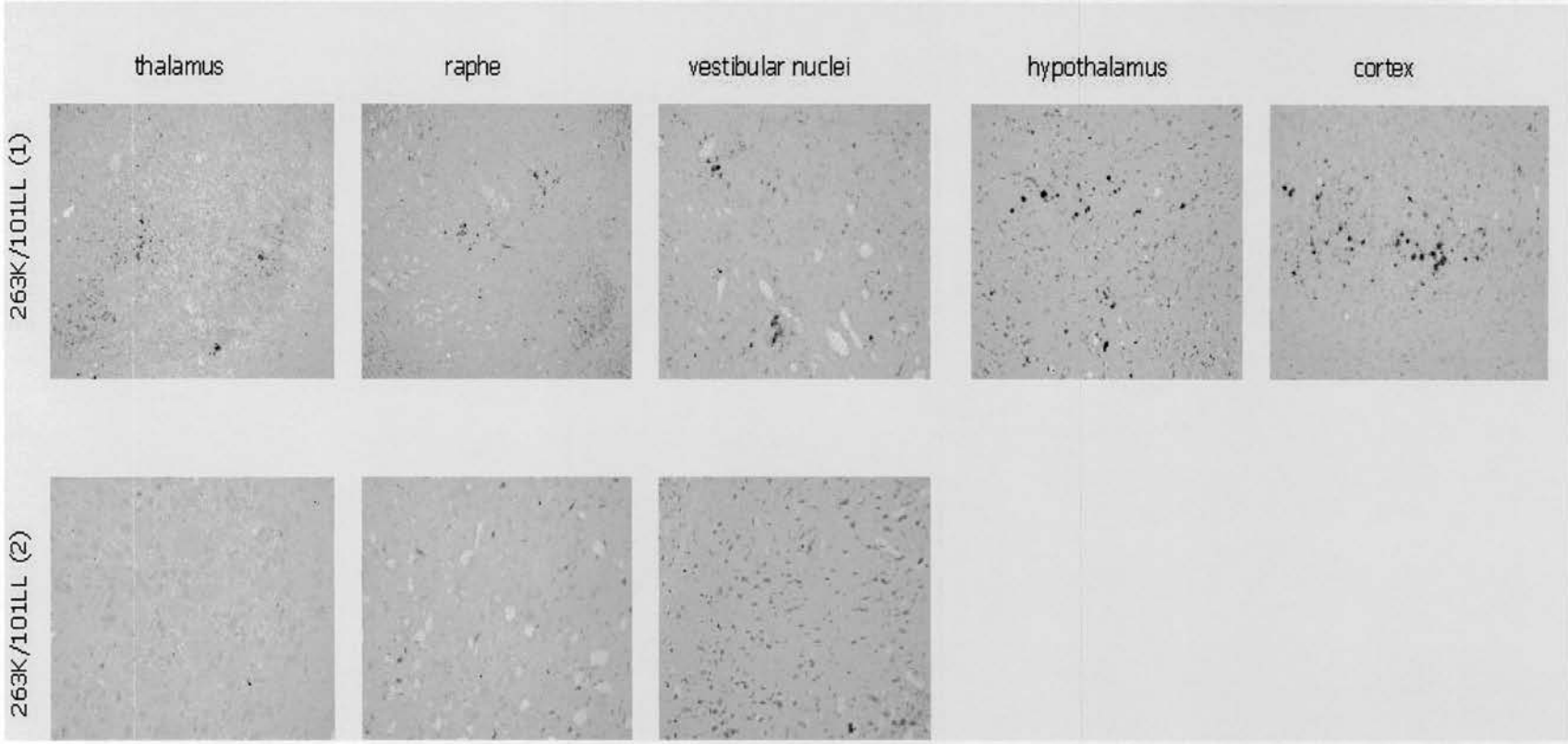

Figure 4.6 Relative PrP deposition in two individual 263K/101LL mice

Immunostaining of two representative 263K/101LL brains in which PrP deposition is seen at different intensities when stained using 6H4 antibody. (A) to (E) 263K/101LL brain 1 has distinct PrP deposition throughout the brain and vacuolation appears to correlate with areas of PrP deposition; (F) to (H) 263K/101LL brain 2 in which PrP deposition is not seen even in thalamus (F), where PrP deposition levels are highest in this model. Vacuolation but not deposition was present in this animal. All sections at x 200 magnification.

4.3.4 Primary pattern of PrP deposition in GSS -infected mice

GSS/101LL brains from six individual TSE-affected animals were stained using polyclonal 1B3 and monoclonal 6H4 antibodies. For each brain investigated, the type, distribution and intensity of deposition was similar for both antibodies. PrP staining was less severe in GSS/101LL mice (figure 4.6) than in the ME7-infected models described previously (figure 4.4). PrP in GSS/101LL mice was found in a punctate deposition (figure 4.7A & B), similar to that found in 263K/101LL brain. As with 263K/101LL brain, PrP staining in GSS/101LL brain was variable, four animals exhibited visible PrP and two appeared to have no PrP. Similar to the 263K/101LL model, staining in GSS/101LL tissues was most intense in the thalamic nuclei, the hypoythalamus, raphe of the midbrain and vestibular nuclei of the hindbrain. PrP deposition in these areas was punctate but unlike that of 263K/101LL, did not appear to be associated with microglia or astrocytes. In the two animals where PrP deposition was not readily visible, small PrP deposits were sometimes visible in the thalamus, raphe and vestibular nuclei when viewed under x400 magnification (figure 4.7D). Similar to the 263K/101LL model, positive control sections were stained as expected, thus diffuse staining may not be characteristic of the GSS/101LL model.

Low/non detectable levels of PrP deposition were seen in GSS/101LL brain sections using the immunohistochemial technique described here. This compared to low PrP^{Sc} levels seen in GSS/101LL brain homogenates detected by immunoblot, thus it appeared that the disease-associated PrP deposited in this model could be PK-resistant PrP^{Sc}.

4.3.5 Comparative PrP deposition between models

To compare the relative amounts of disease-associated PrP deposited in each murine model with the amount of PrP^{Sc} detected by immunoblot a preliminary comparison of PrP deposition was performed across all models. PrP deposition was assessed in seven different grey matter areas of the brain, corresponding to five areas where PrP was known to accumulate

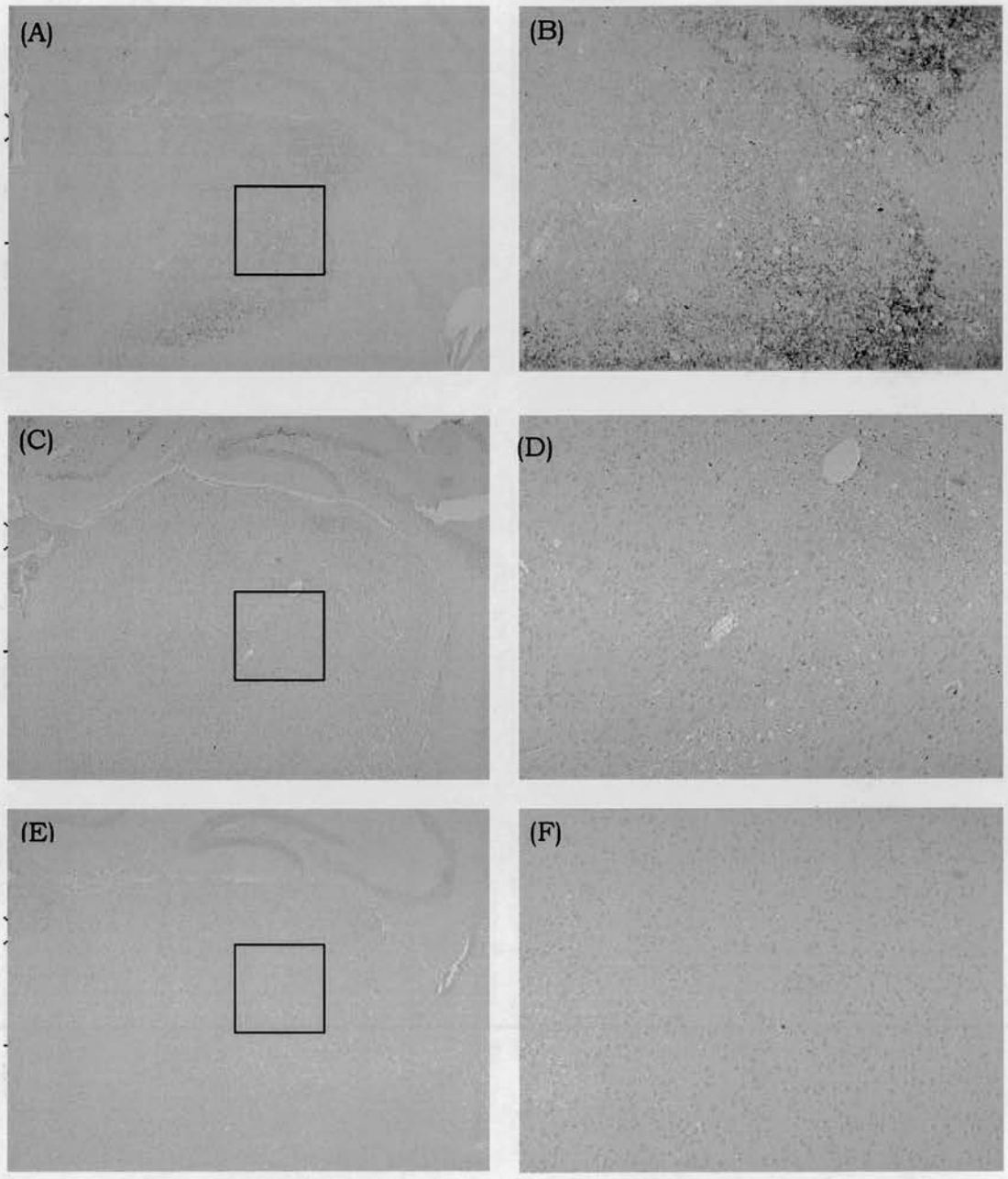

Figure 4.7 Relative PrP deposition in individual GSS/101LL mice

Immunostained brain from GSS infected 101LL mice (GSS/101LL). Sections cut at hippocampus/thalamus level (figure 4.1) and stained using 6H4 monoclonal antibody. (A) & (B) GSS/101LL brain 1; (C) & (D) GSS/101LL brain 2; (E) & (F) GSS/101LL brain 3. (A), (C) & (E) hippocampus and thalamus x 40 magnification; (B), (D) & (F) thalamus x 100 magnification.

in the models (thalamus, hypothalamus hippocampus, vestibular nuclei and raphe) and two areas where PrP accumulation was rarely seen in some models (cortex and cerebellum). PrP deposition in immunostained brain sections was scored on a scale of one to four, where four indicated most intense PrP staining (table 4.1). For a direct comparison of all models it would have been better to compare all sections stained with the same antibody however this was not possible here. ME7 deposition in each model was assessed from 1A8-stained sections since 6H4 and 8H4 sections were incomplete (chapter 4.3.2). No difference in the level or type of PrP deposition was seen in 263K/101LL or GSS/101LL brain when stained with either 1B3 or 6H4 antibodies (figure 4.6 & 4.7) thus deposition was assessed from 6H4-stained sections. The degree of PrP deposition in each model was therefore ranked ME7/101PP > ME7/101LL > 263K/101LL ≥ GSS/101LL (figure 4.8). This is the same ranking given to the models based upon immunoblot PrP^{Sc} detection and may indicate that the disease-associated PrP deposited in these models is indeed PrP^{Sc} (chapter 3).

Brain Area	ME7/101PP [a]	ME7/101LL [a]	263K/101LL [b]	GSS/101LL [b]
Cerebral Cortex	++	+	+	+
Hippocampus	+++	++	+	+
Thalamus	++++	+++	++	+
Hypothalamus	++++	+++	+	++
Raphe	++++	+++	+	++
Vestibular nu[c]	+++	+++	+	++
Cerebellar Cortex[c]	++	++	0	0

Table 4.1 Comparison of PrP deposition levels between models

[a] PrP deposition detected using polyclonal antibody 1A8
[b] PrP deposition detected using monoclonal antibody 6H4
[c] see figure 4.1 for vestibular nuclei (V) and raphe (R) location

The vestibular nucleus and raphe of infected 101LL models exhibit relatively high PrP deposition in comparison to other brain areas (figure 4.7). Thalamic deposition was comparatively high in all models. In the models where PrP^{Sc} levels were low, the thalamus was often the only area where PrP deposition was visible (figure 4.7C). In ME7/101PP mice PrP accumulation in vestibular nuclei and raphe was lower than in thalamus. Although PrP deposition in all areas is higher in ME7-infected mice, it is possible that primary targeting to the vestibular nuclei and raphe in 263K/101LL and GSS/101LL models facilitates a rapid clinical disease in the low PrP^{Sc} models.

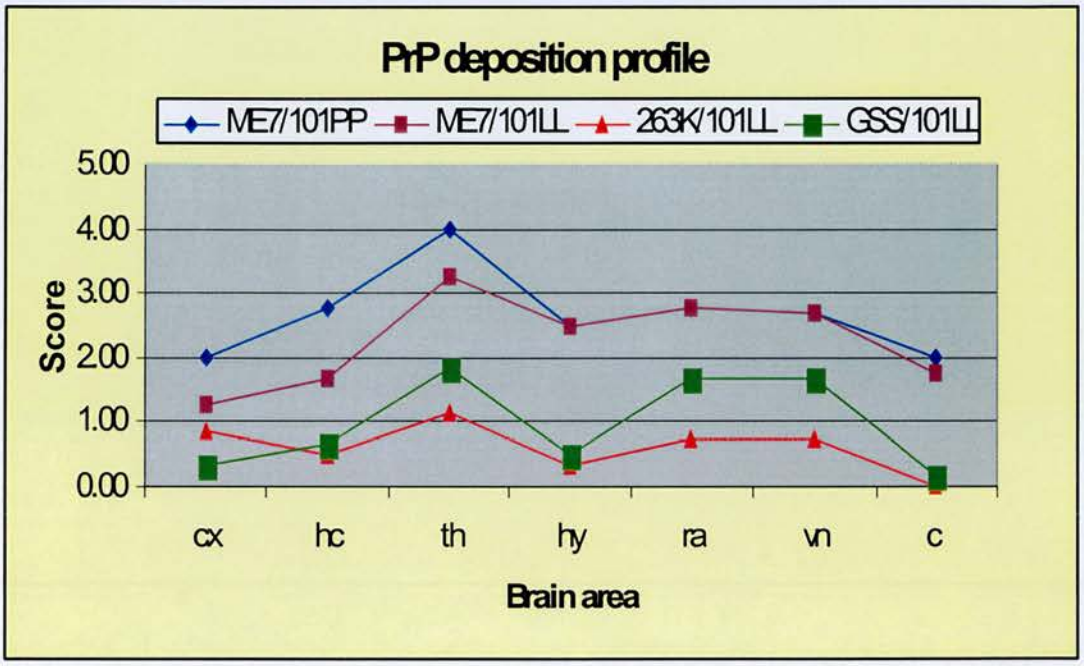

Figure 4.8 Comparative PrP deposition profiles

PrP deposition profiles in seven different grey matter areas in brain. Four to seven animals scored for each model. Scores range from one to four, four indicating most severe PrP deposition. Brain areas scored are cx-cerebral cortex, hc-hippocampus, th-thalamus, hy-hypothalamus, ra-raphe, vn-vestibular nuclei, c-cerebellum (see figure 4.1 for location).

4.3.6 Comparison of PrP deposition and vacuolation in each model

It is not understood whether PrP deposition results in vacuolar pathology, however areas of PrP deposition and vacuolar pathology have been correlated in several TSE models, particularly those where PrP deposition is high (chapter 4.1). A brief comparison of the vacuolation profiles and PrP

deposition profiles of the chosen models was therefore performed here. PrP deposition was examined in grey matter areas where vacuolation was found to be high or low depending on the model thus deposition in thalamus, hippocampus, hypothalamus, cerebellum and cortex was plotted alongside the vacuolation profile for each model (figure 4.9). In ME7/101PP (figure 4.9A), areas of high vacuolation correspond to high PrP deposition and lower vacuolation corresponded to lower PrP deposition. This correlation was generally observed in ME7/101LL (figure 4.9B), 263K/101LL (figure 4.9C), and in GSS/101LL (figure 4.9D). More particularly, the association between vacuolation and deposition was clearly demonstrated in 263K/101LL cortex where PrP accumulated solely around areas of vacuolation (figure 4.6E). Across all the models studied here, where PrP deposition was evident areas of PrP deposition and vacuolation were found to correlate. This is similar to the pathology seen in models where PrP deposition was high (De Armond et al., 1989) and probably demonstrates that the general pathology in the low PrP^{Sc} model is in keeping with that of other TSE-models (Jeffrey et al., 2001).

4.3.7 Other disease-associated pathology

ME7/101LL mice showed limited neuronal loss in the CA1 pyramidal cell layer, which was not as apparent as the neuronal loss in the ME7/101PP CA1 region (figure 4.4). Hippocampal neuronal loss does not appear to be an intrinsic pathological characteristic of 101LL mice since it was not apparent in GSS and 263K-infected 101LL mice (figures 4.5 & 4.7), thus may be a characteristic of the ME7 agent itself. Neuronal loss in other brain areas of infected 101LL mice cannot be ruled out since this pathological characteristic was not investigated outside of the hippocampus in these studies. Time-course studies of neuronal loss in 263K/101LL and GSS/101LL models may find highly targeted neuronal loss in specific brain areas.

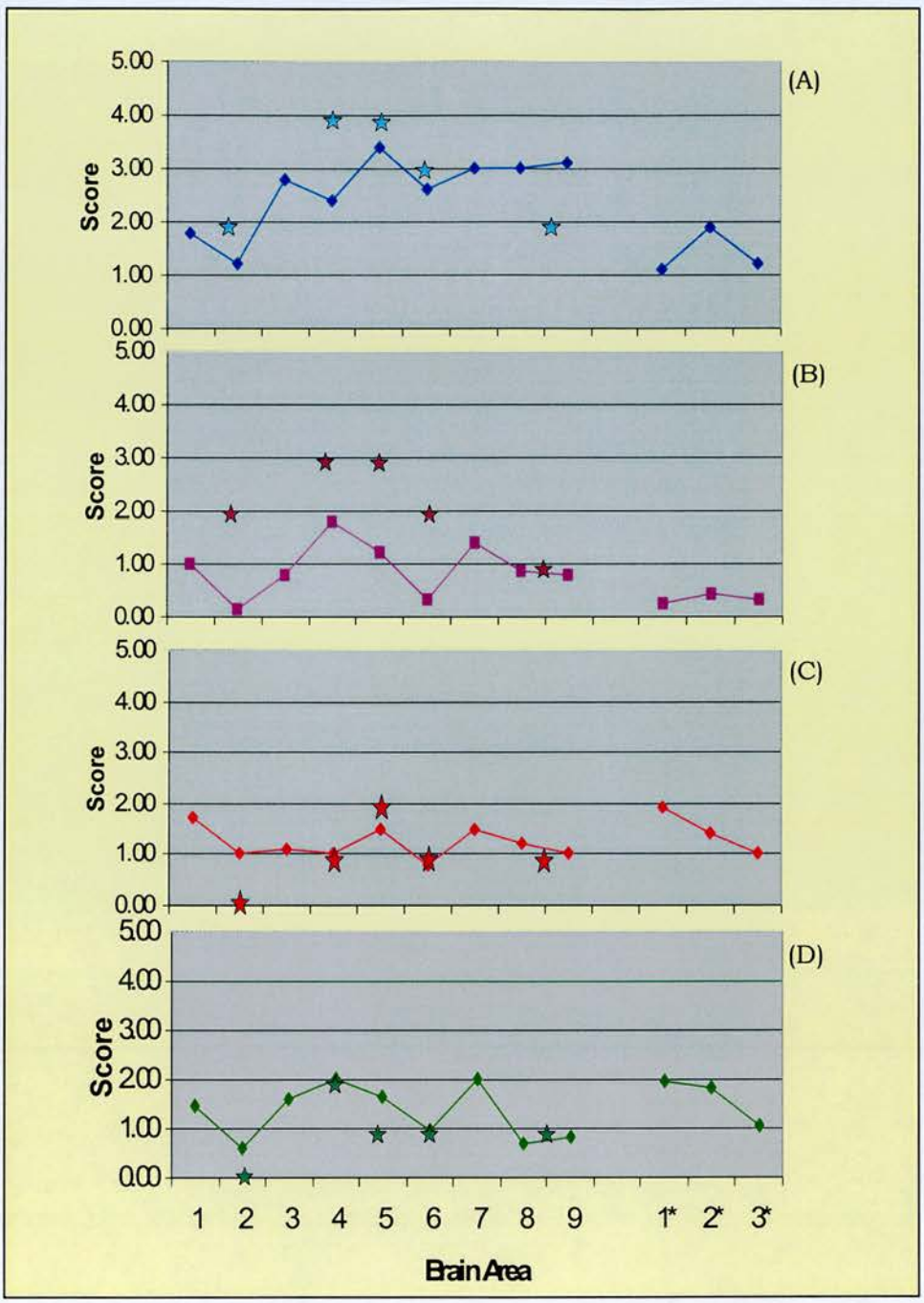

Figure 4.9 The association between vacuolation and PrP deposition

Vacuolation versus PrP deposition in each model, (A) ME7/101PP, (B) ME7/101LL, (C) 263K/101LL, (D) GSS/101LL. Vacuolation profile of nine grey matter areas is shown as a solid line. PrP deposition levels (table 4.1) shown as stars at appropriate brain area. 2-cerebellum, 4-hypothalamus, 5-thalamus, 6-hippocampus; 8 & 9-cortex. Vacuolation in raphe of midbrain and vestibular nuclei not scored.

4.4 Discussion

4.4.1 PrP accumulation correlates with PrP^{Sc} levels

In order to study the correlation between PrP^{Sc} level and titre of infectivity TSE models were chosen which displayed different amounts of PrP^{Sc} as detected my immunoblot (chapter 3). ME7/101PP had high, ME7/101LL intermediate, and 263K/101LL and GSS/101LL low PrP^{Sc} levels. Here, immunostaining of brain sections demonstrated the accumulation of disease-associated PrP in each model. The level of PrP staining corresponded with the amount of PrP^{Sc} exhibited in brain homogenate from each model (chapter 3) where PrP accumulation was high in ME7/101PP, low to undetectable in 263K/101LL and GSS/101LL models and found at intermediate levels in ME7/101LL brain. These findings are consistent with other studies that showed a positive correlation between PrP deposition and PrP^{Sc} level (DeArmond et al., 1987; Jeffrey et al., 2001 McBride, 2001 #284). Deposition of PrP was seen before the onset of pathology however infectivity was detected before the appearance of PrP deposition, suggesting that whilst PrP^{Sc} may be pathogenic it may not be the infectious agent. It may be that aggregated PrP^{Sc} can trigger other pathogenic events in TSE-infected brain that leads to vacuolation and neuronal loss.

Although the study performed here provides additional evidence suggesting that the PrP deposited in TSE affected brain is PrP^{Sc} definitive identification of PrP^{Sc} in these brains is required. PET blot of adjacent brain tissue sections for each model investigated here would have identified the presence of PrP^{Sc} (McBride et al., 2001). This method has been used to track the progression of PrP^{Sc} from the periphery to the central nervous system in hamsters orally infected with 263K. Transfer of protein from paraffin-embedded tissue (PET) to nitrocellulose membrane allows PK-treatment to be performed. Protease resistant PrP^{Sc} can therefore be identified in specific brain areas using this method.

Unlike hamster 263K brain, 263K/101LL and GSS/101LL brain sections did not exhibit diffuse PrP staining. It is unknown whether diffuse staining

is a characteristic of the 263K/101LL and GSS/101LL models since only a limited number of 263K/101LL sections have been immunostained. However formic acid treatment may have affected detection of this diffuse staining. Brain from 263K/101LL and GSS/101LL models was immersed in formic acid for 90 minutes to reduce the occupational exposure of staff to TSE agents when handling and cutting infected brain. Experiments have shown that infectivity in formic acid treated, fixed brain tissue can be reduced by as much as 10^5 ID_{50}/ml, depending on the strain of TSE agent used (Taylor et al., 1997). It has recently been demonstrated that the pretreatment of paraffin-embedded tissues with formic acid to decontaminate infected tissue reduces the amount of detectable PrP in immunostained sections. PrP staining was still detectable, however, in highly affected brain areas such as thalamus and hippocampus (A. Suttie and P McBride, personal communication & figure 4.10). To identify whether diffuse staining does occur in the 263K/101LL and GSS/101LL models brain sections should be re-examined without formic treatment.

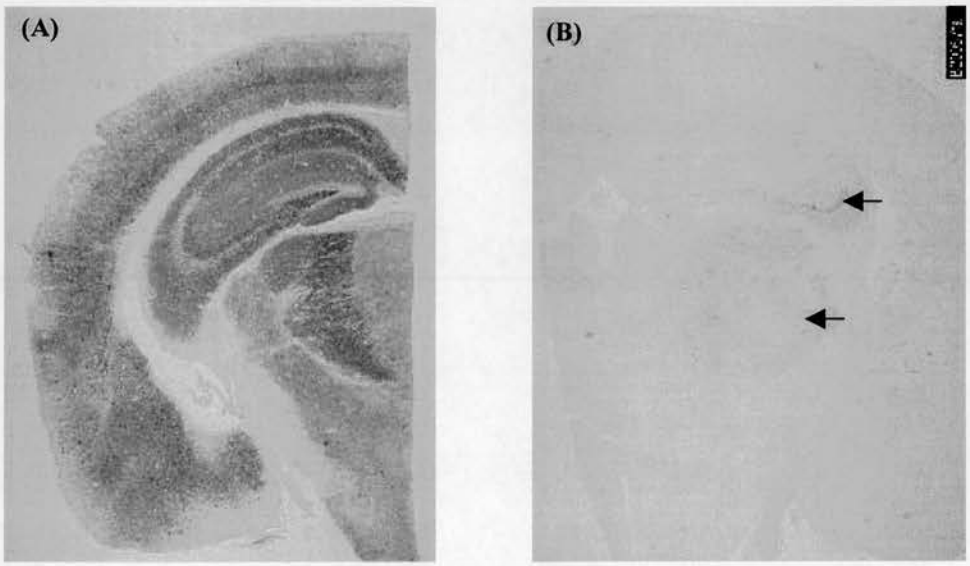

Figure 4.10 The effect of formic acid treatment upon immunostained brain sections.

ME7-infected brain (A) not treated with abundant PrP-specific staining throughout the brain, or (B) formic acid-treated with a loss of PrP-specific staining, PrP staining can be seen very faintly in the hippocampus and thalamus (black arrows). Coronal sections of brain cut at the thalamic/hippocampal level (figure 4.1) immunostained using 6H4 monoclonal antibody. Images courtesy of A. Suttie, NPU, Edinburgh.

Although 263K/101LL and GSS/101LL brain tissue were formic acid treated and the levels of disease-associated PrP were thought to be reduced, levels of PrP in these models were consistent with the low/non-detectable levels of PrP^{Sc} detected using immunoblot (chapter 3). Individual animals within the 263K/101LL and GSS/101LL models displayed variation in the amounts of PrP deposited in the brain. This variation was also seen upon immunoblot detection of PrP^{Sc} in individual brain homogenates (chapter 3). It is reassuring to note that both immunocytochemistry and immunoblot similarly measure the relative levels of disease-associated PrP, or PrP^{Sc}, in each TSE model studied here.

4.4.2 PrP deposition and pathology

PrP^{Sc} deposition is thought to cause TSE-associated pathology and in particular vacuolation has been shown to correlate with areas of PrP^{Sc} deposition (DeArmond et al., 1987). In the studies performed here in areas of high PrP^{Sc} deposition intensity of vacuolation was high and where PrP^{Sc} deposition was low vacuolation intensity was correspondingly low, thus it did appear that vacuolation correlated with the presence of PrP deposition. This agreed with previous studies (De Armond et al., 1989; DeArmond et al., 1987). The studies by DeArmond *et al* and the studies here investigated vacuolation and deposition at disease endpoint and did not plot the progression of vacuolation alongside the appearance of PrP^{Sc} in the brain. Moreover, in other murine TSE models PrP^{Sc} deposition has been shown to precede synapse loss (Jeffrey et al., 2000) and areas of vacuolation and neuronal loss correlated with areas of PrP deposition in an intra-ocular model of murine TSE (Fraser et al., 1995). These studies further suggest that PrP^{Sc} is the cause of TSE pathology.

Whilst the data accumulated by these studies indicate that PrP deposition could be responsible for vacuolation, these parameters did not correlate in all areas of 263K/101LL and GSS/101LL brain. High levels of vacuolation occurred in the paraterminal body of these models and vacuolation was often seen in the superior colliculus yet PrP deposition was rarely recorded in these brain areas. This may indicate that not all TSE vacuolation is

associated with PrP^{Sc}. Thus it is possible that PK-resistant PrP^{Sc} is not the cause of vacuolar pathology in these models.

4.4.3 Targeting of PrP deposition and vacuolation

If PrP^{Sc} were the pathogenic molecule that initiated TSE-associated pathology then the amount of PrP^{Sc} deposited in TSE-infected brain must affect disease incubation time. However Kimberlin *et al* suggest that specific target areas of pathology play a role in the speed of disease progression (Kimberlin & Walker, 1988). Short disease incubation times would occur when specifically vulnerable areas were targeted very soon after acquiring TSE, however upon late targeting of vulnerable areas, the disease incubation time would be longer. In the experiments performed here the targeting of PrP deposition was not dramatically different between models. Thalamic deposition was highest throughout all models except GSS/101LL. PrP staining in GSS/101LL was high in the vestibular nuclei and the raphe. These areas as well as the thalamus were also particularly affected in the 263K/101LL model. Between the models, this is the only visible difference in the distribution of PrP staining. It may be that specific targeting to the vestibular nucleus in these models exacerbates the disease. If these areas are critical in keeping the animal alive, early and specific targeting of pathology to vestibular nuclei may explain the lower disease incubation times in the 263K/101LL and GSS/101LL models. With the specific targeting of PrP deposition to the vestibular nucleus and raphe in the GSS/101LL and 263K/101LL models, it may be expected that specific clinical symptoms would have been apparent during disease. Damage to the acoustic vestibular nuclei may have resulted in impaired hearing or serotonin depletion symptoms such as altered sleep patterns, aggressive behaviour or increase motor activity. Damage to further vestibular nuclei may have resulted in increased symptoms of imbalance. However, such symptoms were not reported during the clinical phase of TSE in GSS and 263K-infected 101LL mice, furthermore, there is no reported correlation between clinical signs and areas of pathology. The 22A model of TSE, for example, shows high levels of cerebellar damage, yet motor function is not impaired to any greater degree in this model compared to than found in

other TSE models (P McBride, personal communication). However it is possible that other differences in the targeting of PrP deposition between models, other than those discussed here, have been overlooked.

If vacuolation was targeting to critical brain areas in each model this may also explain differences in TSE survival times. The targeting of vacuolation (vacuolation pattern) has been shown to differ according to genetic background of the host and the strain of TSE agent used (Bruce et al., 1989). Where possible these variables have been minimised in this study, however it appears that both these variables have an effect on the models studied here. Each model of TSE produced a distinct vacuolation profile according to the different strain of TSE agent used. Additionally the presence of the 101LL allele appeared to affect the intensity of vacuolation with low levels of vacuolation in 263K-, GSS- and ME7- infected 101LL mice. Vacuolation in the hypothalamus appeared particularly high in these models however it is not clear whether comparatively high vacuolation in this brain area in the 101LL models affected animal survival. The hypothalamus is a highly important area of the brain, responsible for homeostatic control in the animal. It has an important neuroendocrine function and can regulate body temperature, the cardiovascular system, food and water intake and stress responses. Thus if severe vacuolation occurs in this area of the brain it is not difficult to see how this may be critical to the survival of the animal.

In order to thoroughly assess and compare the pathological changes in all of the models discussed here, time-course studies (chapter 4.1) should be performed. Parameters such as synaptic loss, neuronal degeneration (Jamieson et al., 2001; Jeffrey et al., 2000) and the appearance of gliosis (De Armond et al., 1989; Jeffrey et al., 1997), which have been studied in other TSE models, should be investigated. In conjunction with a detailed investigation of the deposition of PrP and appearance of vacuolation this would provide a detailed study of whether PrP^{Sc} correlates with TSE-associated pathology in the 263K/101LL and GSS/101LL models.

4.4.4 Is PrP^{Sc} the pathological molecule of TSE?

Low levels of PrP deposition and vacuolation are unlikely to cause death unless they specifically occur in vulnerable brain areas. This specific targeting of pathology may occur in the ME7/101LL, GSS/101LL and 263K/101LL models. If PrP^{Sc} is deposited before vacuolation occurs, it is possible that PrP^{Sc} causes subsequent pathology, however, in certain brain areas there are areas of vacuolation in which no PrP is detected. This may suggest that, if PrP^{Sc} is responsible for vacuolation, it may exert distant as well as local effects. However, in individual mice no PrP deposition was detected yet vacuolar pathology was evident suggesting that PrP^{Sc} may not be responsible for vacuolation.

If PrP^{Sc} triggers pathology in TSE-affected brain, it may be that PrP deposition (as PK-resistant PrP^{Sc}) is a final event in a pathological reaction. There may be an associated cascade of events triggering TSE pathology. Whilst there is speculation that apoptotic events cause the neuronal loss associated with TSE, it is not known how vacuolation occurs. However, if the cascade of events leading to PrP^{Sc} deposition involves other proteins or complexes, it is possible that these other reactions may cause other TSE-related pathology (figure 4.11).

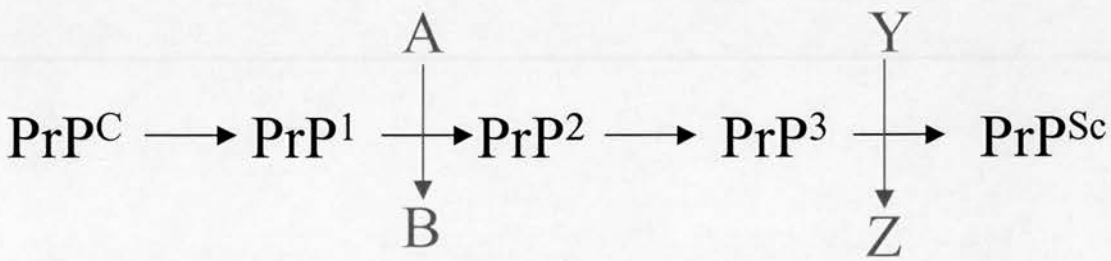

Figure 4.11 PrP deposition cascade and interactions

Apoptotic cascades may interact with intermediate forms of PrP. Neuronal loss or other pathological damage triggered by apoptosis may occur before conversion of intermediate forms of PrP to PrP^{Sc}.

The proapoptotic markers, Fas and caspase 3 have been shown to be upregulated before PrP deposition and clinical signs occurs in an 87V model of TSE (Jamieson et al., 2001). It is possible that the cascade of PrP

deposition may have triggered this upregulation, which ultimately leads to neuronal loss.

In the 263K/101LL and GSS/101LL models, overproduction of B or Z (figure 4.11) may result in the appearance of fatal pathological events at key brain areas, before the accumulation of PrP^{Sc}. There may be different pathways to disease-associated pathology depending on whether PrP^{Sc} is present. These pathways may only be resolved if a detailed time-course experiment was undertaken to investigate the interactions and sequence of pathological changes during TSE disease in the low PrP^{Sc} models.

For the purposes of this thesis a detailed investigation of pathology was not required. Essential for these studies was that each model, ME7/101PP, ME7/101LL, 263K/101LL and GSS/101LL, revealed TSE-associated pathology and that the amount of PrP deposition corresponded to the amount of Pk-resistant PrP^{Sc} previously detected by immunoblot. The actual levels of PrP^{Sc} deposition and titre of infectivity in each model will be quantified further in this thesis.

5. Measurement of infectivity in brain tissue

5.1. Introduction

In conjunction with a clinical evaluation, the deposition of PrP, identification of PrP^{Sc} and appearance of vacuolation identifies a TSE infected animal. However, in order to define TSE, a neurodegenerative disease must be further transmitted from infected tissue. Transmission indicates the tissue contains the infectious agent but it does not quantify how much infectious agent is present. In general, short incubation times indicate a high titre of infectivity. However as demonstrated earlier (chapter 3) these parameters do not always correlate. Therefore, to quantify the infectivity present in infected tissue a full titration is required. There are two approaches to measure titre of infectivity by bioassay. One is the time interval assay (Kascsak et al., 1985; McKinley et al., 1983), the other is the end-point titration assay (Kimberlin & Walker, 1979; Taylor et al., 2000). The time interval assay uses the time from inoculation to onset of illness and applies this to a specific equation to calculate infectivity titre. This relies on the subjective assessment of when clinical symptoms begin in the TSE-infected host. However, due to the subjectivity of the individual carrying out the clinical assessment, the time of onset of clinical disease can vary (V. Thomson, personal communication). Such complications may introduce errors, which affect the incubation time assay. In the end-point titration the appearance of clinical disease in animals can be more clearly identified by continuously assessing the clinical status of animals over several weeks after disease onset. In the experiments here, titre of infectivity was measured using the end-point titration method (Kimberlin & Walker, 1978) (chapter 1.10). The end-point titration requires more animals than the incubation time assay and sufficient dilution of the agent must be performed to ensure that the true end-point is reached. A study to compare this assay with the time interval assay found no significant difference in the calculation of infectivity titres between these assays (Prusiner et al., 1982b). However, the end-point titration assay is thought to be more accurate in

assessing titre of infectivity since this dilutes the infectious material to an end-point.

Bioassay remains the gold standard for measuring TSE infectivity. The presence of one infectious unit of the TSE agent in mice can be measured by bioassay since TSE will progress in affected animals. The hamster 263K model demonstrated that one infectious unit (ifu) contains 10^4 to 10^5 molecules of PrP^{Sc} (Bolton et al., 1982; Hilmert & Diringer, 1984; Hope & Manson, 1991; McKinley et al., 1983) & chapter 1.10, thus any *in vitro* assay must be capable of measuring this amount of PrP^{Sc} if it is to be comparable to bioassay. Infectivity has been identified from brain and placenta in the apparent absence of PrP^{Sc} when detected by immunoblot (Lasmezas et al., 1997; Manson et al., 1999; Onodera et al., 1993), thus most current PrP^{Sc} detection methods are not capable of identifying a single infectious unit of TSE. Recently however, two *in vitro* assays were reported to detect the equivalent of one infectious unit of TSE. The first assay relies on the uptake and detection of PrP^{Sc} in neuroblastoma cells infected with murine RML scrapie strain and assumes that PrP^{Sc} is the causal agent of TSE (Klohn et al., 2003). This assay is strain specific, however and is not useful for the studies performed here. The second assay, CDI, does not rely on the detection of the PK-resistant 27-30kDa core of PrP^{Sc}. Instead, different conformations of PrP^{Sc} that may be present in infected tissues can be detected under increasing denaturing conditions (see chapter 1.9 for full details). This assay has already been used to quantify BSE in infected cows (Safar et al., 2002). CDI requires the use of specific antibodies to identify an epitope that is hidden in the native but exposed in the denatured conformation of PrP in specific samples. Such antibodies have not been identified for the models investigated here.

The aim of this chapter was to calculate the titre of infectivity found in models of TSE containing high (ME7/101PP), intermediate (ME7/101LL), and low (263K/101LL) levels of PrP^{Sc} at disease end-point. This allowed a correlation of PrP^{Sc} level with infectivity titre in each TSE model to test whether high infectivity titres are produced in infected tissue with high levels of PrP^{Sc} in accordance with the prion hypothesis. Infectivity in

ME7/101PP brain in *Prnp-a* mice was previously titrated at 10^8 to 10^9 ifu/g (Carp & Callahan, 1986; Taylor et al., 2000). The titre of infectivity has not been previously reported for ME7/101LL mice however PrP^{Sc} levels in ME7/101LL mice were less than in ME7/101PP mice (Manson et al., 1999) indicating that lower infectivity titres may be expected in ME7/101LL brain. 263K/101LL brain had not been previously titrated however extremely low PrP^{Sc} levels in these mice may indicate that the titre of infectivity in 263K/101LL mice would be lower than in ME7/101PP and ME7/101LL mice. Since PrP^{Sc} levels differ dramatically between individual primary pass animals (chapter 4), three individual 263K/101LL brains were chosen for PrP^{Sc}/titre correlation. ME7 is a stable TSE agent and has been passaged many times in *Prnp*-a mice (chapter 1.12) thus the variability of PrP^{Sc} level between individuals in the ME7 model would be predicted to be less than that in the 263K/101LL model. Therefore only one brain was studied from ME7/101PP and ME7/101LL models.

5.2. Methodology

5.2.1. Brain homogenate titrated

Brains from one animal each of ME7/101PP, ME7/101LL and GSS/101LL models as well as three brains from the 263K/101LL model, (designated 263K/101LL (1), 263K/101LL (2) and 263K/101LL (3)) were prepared. Sterile 10% brain homogenate was serially diluted tenfold, and 20µl of each dilution was inoculated into the right brain hemisphere of each mouse (chapter 2.22).

5.2.2. Number of mice required for titration

To measure infectivity in brain from each model, donor homogenate from the ME7/101PP model was titrated in 101PP mice and homogenate from ME7/101LL and 263K/101LL models was titrated in 101LL mice (table 5.1). This ensured that the assay was not affected by differences in disease transmission caused by genetic differences between the donor and recipient mouse (Bruce & Dickinson, 1987).

Accurate measurement of end-point titration required the serial dilution of homogenate containing the infectious agent to a point where a group of animals do not shown clinical or pathological signs of disease. Previous titration data from ME7-infected *Prnp*-a mice indicated dilution of brain homogenate to at least 10^{-8} was required to achieve a zero-affected group (Taylor et al., 2000). It was not known whether the titre of infectivity in 263K-infected 101LL brain would be higher than that in ME7/101PP mice. Due to time constraints these titration experiments would not be repeatable and it was important to reach the end-point of infectivity therefore all titration experiments performed here were extended to 10^{-11} dilution. Furthermore, because infectivity titre decreases with increasing dilution, fewer mice are affected by TSE therefore increased numbers of mice were required in each dilution group. Thus, mouse group sizes increased with increasing dilution of brain homogenate, with six animals for 10^{-2} dilution, nine animals each for 10^{-3} and 10^{-4} dilutions and 12 animals in each group

thereafter. The mice used were housed in cages of six and this was considered when choosing the number required for each dilution. In addition, another 12 mice were added to the 10^{-2} group of each titration to provide stock tissue for other experiments. Whole brain from six of these animals was stored at –70°C for further passage and titration experiments. These brains could not be pathologically examined thus were not included in vacuolation profile data, which requires at least six animals per group. These experiments would not be repeatable due to time constraints thus the additional animals were included in case of intercurrent deaths within the original six animals injected at 10^{-2} dilution of inoculum. Moreover the addition of extra animals into the 10^{-2} group allowed disease incubation time to be calculated more accurately.

For each titration a total of 108 mice (101PP or 101LL where appropriate) were therefore required to be inoculated. In addition, 18 101PP mice were inoculated with 10^{-2} dilution of each 263K/101LL brain homogenate, 263K/101LL (1), (2) & (3), to identify whether the differences in transmissibility from individual 263K-infected 101LL brain to 101PP mice was a general feature of the 263K/101LL agent.

Donor Mouse	Donor TSE strain	Recipient Mouse
101PP	ME7	101PP
101LL	ME7	101LL
101LL	263K (1)	101LL
101LL	263K (2)	101LL
101LL	263K (3)	101LL
101LL	GSS	101LL

Table 5.1 Genotype of donor inoculum titrated into recipient mice

5.2.3. Age of mice required for titration

Animals would ideally have been inoculated at 6-8 weeks old to keep the age range to a minimum, however due to time and breeding constraints and animal availability 101PP animals available for injection ranged from 11–26 weeks old and 101LL animals ranged from 4-31 weeks old. To obtain 6-8 week old animals, several small batches would have had to be produced

since the logistic of breeding meant that a large batch of animals within this age range could not be produced at one time. The wide age range was preferable to the alternative option of performing staggered inoculations, which would have involved freeze/thawing inoculum. Repeated freezing of inoculum has been shown to alter disease incubation times thus may alter the titre of infectivity in a sample. It was critical in these studies that the titre of infectivity should not be compromised.

5.2.4. Assessment of mouse genotype

Stocks of 101PP and 101LL mice were maintained at a low level prior to these experiments, however before mating, the PrP genotype of each breeding pair was determined (proline or leucine at amino acid 101) to ensure that homozygous 101PP or 101LL animals were produced. DNA was prepared from tail tissue and PrP genotype was assessed using Polymerase Chain Reaction (PCR) (chapter 2.24). PCR of tail DNA was also performed at the end of each experiment to confirm the genotype of each animal.

5.2.5. Assessment of TSE in injected animals

Intracerebral inoculation of mice was performed (chapter 5.2.1). From 90-100 days post-inoculation, animals were assessed weekly for clinical symptoms of TSE and scored accordingly (a positive clinical score is defined in appendix C). When animals were scored TSE positive for three consecutive weeks, or were deemed to be at the terminal stage of disease, they were culled using a Schedule 1 method in accordance with the Animals (Scientific Procedures) Act 1986. Disease status was confirmed by scoring the degree of TSE-associated vacuolar pathology in grey and white matter brain areas (chapter 4). This was essential since TSE-associated vacuolar pathology can be found in some animals that have not shown clinical symptoms (Manson et al., 1999).

Animals exhibiting clinical TSE symptoms and pathology were included in transmission and disease incubation time calculations. Mice culled due to welfare reasons (for example scratched eyes and ears) may be given a negative clinical score but can exhibit positive pathology if culled at the

early stages of disease. TSE transmission did occur in such animals therefore data was used for the transmission but not the incubation time calculation. Animals exhibiting positive clinical signs of disease but not TSE pathology were not confirmed as having TSE thus were not included in transmission or incubation time calculations. This also applied to mice that exhibited no clinical disease or no TSE pathology. Additionally, data not used for either experimental transmission or incubation time calculations came from animals:

- that died immediately post-inoculation or before the start of the scoring regime,
- that died due to inter-current disease, i.e. for reasons other than TSE,
- where brain could not be retrieved for pathological conformation of disease status due to either cannibalism by other animals, autolysis of brain tissue or because whole brain was stored for further use,
- that were of the wrong genotype for the group.

For these reasons, the final group numbers did not always correspond with the original group numbers.

5.3. Results

5.3.1. ME7/101PP brain has a high titre of infectivity

ME7/101PP titration in 101PP mice (produced from breeding stock confirmed as homozygous 101PP, figure 5.1) resulted in a typical ME7 titration pattern. TSE was transmitted to 100% of 101PP mice in the 10^{-2} group in 159 ± 0.3 days, and was transmitted to 100% of animals in subsequent groups down to 10^{-6} dilution of brain homogenate, with increasing incubation times (table 5.2). Only 17% (2/12) of 101PP mice receiving 10^{-7} dilution and 9% (1/11) of animals in 10^{-8} group were affected by TSE (table 5.2). The first "zero group" (no TSE-affected animals in the group) in this titration was at 10^{-9} dilution of brain homogenate (table 5.2).

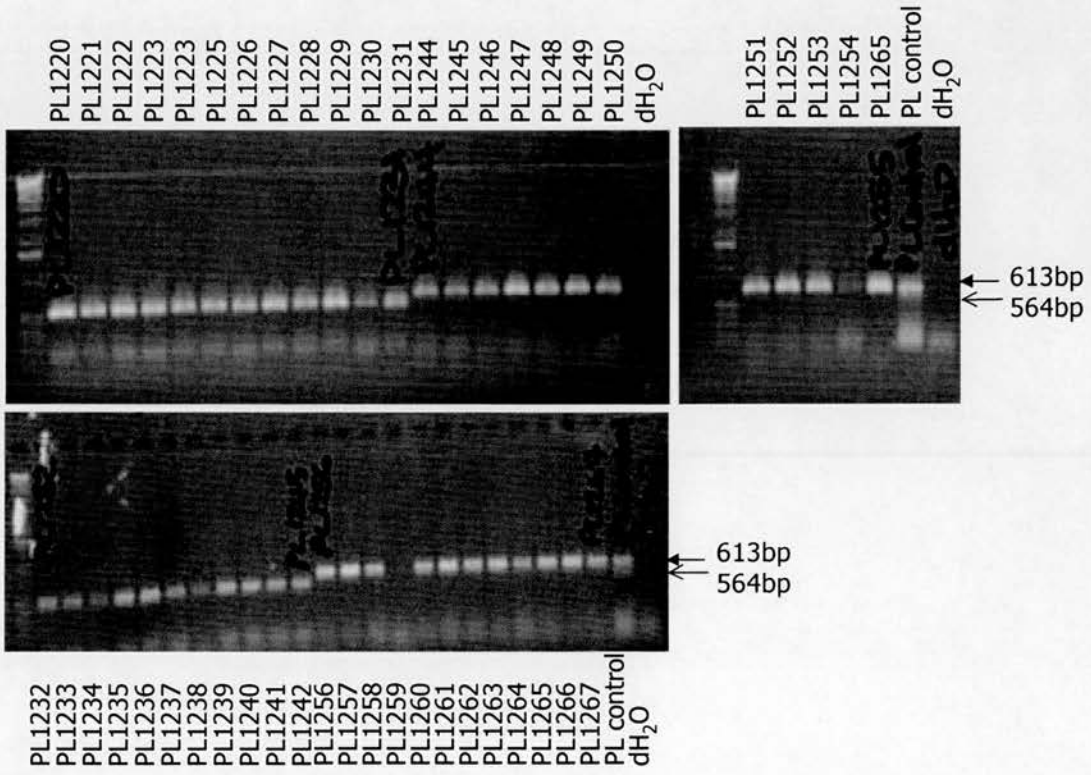

Figure 5.1 PCR of breeding stock mice

1% Agarose gel of DdeI cut DNA from PrP ORF PCR, taken from breeding stock mice and processed in batches of 11 or 12 samples; PL1220-PL1231, PL1244-PL1255, PL1232-PL1243, PL1256-PL1267. Closed arrow at 613bp indicates proline allele only, open arrow at 564bp indicates leucine allele only. PL control DNA from an animal known to be heterozygous, dH_2O lane indicates no contamination of samples.

Dilution Group	ME7/101PP		ME7/101LL		263K/101LL (1)		263K/101LL (2)		263K/101LL (3)	
	n+/nT[a]	Inc Time[b]	n+/nT[a]	Inc Time[b]	n+/nT[a]	Inc Time[b]	n+/nT[a]	Inc Time[b]	n+/nT[a]	Inc Time[b]
10^{-2}	6/6	159±0.3	7/7	220±4	13/13	109±2	13/13	129±2	13/13	262±4
10^{-3}	6/6	170±1	5/5	249±7	6/6	114±1	6/6	134±6	3/6	308±16
10^{-4}	9/9	177±2	9/9	277±4	8/8	125±3	9/9	159±9	6/7	399±9
10^{-5}	9/9	201±5	7/8	313±21	8/8	144±4	6/9	193±22	6/7	398±8
10^{-6}	11/11	269±15	7/12	409±25	11/12	189±16	1/7	226	2/11	401±4
10^{-7}	2/12	291±14	0/10	n/a	5/12	189±6	0/17	n/a	0/9	n/a
10^{-8}	1/11	244	0/12	n/a	1/11	228	1/12	186	0/12	n/a
10^{-9}	0/11	n/a	0/11	n/a	0/9	n/a	0/9	n/a	0/8	n/a
10^{-10}	0/11	n/a	0/11	n/a	0/10	n/a	0/11	n/a	0/9	n/a
10^{-11}	0/11	n/a	0/8	n/a	0/11	n/a	0/11	n/a	0/8	n/a
10^{-2} 101PP	n/a	n/a	n/a	n/a	0/9	n/a	12/12	296±24	0/17	na
ID_{50}	**$10^{6.76}$**		**$10^{5.96}$**		**$10^{6.93}$**		**$10^{5.39}$**		**$10^{4.9}$**	
ID_{50}/g	**$10^{8.5}$**		**$10^{7.7}$**		**$10^{8.6}$**		**$10^{7.1}$**		**$10^{6.6}$**	

[a] n+= number TSE positive animals (assessed by clinical and pathological examination); nT= total number of animals per group.

[b] Mean incubation time (days) of animals scored pathologically positive ± standard error

n/a not applicable

nd not determined

ID_{50} value for inoculated brain tissue (= 20mg) – calculated using the Karber method (chapter 2.22.4). For additional data see appendix D.

ID_{50} value per g brain tissue ([a] x50)

Data correct at 10 January 2004

Table 5.2 Titration of infectivity in TSE models exhibiting high, low and intermediate levels of PrP^{Sc}

At 10^{-8} dilution only one 101PP animal had succumbed to TSE disease with an incubation time of 244 days (table 5.2). This was a shorter incubation time than those animals receiving 10^{-6} homogenate dilution and it is possible that if the inoculum at 10^{-8} dilution was not homogeneous, the animal may have received a clump of TSE agent that was responsible for causing rapid disease. In the study here, the dilution of brain homogenate that resulted in 50% of animals affected by TSE was $10^{-6.76}$ (table 5.2). The titre of infectivity per gram of brain is therefore $10^{8.5}$ infectious units (ifu) (table 5.2), similar to those previously reported for ME7-infected *Prnp*-a mice (Carp & Callahan, 1986; Taylor et al., 2000).

5.3.2. ME7/101LL brain has a lower titre of infectivity than ME7/101PP

TSE was transmitted from primary pass ME7/101LL brain to 100% of 101LL animals (produced from stock mice confirmed 101LL homozygous, figure 5.1) receiving 10^{-2} dilution of inoculum in 220 ± 4 days (table 5.2). At 10^{-3} and 10^{-4} dilution of brain homogenate 100% of 101LL mice were affected by TSE (table 5.2). Disease was transmitted to 88% (7/8) of animals receiving 10^{-5} dilution and 58% (7/12) of animals receiving 10^{-6} dilution. The first "zero group" was at 10^{-7} dilution with no 101LL mice exhibiting TSE disease in this or subsequent groups (table 5.2). The dilution at which 50% of 101LL animals were affected by TSE was $10^{-5.96}$ (table 5.2). The titre of infectivity in ME7/101LL brain was therefore $10^{7.7}$ ifu/g (table 5.2) and was lower than that in ME7/101PP brain. Thus lower titre of infectivity in ME7/101LL brain corresponds with lower levels of PrP^{Sc} exhibited in ME7/101LL compared to ME7/101PP brain. This may suggest that in these models PrP^{Sc} is the infectious agent of TSE.

5.3.3. 263K /101LL brains exhibit high titres of infectivity

Brain homogenate from three separate 263K/101LL animals (chapter 4) were prepared for titration in 101LL mice. Using 263K/101LL (1), TSE was transmitted to 100% of 101LL mice that received 10^{-2} to 10^{-5} dilution of brain homogenate, 92% (11/12) of 101LL mice receiving 10^{-6} dilution, 42% (5/12) of 101LL mice receiving 10^{-7} dilution and 9% (1/11) of 101LL animals

that received 10^{-8} dilution (table 5.2). At 10^{-9} dilution and above, there were no cases of TSE transmission (table 5.2). The dilution of TSE agent that caused disease in 50% of cases was therefore $10^{-6.93}$, and the titre of infectivity for 263K/101LL (1) was $10^{8.6}$ ifu/g (table 5.2), the same titre of infectivity found in ME7/101PP brain.

The second titration experiment was performed using 263K/101LL (2) brain. TSE was transmitted to 100% of 101LL animals in 10^{-2} to 10^{-4} dilution groups, 67% (6/9) of 101LL mice at 10^{-5} dilution and 14% (1/7) of animals at 10^{-6} dilution (table 5.2). No animals succumbed to TSE at 10^{-7} dilution however one animal receiving 10^{-8} dilution of brain homogenate displayed the clinical and pathological symptoms of TSE. In subsequent dilution groups there were no TSE cases (table 5.2). It is not clear whether TSE in the single animal inoculated with 10^{-8} dilution of homogenate was, again, a result of an aggregation of the agent in a non-homogeneous inoculum. The first "zero group" was at 10^{-9} dilution of brain homogenate. The dilution of the 263K/101LL (2) TSE agent that transmitted TSE to 50% of 101LL mice was $10^{-5.39}$ (table 5.2). Thus, the titre of infectivity in 263K/101LL (2) brain was $10^{7.1}$ ifu/g (table 5.2). Given that the degree of accuracy of titration is 0.5 log (Kimberlin, 1976a; Prusiner et al., 1982b), ME7/101LL and 263K/101LL (2) brains can be considered to contain similar titres of infectivity.

Using 263K/101LL (3) brain homogenate, TSE was transmitted to 100% of 101LL animals receiving 10^{-2} dilution only (table 5.2). Transmission of TSE occurred in 50% (3/6) of 101LL mice receiving 10^{-3} dilution, 86% (6/7) of 101LL animals receiving 10^{-4} and 10^{-5} dilutions and 18% (2/11) of 101LL animals at 10^{-6} dilution of brain homogenate (table 5.2). In all subsequent dilution groups TSE was not transmitted thus the first zero group was at 10^{-7} dilution (table 5.2). The dilution of 263K/101LL (3) TSE agent at which 50% of animals succumbed to TSE was $10^{-4.9}$ (table 5.2). The infectivity titre of brain from 263K/101LL (3) was therefore $10^{6.6}$ ifu/g (table 5.2).

In all three 263K/101LL titration experiments performed here the titre of infectivity was greater than expected. The variability of titre of infectivity in

individual 263K/101LL brain homogenates was not unexpected since PrP^{Sc} levels varied in individual mice. This is probably due to the primary passage of the hamster 263K TSE agent into a new host, 101LL mice. It has been previously shown that incubation period, titre of infectivity and PrP^{Sc} deposition levels can differ in individual animals of the same model upon primary passage but that this variation becomes stable upon subsequent passage (Bruce, 1985a; Bruce et al., 2002). Given that PrP^{Sc} levels in all three 263K/101LL brains were substantially lower than in ME7/101PP and ME7/101LL brains (chapter 3) it was expected that the titre of infectivity in 263K/101LL brain would be lower than that in the ME7-infected mouse brains. However, titres of infectivity in 263K/101LL mice were equivalent to those found in ME7-infected mice. Results here indicate that PrP^{Sc} is not the infectious agent of TSE in the 263K/101LL model.

In all three 263K/101LL titration experiments, disease incubation times lengthened and the variation of incubation time within each group increased upon dilution of TSE agent. For 263K/101LL (1) and 263K/101LL (2), disease incubation times at 10^{-2} dilution were extremely short, at 109 ± 2 days and 129 ± 2 days, respectively (table 5.2). Brain homogenate from 263K/101LL (3), at 10^{-2} dilution, produced a disease incubation time of 262 ± 4 days (table 5.2). All three 263K/101LL isolates were transmitted, at 10^{-2} dilution, to 101PP mice. Only 263K/101LL (2) resulted in TSE, with a mean incubation time of 296 ± 24 days.

5.4. Discussion

5.4.1. High titres of infectivity are found in brain with low PrP^{Sc} levels

Titrated brain from ME7/101PP contained $10^{8.5}$ ifu/g (table 5.4). This is a high titre of infectivity and it was not surprising to find such high levels of infectivity in a brain exhibiting high PrP^{Sc} levels at disease end-point (chapter 3). It was surprising however, to find that brain from 263K/101LL (1), that exhibited extremely low PrP^{Sc} levels at disease end-point (chapter 3) contained the same high levels of infectivity at $10^{8.6}$ ifu/g (table 5.4). Despite the absence of detectable PrP^{Sc} in 263K/101LL (2) brain homogenate (chapter 3), similar titres of infectivity were found in ME7/101LL ($10^{7.7}$ ifu/g) and 263K/101LL (2) brain ($10^{7.1}$ ifu/g)(table 5.4). Moreover, 263K/101LL (3) also exhibited no detectable PrP^{Sc} in brain homogenate (chapter 3) but contained appreciable amounts of infectivity, $10^{6.5}$ ifu/g (table 5.4), similar to ME7/101LL brain.

This is the first time substantial levels of infectivity have been reported in transmissible brain containing non-detectable levels of PK-resistant PrP^{Sc}. However, preliminary investigations in the GSS/101LL model (Manson et al., 1999) also found similarly high titres of infectivity ($10^{6.4}$ ifu/g) in transmissible brain exhibiting extremely low PrP^{Sc} levels. Moreover, similar to the 263K/101LL model, short disease incubation times were found in the GSS/101LL model, at 134 days (R. Barron, unpublished data – appendix F). Although the correlation between PrP^{Sc} level and infectivity titre has not been thoroughly investigated in the GSS/101LL model, these data may indicate that infectivity in the GSS/101LL and 263K/101LL models is not conferred by PK-resistant PrP^{Sc}.

If PK-resistant PrP^{Sc} is the infectious agent of TSE, it is surprising that brain from 263K/101LL (2) & (3) contains relatively high titres of infectivity. Across all of the models investigated here, the lack of correlation between PrP^{Sc} and infectivity suggests that either (i) there is more PK-resistant PrP^{Sc} in 263K /101LL brain that is not detected by immunoblot, or (ii) PK-resistant PrP^{Sc} alone is not the infectious agent of TSE. If PrP^{Sc} is the

infectious agent of TSE then TSE-infected tissue containing high levels of PrP^{Sc}, should contain a high titre of infectivity and TSE should be transmitted in short incubation times. If PK-resistant PrP^{Sc} is the infectious agent of TSE why do models with the same titre of infectivity in brain not contain the same level of PrP^{Sc} in brain, regardless of TSE strain?

One infectious unit (ifu) of TSE is proposed to contain 10^4 to 10^5 molecules of PrP^{Sc} as identified from hamster 263K experiments (Beekes, Baldauf & Diringer, 1996; Hope & Manson, 1991; McKinley et al., 1983). The data presented here may suggest that the number of molecules per ifu differs in different TSE models. This may explain why ME7/101PP and 263K/101LL (1) brains exhibit the same titre of infectivity yet ME7/101PP contains more PK-resistant PrP^{Sc}. If PrP^{Sc} is the infectious agent in TSE this may indicate that there are intrinsic differences in the PrP^{Sc} in different models.

5.4.2. Variable disease incubation times from individual brains

Using 263K-infected hamsters an inverse relationship between incubation time and titre of infectivity was demonstrated (Prusiner et al., 1982b) where short incubation times of TSE transmission correlated with high titre of infectivity. Within the ME7 models studied here, at secondary passage, this inverse relationship also occurs. ME7/101PP has a higher titre of infectivity and shorter incubation time than ME7/101LL. This relationship also appears to correlate within the secondary passage of 263K/101LL isolates, where 263K/101LL (1) has the shortest incubation time and highest titre of infectivity and 263K/101LL (3) has the lowest titre of infectivity and longest incubation time. However, the correlation between incubation time and infectivity titre did not appear to hold across all of the different models. ME7/101PP and 263K/101LL (1) models have the same infectivity titre yet 263K/101LL (1) has the shortest incubation time. Furthermore ME7/101LL and 263K/101LL (2) have similar titres of infectivity yet 263K/101LL (2) has a shorter incubation time. It is not clear why there are differences in disease incubation times between models with the same titre of infectivity.

Since variability of TSE incubation time and titre of infectivity was demonstrated within the 263K/101LL model, it may have been prudent to investigate more than one brain in the ME7/101PP and ME7/101LL models. One animal from the ME7 models was investigated since it had been shown that ME7 is stable upon passage in *Prnp*-a mice. However, it is known that genes other than *Prnp* can affect TSE incubation time (Lloyd et al., 2001; Manolakou et al., 2001). The ME7 TSE agent used in these experiments originated from a C57Bl mouse thus the subtle differences in genetic background from C57Bl to 129/Ola mice expressing 101PP and 101LL alleles may cause this to behave like a primary pass agent. In the ME7/101PP and ME7/101LL models individual mice may exhibit differences in intensity of PrP deposition, vacuolation and disease incubation time. These animals may have provided additional data in the correlation experiments performed here, however due to space, breeding and time constraints it was not possible to perform additional titration experiments.

5.4.3. What causes different TSE incubation times in each model?

The three 263K/101LL isolates studied here each produced different disease incubation times at 10^{-2} dilution. It is not clear whether incubation time is controlled by the titre of infectivity or different strain effects upon passage. Each 263K/101LL isolate originates from a single hamster 263K source, and it is not clear whether each brain contained a different TSE isolate that is being selected for upon passage of each brain. To investigate this, dose response curves for each experiment were plotted. A dose response curve plots the relationship between dose of TSE agent and disease incubation time (Kimberlin & Walker, 1978). By normalising the titre of infectivity and plotting this against incubation time at each dilution (see appendix E for data) each titration experiment produced distinct dose response curves (figure 5.5). The curves indicated that TSE incubation time was controlled by strain of TSE agent, rather than the titre of infectivity *per se* of each isolate. In 101LL mice, each isolate of 263K/101LL produced a distinct curve thus indicating TSE strain control over TSE incubation time. (Additionally, the GSS/101LL isolate also produced a distinct curve in

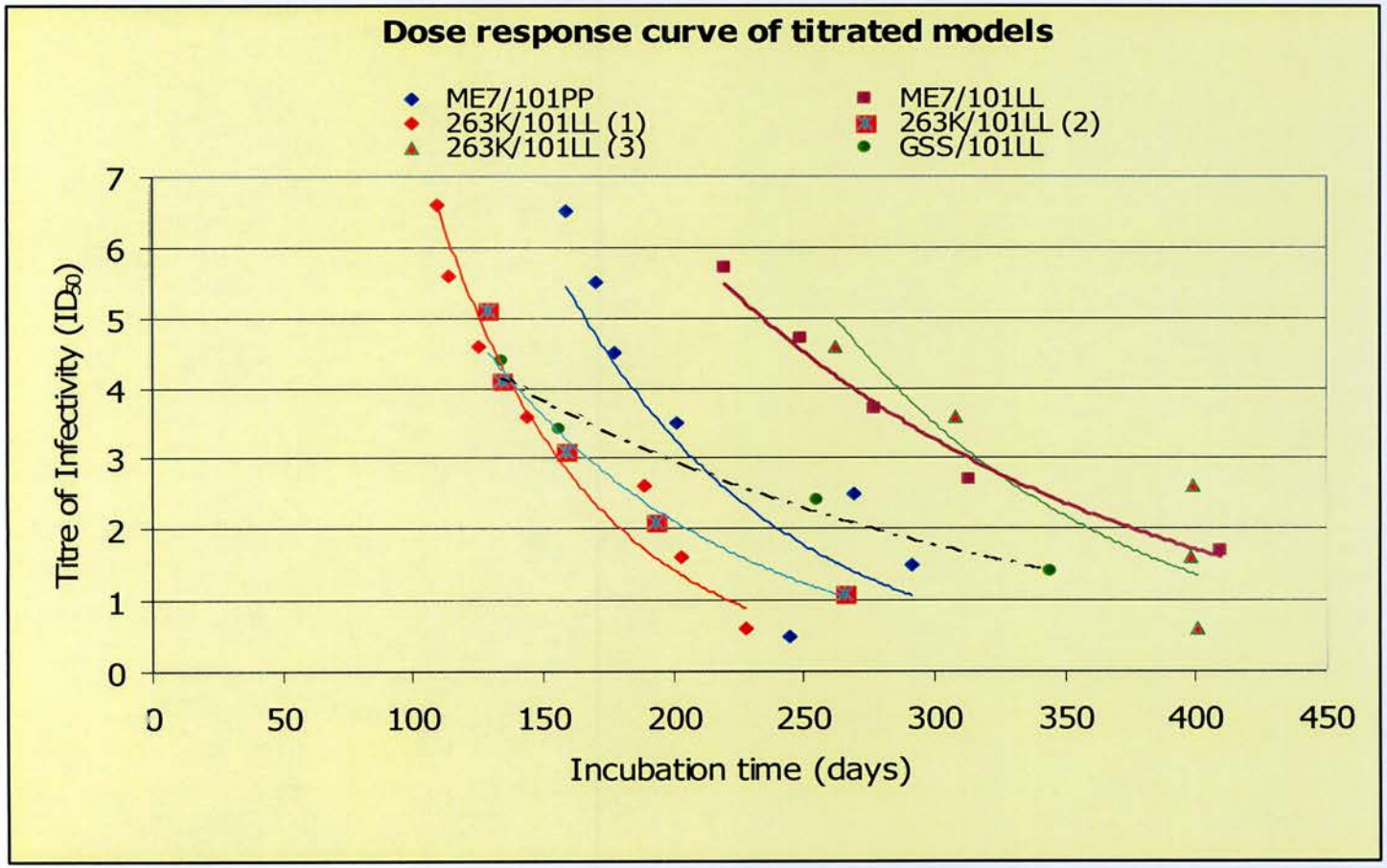

Figure 5.2 Bioassay dose response curves

Titre of infectivity is normalised for each injected dilution of TSE agent (data in appendix D) and plotted against mean disease incubation time for each group. Each line represents one TSE agent. The position of each line indicates the effect TSE agent has upon disease incubation time. Where curves are superimposed, this represents TSE agents that behave in a similar manner, affecting disease incubation time in the same way.

101LL mice indicating an effect of TSE strain upon TSE incubation time.) Moreover, ME7/101PP and ME7/101LL experiments produced distinct curves indicating that host factors may also play a role in determining disease incubation time.

It is not known how host control may be exerted. The deposition of PrP^{Sc} may control disease incubation time. Whilst PrP^{Sc} deposition is extremely low in all three 263K/101LL models, PrP^{C} conversion to PrP^{Sc} may trigger rapid apoptosis and the onset of neuronal loss may account for earlier death in 263K/101LL (1) and (2). Targeting of disease-associated pathology other than PrP^{Sc} deposition, such as vacuolation, neuronal loss, apoptosis and astrocytosis, may affect the survival time of animals infected with a particular TSE isolate. Vacuolation was present in all models studied here (appendix G) however it is not clear whether specific vacuolar targeting to critical brain areas may have caused the death of TSE-infected animals in the studies here. The correlation between vacuolation and PrP^{Sc} levels at secondary pass could be further studied to investigate the role of pathology in these models. In contrast, as suggested by Kimberlin *et al*, it is possible that a genetic component of the TSE strain could target disease-associated pathology to critical brain areas at different times (Kimberlin & Walker, 1988). This may account for different disease incubation times in different models. To clarify whether TSE-associated pathology, driven by the presence of PK-resistant PrP^{Sc}, is responsible for the death of TSE-infected mice in the models studied here, time course assessment of the onset of PrP^{Sc} deposition, vacuolation, neuronal loss and the presence of pro-apoptotic markers should be performed in secondary pass brain tissue.

The studies described in this thesis were designed to investigate the correlation between PK-resistant PrP^{Sc} and infectivity in TSE models exhibiting different levels of PrP^{Sc} in brain. In this chapter it has been demonstrated that high titres of infectivity are present in brain that exhibits low PrP^{Sc} levels. Therefore to fully assess the correlation between PrP^{Sc} and infectivity, and to investigate the number of molecules of PrP^{Sc} per ifu in

each TSE model studied here, the detailed quantification of the levels of PK-resistant PrP^{Sc} in each model was subsequently performed.

6. Measurement and Quantification of PrP

6.1. Introduction

As TSE disease progresses toward the terminal stages, PrP^{Sc} accumulates in the brain of TSE-infected animals (Beekes et al., 1996; Czub et al., 1986b; De Armond et al., 1989; Jeffrey et al., 2001). This contributes to an increase in the amount of total PrP (PrP^{C} plus PrP^{Sc}) in brain, which can be as much as 10 to 20-fold more than the total PrP in uninfected animals (DeArmond et al., 1987). The amount of PrP^{C} in diseased animals has been reported to be similar to that in uninfected animals (Meyer et al., 1986). Furthermore, the amount of PrP^{Sc} in brain at disease end-point differs between affected individuals and between different experimental models (Gambetti, Parchi & Chen, 2003; Hope et al., 1999; Kuczius & Groschup, 1999). In human sporadic CJD different brain areas have been found to exhibit different levels of PrP^{Sc} (MacDonald, Sutherland & Ironside, 1996), this has also been described in the hamster 263K model (DeArmond et al., 1987).

In vitro studies have shown the conversion of a PK-sensitive form of PrP (PrP-sen) to a PK-resistant form of PrP (PrP-res) and demonstrate the principal of PrP^{C} directly binding to PrP^{Sc} (chapter 1.3.5). It has not yet been shown that the *in vitro* production of PrP-res in various systems produces a concurrent increase in infectivity thus it is arguable whether PrP^{Sc} alone is the infectious agent. Moreover, preparations of PrP^{Sc} have been shown to contain additional proteins (Bolton et al., 1987; Kocisko et al., 1995). Thus, in the infectious process, the involvement of molecules other than PrP^{Sc} cannot be ruled out. The relationship between PrP^{Sc} and other molecules is not yet understood, although PrP has been shown to interact with the laminin receptor (Rieger et al., 1999) and small RNA molecules (Weiss et al., 1997). Indeed conversion of PrP^{C} to PrP^{Sc} in a cell-free system has been shown to be enhanced by the presence of RNA (Deleault et al., 2003). It is not yet clear whether such molecules assist with the normal function of PrP^{C} or if they assist in the production of an

infectious PrP. No disease-associate nucleic acid has yet been found, however there is no doubt that PrP plays a role in TSE disease (chapter 1.8.2).

Studies that suggested a strong correlation between PK-resistant PrP^{Sc} and infectivity have also demonstrated that one infectious unit (ifu) is comprised of more than one molecule of PrP^{Sc}. Early investigations of 263K-infected hamster calculated the number of molecules of PrP^{Sc} in one infectious unit at 10^4 to 10^5 molecules (McKinley et al., 1983; Meyer et al., 1986). In the hamster 263K model purification of PrP^{Sc} as SAF (scrapie associated fibrils) also calculated 10^4 to 10^5 molecules of PrP^{Sc} per infectious unit in the same TSE model (Hilmert & Diringer, 1984). These figures were verified by other investigators (Hope & Manson, 1991). The PrP^{Sc} molecule to infectivity ratio assumes an average molecular weight for PrP of 30kDa and does not rule out the possibility that forms of PrP other than PrP^{Sc} may contribute to infectivity. Just as each TSE model has distinct pathology in terms of PrP deposition pattern and vacuolation profile so the number of PrP^{Sc} molecules that make up one infectious unit may differ in each model. The contribution of PK-resistant PrP^{Sc} to the disease as a whole may therefore be different for each TSE model.

In order to correlate PrP^{Sc} levels in terminal brain with the titre of infectivity, PrP^{Sc} levels were quantified in TSE-infected mouse brain. Since it has been shown that there are different PrP^{Sc} levels in different areas of the same brain (De Armond et al., 1989), PrP^{Sc} levels were measured from whole brain homogenate rather than from specific brain areas. To ensure a direct correlation with the titration data, PrP^{Sc} was quantitatively measured in the same brain homogenates that were used to titrate infectivity, from one ME7/101PP and one ME7/101LL animal and from three separate 263K/101LL animals, 263K/101LL (1), (2) and (3) (chapter 5). The quantification of PrP^{Sc} in these models allowed the calculation of the number of PrP^{Sc} molecules per infectious unit to be performed to investigate whether this agreed with previous data or differed in these models.

Immunoblot is generally used as a qualitative assay. ELISA is a quantitative method, which relies on antibody detection of the protein of interest. However immunoblot samples can be quantified using careful densitometric analysis performed on serial dilutions of homogenate containing the protein of interest. For accurate measurement by immunoblot, the protein of interest must be diluted to the limit of detection. Given that previous studies had reported high reproducibility of results using immunoblot to detect PrP^{Sc} (Schaller et al., 1999), and that sample numbers in the study performed in this thesis were small, immunoblot was chosen to quantitatively measure PrP in the samples here. During the course of this work an ELISA became available, therefore the DELFIA methodology (Detection Enhanced Lanthanine Fluorometric ImmunoAssay - described in chapter 1.8.1) was also employed in these studies.

6.2. Methodology

6.2.1. Preparation of brain homogenate for immunoblot

The same brain homogenates as previously used for the titration experiments (chapter 5) were used here. Brain homogenate inoculum was prepared in PBS (chapters 2.22.2 & 5.2.1) from one ME7/101PP animal, one ME7/101LL animal and three separate 263K/101LL mice (263K/101LL (1), 263K/101LL (2) and 263K/101LL (3)), previously described (chapters 3 & 4).

For immunoblot, equal volumes of inoculum (10% brain homogenate) and 2x NP40 detergent buffer were mixed and further homogenised. This gave rise to a 5% homogenate (chapter 2.6.2). This was stored at –70°C in 20µl aliquots and a fresh aliquot was used for each immunoblot.

6.2.2. Immunoblot quantification of PK-resistant PrP^{Sc} and total PrP

A two-fold serial dilution of five percent brain homogenate was prepared using PK-treated (chapter 2.7.1) (at 20µg/ml final concentration) homogenate for PrP^{Sc} detection and untreated homogenate for total PrP detection. Brain homogenate was diluted in uninfected, PK-treated (20µg/ml final PK concentration) brain homogenate (101PP or 101LL appropriate for each model) for PrP^{Sc} detection and in PBS for total PrP detection. Each diluted sample (10µl) was mixed with loading buffer and sample reducing agent (1x final concentration of each) and 20µl of each sample was loaded per well for gel electrophoresis (chapter 2.10). Samples were loaded across two 12% tris/glycine gels (Invitrogen), at brain homogenate concentrations ranging from 2% to 0.000975% brain equivalent (equivalent to 400µg to 0.2µg wet weight of brain). Non PK-treated samples were loaded to control for PrP detection by the antibodies, and a control sample of 50ng recombinant PrP (rPrP) was added to one lane on each SDS-PAGE gel to control for blot-to-blot variation (chapter 2.13). Where possible experiments were repeated three times to control for experimental error. PrP^{Sc} was detected using the monoclonal antibody 8H4

(chapter 2.2) and visualised with secondary rabbit α-mouse (chapter 2.3) and West Dura substrate. Chemiluminesence was captured on x-ray film for 30 seconds and then one minute before mounting the blot on the Kodak Image Station 440 to digitally capture the chemiluminesence for one hour (chapter 2.14).

For each lane in each immunoblot, the intensity of PrP^{Sc} detected was measured using the Kodak image analysis software and expressed as a number of pixels making up that image (chapter 2.14) (see appendix H for data). Each sample intensity was compared to the intensity of 50ng rPrP on that blot, and was quantified accordingly. Each sample lane represented a dilution of homogenate and this dilution factor was applied to each lane to give values for the loaded 10% brain homogenate. Due to experimental error, the values varied between each experimental run and for each dilution within the run, therefore a mean value was calculated for all diluted samples run per TSE model. The standard deviation of samples loaded onto the same blot, and between blots indicated the variability of PrP detection using immunoblot. Due to the doubling dilution series, this assay will not distinguish less than a 2-fold difference in PrP level between samples.

6.2.3. Quantification of PrP using DELFIA

DELFIA measures PrP^{C} and PrP^{Sc} based on their relative solubility in 1M GndHCl. The critical measurement of infectivity titre and the quantification of PrP had limited the availability of each brain homogenate used in these studies. Fresh brain from each model was therefore used in the DELFIA analysis of PrP. Although these brains were representative of each model, infectivity was not titrated consequently PrP^{Sc} levels could not be directly correlated with titre of infectivity. PrP^{Sc} and PrP^{C} were measured in homogenate that originated from one uninfected 101LL, one ME7/101LL and two 263K/101LL mice, designated (a) and (b). Additionally, the PrP isoforms were also measured in one GSS/101LL brain (the non-titrated brain described in chapter 5). From each brain, 10% homogenate was prepared (chapter 2.6.1) and the DELFIA methodology followed (chapter

2.25). These experiments were kindly performed by D King (NPU, Edinburgh, UK), who optimised the DELFIA process.

6.3. Results

6.3.1. Sensitivity of Immunoblot detection

To determine the sensitivity of immunoblot pure recombinant PrP (rPrP), which produced a single band on coomassie stained gels (figure 6.1A), was imunoblotted using the monoclonal antibody 8H4. This protein was used as a control for the experiments described here since it produces a single band upon immunoblot, which can be easily quantified. Recombinant PrP was used to control for blot-to-blot variation and to enable PrP levels to be quantified. This was consistently detected at 5-10ng as a single band at around 28kDa (figure 6.1B) as observed previously (Takekida et al., 2002). If present, degradation products of rPrP were detected below 20kDa.

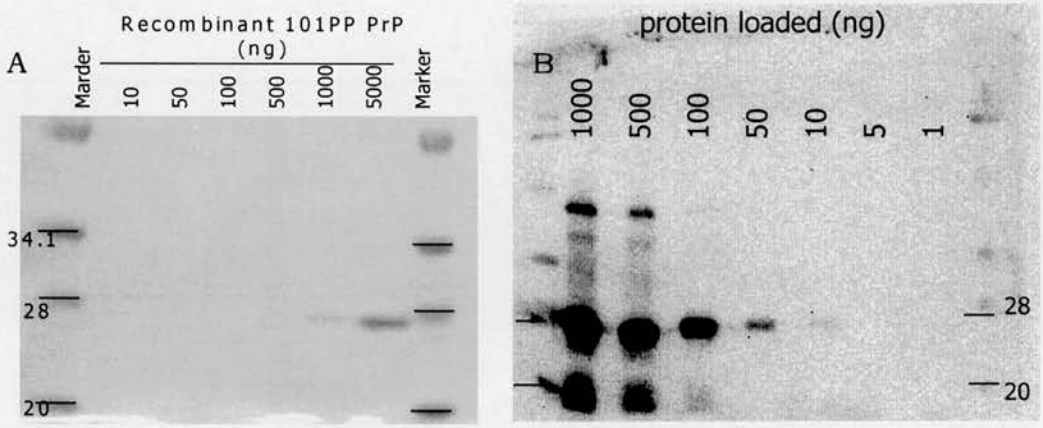

Figure 6.1 Sensitivity of detection of recombinant PrP

Wild type 101PP recombinant PrP analysed using 12% tris/glycine SDS-PAGE (A) serially diluted, loaded at 10-5000 ng per well and coomassie-blue stained (chapter 2.15.2), and, (B) serially diluted, loaded at 1-1000ng and immunoblot detected (chapter 2.12). PrP detected using 8H4 and visualised using secondary rabbit anti-mouse antibody and West Dura substrate (chapters 2.2 & 2.3). rPrP was diluted in PBS before loading 20μl per well of indicated concentrations. Sizes of markers are shown in kDa.

A preliminary investigation was undertaken to assess the usefulness of deglycosylating PrP for measurement of the resultant single band rather than the three bands of glycosylated PrP. In this experiment the amount of PrP measured in deglycosylated samples was less than measured in untreated samples (figure 6.2 & table 6.1 - compare PNGase treated against untreated samples). This may have been due to loss of some PrP during the deglycosylation process. Additionally, incomplete deglycosylation meant that all bands in a sample lane were measured, thus proving of no

advantage over the measurement of all three glycosylated bands of PrP. Sample deglycosylation was therefore was not used for PrP quantification studies.

Figure 6.2 Comparison of glycosylated and deglycosylated 139A brain homogenate

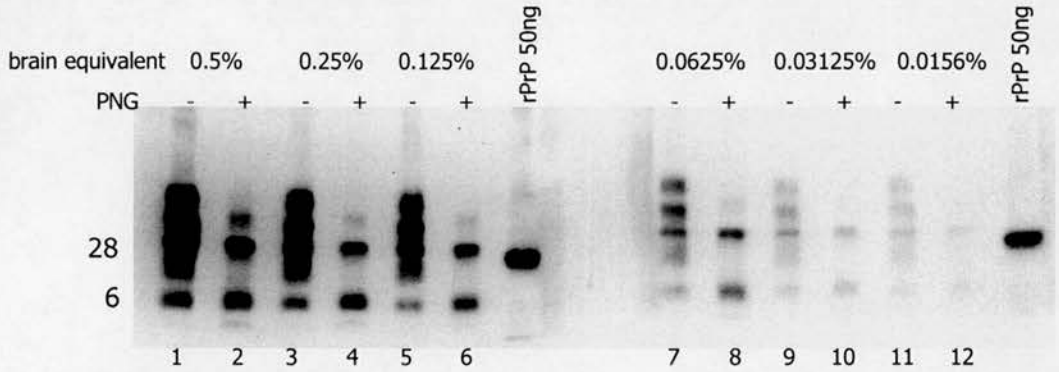

Total PrP quantification (chapter 6.2.2) in PNGase treated (PNG+ lanes) or untreated (PNG- lanes) brain homogenate from 139A-infected mouse. 0.5% to 0.0156% brain homogenate was loaded across two SDS-PAGE gels. Control recombinant PrP (rPrP) was loaded at 50ng per well in one well per SDS-PAGE gel. PrP was detected by immunoblot using monoclonal antibody 8H4 (chapter 2.2) and visualised using secondary rabbit α-mouse antibody (chapter 2.3) and West Dura substrate. Marker sizes are indicated in kDa. * indicates the typical 3-band pattern of di-, mono- and unglycosylated PrP. Deglycosylated PrP was detected at 30kDa. Recombinant PrP was detected at 28kDa. Incomplete deglycosylation of di- and monoglycosylated bands visible at 33kDa. The lower 6kDa band probably represents natural degradation products of deglycosylated PrP. Lane numbers correspond to data in table 6.1.

Lane	PNGase	Band intensity (pixels)	ng equivalent (compared to rPrP)
1	-	283590	280
2	+	48515	48
3	-	164590	162
4	+	26580	26
5	-	34101	34
6	+	21780	21
7	-	26339	26
8	+	35039	35
9	-	13621	13
10	+	7950	8
11	-	1549	2
12	+	1207	1
rPrP	n/a	50719	50

Table 6.1 Quantification of glycosylated and deglycosylated PrP in 139A brain homogenate

Measurement of PrP in brain homogenate, untreated (PNG-) or treated with PNGase (PNG+) to deglycosylate the protein. The pixel intensity of each band per lane, as depicted in figure 6.2, was detected. The sum of individual bands was taken where multiple bands were detected in one lane. Using a recombinant protein control, the pixel intensity was converted to a ng equivalent (chapter 6.2.2).

6.3.2. Detection of PK-resistant PrP^{Sc} in infected brain from each model

PrP^{Sc} levels in ME7/101PP brain homogenate (figure 6.3) were judged to be approximately two-fold higher than PrP^{Sc} levels in ME7/101LL brain homogenate (figure 6.4) when detected by immunoblot. PrP^{Sc} levels in 263K/101LL brain homogenates (figures 6.5 & 6.6) were judged to be at least five-fold lower than in ME7/101PP homogenate and at least two and a half-fold lower than in ME7/101LL homogenate. The mean value of PrP^{Sc} detected in each brain homogenate was 4010 ± 511ng (± standard error) for ME7/101PP (figure 6.3), 1979 ± 462ng for ME7/101LL (figure 6.4) and 872 ± 292ng for 263K/101LL (1) (figure 6.5). No PrP^{Sc} was detected in brain homogenate from 263K/101LL (2) or (3) (figure 6.6), indicating variable levels of PrP^{Sc} from individual 263K/101LL brain.

It is not clear why there was less PK-resistant PrP^{Sc} in the ME7/101LL and 263K/101LL brain homogenates compared to ME7/101PP homogenate. This may reflect a general reduction in the amount of total PrP in the 101LL mice. This reduction may perhaps be due to differential processing of PrP^{C} in these animals or differences in the production of PrP^{Sc} during the conversion process.

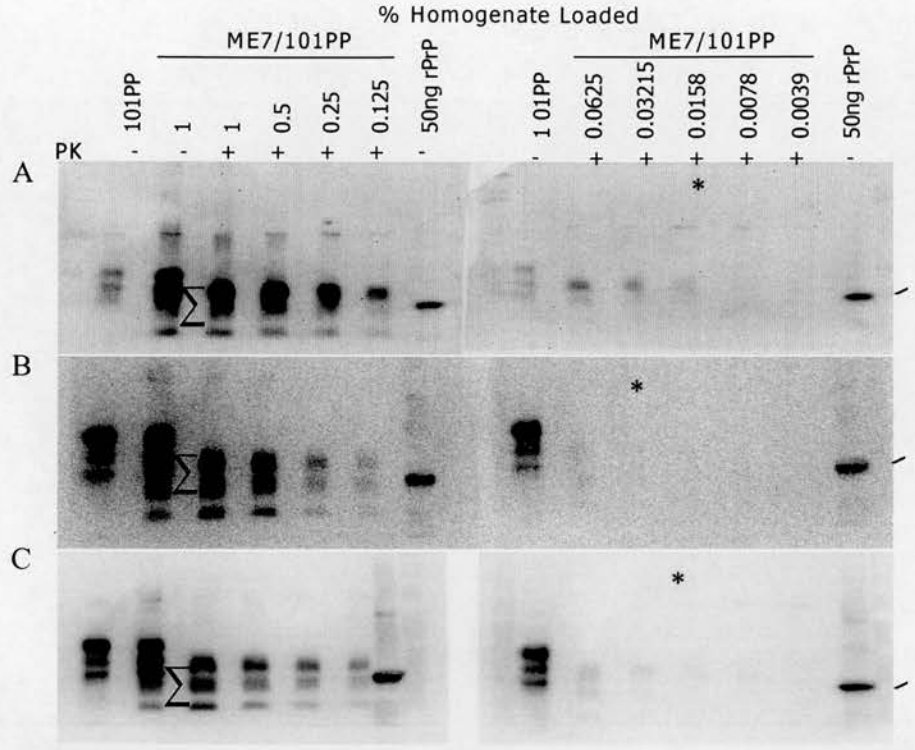

% homogenate loaded	Concentration of PrP^{Sc} in ME7/101PP brain homogenate (ng)		
	Blot A	Blot B	Blot C
1	3715	3485	3671
0.5	5716	5732	3273
0.25	5127	3287	3704
0.125	4495	2719	4975
0.0625	8696	392	1162
0.0313	7241	0	1509
0.0156	2901	0	0
0.0078	0	0	0
0.0039	0	0	0
0.0020	0	0	0
Mean PrP^{Sc} ± SE	4010 ± 511		

Figure 6.3 Quantification of PK-resistant PrP^{Sc} in ME7-infected 101PP brain homogenate

PrP^{Sc} detected in ME7/101PP brain homogenate treated with PK (20μg/ml final concentration), then two-fold serially diluted in uninfected 101PP brain homogenate (PK-treated at 20μg/ml) to give dilutions of brain from 1 to 0.0039% when loaded onto 12% tris/glycine SDS-PAGE gels. Control homogenates (loaded at 1%) of uninfected 101PP and ME7/101PP brain, PK untreated, were also included. PrP was detected using 8H4 monoclonal antibody (chapter 2.2) and visualised using West Dura substrate. Blots (A), (B) & (C) represent three separate experiments performed on different days. On each blot the limit of detection is marked*. Recombinant PrP is indicated at 28kDa (<). The three glycosylated bands of PrP were detected in each lane (Σ) and the sum of the pixel intensities was taken. Compared to recombinant PrP, pixel intensity was converted to ng and the homogenate dilution factor was taken into account to provide a concentration of PrP^{Sc} for 10% brain homogenate (table 6.2). A mean of the PrP^{Sc} concentrations obtained for each lane over all blots was then calculated. A value of zero indicates no PrP^{Sc} was detected.

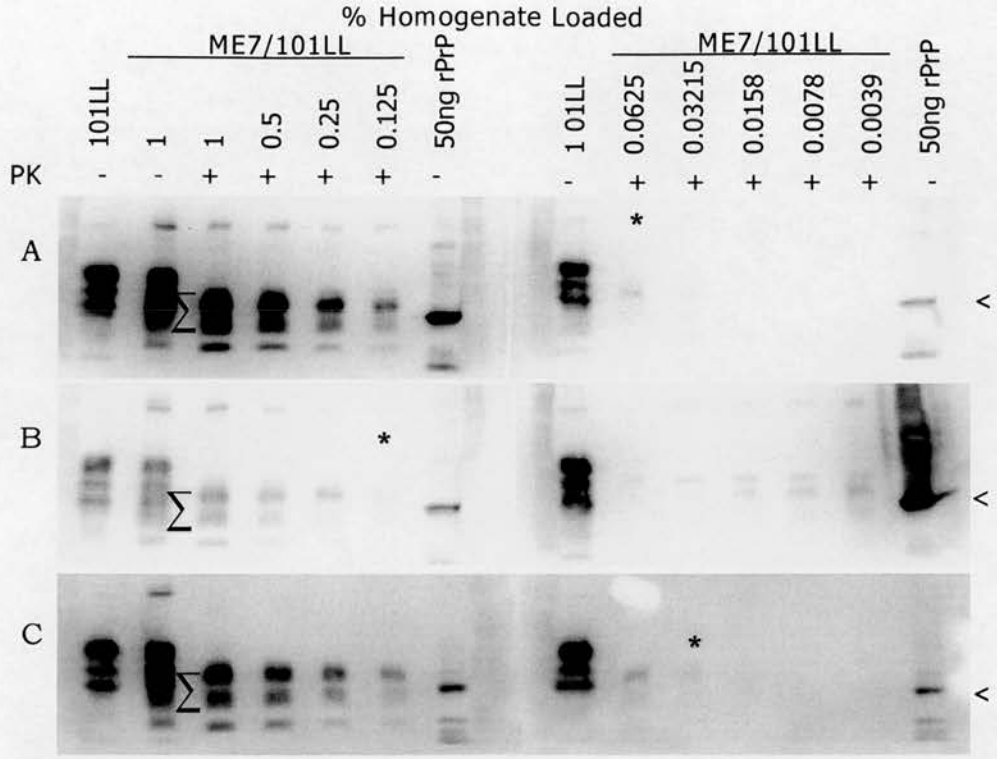

% homogenate loaded	Concentration of PrP^{Sc} in ME7/101LL brain homogenate (ng)		
	Blot A	Blot B	Blot C
1	4785	1330	1091
0.5	4323	1723	1007
0.25	5757	1150	1268
0.125	7463	1177	332
0.0625	4176	941	319
0.0313	3178	1140	225
0.0156	0	0	168
0.0078	0	0	48
0.0039	0	0	0
0.0020	0	0	0
Mean PrP^{Sc} ± SE	1979 ± 462		

Figure 6.4 Quantification of PK-resistant PrP^{Sc} in ME7/101LL brain homogenate

PrP^{Sc} detected in ME7/101LL brain homogenate treated with PK (20μg/ml final concentration), then two-fold serially diluted in uninfected 101LL brain homogenate (PK-treated at 20μg/ml) to give dilutions of brain from 1 to 0.0039% when loaded onto 12% tris/glycine SDS-PAGE gels. Control homogenates of uninfected 101LL and ME7/101LL brain, PK untreated, were also loaded at 1% homogenate each. PrP was detected as before (figure 6.3) Blots (A), (B) & (C) represent three separate experiments performed on different days. On each blot the limit of detection is marked*. Recombinant PrP is indicated at 28kDa (<). The three glycosylated bands of PrP were detected in each lane (Σ). The pixel intensities for each band were converted to ng as previously detailed (figure 6.3). A value of zero indicates no PrP^{Sc} was detected.

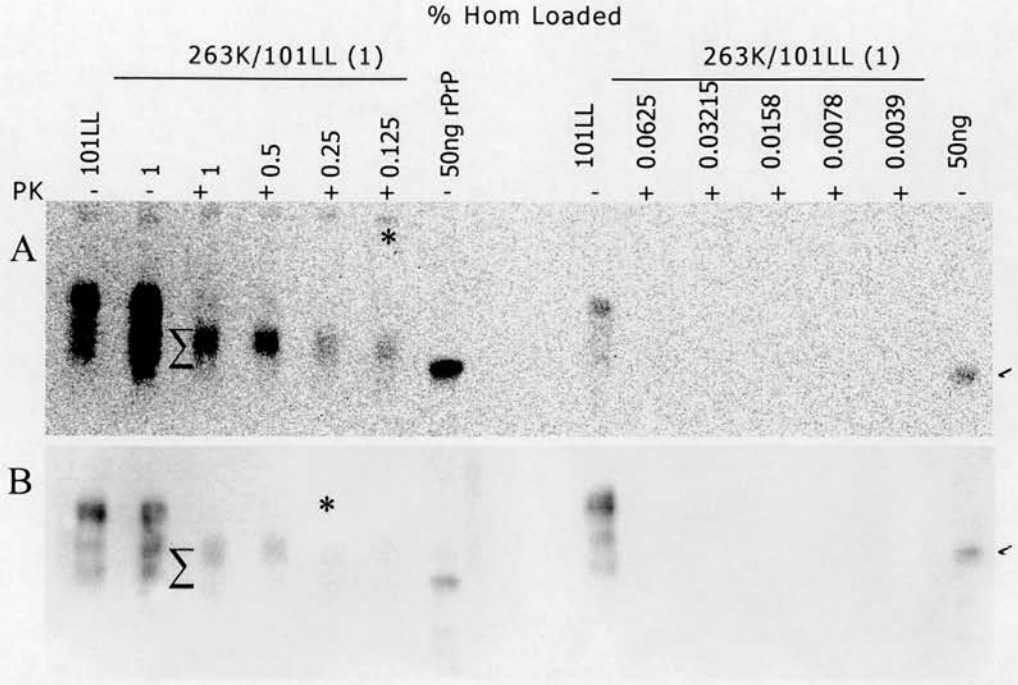

% homogenate loaded	Concentration of PrP^{Sc} in 263K/101LL (1) brain homogenate (ng)	
	Blot A	Blot B
1	439	739
0.5	826	1371
0.25	396	2667
0.125	537	0
0.0625	0	0
0.0313	0	0
0.0156	0	0
0.0078	0	0
0.0039	0	0
Mean PrP^{Sc} ± SE	872 ± 292	

Figure 6.5 Quantification of PK-resistant PrP^{Sc} in 263K-infected 101LL (1) brain homgenate

PrP^{Sc} detected in 263K/101LL (1) brain homogenate treated with PK (20μg/ml final concentration), then two-fold serially diluted in uninfected 101LL brain homogenate (PK-treated at 20μg/ml) to give dilutions of brain from 1 to 0.0039% when loaded onto 12% tris/glycine SDS-PAGE gels. Control uninfected 101LL and 263K/101LL brain homogenates, PK untreated, were loaded at 1% homogenate. PrP was detected as before (figure 6.3) Blots (A) & (B) represent two separate experiments performed on different days. On each blot the limit of detection is marked*. Recombinant PrP is indicated at 28kDa (<). The three glycosylated bands of PrP were detected in each lane (Σ). The pixel intensities for each band were converted to ng as previously detailed (figure 6.3). A value of zero indicates no PrP^{Sc} was detected.

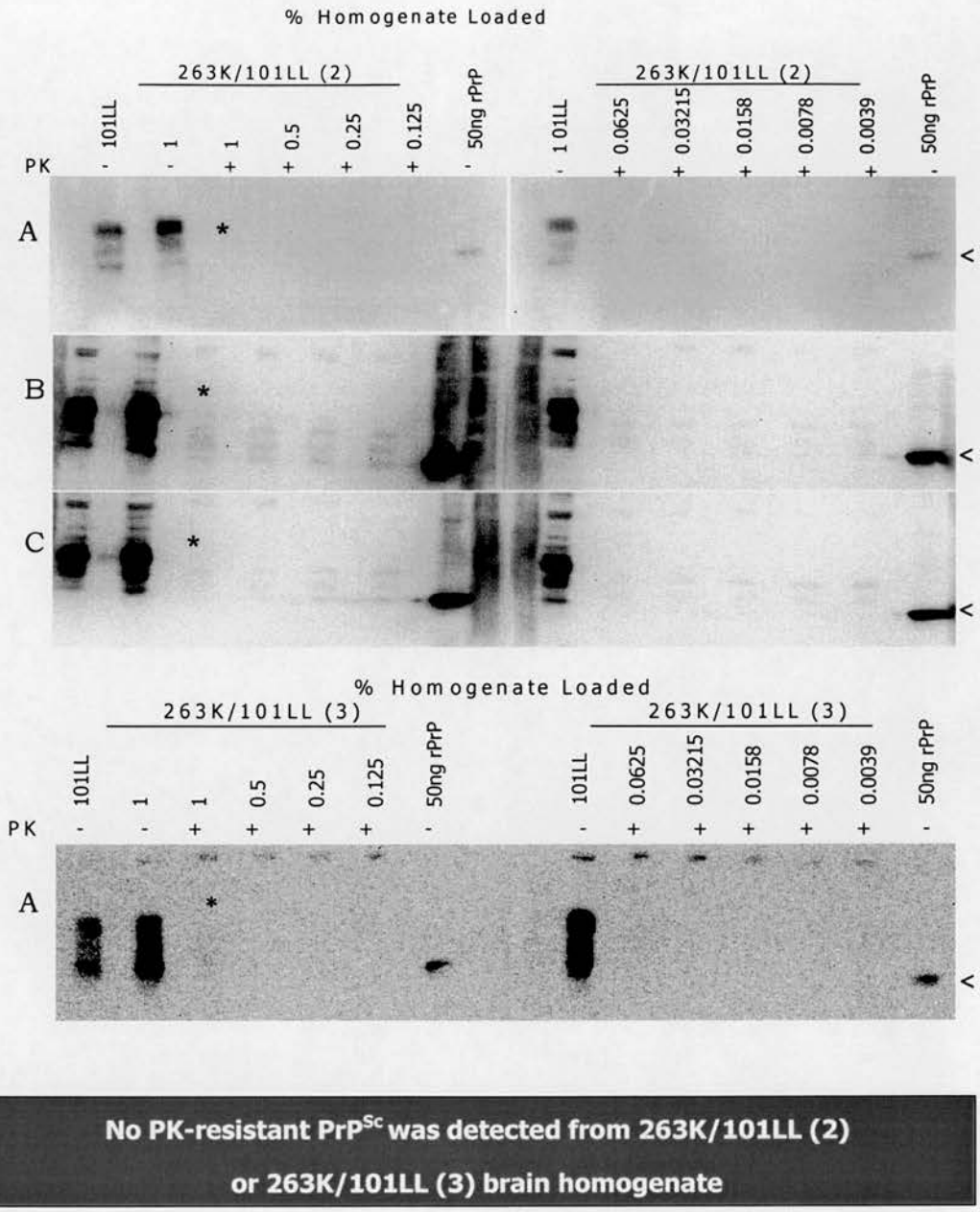

No PK-resistant PrP^{Sc} was detected from 263K/101LL (2) or 263K/101LL (3) brain homogenate

Figure 6.6 Quantification of PK-resistant PrP^{Sc} in 263K-infected 101LL (1) brain homgenate

PrP^{Sc} detected in 263K/101LL (2) and 263K/101LL (3) brain homogenate treated with PK (20μg/ml final concentration), then two-fold serially diluted in uninfected 101LL brain homogenate (PK-treated at 20μg/ml) to give dilutions of brain from 1 to 0.0039% when loaded onto 12% tris/glycine SDS-PAGE gels. Control uninfected 101LL and 263K/101LL brain homogenates, PK untreated, were loaded at 1% homogenate. PrP was detected as before (figure 6.3). For 263K/101LL (2) blots (A), (B) & (C) represent three separate experiments performed on different days. Only one experiment (blot A) was performed using 263K/101LL (3). On each blot the limit of detection is marked*. Recombinant PrP is indicated at 28kDa (<). The three glycosylated bands of PrP were detected in each lane (Σ). The pixel intensities for each band were converted to ng as previously detailed (figure 6.3). In all analysis, only zero values were obtained for all PK-treated lanes.

6.3.3. Total PrP detection in titrated brain

To address whether total PrP levels differed in each model, and to be able to assess the amount of PrP^{C} in each infected animal, the total amount of PrP was examined in the same brain homogenate as used for PrP^{Sc} measurement (chapter 6.3.2). Uninfected 101PP and uninfected 101LL brain homogenates were found to contain a similar amount of total PrP, with 3314 ± 716 (SE) ng total PrP present in 101PP and 3834 ± 709 ng present in 101LL brain homogenates (figure 6.7). ME7/101PP brain homogenate contained 6180 ± 1431 ng total PrP (figure 6.8), approximately 4-fold more than the total PrP detected in ME7/101LL brain homogenate, which contained 2292 ± 571 ng total PrP (figure 6.9). This large difference was initially attributed to less PrP^{Sc} produced in 101LL compared to 101PP mice during disease, however it was subsequently found that it was probably due to a degradation of PrP during storage of this sample (chapter 6.3.4). It is not clear why this sample in particular was affected since all samples were stored in the same –70°C freezer. In 263K/101LL (1) brain homogenate 5730 ±1062 ng total PrP was detected (figure 6.10) and 263K/101LL (3) exhibited 4114 ± 928 ng total PrP (figure 6.11). These data indicated that ME7/101PP and 263K/101LL (1) contained approximately 2-fold more total PrP than found in uninfected animals and that 263K/101LL (3) contained approximately the same amount of total PrP as in uninfected animals. Total PrP levels were found to be similar in 263K/101LL (1) and 263K/101LL (3) brain homogenates. The detection limits of 263K/101LL (1) and (3) were within a 2-fold range of that for ME7/101PP. Therefore, there did not appear to be a major difference between total PrP levels in ME7/101PP, 263K/101LL (1) and 263K/101LL (3) brain homogenates.

Infected animals have been shown to contain up to 10x more total PrP than uninfected animals (Meyer et al., 1986). The finding here that uninfected and infected brain exhibited only up to 2-fold differences in total PrP levels was therefore surprising since the production of PrP^{Sc} during disease should increase total PrP levels in infected compared to uninfected animals.

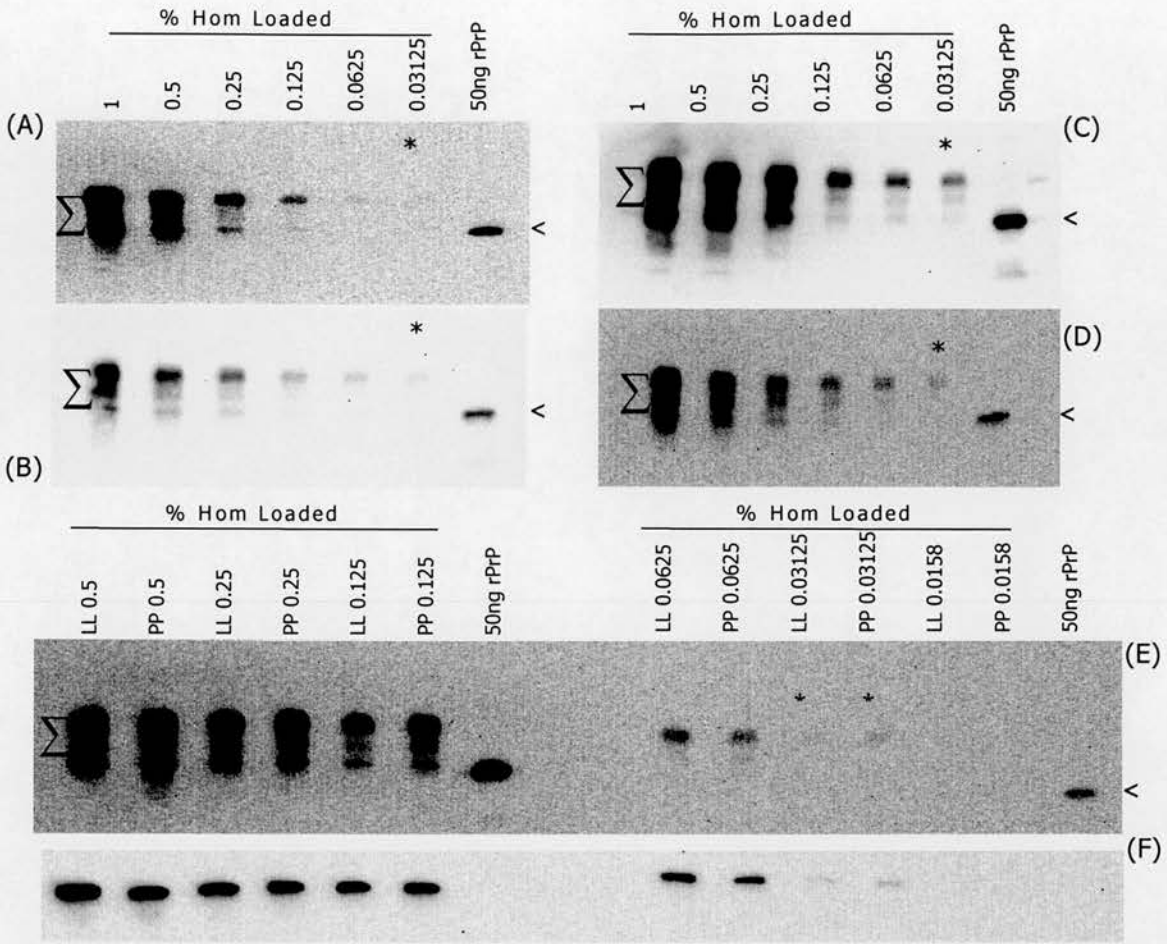

% homogenate loaded	Concentration of Total PrP in uninfected brain homogenate (ng)					
	Uninfected 101PP			Uninfected 101LL		
	Blot A	Blot B	Blot E	BlotC	Blot D	Blot E
1	1077	11297	nd	4510	4716	nd
0.5	2325	6966	3910	5662	3707	2903
0.25	3127	2598	3438	5494	2200	3216
0.125	1387	1030	3909	2583	1097	1779
0.0625	1740	304	6675	2689	1911	10684
0.0313	1444	544	10328	2449	2221	8919
0.0158	nd	nd	0	nd	nd	0
Mean PrP ± SE	3314 ± 716			3834 ± 709		

Figure 6.7 Quantification of total PrP in uninfected 101PP and 101LL brain homogenate

Detection of total PrP in uninfected 101PP and 101LL brain homogenate two-fold serially diluted in PBS to give dilutions of brain homogenate from 1 to 0.0158% when loaded onto 12% tris/glycine SDS-PAGE gels. PrP was detected using 8H4 monoclonal antibody (chapter 2.2) and visualised using West Dura substrate. Blots (A) & (B) and (C) & (D) represent two separate 101PP and 101LL experiments respectively. Blot (E) is an independent experiment with 101PP and 101LL homogenate dilutions loaded across the same SDS-PAGE gel. All blots were performed on different days. On each blot the limit of detection is marked*. Recombinant and glycosylated PrP are marked as previously (figure 6.3) and total PrP was detected as for PrP^{Sc} (figure 6.3). (F) Immunoblot E also probed with GAPDH (chapter 2.2) to ensure equivalent amounts of protein were loaded at each dilution from each brain.

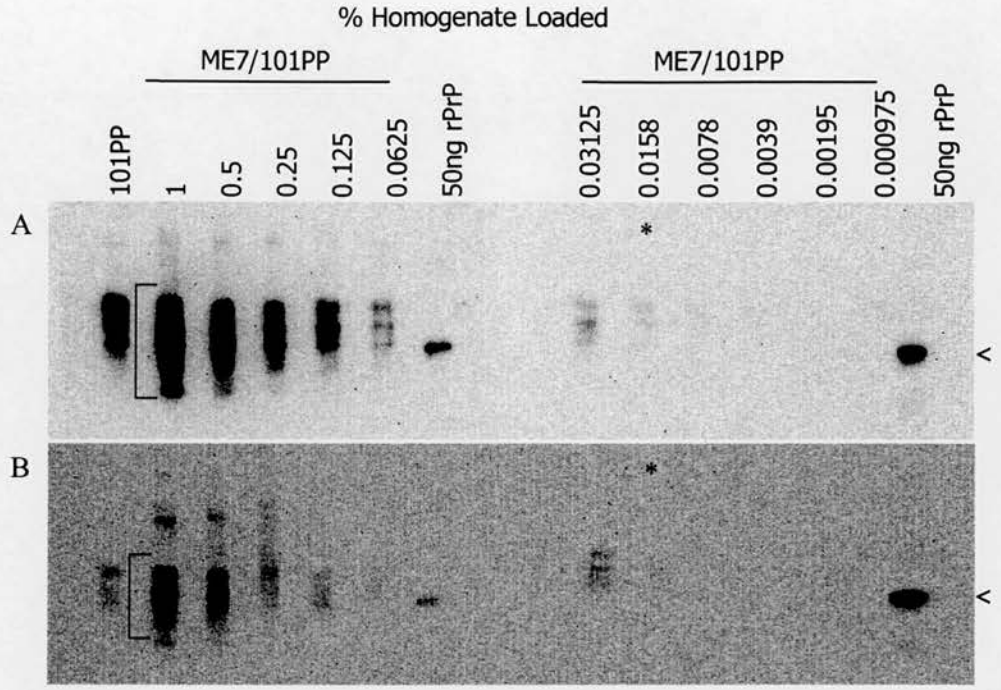

% homogenate loaded	Concentration of Total PrP in ME7/101PP brain homogenate (ng)	
	Blot A	Blot B
1	11970	14539
0.5	8222	10721
0.25	8765	3926
0.125	15550	1356
0.0625	4390	1400
0.0313	1783	2985
0.0156	650	247
0.0078	0	0
0.0039	0	0
0.0020	0	0
Mean PrP ± SE	6180 ± 1431	

Figure 6.8 Quantification of total PrP in ME7-infected 101PP brain homogenate

Total PrP detected in ME7/101PP brain homogenate two-fold serially diluted in PBS to give dilutions of brain from 1 to 0.001% when loaded onto 12% tris/glycine SDS-PAGE gels. PrP was detected as before (figure 6.3). Control homogenate of uninfected 101PP brain (PK-) were loaded at 1% homogenate concentration per well. Blots (A) & (B) represent two separate experiments performed on different days. On each blot the limit of detection is marked*. Recombinant PrP is indicated at 28kDa (<). The three glycosylated bands of PrP were detected in each lane (bracketed). The pixel intensities for each band were converted to ng as previously detailed (figure 6.3). A value of zero indicates no PrP was detected.

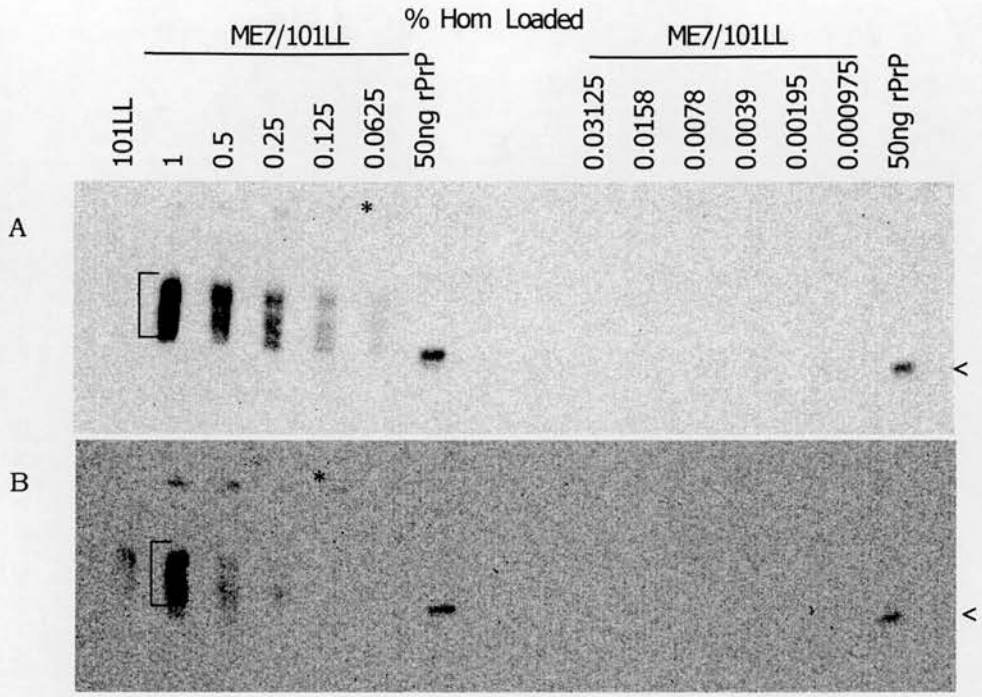

% homogenate loaded	Concentration of Total PrP in ME7/101LL brain homogenate (ng)	
	Blot A	Blot B
1	3997	3022
0.5	2781	1578
0.25	3663	147
0.125	5137	0
0.0625	2594	0
0.0313	0	0
0.0156	0	0
0.0078	0	0
0.0039	0	0
0.0020	0	0
Mean PrP ± SE	2292 ± 571	

Figure 6.9 Quantification of total PrP in ME7-infected 101PP brain homogenate

Total PrP detected in ME7/101LL brain homogenate two-fold serially diluted in PBS to give dilutions of brain from 1 to 0.002% when loaded onto 12% tris/glycine SDS-PAGE gels. PrP was detected as before (figure 6.3). Control homogenate of uninfected 101LL brain (PK-) were loaded at 1% homogenate concentration per well. Blots (A) & (B) represent two separate experiments performed on different days. On each blot the limit of detection is marked*. Recombinant PrP is indicated at 28kDa (<). The three glycosylated bands of PrP were detected in each lane (bracketed). The pixel intensities for each band were converted to ng as previously detailed (figure 6.3). A value of zero indicates no PrP was detected.

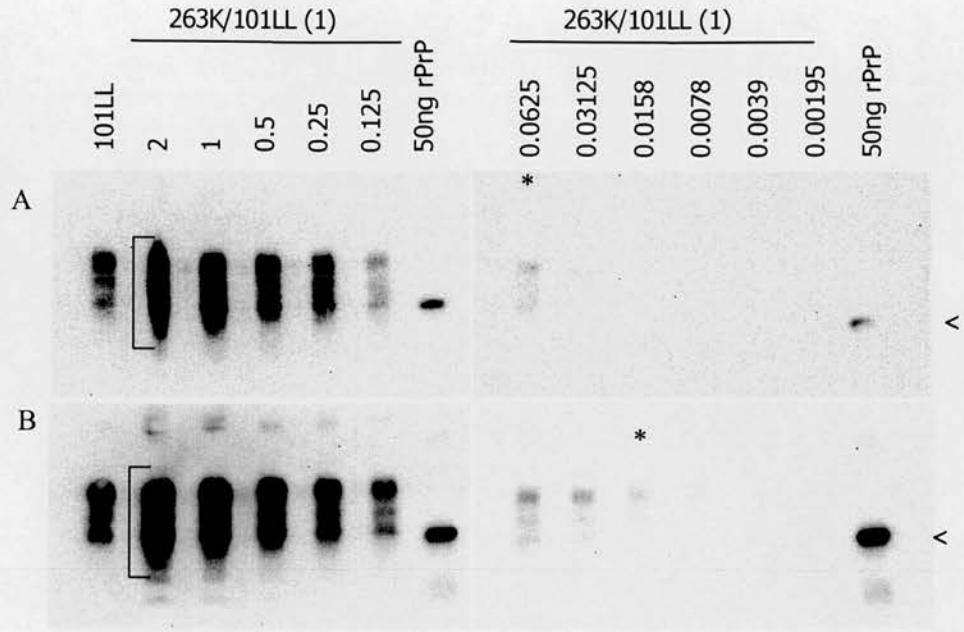

% homogenate loaded	Concentration of Total PrP in 263K/101LL (1) brain homogenate (ng)	
	Blot A	Blot B
2	8215	1678
1	9663	3846
0.5	9563	4160
0.25	14665	6144
0.125	6206	6088
0.0625	11856	2846
0.0313	0	5471
0.0156	0	1270
0.0078	0	0
0.0039	0	0
0.0020	0	0
Mean PrP ± SE	5730 ± 1062	

Figure 6.10 Quantification of total PrP in 263K-infected 101LL brain homogenate

Total PrP detected in 263K/101LL (1) brain homogenate two-fold serially diluted in PBS to give dilutions of brain from 2 to 0.002% when loaded onto 12% tris/glycine SDS-PAGE gels. PrP was detected as before (figure 6.3). Control homogenate of uninfected 101LL brain (PK-) were loaded at 1% homogenate concentration per well. Blots (A) & (B) represent two separate experiments performed on different days. On each blot the limit of detection is marked*. Recombinant PrP is indicated at 28kDa (<). The three glycosylated bands of PrP were detected in each lane (bracketed). The pixel intensities for each band were converted to ng as previously detailed (figure 6.3). A value of zero indicates no PrP was detected.

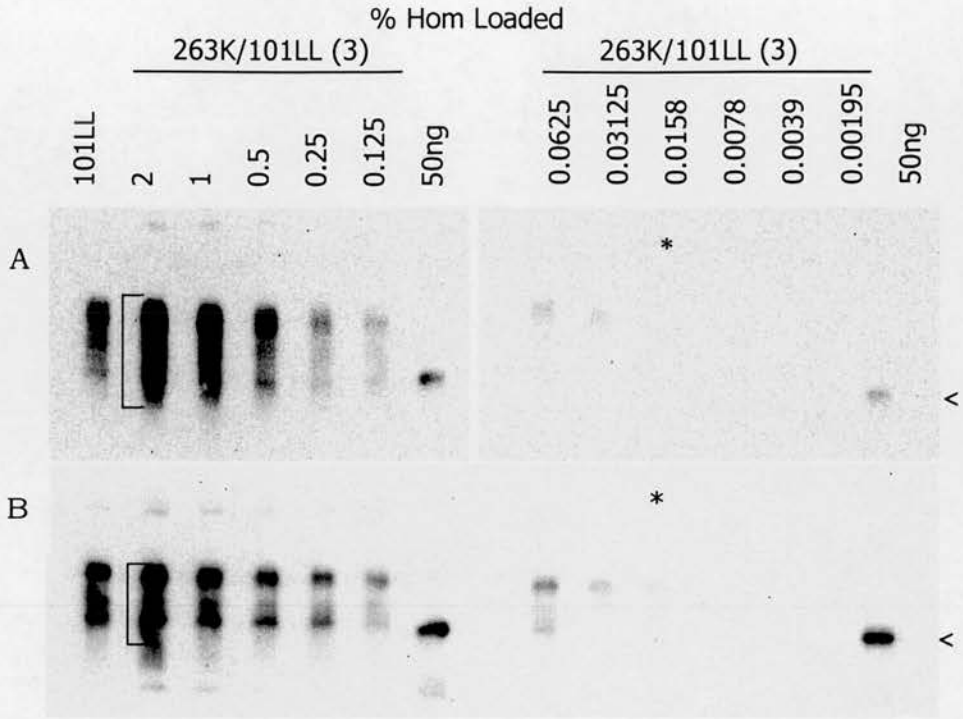

% homogenate loaded	Concentration of Total PrP in 263K/101LL (3) brain homogenate (ng)	
	Blot A	Blot B
2	6928	497
1	11551	981
0.5	9237	1269
0.25	5116	2098
0.125	3707	1634
0.0625	10330	5185
0.0313	4937	1361
0.0156	0	987
0.0078	0	0
0.0039	0	0
0.0020	0	0
Mean PrP ± SE	4114 ± 928	

Figure 6.11 Quantification of total PrP in 263K-infected 101LL brain homogenate

Total PrP detected in 263K/101LL (3) brain homogenate two-fold serially diluted in PBS to give dilutions of brain from 2 to 0.002% when loaded onto 12% tris/glycine SDS-PAGE gels. PrP was detected as before (figure 6.3). Control homogenate of uninfected 101LL brain (PK-) were loaded at 1% homogenate concentration per well. Blots (A) & (B) represent two separate experiments performed on different days. On each blot the limit of detection is marked*. Recombinant PrP is indicated at 28kDa (<). The three glycosylated bands of PrP were detected in each lane (bracketed). The pixel intensities for each band were converted to ng as previously detailed (figure 6.3). A value of zero indicates no PrP was detected.

6.3.4. Total PrP detection in non-titrated brain

A second study of total PrP levels in infected animals was undertaken to confirm the data described previously (chapter 6.3.3). Freshly prepared brain homogenate was analysed from representative animals from each model. Infectivity titres in these tissues were not investigated due to time and breeding constraints. Fresh brain was investigated from one ME7/101PP and one ME7/101LL animal and from two separate 263K/101LL animals, designated 263K/101LL (a) and 263K/101LL (b). Due to time constraints, only one immunoblot experiment per homogenate was carried out. There appeared to be similar amounts of total PrP in each sample. ME7/101PP brain homogenate contained 4132 ± 1241 ng total PrP (± standard error), ME7/101LL contained 3866 ± 2107 ng, 263K/101LL (a) exhibited 671 ± 315 ng and 263K/101LL (b) contained 1398 ± 749 ng total PrP (figure 6.12). When plotted alongside the uninfected data (taken from figure 6.7) total PrP levels in ME7/101PP, ME7/101LL and 263K/101LL (b) infected brain homogenate appeared equivalent, when error bars were taken into consideration (figure 6.13). When considering the error bars, the total PrP detected in 263K/101LL (a) and 263K/101LL (b) homogenates appeared equivalent, however 263K/101LL (a) appeared to contain less total PrP than detected in uninfected and ME7-infected 101PP and 101LL brain homogenates. It should be noted however, that these experiments were only performed once, using one representative brain per model. This may explain the large standard error in these experiments and why it was difficult to distinguish the limits of detection between the samples.

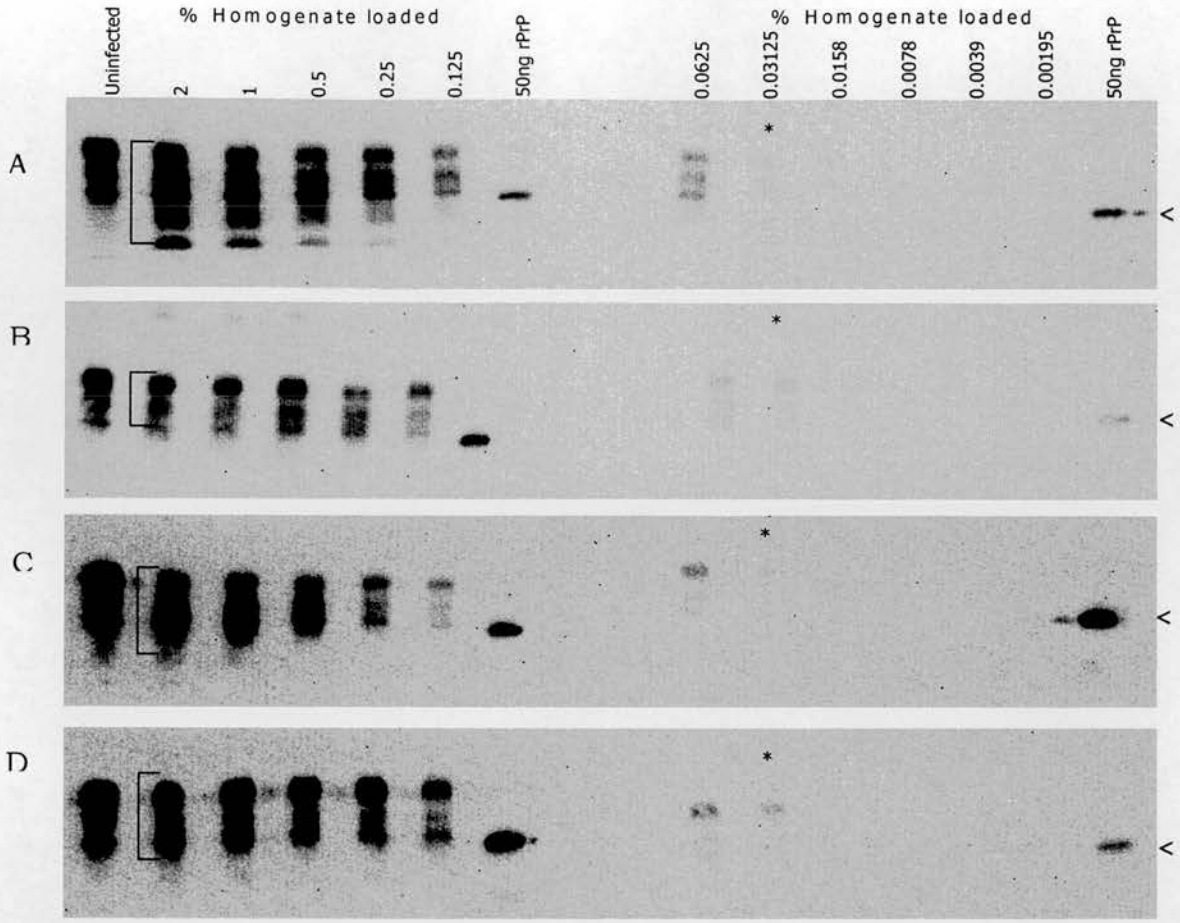

% homogenate loaded	Concentration of Total PrP in freshly prepared brain homogenates (ng)			
	ME7/101PP	ME7/101LL	263K/101LL (a)	263K/101LL (b)
2	4383	491	3147	175
1	5806	639	1815	561
0.5	8432	2052	858	913
0.25	10370	2788	771	1335
0.125	7446	2249	534	1351
0.0625	8360	16058	226	7958
0.0313	656	18244	26	3086
0.0156	0	0	0	0
0.0078	0	0	0	0
0.0039	0	0	0	0
0.0020	0	0	0	0
Mean PrP ± SE	4132±1241	3866±2107	671 ± 315	1398 ± 749

Figure 6.12 Quantification of total PrP in 263K-infected 101LL brain homogenate

Total PrP detected in freshly prepared brain homogenate from (A) ME7/101PP, (B) ME7/101LL, (C) 263K/101LL (a), (D) 263K/101LL two-fold serially diluted in PBS to give dilutions of brain from 2 to 0.002% when loaded onto 12% tris/glycine SDS-PAGE gels. PrP was detected as before (figure 6.9). The limit of detection is marked*. Recombinant PrP is indicated at 28kDa (<). The three glycosylated bands of PrP were detected in each lane (bracketed). The pixel intensities for each band were converted to ng as previously detailed (figure 6.9). A value of zero indicates no PrP was detected.

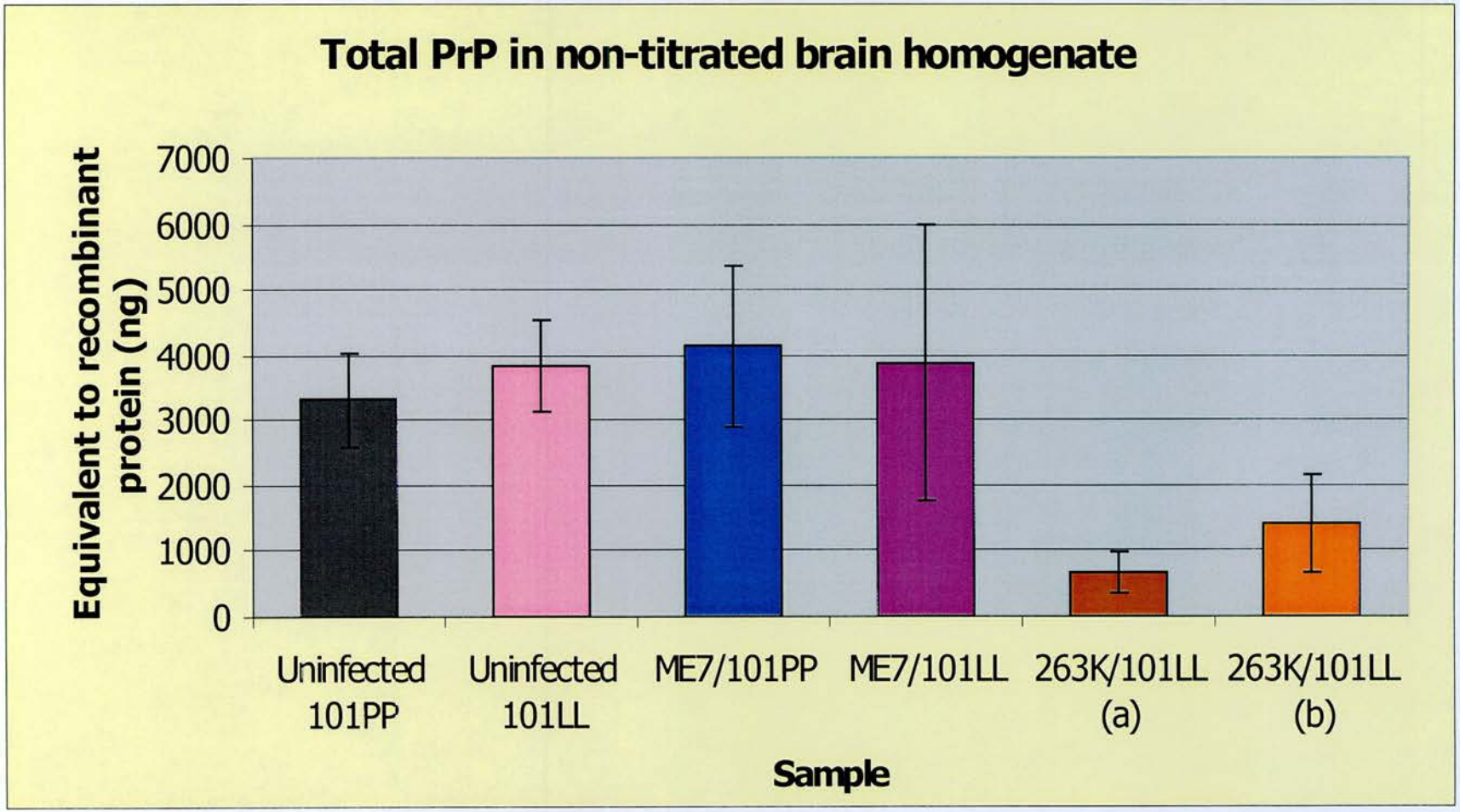

Figure 6.13 Total PrP levels in non-titrated brain homogenate

Quantification of total PrP in non-titrated brain calculated in comparison to 50ng of recombinant PrP as measured by immunoblot (figure 6.12). Data represents mean ± SE from one brain per model.

6.3.5. PrP^C levels in infected brain

For each brain homogenate (titrated brain), PrP^C levels were calculated by subtracting the mean PK-resistant PrP^{Sc} level detected in a homogenate from the mean total PrP level detected (table 6.2). Since PrP^C levels were not directly measured using immunoblot, this calculation only inferred to the amount of PrP^C in each brain homogenate studied here. These calculations indicated that across all of the models studied, total PrP levels remained relatively constant whereas PrP^{Sc} levels and PrP^C levels varied across all infected animals. In ME7/101PP, PrP^C made up 35% of total PrP, whilst in ME7/101LL, it only made up 14% of total PrP. In 263K/101LL (1) and (3) PrP^C constituted 85% and 100% of total PrP, respectively (table 6.2).

Model	Total PrP (ng) [a] =100%	Relative % PK-res PrP^{Sc} (ng)[b]	Relative %PrP^C (ng)[c]
Uninfected 101PP	3314	NA	100%
Uninfected 101LL	3834	NA	100%
ME7/101PP	6180	65% (4010)	35% (2170)
ME7/101LL	2292	86% (1979)	14% (313)
263K/101LL (1)	5730	15% (872)	85% (4858)
263K/101LL (2)	ND	0	NA
263K/101LL (3)	4114	0	100% (4114)

[a] Total PrP detected in each brain homogenate (ng) (chapter 6.3.3) contributes to 100% of PrP per homogenate

[b] PK-resistant PrP^{Sc} detected in each brain homogenate (ng) (chapter 6.3.2) converted to a percentage relative to total PrP.

[c] PrP^C levels inferred for each brain homogenate by calculating total PrP minus PK-resistant PrP^{Sc} (ng) converted to a percentage relative to total PrP.

NA Not applicable

ND Not determined – non enough homogenate to measure the parameter

Table 6.2 Relative contributions of PrP^C and PK-resistant PrP^{Sc} in brain homogenate from each TSE model

Since PrP^C was not actually detected in the experiments performed thus far, PrP^C levels were further investigated using a different detection method. The ELISA-based assay, DELFIA was therefore used to detect both PrP^C and PrP^{Sc} levels from brain homogenate taken from each TSE model studied here.

6.3.6. Measurement of PrP using DELFIA

During the course of these studies the DELFIA assay became available. This assay is more quantitative than the immunoblot system used above thus PrP^{Sc} levels in infected brain and PrP^{C} levels in uninfected and infected brain could be quantified. Accordingly, the brain homogenate used to quantify total PrP levels by immunoblot (i.e. the non-titrated homogenate used in chapter 6.3.4) was investigated using DELFIA since the stocks of titrated brain homogenate were no longer available. In 1M guanidine hydrochloride solution [GndHCl] PrP^{Sc} is GndHCl-insoluble and PrP^{C} is GndHCl-soluble therefore these fractions can be separated and PrP content measured (chapter 6.2.3). PrP levels in experimental samples were measured relative to a standard curve produced using recombinant PrP. In uninfected 101LL homogenate PrP was detected only in the 1M GndHCl-soluble phase, none was detected in the GndHCl-insoluble phase (table 6.3). This showed good separation of PrP in GndHCl soluble and insoluble phases using this methodology (table 6.3). In ME7/101LL, PrP was recovered mainly from the GnHCl-insoluble phase, indicating a high PrP^{Sc} content (table 6.3).

Sample	GndHCl-soluble PrP (ng)	GndHCl-insoluble PrP (ng)	Total PrP (ng)	% Insoluble PrP
Uninfected 101LL	0.13	0	0.13	0
ME7/101LL	0.20	4.58	4.78	96
263K/101LL (a)	0.38	0.01	0.39	3
263K/101LL (b)	0.22	1.42	1.64	87
GSS/101LL	0.71	0	0.71	0

PrP detected in the 1M GndHCl-soluble phase is probably PrP^{C}
PrP detected in the 1M GndHCl-insoluble phase is probably PrP^{Sc}
Total PrP is inferred from the addition of PrP in soluble and insoluble phases.
The precentage of GndHCl-insoluble PrP in each sample probably represents the contribution of PrP^{Sc}. Data courtesy of D King, NPU, Edinburgh.

Table 6.3 DELFIA measurement of PrP in brain

In 263K/101LL (a) most PrP was detected from the GndHCl-soluble fraction, however 3% of PrP was recovered in the GndHCl-insoluble phase

(table 6.3). This suggests that there may be a small amount of PrP^{Sc} in this brain but that the majority is probably PrP^{C}. Conversely, in 263K/101LL (b) most PrP was recovered in the GndHCl-insoluble phase (table 6.3) suggesting the majority of PrP in this brain was PrP^{Sc}, however 13% of PrP was also recovered in the GndHCl-soluble fraction, suggesting this was PrP^{C}. Total PrP in 263K/101LL (a) was less than in 263K/101LL (b), and concurred with previous immunoblot data (figure 6.12). ME7/101LL brain homogenate contained 12-fold more total PrP than 263K/101LL (a) homogenate and three-fold more total PrP than detected in 263K/101LL (b) brain homogenate (figure 6.14).

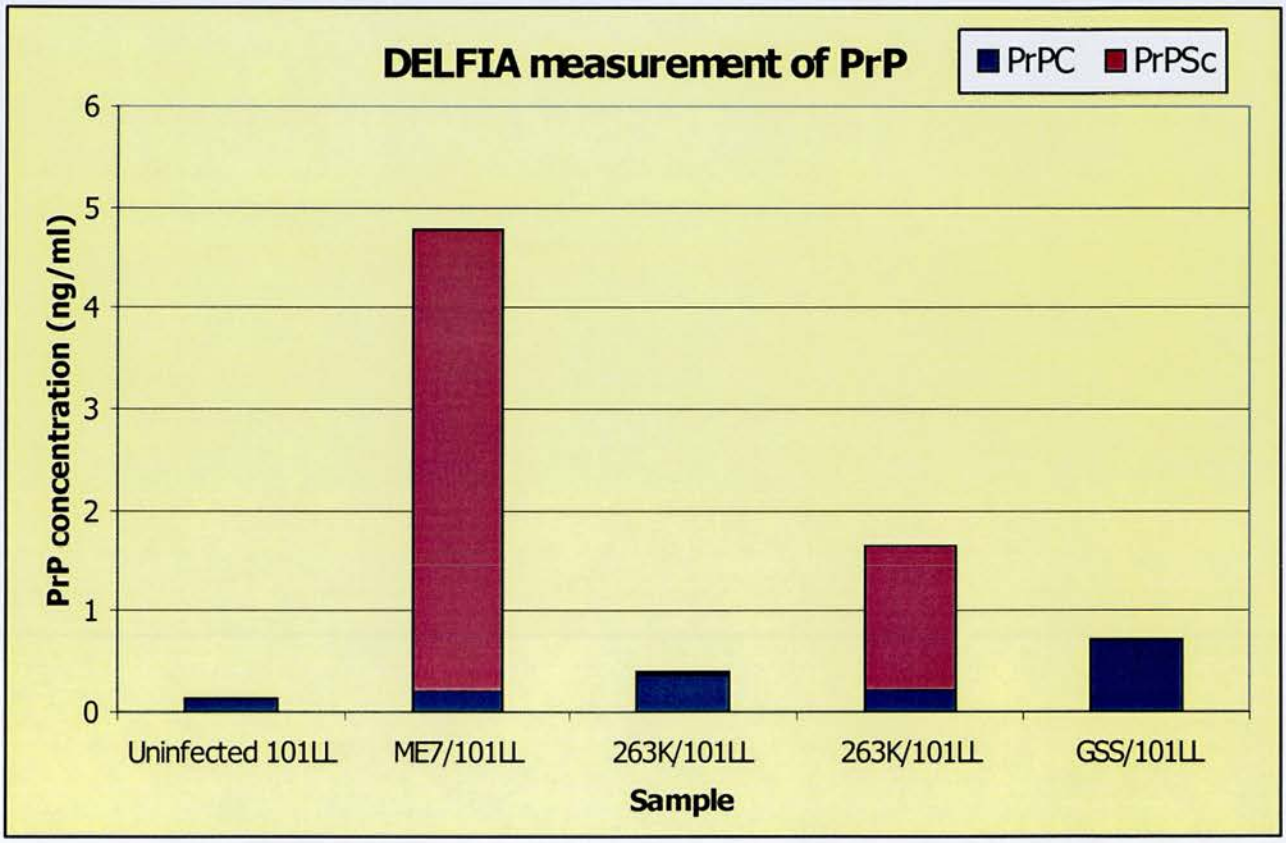

Figure 6.14 DELFIA measurement of PrP in brain

PrP^{C} and PrP^{Sc} separated by differential solubility in 1M guanidine hydrochloride were detected using monoclonal antibodies, FH11 at 1µg/ml for capture and europium-labelled 7A12 for detection. Data represents a single measurement performed on a single representative brain homogenate from each TSE model, except the 263K/101LL model where two individual brain homogenates were investigated.

Immunoblot had also measured three-fold more total PrP in ME7/101LL than in 263K/101LL (b), but had measured only six-fold more total PrP in ME7/101LL compared to 263K/101LL (a) (figure 6.12). This may be due to less sensitive detection of PrP by immunoblot. Importantly, PrP was not detected in the GndHCl-insoluble fraction of GSS/101LL brain, suggesting that if present, PrP^{Sc} levels in this homogenate are extremely low.

6.4. Discussion

6.4.1. Sensitivity of PrP detection

The sensitivity of immunoblot was determined using pure recombinant PrP (rPrP), which producing a single band on coomassie-stained SDS-PAGE. This was consistently detected at 5-10ng, comparable to a previous study where bovine recombinant PrP was detected down to 1ng by immunoblot (Takekida et al., 2002). Immunoblot detected PrP in the ng range, similar to previous immunoblot investigations (Lasmezas et al., 1997). DELFIA detected PrP in the pg range, similar to the sensitivity of other ELISA-based assays (Grassi et al., 2000). In other studies, immunoblot and ELISA sensitivity has been improved by concentrating PrP from a whole sample, using centrifugation or precipitation techniques (Lee et al., 2000; Polymenidou et al., 2002; Safar et al., 1998). However, due to limited availability of brain homogenate in which infectivity was titrated and PrP^{Sc} levels were assessed, these techniques were not used to analyse the samples described here.

In ME7/101PP brain 2mg wet weight contained 4µg PK-resistant PrP^{Sc} (2ug PrP^{Sc}/mg brain). A total mouse brain, 500mg wet weight, has been reported to contain up to 4µg PK-resistant PrP^{Sc} (8ng/mg) (R. Barron, IAH, Edinburgh, personal communication) thus the absolute amounts of PrP^{Sc} detected by immunoblot here probably over-represent those present in the whole brain. DELFIA analysis of infected brain detected 4ng PrP^{Sc} in 20mg wet weight of ME7/101LL brain (0.2ng PrP^{Sc}/mg) therefore probably under-represents the amount of PrP^{Sc} present in whole mouse brain.

The quantification of immunoblots relied on the accurate measurement of rPrP concentration and if this was over-estimated then the sample values are likely to be over-estimated. The concentration of rPrP was estimated using the BSA assay and it is possible that this was not accurate. It may have been more appropriate to perform a dilution series of rPrP on each blot to provide a standard curve for PrP measurement, however space constraints on each SDS-PAGE gel did not allow this. In addition the densitometric analysis of PrP may not have been accurate. Where samples were overloaded the chemilluminescent signal may not have been completely captured. Alternatively the detection antibody may have a different affinity to rPrP compared to native samples. Recombinant PrP is produced in a prokaryotic system thus is unglycosylated and lacks the GPI-anchor, which may affect the antibody affinity. In DELFIA it has been demonstrated that anti-PrP antibodies have an increased affinity to rPrP giving higher concentration values, compared to those of brain homogenate samples (D King, unpublished results). If this also occurs during immunoblot detection, this may explain why PrP levels in brain homogenate measured by immunoblot here appear lower than previously reported.

In all of the quantification experiments it must be remembered that for each model, except 263K/101LL, only one representative brain was chosen for investigation. It is possible that, similar to the 263K/101LL model, different amounts of PrP would be detected in other brains from the ME7/101PP and ME7/101LL models. However, all of the samples examined here have been compared to the same recombinant control and are similarly affected by any error in measuring rPrP concentration. Important for this study is the correlation between the relative amount of PK-resistant PrP^{Sc} in each sample and the relative titre of infectivity found in each sample. The percentage of PrP^{Sc} in each sample remains unchanged even if the rPrP concentration was not accurately measured. Clearly, 263K/101LL (1) brain has five-fold less PK-resistant PrP^{Sc} than ME7/101PP yet both samples contain the same titre of infectivity.

6.4.2. Immunoblot variability

The detection of similar total PrP levels in each of the brain homogenates investigated by immunoblot indicated that the limit of PrP detection had been reached at the equivalent dilution for each brain homogenate. Immunoblot, however, was sensitive enough to distinguish different amounts of PrP within this dilution. The standard errors for each measurement indicated a relatively high degree of variability for each sample investigated using immunoblot and this probably contributed to total PrP values appearing to be the same. Immunoblot variation can occur within each blot, from sample to sample because of dilution and pipeting errors, and can also occur between blots performed on different days, again due to dilution and pipeting errors but also experimental conditions. In general, where the dilution of homogenate increased, sample variability increased, indicating that with each dilution errors increased. Generally, inter-blot variation was greater than intra-blot variation, suggesting that the variation in the day-to-day conditions contributed most to the variation in PrP measurement. Although blot to blot variation occurred, the presence of the rPrP on each blot allowed this variation to be controlled.

6.4.3. Immunoblot detected equivalent amounts of total PrP in brain

Previous studies had indicated that compared to uninfected animals, TSE-infected animals displayed total PrP levels that increased 5 to 10-fold (Meyer et al., 1986) or 4 to 7-fold (Somerville & Dunn, 1996), and that this increase was due to the accumulation of PK-resistant PrP^{Sc} during disease. It was considered that for samples containing high amounts of PK-resistant PrP^{Sc}, the total PrP should be high, but the data described herein does not agree with this. ME7/101PP homogenate contained 5 to 8-fold more PK-resistant PrP^{Sc} than found in 263K/101LL (1), however there was not an equivalent 5 to 8-fold difference in total PrP levels, indeed total PrP levels in these homogenates were similar (figure 6.15). Surprisingly, brain homogenate from all models studied here, including uninfected 101PP and 101LL mice, appeared to contain similar amounts of total PrP, when assessed by immunoblot (figure 6.15).

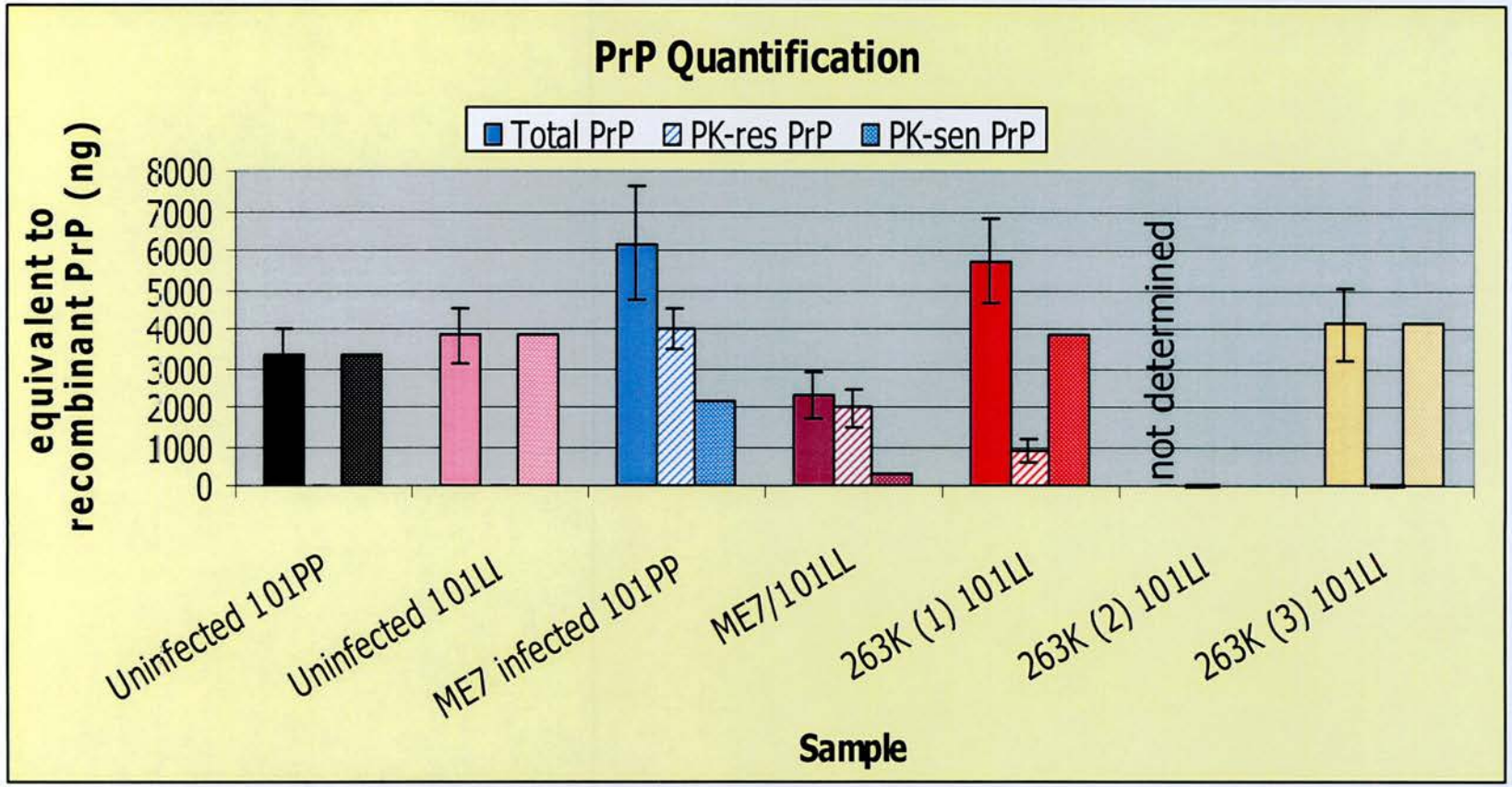

Figure 6.15 PrP levels detected by immunoblot in each TSE model

Quantification of PrP in 2mg wet weight equivalent from each titrated model. PK-resistant PrP or PrP^{Sc} (hatched bars) and total PrP (solid bars) calculated in comparison to 50ng of recombinant PrP as measured by immunoblot (table 6.5 and 6.8). The amount of PK-sensitive PrP or PrP^{C} (dotted bars) was inferred by subtracting the measured amount of PrP^{Sc} from the measured amount of total PrP. Error bars (±SE) are shown only for measured values.

Moreover, quantification of total PrP in infected brain homogenate found PrP levels to be no more than 2-fold higher than in uninfected brain (figure 6.15). Importantly, a second set of brain homogenates taken from the same experimental models confirmed the total PrP data. In contrast, DELFIA measurement of total PrP from the second set of brain homogenates revealed different levels of total PrP in each homogenate with total PrP in ME7/101LL brain homogenate 38-fold more than in uninfected brain. Homogenate from 263K/101LL (a) contained 5-fold more and 263K/101LL (b) contained 13-fold more total PrP than found in uninfected 101LL brain.

It is not clear why there was a difference between the two quantitative methods used here. ELISA is a more sensitive technique than immunoblot and may indicate more clearly the amount of PrP in each sample. In immunoblot, the indirect measurement of the number of pixels contributing to the PrP image for each sample may not accurately measure the amount of chemiluninescence generated by the sample. It may be that the 2-fold dilution factor chosen to assess these brain homogenates by immunoblot was not sufficient to distinguish a 2 to 3-fold difference in PrP levels between samples, however differences greater than 4-fold should be easily distinguishable. DELFIA analysis of total PrP was more consistent with previous reports that found an increase in total PrP with increasing PrP^{Sc} levels (Meyer et al., 1986; Somerville & Dunn, 1996).

6.4.4. Amount of PK-resistant PrP^{Sc} varies in infected animals

In previous experiments 101LL mice inoculated with ME7 or 263K produced less PK-resistant PrP^{Sc} in brain than ME7-infected 101PP mice (Barron et al., 2001; Manson et al., 1999). These findings were confirmed here. Immunoblot indicated that PrP^{Sc} levels in ME7/101LL brain were 2-fold less, and in 263K/101LL (1) were 5 to 8-fold less, than in ME7/101PP brain (figure 6.15). No PK-resistant PrP^{Sc} was detected in 263K/101LL (2) and 263K/101LL (3) brain homogenates by immunoblot (figure 6.15), consistent with the variation in PrP^{Sc} levels found within in this TSE model, as previously described (chapters 3 & 4). DELFIA analysis confirmed immunoblot data, detecting variable PrP^{Sc} levels between individual

263K/101LL brains. DELFIA also detected pg levels of PrP^{Sc} in some 263K/101LL brain homogenates. Given that DELFIA detection of PrP is more sensitive immunoblot detection, it is feasible that extremely low levels of PrP^{Sc} in 263K/101LL (2) and (3) brain homogenates, which were not detected by immunoblot, may have been detectable by DELFIA.

PrP^{Sc} was not detected by immunoblot or DELFIA in GSS/101LL brain homogenate. TSE was had successfully transmitted to uninfected 101LL mice using this homogenate (chapter 5). 263K/101LL (2) and 263K/101LL (3) brain homogenates also transmitted TSE to uninfected 101LL mice (chapter 5) and it is possible that DELFIA may not detect the presence of PrP^{Sc} in these homogenates. Since infectivity was transmitted from all 263K/101LL and GSS/101LL homogenate investigated by immunoblot it is possible that infectivity may associate with something other than PK-resistant PrP^{Sc} . It is possible that other soluble, intermediate forms of PrP may be extracted along with PrP^{C} during the DELFIA process, thus a soluble, non-PrP^{C} form of PrP could be the infectious agent.

6.4.5. Variability in PrP^{C} levels in infected animals

The inferred PrP^{C} levels obtained from immunoblot data indicated that PrP^{C} levels varied in infected animals (figure 6.15), and that in some infected animals PrP^{C} levels were lower than found in uninfected animals. This was contrary to a previous study that showed PrP^{C} levels in infected animals were similar to those found in uninfected animals, with PrP^{C} constituting 10% of the total PrP in an infected animal (Meyer et al., 1986). In the immunoblot studies here only ME7/101LL brain homogenate contained PrP^{C} representing 10% of the total PrP. Notably, PrP^{C} levels in 263K/101LL (3) brain homogenate, which appeared to contain only PrP^{C} , were similar to PrP^{C} levels found in uninfected 101PP and 101LL mice. TSE was transmitted from 263K/101LL (3) homogenate, however, indicating that the PrP detected in this brain may be a PK-sensitive form of infectious PrP. Such forms of PrP were recently described in a murine model of GSS (Tremblay et al., 2004). DELFIA analysis of PrP^{C} confirmed the variable, and sometimes low, PrP^{C} levels in infected animals.

DELFIA measurement of GSS/101LL brain, that transmitted infectivity to 101LL mice, detected PrP^{C} levels higher those in uninfected 101LL mice, yet detected no PrP^{Sc}, suggesting that the 1M GnHCl-soluble fraction, in which PrP^{C} is found, may contain other soluble forms of PrP. Intermediate forms of PrP have been isolated from 263K-infected hamster brain as small, PK-sensitive forms of PrP (Tzaban et al., 2002), and it is possible that these intermediates may also be present in the GndHCl-soluble fraction. Using immunoblot alone it would be difficult to separate infectious and non-infectious soluble forms of PrP^{Sc} since both are PK-resistant. The differential extraction method of DELFIA may be useful in isolating soluble forms of PrP, which could then be titrated to identify whether they were infectious. Alternatively, gel filtation studies, similar to those described by Tzaban *et al* may be useful in identifying fractions of brain that contain infectivity.

6.4.6. The correlation between PK-resistant PrP^{Sc} and infectivity

The aim of these experiments was to quantify PK-resistant PrP^{Sc} levels for correlation with infectivity titres. Importantly, each parameter was measured in the same brain homogenate thus correlating infectivity with PK-resistant PrP^{Sc} in a single animal. This provides an accurate correlation for each model since PrP^{Sc} levels and titre of infectivity can vary between individual animals. However, due to the limitations of the number of TSE models studied and low the number of individual brains studied per model (one from ME7/101PP, one from ME7/101LL and three from the 263K/101LL model) it was not possible to perform a statistical correlation. With hindsight, at least another two models, exhibiting high and intermediate levels of PrP^{Sc}, should have been examined for comparison with ME7/101PP and ME7/101LL, and more individual brain homogenates should have been examined from each model. Due to both time and space constraints however, it was not possible to assess the titre of infectivity in brain from a large number of animals.

General observation of the data here suggests that where one strain of TSE agent is used, titre of infectivity increased with increasing PrP^{Sc} level, in

accordance with the prion hypothesis. Within the 263K/101LL model, homogenate from 263K/101LL (1) contained highest PrP^{Sc} levels and infectivity titre and within the ME7-infected animals ME7/101PP contained the highest titre of infectivity and PrP^{Sc} level. However, this relationship is not consistent between the different models since homogenate from 263K/101LL (1) contains five times less PrP^{Sc} than found in ME7/101PP homogenate yet titres of infectivity are equal. No PK-resistant PrP^{Sc} was detected in homogenate from 263K/101LL (2) and 263K/101LL (3), yet titre of infectivity in 263K/101LL (2) and 263K/101LL (3) were similar to that found in ME7/101LL homogenate. If PK-resistant PrP^{Sc} is the infectious agent in these diseases, this data suggests that this form of PrP is intrinsically different in each model.

6.4.7. The number of PrP molecules per infectious unit

The hamster 263K model indicated that one infectious unit contains 10^4 to 10^5 molecules of PrP^{Sc} (McKinley et al., 1983; Meyer et al., 1986). High titres of infectivity were found in ME7/101PP and in 263K/101LL (2) and (3) brain homogenates, however PrP^{Sc} was not detected in 263K/101LL (2) and (3) brain. This suggests that in different TSE models, if PK-resistant PrP^{Sc} is the infectious agent, one infectious unit may be comprised of a different number of PrP^{Sc} molecules. From the quantification of PK-resistant PrP^{Sc} in each brain homogenate (measured in this chapter) and of the titre of infectivity determined in each homogenate (chapter 5), it was possible to estimate the number of molecules of PrP^{Sc} per infectious for each brain homogenate studied here (table 6.4). In ME7/101PP, ME7/101LL and 263K/101LL (1) brain homogenates, where PK-resistant PrP^{Sc} could be detected, the number of PrP^{Sc} molecules per infectious unit fell within previously detected limits (Beekes et al., 1996; McKinley et al., 1983; Meyer et al., 1986). ME7/101PP exhibited $10^{5.4}$ molecules, ME7/101LL exhibited $10^{5.9}$ molecules and 263K/101LL (1) exhibited $10^{4.6}$ molecules PrP^{Sc} in one infectious unit (ifu) (table 6.4). This suggests that in these models PK-resistant PrP^{Sc} does correlate with infectivity.

Brain homogenate	Infectivity titre[a] (ID_{50}/g brain)	Molecules PrP per infectious unit[b] PrP^{Sc}	PrP^{C}
ME7/101PP	$10^{8.5}$	$10^{5.4}$	$10^{5.1}$
ME7/101LL	$10^{7.7}$	$10^{5.9}$	10^{6}
263K/101LL (1)	$10^{8.6}$	$10^{4.6}$	$10^{5.4}$
263K/101LL (2)	$10^{7.1}$	na ($^{f}10^{3.3}$)	na
263K/101LL (3)	$10^{6.6}$	na ($^{f}10^{3.7}$)	$10^{7.4}$

[a] Infectivity titre determined by end-point titration (chapter 5)
[b] Amount of PK-resistant PrP^{Sc} measured by immunoblot. Amount of PrP^{C} inferred from immunoblot detection of total PrP level minus PrP^{Sc} level
Number of molecules per infectious unit calculated; $\frac{\text{no. molecules in sample}^{d}}{\text{titre of infectivity}}$
[d] Number of molecules in sample calculated; $\frac{\text{PrP detected (g)} * \text{Avagadro's number}^{e}}{\text{PrP molecular weight (assumed to be 30,000 Da)}}$
[e] Avagadro's number of molecules in 1mole of solution = 6.022×10^{23}
[f] Assumed measurement of PrP^{Sc} to be 1ng
nd Not determined
na Not applicable

Table 6.4 Number of molecules of PrP per infectious unit calculated from immunoblot detection of PK-resistant PrP^{Sc} and end-point titration of brain homogenate from each TSE model

PK-resistant PrP^{Sc} in homogenate from 263K/101LL (2) and (3) was not detected using immunoblot or DELFIA, however if infectious PrP^{Sc} was present in these homogenates it may be <5ng, below the limit of detection of immunoblot. The value of 1ng PrP^{Sc} was therefore assigned to 263K/101LL (2) and (3) to calculate the number of molecules of PrP^{Sc} per infectious unit in each homogenate. There are $\leq 10^{3.3}$ molecules PrP^{Sc} per ifu in 263K/101LL (2) and $\leq 10^{3.7}$ molecules PrP^{Sc} per ifu in 263K/101LL (3) homogenates (table 6.4). Therefore the number of PrP^{Sc} molecules in one infectious unit in the 263K/101LL models was less than those found in the ME7-infected models. This infers that if PK-resistant PrP^{Sc} is the infectious agent in these brains, one molecule of PK-resistant PrP^{Sc} in 263K/101LL-infected brain may be more virulent than one molecule of PK-resistant PrP^{Sc} in ME7-infected brain. However, if another molecule (or complex of molecules) contributes to infectivity then 263K/101LL brain may contain more of this unidentified molecule than ME7-infected brain.

PK-resistant PrP^{Sc} levels do not correlate with infectivity titre in 263K/101LL (2), (3) and (b) brains, as well as in the GSS/101LL brain investigated in this thesis (chapter 3). Thus the correlation between PK-resistant PrP^{Sc} and infectivity, as defined by Prusiner et al (McKinley et al., 1983; Prusiner, 1982), is not exclusive. It has been suggested that other forms of PrP, particularly exhibiting PrP^{C}-like biochemical properties (eg. PK-sensitivity) may be present in TSE-infected brain (Safar et al., 1998; Tremblay et al., 2004; Tzaban et al., 2002). It is not known whether these forms of PrP contribute to infectivity. In the studies here, PrP^{Sc} was identified using PK thus alternative PK-sensitive forms of PrP (PrP-sen) may have been degraded along with PrP^{C}. PrP^{C} levels identified by immunoblot indicated that the number of PrP-sen molecules per ifu in each homogenate was similar, if not higher than the number of PrP^{Sc} molecules per ifu. These data, and DELFIA detection of PK-sensitive PrP in the GndHCl-soluble fraction from transmissible 263K/101LL and GSS/101LL brain, may indicate the influence of PK-sensitive molecules, other than PrP^{C}, on infectivity in 263K/101LL and GSS/101LL models. Further studies to identify PK-sensitive PrP in these models is therefore required.

Other studies have expressed the amount of PrP^{Sc} found in brain preparations as absolute amounts, however such studies have attempted to purify the scrapie agent, as PrP 27-30 or as SAF (Gibson et al., 1987; Hilmert & Diringer, 1984; Kascsak et al., 1985; McKinley et al., 1983). However in such experiments proteins other than PrP were also purified (Bolton et al., 1987) thus may be associated with infectivity. The experiments described in this chapter quantified PK-resistant PrP^{Sc} from crude brain homogenate rather than from a purified SAF or PrP27-30 preparation. Thus, the study here, in common with other studies correlating PrP^{Sc} and infectivity, may measure additional molecules that contribute to infectivity.

The presence of alternative forms of PrP may explain why PK-resistant PrP^{Sc} levels in individual brain from the 263K/101LL and ME7-infected models can differ by at least five-fold yet infectivity titres remain similar. In the

next chapter, therefore, the presence of other forms of PrP in brain homogenate from GSS/101LL and 263K/101LL models was investigated.

7. Alternative forms of PrP

7.1. Introduction

The studies performed in this thesis have indicated that there is a lack of correlation between PK-resistant PrP^{Sc} and infectivity titre. This lack of correlation is evident in the 263K/101LL model where individual brains exhibited extremely low levels or no detectable PK-resistant PrP^{Sc}, yet contained appreciable amounts of infectivity (chapters 5 & 6). Concentration of the PrP in such samples may reveal the presence of extremely low levels of PK-resistant PrP^{Sc}. If the prion hypothesis is correct PK-resistant PrP^{Sc} should have been detected in 263K/101LL mouse brain from which TSE was transmitted, however it is possible that alternative forms of infectious PrP, other than PK-resistant PrP^{Sc} are present in the brain. It has been shown that alternative forms of PrP are present in human GSS caused by the A117V mutation and CJD caused by the insertion of nine extra octapeptide repeat regions (chapter 1). Additionally, alternative forms of PrP, such as cyPrP, have been suggested to be neurotoxic (Ma et al., 2002; Stewart & Harris, 2003) and these may be present in cases of TSE where PrP^{Sc} is absent. Moreover if, as suggested by the prion hypothesis, there is an infectious template that allows the conversion of PrP^{C} from an uninfectious to an infectious form, it may be an alternative form of PrP and not PK-resistant PrP^{Sc} that acts as the template.

The concept of PrP^{C} to PrP^{Sc} conversion has evolved from the suggestion of a simple one step process to a complex conversion pathway, along which there may exist several different structural forms of PrP (figure 7.1). These different forms of PrP may have different PK-cleavage sites exposed and differential biochemical properties to PrP^{C} or PrP^{Sc}, resulting in differential PK-sensitivity and/or detergent solubility. Due to the unknown nature of PrP intermediates they are often referred to as PrP* (Weissmann, 1991).

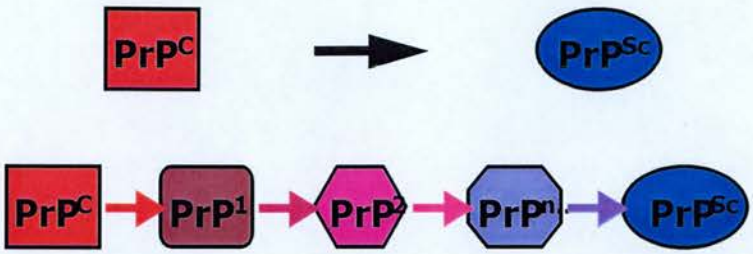

Figure 7.1 Does PrP conversion follow a simple or complex pathway?

If PK-resistant, detergent insoluble PrP^{Sc} is the infectious agent of TSE, why does the 263K/101LL model have high titres of infectivity associated with low PrP^{Sc} levels? Furthermore, why was no PK-resistant PrP^{Sc} detected in GSS/101LL brain by immunoblot or DELFIA yet the same brain homogenate was capable of transmitting infectivity? Both 263K/101LL and GSS/101LL brain may contain infectious but PK-sensitive PrP and could explain why there is a lack of PK-resistant, detergent insoluble PrP^{Sc} in these models.

This chapter investigates the possibility that infectivity is associated with a form of PrP other than PK-resistant PrP^{Sc}. The biochemical characteristics of PrP found in disease end-point brain in all of the models was therefore analysed to determine whether the PrP present conformed to the detergent insoluble, PK-resistance of PrP^{Sc} or the detergent soluble, PK-sensitivity of PrP^{C}. At the time of commencing these studies it was not known whether the transmembrane PrP associated with the A117V GSS model was infectious. Since the P101L mutation causes GSS, the possible presence of transmembrane PrP was also investigated in infected 101LL mice. The implications of disease transmission with respect to the forms of PrP found in each model are also discussed.

7.2. Methodology

7.2.1. Brain homogenate investigated from each model

Brain homogenate from ME7/101PP, ME7/101LL and 263K/101LL models was investigated. Where possible brain homogenate that had previously been used to quantify PK-resistant PrP^{Sc} (chapter 6) and calculate titre of infectivity (chapter 5) was used. All homogenates had transmitted TSE (chapter 5), however, 263K/101LL (1) contained five-fold less PrP^{Sc} than ME7/101PP and 263K/101LL (2) & 263K/101LL (3) both contained no detectable PrP^{Sc} (chapter 6). Additionally, one brain from GSS-infected 101LL mice that contained no detectable PrP^{Sc} yet transmitted TSE (non-titrated brain - chapter 5) was also examined.

7.2.2. PK sensitivity of PrP in each model

Five percent brain homogenate prepared in detergent (chapter 2.6.2) was incubated with varying amounts of PK (chapter 2.7.1) at final concentrations of 1000, 500, 400, 300, 200, 100, 50, 20, 10, 5, 2, and 1μg/ml. PK reactions consisted of 9μl homogenate and 1μl appropriately diluted PK in a total of 10μl. Reactions were incubated at 37°C for 60 minutes and terminated by adding 1μl of 100mM PMSF. Control reactions of PK-treated (20μg/ml final concentration) and PK-untreated uninfected brain were also performed. Samples were examined by immunoblot (chapter 2.12). PrP^{Sc} with different PK-resistant properties may have different structural conformations not visible to one monoclonal antibody. Blots were therefore probed using monoclonal antibody, 8H4, or polyclonal antibody, 1B3 (chapter 2.2).

7.2.3. Detergent solubility of PrP in each model

Brain was prepared as 10% homogenate from infected ME7/101PP, ME7/101LL, 263K/101LL (1), 263K/101LL (2), 263K/101LL (3) and GSS/101LL and from uninfected 101PP and 101LL mice, and was analysed

using the detergent solubility protocol (chapter 2.22). Resuspended fractions (P1, P2 and S2) were split into two samples to identify PrP^{C} and PrP^{Sc} proportions in each fraction. One sample was PK-treated (20µg/ml final concentration - chapter 2.7.1). Each reaction was added to SDS-PAGE loading buffer and sample reducing agent then protein was separated by electrophoresis and analysed using immunoblot (chapter 2.9).

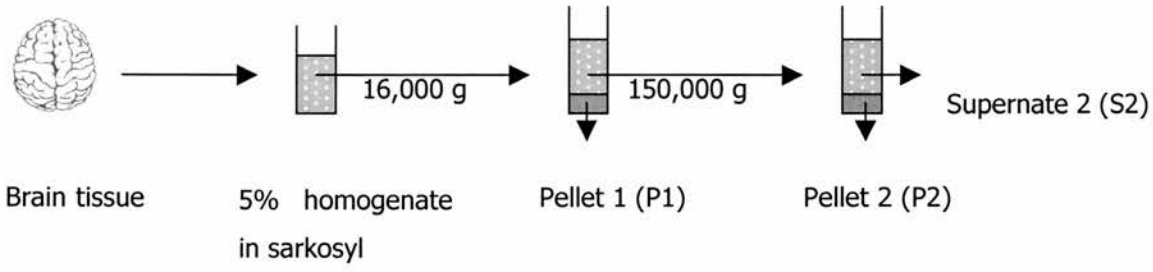

Figure 7.2 Separation of detergent soluble and insoluble PrP fractions by centrifugation

Pellet 1 (P1) produced after first spin contains cellular debris with PK-resistant and PK-sensitive PrP present. Supernate 2 (S2) produced after first spin contains soluble PrP which is PK-sensitive and is likely to represent PrP^{C}. Pellet 2 (P2) produced after second spin contains insoluble PrP which is PK-resistant and is probably PrP^{Sc}.

7.2.4. Identification of transmembrane PrP

Microsomal membranes were prepared (chapter 2.13) from brain tissue of one animal each of ME7/101PP, ME7/101LL and 263K/101LL models as well as from uninfected 101PP and 101LL animals. These tissues were taken from the same experiments as the titrated tissues, but were from different animals. The resultant microsomes were examined using the PK-protection assay to analyse for transmembrane PrP. For each preparation, the identification of calnexin, a ubiquitous transmembrane protein, was crucial in determining whether membranes were intact before proceeding with transmembrane identification. These methods were modified from published protocols (Hegde et al., 1998; Stewart & Harris, 2001).

7.2.4.1. Calnexin identification

To determine whether microsomal membranes remained intact after storage at -70^{0}C microsomal membranes were treated with PK (chapter 2.15). Transmembrane calnexin protein was identified using a purified IgG, mouse monoclonal, anti-calnexin antibody (chapter 2.2), visualised using goat α-rabbit secondary (chapter 2.3) and POD substrate and viewed using x-ray film. A shift from full-length 98kDa calnexin in PK-untreated reactions to a cleaved 64kDa protein in PK-treated reactions indicated intact microsomes.

7.2.4.2. Transmembrane PrP identification

^{Ntm}PrP was detected using monoclonal antibody 8B4 and ^{Ctm}PrP was detected using monoclonal antibody 8H4 (chapter 2.2). PrP was visualised using secondary rabbit α-mouse (chapter 2.3) and POD substrate using x-ray film (chapter 2.12).

7.3. Results

7.3.1. The relative PK-sensitivity of PrP

PrP^{Sc} is described as having a PK-resistant core of 27-30kDa, whereas PrP^{C} is completely degraded upon treatment with PK (McKinley et al., 1983; Meyer et al., 1986). Diagnostic and research laboratories generally use ≥ 20μg/ml PK to identify the PK-resistant core of PrP. PK-resistant PrP^{Sc} was not detected in brain homogenate from individual 263K/101LL and GSS/101LL mice, which subsequently transmitted TSE (chapters 5 & 6), therefore it was possible that infectious PrP in these models had an alternative PK-resistant pattern to PrP^{Sc} found in the ME7/101PP and ME7/101LL models. PrP in both 101PP and 101LL uninfected brain was sensitive to ≥5 μg/ml PK, when detected with 8H4 (figure 7.3A&B) and ≥ 10 μg/ml PK when detected with 1B3 (figure 7.4A&B). ME7/101PP exhibited PrP^{Sc} that appeared to have a high degree of PK-resistance, with the protease-resistant core still visible using 1000μg/ml PK (figure 7.4C). The quantification of PK-resistant PrP^{Sc} in ME7/101LL brain indicated that this homogenate contained half the amount of PrP^{Sc} compared to ME7/101PP (chapter 6). However PrP from both models exhibited the same high degree of PK-resistance, exhibiting the protease resistant core at 1000μg/ml , when detected with 1B3 (figure 7.4D).

The PrP in 263K/101LL mice showed variability in PK-resistance. Homogenate from 263K/101LL (1) showed a PK-resistance at 20 μg/ml when detected with 8H4 and up to 1000 μg/ml when detected with 1B3 (figures 7.3C & 7.4E). thus PrP in this homogenate displayed a high degree of PK-resistance, similar to the PrP^{Sc} in ME7/101PP and ME7/101LL brain homogenate. However, homogenate from 263K/101LL (2) and 263K/101LL (3) was sensitive to PK ≥ 5 μg/ml, similar to that found in uninfected animals (figures 7.3D & 7.4F). When immunoblotted with 8H4, PrP in GSS/101LL brain homogenate was also sensitive to ≥ 5μg/ml PK (figure 7.3E), similar to the PK resistance of PrP in homogenate from uninfected and 263K/101LL (2) and (3) mice. In 1B3 blots,

the intensity of the upper band at approximately 33kDa (figure 7.4 C-F) increased with increasing PK concentration and probably represents PK itself since this has an approximate molecular weight of 29kDa (Sambrook & Russell, 2003).

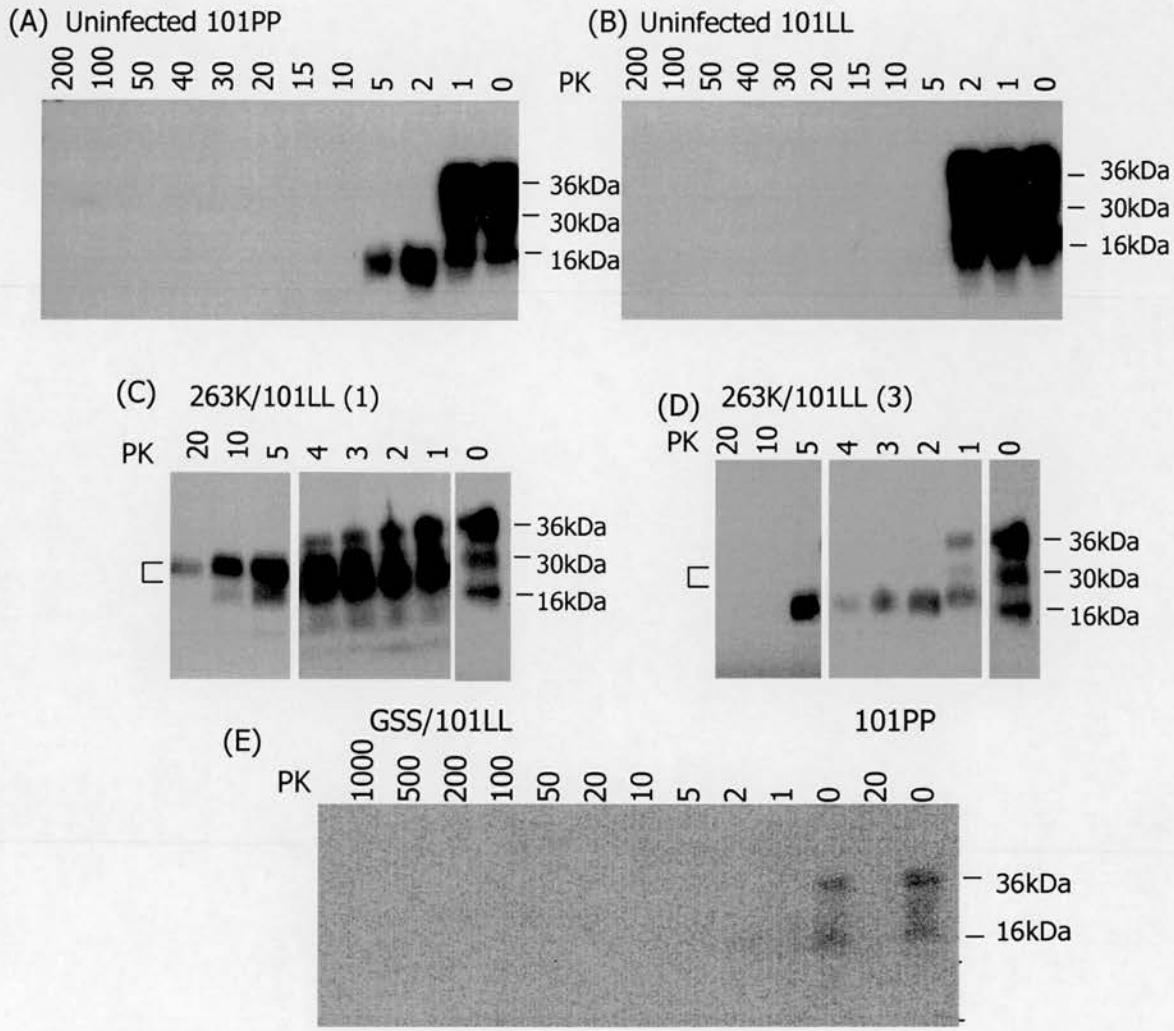

Figure 7.3 PK-titration of brain homogenate detected using monoclonal antibody 8H4

1% brain homogenate PK-treated with up to 200µg/ml PK from (A) uninfected 101PP, (B) uninfected 101LL, (C) 263K/101LL brain homogenate- 1, (D) 263K/101LL brain homogenate - 3, and (E) GSS/101LL brain homogenate, including uninfected 101PP brain homogenate control, untreated and PK-treated (20µg/ml final concentration). Detected using 8H4 monoclonal antibody (chapter 2.2) and visualised using rabbit α-mouse secondary antibody (chapter 2.3) and POD substrate. Bracket indicates PK-resistant core of PrP^{Sc} at 27-30kDa.

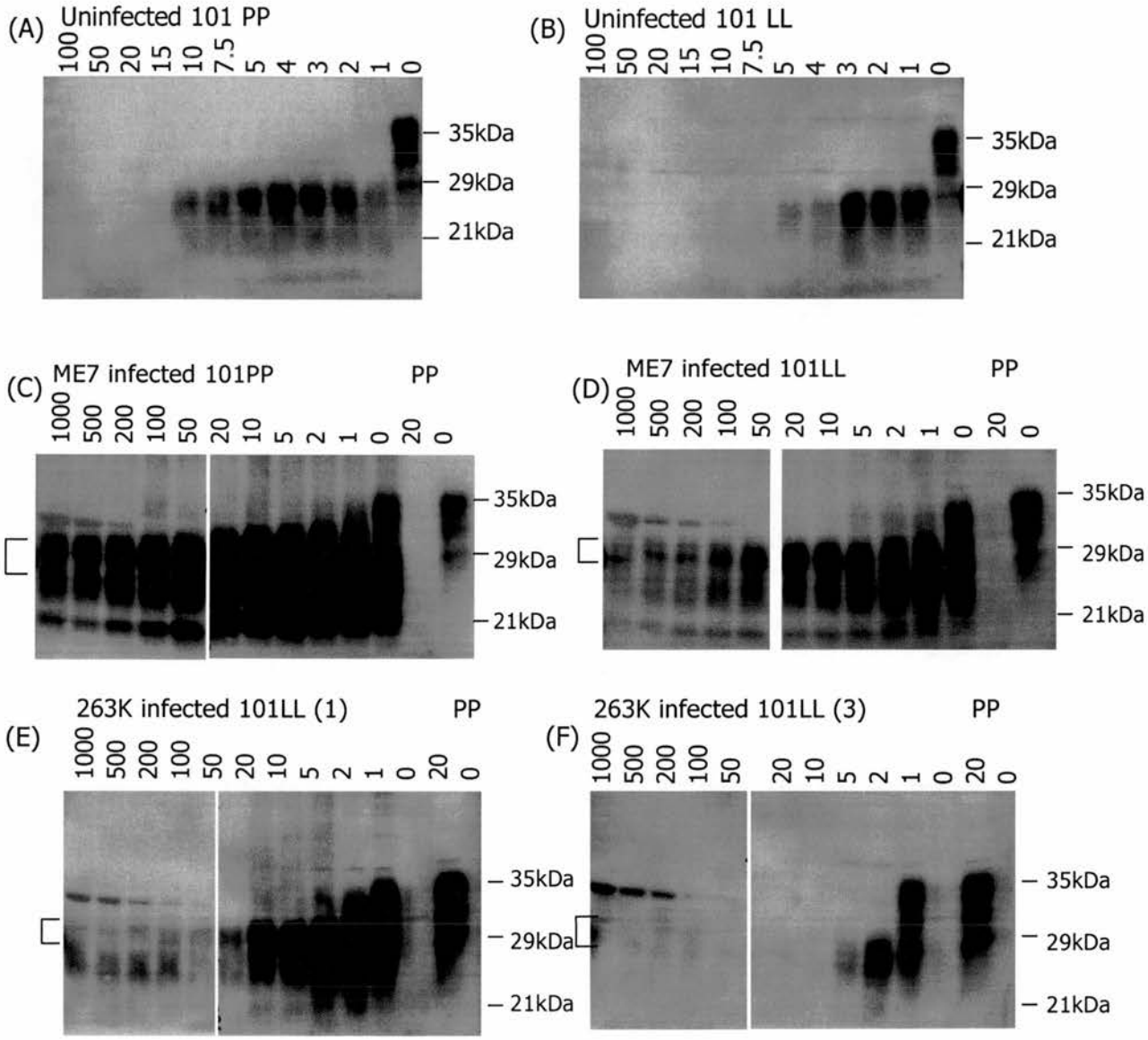

Figure 7.4 PK-titration of infected and uninfected brain homogenate detected using 1B3

1% brain homogenate from (A) uninfected 101PP and (B) uninfected 101LL models, treated with 1-100µg/ml PK (final concentration). 1% brain homogenate from (C) ME7/101PP, (D) ME7/101LL, (E) 263K/101LL (1) and (F) 263K/101LL (3) models treated with 1-1000µg/ml PK (final concentration), with uninfected 101PP brain (PP), untreated an PK-treated (20µg/ml final concentration) as a control. Detected using polyclonal antibody 1B3 (chapter 2.2) and visualised using secondary antibody (chapter 2.3) and POD substrate. Bracket indicates PK-resistant core of PrP^{Sc} at 27-30kDa. * indicates the presence of PK itself at ~33kDa.

7.3.2. The detergent solubility of PrP

PrP^{Sc} is described as a PK resistant protein, however this was not detected from transmissible 263K/101LL or GSS/101LL brain homogenate using PK concentrations ≥20mg/ml. PrP^{Sc} is further biochemically characterised as a detergent insouble protein, compared to PrP^{C}, which is detergent soluble. This difference in solubility is thought to occur because of different conformations of PrP. Therefore, to determine whether the low levels of PrP^{Sc} in 263K/101LL and GSS/101LL models were due to different forms of PrP, the detergent solubility of PrP from all models was investigated using the methodology described (figure 7.2). Brain homogenate from uninfected 101PP and 101LL mice and from infected animals that had been investigated in the PK-resistance experiments was used in these experiments. Initially samples were resuspended in 100µl buffer (chapter 2.9) therefore were not concentrated.

Brain homogenate from uninfected 101PP and 101LL mice produced only the expected detergent soluble, PK-sensitive PrP^{C}, in S2 with no PrP detectable in the other fractions (figure 7.5A & B). Brain homogenate from ME7/101PP and ME7/101LL mice exhibited PrP in all fractions: P2 contained detergent insoluble, PK-resistant PrP^{Sc}, S2 contained PK-sensitive PrP^{C} and P1 contained PrP^{Sc}, indicating that not all of the abundant PrP in these tissues was released during homogenisation (figure 7.5A & B). There were different patterns of detergent solubility in the three different 263K/101LL brain homogenates investigated. 263K/101LL (1) exhibited detergent insoluble PrP^{Sc} in P2, similar to ME7-infected brain, whereas 263K/101LL (2) exhibited only detergent soluble PrP^{C} in the S2 fraction, similar to PrP in uninfected brain (figure 7.5C). Detergent insoluble PrP was found in the P2 fraction of 263K/101LL (3) brain homogenate. PrP detected in the PK+ lane was faint, but appeared to be PK-resistant (figure 7.5C). However since the pellets produced using this method were viscous and difficult to load onto the elecrophoresis gels, it was not initially clear whether a small amount of PrP from the S2 PK- lane had spilled into the PK+ lane during loading.

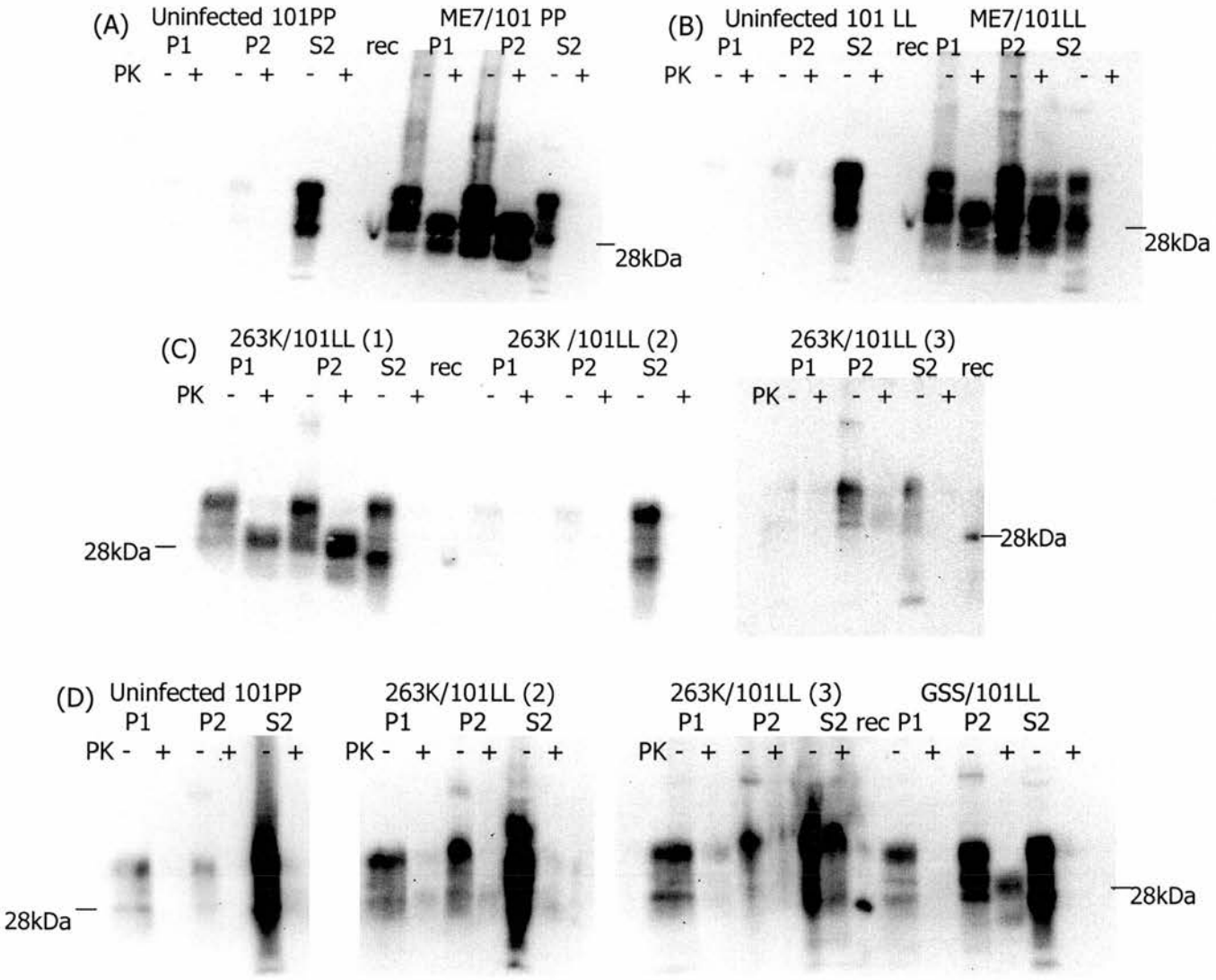

Figure 7.5 Detergent solubility of PrP

Detergent solubility of PrP from all models assessed in (A) 2% brain homogenate from uninfected 101PP and ME7/101PP mice, (B) 2% brain homogenate from uninfected 101LL and ME7/101LL mice, (C) 2% brain homogenate from 263K/101LL (1), (2) & (3). (D) 5x concentrated samples from uninfected 101PP, 263K/101LL (2) & (3) and GSS/101LL homogenate. PK-treated brain (PK+ lanes) treated with 20µg/ml final concentration. PrP detected using antibody 8H4, with West Dura substrate as before (figure 7.3). For band sizes, compare to recombinant PrP (rec) at 28kDa.

To identify whether low levels of PrP^{Sc} were present in infected brain, homogenate from the 263K/101LL and GSS/101LL models, pellets were re-suspended to a five-fold concentration (chapter 2.9). When compared to the previous data, all concentrated samples showed an increase in the concentration of PrP in each fraction (figure 7.5D). In uninfected homogenate, only PK-sensitive PrP^{C} was detected in the detergent soluble S2 fragment, however, compared to the un-concentrated samples, an increased amount of PK-sensitive PrP was found in the P2 fraction (figure 7.5D). This probably represents a small amount of PrP^{C} that was not completely removed from this fraction before P2 was resuspended. PrP in 263K/101LL (2) and 263K/101LL (3) homogenates showed the uninfected pattern of detergent solubility with the majority of PrP present in the S2 fraction and PK-sensitive. In 263K/101LL (3), however, PrP was detected in the S2 PK+ lane (figure 7.5D). Protein was present at 30-35kDa, reminiscent of PrP^{C}, and probably represented spill-over from the S2 PK- lane rather than detergent soluble PK-resistant PrP, which would be seen at 27-30kDa. PrP from 263K/101LL (2) and (3) therefore exhibit a PrP^{C}-like detergent solubility. The GSS/101LL brain homogenate revealed PrP with detergent solubility similar to that of ME7 infected tissues with PK-resistant, detergent insoluble PrP^{Sc} found in the P2 fraction and PK-sensitive, detergent soluble PrP^{C} found in the S2 fraction. Moreover, PrP^{Sc} was visible in this tissue where it had not been seen before indicating that concentration of brain homogenate was required to detect low amounts of PrP^{Sc} in brain homogenate. Concentration of homogenate from 263K/101LL mice to greater than five-fold may have revealed PrP^{Sc} in this model.

7.3.3. Investigation of transmembrane PrP

The PrP detected in 263K/101LL brain homogenate appeared to be consistent with the non-infectious PrP^{C} form (PK-sensitive and detergent soluble), however 263K/101LL brain transmitted infectivity to 101LL mice (chapter 5) thus this homogenate contained more than non-infectious PrP^{C}. It was therefore possible that infectious PrP other than PrP^{Sc} was present in this model.

Transmembrane PrP had been described in murine and human brain exhibiting TSE pathology in the absence of PrP^{Sc} (Hegde et al., 1998). At the time of performing the studies here it was not known if transmembrane PrP was infectious, thus transmembrane PrP was investigated in the models studied here.

Microsomal membranes were prepared from brain homogenate from one representative animal from each model (ME7/101PP, ME7/101LL and 263K/101LL) and from uninfected 101PP and 101LL mice. The original protocol devised for studying transmembrane PrP was performed on fresh brain (Hegde et al., 1998; Stewart & Harris, 2001). Brain tissue from the models used in this study had been frozen therefore it was essential to assess whether frozen brain was suitable for this study. Calnexin, a membane-spanning protein, was used as a control to verify that microsomal membranes remained intact after removal from -70°C storage. The full length 98kDa calnexin protein spans the ER membrane with a 64kDa portion remaining in the lumen. When microsomes were incubated with PK, the protein outside of the lumen was cleaved. After PK cleavage the protected 64kDa protein was identified using immunoblot. Microsomes prepared from fresh and frozen brains displayed the 64kDa fragment after incubation with PK (figure 7.6), indicating that frozen brains could be used to identify transmembrane PrP.

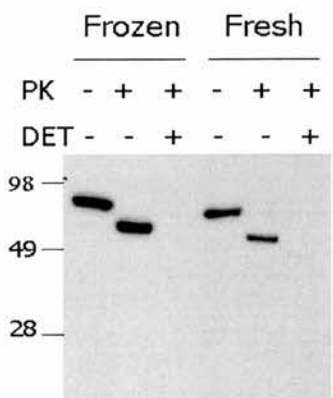

Figure 7.6 Suitability of microsomes preparations from frozen compared to fresh brain from uninfected 101PP mice.

Detection of transmembrane calnexin using an α-calnexin antibody (chapter 2.2) indicates the shift from full length 90 kDa to 64 kDa calnexin.

Transmembrane PrP is found in two forms, ^{Ctm}PrP and ^{Ntm}PrP (chapter 1.11.2) thus antibodies that recognise the C- and N-terminus of PrP were used to identify these forms of PrP. 8H4 had been used

to detect PrP previously (chapters 3, 4 & 6) this recognises the C-terminal epitope at amino acid residues 175-190 of PrP (appendix B). Two N-terminal antibodies had been described, 8B4 and 5B2, which recognise epitopes at amino acid residues 36-43 and 34-52 respectively ((Li et al., 2000) & appendix B). Compared to 5B2, 8B4 was found to have a higher affinity to PrP from uninfected 101PP and 101LL brain homogenate and appeared to preferentially detect the diglycosylated form of PrP at 35kDa (data not shown).

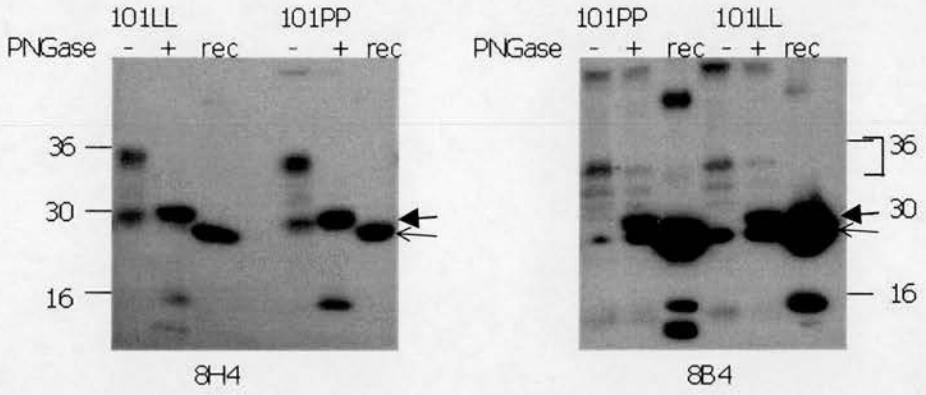

Figure 7.7 Detection of PrP using antibodies that recognise epitopes at the N-terminus

Brain homogenate from uninfected 101PP and 101LL mice was used to determine the usefulness of antibodies that recognise PrP epitopes in the N- and C- terminal region. 2% brain homgenate from 101PP and 101LL mice, untreated (PNG- lane) and deglycosylated as before (PNGase+ lane), control of 25ng recombinant PrP (rec) (naturally deglycosylated at 28kDa, open arrow) detected using C- and N- terminal antibodies, 8H4 (left) and 8B4 (right) respectively. The typical 3-band pattern of PrP^C can be seen in PNGase– lanes at 30-35kDa. The bracket on the right blot indicates probable dimers of rPrP and full length PrP. All immunoblots visualised using secondary rabbit α-mouse antibody and POD substrate (chapter 2.3). Markers indicate kDa sizes.

Monoclonal antibody 8B4 had a similar affinity for PrP from 101PP and 101LL brain homogenate (figure 7.7) and in common with the antibody 8H4, this detected deglycosylated PrP from uninfected 101PP and 101LL brain at 30kDa (figure 7.7). Both antibodies also detected naturally deglycosylated recombinant PrP at 28kDa (figure 7.7). It was important to verify that both antibodies detected deglycosylated PrP since all transmembrane reactions were PNGase treated. Compared to the 8H4 blot results in the 8B4 blot were difficult to interpret because of incomplete deglycosylation (figure 7.7). In both

blots the typical 3-band pattern of PrP^C was seen in PNGase- lanes at 30-35kDa. Deglycosylated PrP^C in PNGase+ lanes was present at 30kDa (closed arrow). The recombinant PrP (rPrP or rec) is non-glysosylated and is present at 28kDa (open arrow), but has been overloaded in the 8B4 blot. In the 8B4 blot the lower 28kDa band in PNGase+ lane (open arrow) probably represents incomplete deglycosylation of PrP from the mono- and diglycosylated bands, additional bands <16kDa in the rec lanes probably represent natural cleavage products of rPrP and additional bands at >50kDa probably represent dimerisation of full-length and recombinant PrP (bracket in figure 7.7).

Control reactions for transmembrane PrP were kindly provided by D. Harris and R. Stewart (Washington University School of Medicine, St Louis, USA). These consisted of reticulocyte lysate translation reactions (L9R-3AV) in which PrP was produced that contained three alanine to valine mutations at PrP amino acid residues 112, 114 and 117. These residues have been shown to induce the production of ^{Ctm}PrP (Stewart & Harris, 2001). The leucine to arginine mutation at residue 9, within the signal sequence, enhances the production of ^{Ctm}PrP (Stewart, Drisaldi & Harris, 2001). In translation reactions a combination of these mutations allows the production of ^{Ctm}PrP alone (Stewart & Harris, 2003).

Half brain was taken from one uninfected 101PP and 101LL mouse and from one ME7/101PP, ME7/101LL and 263K/101LL mouse, and microsomal membranes were prepared (chapter 2.17). The calnexin control assay verified the membranes were in tact (figure 7.8) before the presence of transmembrane PrP was investigated from each preparation.

PrP detection was controlled using homogenates of uninfected 101PP and 101LL brain that were either untreated or PNGase-treated (figure 7.9B). Transmembrane PrP, ^{Ctm}PrP at 19kDa and ^{Ntm}PrP at 14kDa, should have been detected in the control L9R-3AV samples, however no PrP was detected these samples (figure 7.9B). This was possibly due to damage caused by the transit of the control from the USA or by long-term storage at -70^0C. Alternatively, the

harsher conditions of the PK-protection assay used here (37°C for 30 minutes) compared to those previously described (4°C for 60 minutes) (Stewart & Harris, 2001), may also explain the lack of detection of transmembrane PrP.

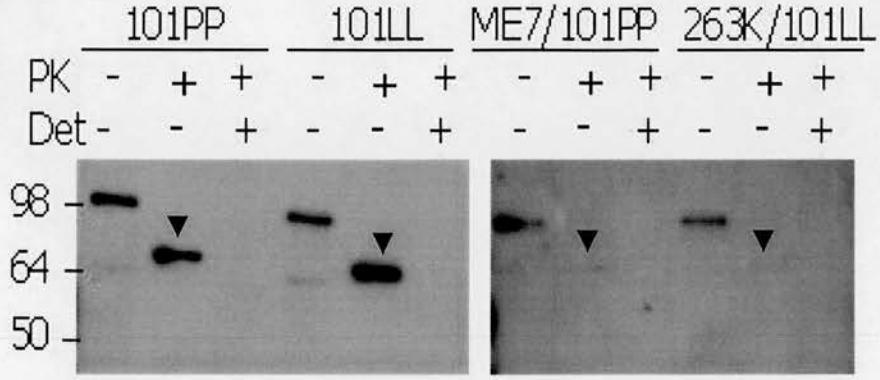

Figure 7.8 Verification of intact microsome preparations

In tact microsomal membrane preparations were confirmed in uninfected 101PP and 101LL as well as ME7/101PP and 263K/101LL brain homogenates, using α-calnexin antibody (chapter 2.2) and visualised using goat α-rabbit secondary antibody (chapter 2.3) and POD substrate. The upper 98kDa band * indicated the presence of full-length calnexin. The lower 64kDa band (downward arrow) indicated the presence of the internal portion of calnexin protected from PK cleavage by the intact microsomal membrane. Marker sizes in kDa.

There is no 19 kDa band in the PK+/Det- lane in any of the samples (figure 7.9B) suggesting that ^{Ctm}PrP is not present at detectable levels in any of these brain samples. All brain homogenates show similar results (figure 7.9B) suggesting no difference in the transmembrane PrP between models. Detection of PrP in the control brain homogenates using 8H4 indicated that the samples were not fully deglycosylated and the resultant PrP was difficult to distinguish (figure 7.9B). Deglycosylated PrP exhibits a major band at 28 kDa and another band at 19-21 kDa, which represents the deglycosylated form of naturally cleaved PrP. These fragments were present on the blots here as major bands at 28 kDa and ~19 kDa (figure 7.9B). However, because PrP was not fully deglycosylated, there were extra bands representing monoglycosylated full length PrP at ~32 kDa and the naturally cleaved glycosylated fragment at ~22 kDa (figure 7.9B). The presence of PK-resistant PrP in the PK+/Det- and PK+/Det+ lanes of ME7/101PP indicates that there is PK-resistant PrP^{Sc} present in this brain. However, curiously, PK-resistant PrP^{Sc} is not present in

these lanes of the ME7/101LL brain. Only one ME7/101LL brain was investigated here and the absence of PK-resistant PrP^{Sc} in this homogenate may be due to experimental error. However, this may also suggest that there is an extremely low level of PrP^{Sc} in this particular ME7/101LL brain homogenate. Unfortunately no immunostaining or immunoblot analysis was performed on this brain prior to use therefore the levels of PrP^{Sc} in this animal is not known.

In this assay, the 8B4 detection of PrP was poor and it is not clear why since 8B4 is clearly capable of detecting PrP (figure 7.7). PrP was faintly detected in PNGase-treated uninfected 101PP and 101LL brain homogenate, but was not detected in untreated samples. PrP was only detected in microsomal preparations from uninfected 101LL homogenate as a deglycosylated fragment of 28 kDa (figure 7.9B). This fragment was also faintly detected at 28 kDa in the PK-/Det+ lane of ME7/101PP (figure 7.9B). No ^{Ntm}PrP was found at 14 kDa in the PK+/Det- lanes for any of the samples (figure 7.9B). The action of freeze-thawing the microsomal membranes, however, may explain the lack of PrP detected from the preparations made here. This action may have fractured the membranes and allowed PK to digest all the PrP, including transmembrane forms.

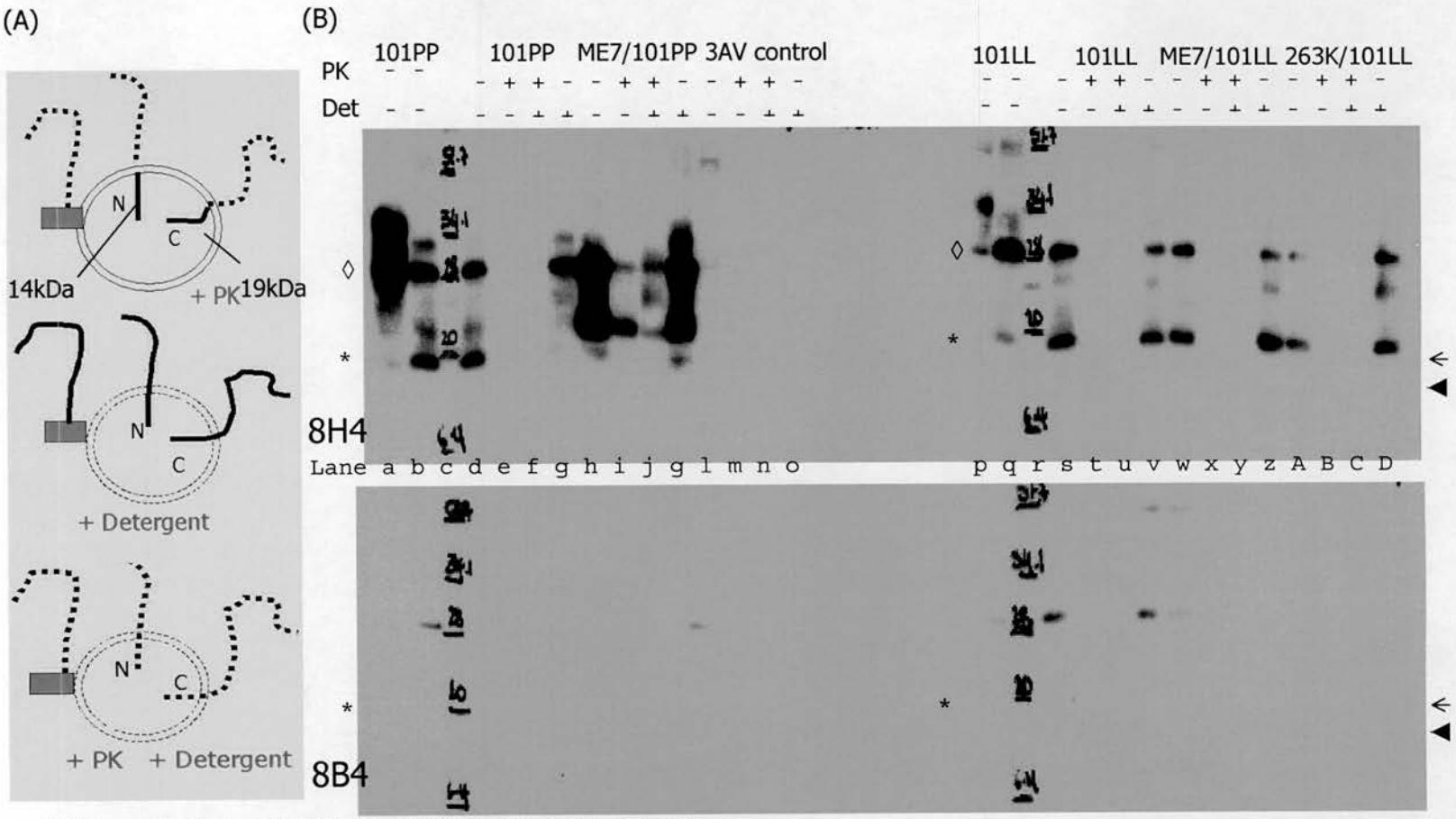

Figure 7.9 Investigation of transmembrane PrP from brain microsomes

Identification of transmembrane PrP from microsome preparations. (A) microsomes treated PK+/Det- contain only the transmembrane forms, ^{Ctm}PrP at 19kDa (open arrow) and ^{Ntm}PrP at 14kDa (closed arrow), PK-/Det+ contain full length transmembrane and cell surface PrP, PK+/Det+ no PrP detected. (B) Transmembrane PrP detected in microsomes prepared from control L9R-3AV reactions (lanes l-o), uninfected 101PP (lanes d-g) and 101LL (lanes s-v) brain and infected ME7/101PP (lanes h-k), ME7/101LL (lanes w-z) and 263K/101LL (lanes A-D) brain, using 8H4 to detect ^{Ctm}PrP (upper blot) and 8B4 to detect ^{Ntm}PrP (lower blot), visualised using rabbit anti-mouse secondary antibody and POD substrate. Control brain homogenate, 1% 101PP(lanes a,b) and 101LL (lanes p,q) (PNGase-/+) loaded to the left of each marker. * 19-21kDa deglycosylated, naturally cleaved PrP. ◊ monoglycosylated full length PrP at ~32 kDa. Marker sizes are indicated at 51, 34, 28, 20 and 6kDa in lanes c & r.

7.4. Discussion

Investigations were performed here to identify the presence of alternative forms of PrP that did not conform to the previously described biological characteristics of PrP^{Sc} (Meyer et al., 1986). Such forms of PrP may explain the apparent absence of PK-resistant PrP^{Sc} in brain homogenate that contain high titres of infectivity.

7.4.1. Transmissible brain contains PrP with PrP^{C}-like characteristics

PrP^{Sc} is classically defined as detergent insoluble and PK-resistant whereas PrP^{C} is PK sensitive and detergent soluble (Meyer et al., 1986). The studies performed here found that uninfected 101PP and 101LL mouse brain contained detergent soluble/PK sensitive PrP, reminiscent of PrP^{C}, however this PrP did display partial PK-resistance at low PK concentrations. This single 28kDa intermediate form was previously described (Buschmann et al., 1998) and is thought to represent an N-terminally cleaved product of full length PrP^{C}. The flexible N-terminal region of PrP is thought to be more accessible to PK than the structured region, therefore the N-terminus is thought to be cleaved before the 28kDa C-terminal globular domain (Buschmann et al., 1998). Homogenate from 263K/101LL (2) and (3) contained PrP with PrP^{C} characteristics; detergent soluble and PK-sensitive, and is consistent with the lack of PK-resistant PrP^{Sc} detected upon immunoblot (chapters 3 & 6). Studies here did not indicate the presence of PrP intermediate to PrP^{C} and PrP^{Sc} in 263K/101LL (2) and 263K/101LL (3) brain homogenates. Where PrP^{Sc} was readily detected; in 263K/101LL (1), ME7/101PP and ME7/101LL homogenate (chapter 6), PrP was detergent insoluble and PK-resistant, consistent with the biochemical definition of PrP^{Sc}. However, the PrP in 263K/101LL (1) appeared less PK-resistant than that in the ME7 models, consistent with a previous study describing the ME7 agent as more PK-resistant than 263K (Kuczius & Groschup, 1999).

The resistance of PrP^{Sc} to PK may be due to the highly aggregated nature of PrP^{Sc}. A tighly packed aggregate of PrP in ME7/101PP brain may not allow PK to access the aggregate to completely cleave the protein. However, if PrP

is aggregated loosely in 263K/101LL brain this may allow PK to access PrP and cleave the protein. Low concentrations of PK may therefore be effective in completely cleaving 263K/101LL whereas high concentrations of PK would be required to completely cleave PrP in ME7/101PP brain. Moreover, given that PrP in 263K/101LL (1) is less PK-resistant than PrP in the ME7 models this may indicate the presence of smaller amounts of highly aggregated PrP^{Sc} in 263K/101LL (1) compared to the ME7 models. PrP in ME7/101PP and ME7/101LL brain homogenate was resistant to similar concentrations of PK even though the ME7/101LL homogenate contained half the amount of PrP^{Sc} than the ME7/101PP homogenate (chapter 6). These data probably indicate that PrP found in brain from ME7/101PP and ME7/101LL models is likely to be highly aggregated whereas PrP in 263K/101LL is less so.

Concentration of PrP^{Sc} in GSS/101LL brain revealed the presence of a small amount of PK-resistant PrP^{Sc}. This may account for the transmission of TSE from this brain homogenate to 101LL mice (chapter 5). Brain homogenate from 263K/101LL (2) and 263K/101LL (3) also transmitted infectivity to 101LL mice however no PK-resistant PrP^{Sc} was detected in these brains even upon 5x concentration of the homogenate. This 5x concentration may not have been enough to reveal exceedingly small amounts of PK-resistant PrP^{Sc} in these homogenates thus methods of PrP^{Sc} concentration such as precipitation of PrP^{Sc} using salts (Polymenidou et al., 2002; Wadsworth et al., 2001) should have been considered. It was not possible to perform such experiments on the exact brain homogenates investigated here due to limited availability however it may have been prudent to use fresh brain from representative animals of each model.

Infectivity was transmitted from all three 263K/101LL brain homogenates yet in 263K/101LL (2) and (3) the only PrP detected had PrP^{C}-like characteristics. This may suggest that in these particular brain homogenates, if PrP is the infectious molecule, a detergent soluble, PK-sensitive form can confer infectivity. Since no PK-resistant PrP was present in 263K/101LL (2) and 263K/101LL (3) brain homogenate PK-sensitive PrP is likely to make up the majority of infectious PrP in these brains. This

may suggest that the acquisition of infectivity may occur at a very early stage during $PrP^{C} \rightarrow PrP^{Sc}$ conversion so that infectious PrP may have a PrP^{C}-like conformation (e.g. PrP^{I} portrayed in figure 7.1). If the infectious agent is a molecule (or complex of molecules) associated with PrP, this association may occur at a very early stage of disease. Moreover, taking into consideration previous *in vitro* data indicating the conversion of PrP^{C} to a PK resistant form of PrP which is not infectious (Hill et al., 1999a), then it may be that a PrP-associated infectious molecule, present *in vivo*, is not critical to the *in vitro* conversion process *per se*. If this molecule was the infectious agent of TSE then this would suggest that the infectious mechanisms of TSE are separate from PrP conversion mechanisms.

7.4.2. 101LL mice are unlikely to contain transmembrane PrP

Brain tissue from all models investigated here was analysed for the presence of transmembrane forms of PrP as ^{Ctm}PrP and ^{Ntm}PrP. No transmembrane PrP was detected in uninfected 101PP and 101LL mouse brain. This agrees with other studies that have failed to find transmembrane PrP associated with the P101L mutation (D. Harris, Washington University, USA, personal communication) and in models with disease-causing mutations outside of the hydrophobic region of PrP (Stewart & Harris, 2001). Infection of 101LL mice with ME7 or 263K TSE agents did not result in detection of ^{Ctm}PrP in these animals. However, ^{Ctm}PrP and ^{Ntm}PrP were not detected from the appropriate controls, thus the presence of ^{Ctm}PrP in infected 101LL mice cannot be completely ruled out. Additionally transmembrane PrP was not identified from the single experiment performed here. Since this was not repeated, the presence of transmembrane PrP in the brain samples studied here cannot be completely ruled out. Moreover, the concentration of microsomal membranes recovered from the brains investigated here may have been low, thus low amounts of transmembrane PrP may not have been visible in these preparations.

In the experiments performed here, however, the suggested absence of ^{Ctm}PrP in infected 101LL mice is consistent with the finding that ^{Ctm}PrP

production is not enhanced during TSE infection (Stewart & Harris, 2003). Given that ^{Ctm}PrP has been reported to represent ~1% of the total PrP, it is possible that the experiments performed in this thesis are not sensitive enough to detect extremely low levels of ^{Ctm}PrP. Previous data here have indicated that immunoblot of PrP can detect ≥5ng PrP (chapter 6), thus if ^{Ctm}PrP is present, levels must be <5ng. The use of the recently reported ^{Ctm}PrP-specific antibody, anti-SP (Stewart & Harris, 2003), may enhance the detection of this form of PrP. Evidence from *in vitro* and *in vivo* experiments suggests that only mutations within the hydrophobic domain of PrP (residues 111-134) result in an increased amount of transmembrane PrP (Hegde et al., 1998; Stewart & Harris, 2001). The GSS mutation, A116V, was shown to increase ^{Ctm}PrP production *in vitro* and *in vivo* (Hegde et al., 1998; Stewart & Harris, 2001). However the P101L GSS mutation lies out-with the hydrophobic domain therefore would not be predicted to cause an increase in transmembrane PrP in the 101LL mice studied here. Other *in vitro* studies in which human neuroblastoma cells expressed PrP^{C} with the P101L mutation have suggested that, compared to cells that do not contain the P101L mutation, there is an increased concentration of a 20 kDa fragment of PrP apparently derived from ^{Ctm}PrP (Mishra et al., 2002). To explain the lack of PrP^{Sc} found in human GSS cases and in animal models of GSS, the authors of this paper suggest that the P101L mutation causes an increased production of ^{Ctm}PrP during disease (Mishra et al., 2002). Furthermore, they suggest that the increased presence of ^{Ctm}PrP, associated with the P101L mutation, causes an increase in disease susceptibility (Mishra et al., 2002). However, this is contradictory to the extended incubation times reported for transgenic 101LL mice infected with human vCJD or with murine TSE agents 22A and 79V (Barron et al., 2001; Barron et al., 2003). These mice show extended rather than shortened incubation times compared to mice without the P101L mutation and suggests that the 101LL polymorphism can decrease as well as increase susceptibility to disease. Transmembrane forms of PrP have been suggested to be the neurotoxic agent in models of TSE where PrP^{Sc} is non-detectable (chapter 1.11), however from the experiments performed here and elsewhere (Stewart & Harris, 2001; Stewart & Harris, 2003), these forms are unlikely to be involved in the disease process in 101LL mice.

7.4.3. 101LL mice may contain other forms of PrP

Cystolic PrP (cyPrP) along with ^{Ctm}PrP have not yet been demonstrated to be infectious however these forms have been suggested, to cause neurotoxicity in TSE disease (Ma et al., 2002; Stewart & Harris, 2003)(chapters 1.11 & 1.12). The accumulation of cyPrP may occur when cellular quality control mechanisms are overwhelmed, with an increase in improperly folded PrP^{C} leading to a build-up of a PrP^{Sc}-like protein (detergent insoluble/partially PK-resistant) that is neurotoxic (Dimcheff, Portis & Caughey, 2003b). Other investigators suggest that cyPrP is not toxic to cultured human primary neurons thus cyPrP is not applicable to human disease (Roucou et al., 2003). Indeed these authors suggest that cyPrP (and normal PrP) is neuro-protective and directly interacts with the neuronal-specific proapoptotic protein, Bax, to inhibit neuronal apoptosis (Roucou et al., 2003). The involvement of cyPrP in TSE disease has therefore yet to be fully resolved. Cytosolic PrP can apparently cause neurodegenerative disease in the absence of PK-resistant PrP^{Sc} however since cyPrP has not been shown to be infectious it is unlikely that this form of PrP would be present in the 101LL mice.

It is more likely that 263K/101LL (2) and 263K/101LL (3) brain homogenates, and perhaps some GSS/101LL brains, contain an infectious and PK-sensitive form of PrP. Using an alternative PK-treatment regime and the CDI assay PK-sensitive PrP^{Sc} ($sPrP^{Sc}$) has been described transgenic mice, containing the P101L mutation, that have been TSE-infected or become spontaneously ill (Tremblay et al., 2004). Since Tg2866 mice succumb to spontaneous neurodegenerative disease and TSE can be further transmitted from brain, the detection of $sPrP^{Sc}$ in these mice is thought to represent the infectious agent. However the indicator Tg196 mice in which spontaneously ill Tg2866 brain homogenate was transmitted also succumb to spontaneous disease. Tg196 brain homogenate does not contain PK-resistant PrP^{Sc} or $sPrP^{Sc}$ thus it is not clear whether $sPrP^{Sc}$ is an infectious form of PrP. If $sPrP^{Sc}$ was detected in 263K/101LL (2) and 263K/101LL (3) brain this may provide more definitive evidence in support of the suggestion that $sPrP^{Sc}$ may be the infectious agent in some cases of TSE.

It is possible that there are subtle differences in $PrP^{C} \rightarrow PrP^{Sc}$ conversion process in 101PP and 101LL mice that causes the appearance of PK-sensitive, infectious PrP in the 263K-infected 101LL mice. Alongside the presence of PK-sensitive PrP the presence of ^{Ctm}PrP or cyPrP in these mice may indicate that there is an alternative processing of PrP that causes the rapid accumulation of these neurotoxic forms thus the rapid death of infected 101LL mice. The use of the anti-SP antibody (Stewart & Harris, 2003), may help verify whether ^{Ctm}PrP and indeed cyPrP are present. Isolation of these forms of PrP followed by purification of PrP and application *in vivo* or *in vitro* may indicate whether these are associated with neurotoxicity rather than infectivity (chapter 1.12). This would indicate that the neurotoxic characteristic of PrP is separate from the infectious characteristic of TSE.

8. Discussion

8.1. PK-resistant PrP^{Sc} does not definitively correlate with infectivity

The correlation between PK-resistant PrP^{Sc} and infectivity is a central issue in the field of TSE disease. PrP^{Sc} is found only in infected tissues and the prion hypothesis, which predicts that PK-resistant PrP^{Sc} alone is the infectious agent of TSE, was formulated from experiments that co-purified PrP^{Sc} and infectivity from infected brain from models exhibiting abundant PK-resistant PrP^{Sc} at the terminal stages of disease (chapter 1.2). Indeed in hamsters infected intracerebrally and orally with TSE, there is a strong correlation between PrP^{Sc} level and titre of infectivity (Beekes et al., 1996; McKinley et al., 1983; Prusiner, 1982). The detection of PK-resistant PrP^{Sc} from BSE-infected cattle brain has also been shown to be consistent with the correlation between PrP^{Sc} and infectivity (Deslys et al., 2001).

Despite the demonstration that PK-resistant PrP^{Sc} correlates with infectivity in these models there are cases of TSE where this form of PrP does not appear to correlate with the presence of TSE or infectivity. PrP^{Sc} was not detected in the brain of scrapie infected goats (Foster et al., 2001a), nor in humans affected by FFI (Dorandeu et al., 1998) or GSS (Tateishi et al., 1990). The lack of detectable PK-resistant PrP^{Sc} in these brains may be explained by the presence of extremely low titres of infectivity in affected brain. PrP^{Sc} levels in such brain may be so low they are extremely difficult to detect. It is also possible that PK-resistant PrP^{Sc} may not be the infectious agent in these cases of TSE. An alternative form of PrP or a molecule other than PrP may be the infectious agent. Murine models of TSE have been described in which disease can be transmitted from brain that contains no detectable PrP^{Sc} (chapter 1.9). The murine model of BSE transmission to C57Bl/6 mice (Lasmezas et al., 1997) and the transgenic model of GSS in Tg174 mice (Hsiao et al., 1994) have both described undetectable or extremely low levels of PK-resistant PrP^{Sc} in the brains of TSE-affected mice, yet brain material from each of these models can transmit infectivity. The model of Lasmezas *et al* in particular definitively

demonstrates the presence of infectivity in the apparent absence of PK-resistant PrP^{Sc} and may suggest that PK-resistant PrP^{Sc} is not the infectious agent.

In addition to the Lasmezas model, the 263K/101LL model of TSE was previously found to transmit TSE in the apparent absence of PK-resistant PrP^{Sc} (Barron et al., 2001). It was thought that this model was useful for further investigation into the correlation between PK-resistant PrP^{Sc} and infectivity since high PrP^{Sc} levels would not obscure the real infectious agent. In the studies here, the correlation between PK-resistant PrP^{Sc} and infectivity appeared to hold where mice were infected with the same strain of TSE agent (chapters 5 & 6). ME7/101PP exhibited two-fold more PrP^{Sc} and one log more infectivity than ME7/101LL. Of all the 263K/101LL brain homogenates studied here 263K/101LL (1) exhibited most PrP^{Sc} and had the highest infectivity titre. However, PK-resistant PrP^{Sc} and infectivity did not appear to correlate across all of the models investigated (chapters 5 & 6). Surprisingly, brain homogenates from 263K/101LL (1) and one ME7/101PP animal both exhibited the same titre of infectivity yet ME7/101PP homogenate contained five-times more PrP^{Sc} than 263K/101LL (1) homogenate. Furthermore, in 263K/101LL (2) and 263K/101LL (3) brain homogenates there was no detectable PK-resistant PrP^{Sc} yet these contained similar titres of infectivity to one brain homogenate from the ME7/101LL model, which contained only two-fold less PrP^{Sc} than ME7/101PP homogenate. These data (summarised in figure 8.1) appear contrary to the prion hypothesis.

The model of TSE studied here was not unique in showing that infectivity could be transmitted in the absence of detectable PK-resistant PrP^{Sc}. However the data presented in this thesis is the first to clearly demonstrate high titres of infectivity in brain where PK-resistant PrP^{Sc} cannot be detected.

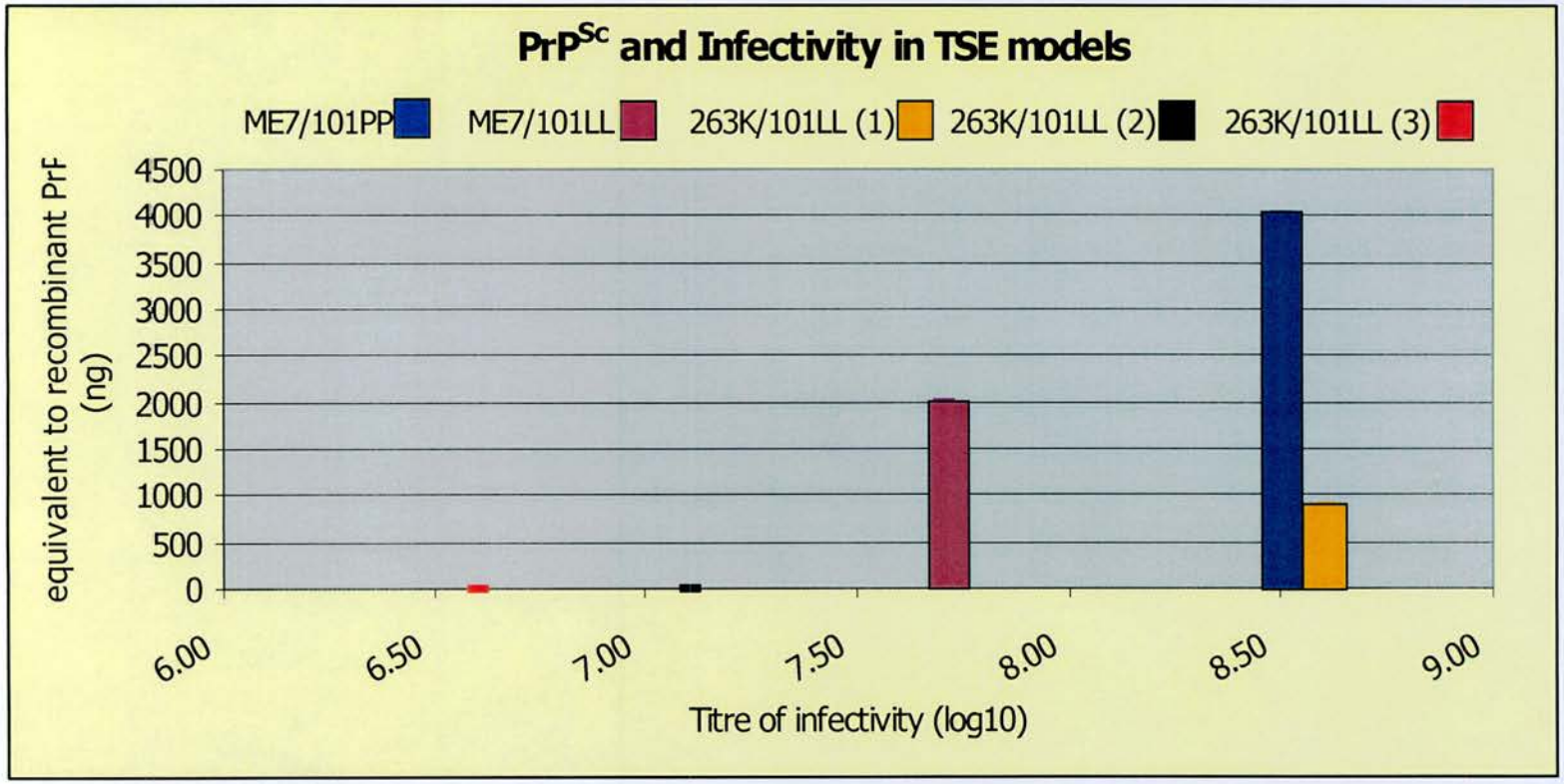

Figure 8.1 Amount of PK-resistant PrP^{Sc} and infectivity detected in high, intermediate and low PrP^{Sc} models

Titre of infectivity for each model plotted against the corresponding amount of PK-resistant PrP^{Sc} detected by immunoblot relative to 50ng recombinant PrP, using 8H4 monoclonal antibody. One brain each from ME7/101PP and ME7/101LL models and three separate brains from the 263K/101LL model were investigated.

8.2. PK-resistant PrP^{Sc} may not be the causal agent of TSE

In cases of TSE where there is an absence of PK-resistant PrP^{Sc} it has been proposed that the infectious agent may be an alternative form of PrP. Human brain affected by GSS/A117V has been shown to contain increased amounts of transmembrane PrP as ^{Ctm}PrP (Hegde et al., 1998). Increased amounts of ^{Ctm}PrP were also seen in a transgenic model of GSS/A116V (Hegde et al., 1999). However, neither brain from the human case or the murine model investigated was capable of transmitting TSE further thus it is possible that ^{Ctm}PrP is a neurotoxic rather than infectious molecule. Since the 263K/101LL mice investigated in the studies in this thesis contained very little if any PrP^{Sc} in the brain, attempts were made to identify whether transmembrane PrP was present in these mice. The single experiment performed here did not allow a definitive conclusion to be drawn as to whether ^{Ctm}PrP forms were present in the 263K/101LL model, however it indicated that ^{Ctm}PrP may be absent from this model. It is unlikely that such forms would be present since the 101LL mice used in this model have a *Prnp* mutation out-with the transmembrane domain and it has been shown that only mutations in the transmembrane domain can induce the production of ^{Ctm}PrP (Stewart & Harris, 2001).

Other cases of TSE in which no PK-resistant PrP^{Sc} was detected in infected brain are those of the human octapeptide repeat insertion and the murine model of this disease in PG14 mice (Chiesa et al., 1998). These mice displayed a neurological disease reminiscent of TSE, however, in accordance with the suggestion that only mutations within the transmembrane domain of PrP caused the production of ^{Ctm}PrP, no transmembrane PrP was found in the brain of affected animals from this model (Stewart & Harris, 2001). Instead, PrP with altered PK-sensitivity was found in brain homogenate treated with low concentrations of PK (Chiesa et al., 1998). This brain material was not capable of transmitting TSE thus the PK-sensitive PrP in this model is not infectious. The discovery of non-infectious, PK-sensitive PrP in PG14 mice differs from the findings in this thesis. 263K/101LL brain homogenate contained high titres of

infectivity and did transmit infectivity to 101LL mice, however there appeared to be only PK-sensitive, detergent soluble PrP present where no PrP^{Sc} was detected (chapter 7). This implied that a proportion of PK-sensitive PrP detected in these brain homogenates was infectious and further investigation is ongoing to definitively identify whether PK-sensitive PrP is the infectious agent in the 263K/101LL model. These data may suggest that the PK-sensitive PrP present in the PG14 model represents a neurotoxic rather than infectious molecule.

Another study has linked PK-sensitive PrP to TSE. PK-sensitive PrP^{Sc} ($sPrP^{Sc}$) was identified in spontaneously sick Tg2866 and TSE-infected Tg196 transgenic mice, which both carry the GSS/P101L mutation (Tremblay et al., 2004). Both these lines of mice become spontaneously sick, with 100% incidence in Tg2866 mice by 132 days and 20-30% incidence in Tg196 mice by approximately 550 days (Kaneko et al., 2000; Tremblay et al., 2004). In these mice PK-sensitive PrP^{Sc} was detected using an alternative PK regime, treating brain homogenate with 250µg/ml PK for one hour at 4^0C. PK-sensitive PrP^{Sc} appeared as a single band at 22-24kDa upon immunoblot of all infected Tg196 and spontaneous Tg2866 brains investigated. However, it was not clear whether $sPrP^{Sc}$ was present in uninfected Tg196 mice, whether spontaneously ill or not, thus it is difficult to say whether $sPrP^{Sc}$ is truly associated with infectivity. Clarification of this issue is required before $sPrP^{Sc}$ can be described as a disease-associated form of PrP in the Tg196 and Tg2866 models.

It may be that the PK-sensitive PrP described in 263K/101LL mouse brain is similar to the $sPrP^{Sc}$ form described by Tremblay *et al*, therefore it would be prudent to perform the alternative PK regime on 263K/101LL brain homogenate. Furthermore, since infectivity is not associated with PK-resistant PrP^{Sc} in the 263K/101LL model, the presence of $sPrP^{Sc}$ in this model may provide a clearer indication of whether this form of PrP is indeed infectious. Since the 263K/101LL model is a true TSE and is not complicated by evidence of a spontaneous disease in the transgenic 101LL mice, this provides a more elegant model to study the proposed link between infectivity and $sPrP^{Sc}$. If $sPrP^{Sc}$ is infectious, this may represent

one of the intermediate PrP* forms proposed to exist during the conversion of $PrP^{C} \rightarrow PrP^{Sc}$ (Weissmann, 1991).

8.3. PK-resistant PrP^{Sc}: A metabolic end product?

The prion hypothesis suggests that the normal protein, PrP^{C} undergoes a conformational change to become infectious PK-resistant PrP^{Sc} (Pan et al., 1993). It is not known how or where during the conversion process PrP^{Sc} acquires infectivity. It has been suggested that the conformational change itself can confer infectivity, however studies have shown that PK-resistant PrP produced via *in vitro* conversion is not infectious (Hill et al., 1999a). This indicates that conformational change itself is not enough to make PK-resistant PrP infectious and may suggest that PrP^{Sc} is not the infectious agent. Moreover, experiments using heat treatment have dissociated infectivity from the PK-resistant property of PrP (Somerville et al., 2002) and further suggest that PK-resistant PrP^{Sc} is not the infectious agent of TSE. If the infectious agent is not PrP another molecule or complex of molecules may be the infectious agent, and may associate with PrP. *In vitro* studies and studies in yeast have demonstrated the principal of PrP conversion (Kirby et al., 2003; Kocisko et al., 1994; Liebman, 2002) and it is possible that PrP^{Sc} is simply the final product in the conversion process rather than the infectious agent *per se*.

The fact that PK-resistant PrP^{Sc} is present in most TSE cases may be an indication that $PrP^{C} \rightarrow PrP^{Sc}$ conversion usually occurs at a rapid rate. In some TSE models the conversion process may proceed rapidly towards the PrP^{Sc} endpoint, with the infectious agent associating with PrP^{Sc}. In other models, such as 263K/101LL, this conversion process may occur more slowly, with a detergent soluble, PK-sensitive intermediate form of PrP produced. The experiments performed in this thesis may indicate that in the cases of TSE where PrP^{Sc} is not detected the conversion reaction may not have reached the PrP^{Sc} endpoint and PrP^{Sc} may not be produced by the time the animal dies. It is not clear why there should be differences in the rate of conversion of PrP between different TSE models. More particularly it is not clear why PrP conversion would occur at an extremely slow rate in the

263K/101LL model studied here. It would be interesting to use brain homogenate from the 263K/101LL model in cell-free conversion (Kocisko et al., 1994) and PMCA experiments (Saborio et al., 2001) to identify whether the PrP in this model is capable of forming PrP^{Sc}. If PK-resistant PrP^{Sc} were formed from this material it would add to the data in support of the prion hypothesis. However, the titre of infectivity of the resultant material would also have to be assessed to investigate whether additional PrP^{Sc} formed was infectious.

Subpassage of a TSE agent in the same species usually results in an increased accumulation of PK-resistant PrP^{Sc} in the brain as the TSE strain stablises. Further studies of the 263K/101LL model have indicated that upon subsequent passage of two of the three isolates described in this thesis (chapter 5) PK-resistant PrP^{Sc} became evident in brain homogenate. However, passage of one 263K/101LL isolate resulted in disease with a continued absence of PrP^{Sc} in brain homogenate. It is not known whether, in accordance with the prion hypothesis, the titre of infectivity increased with an increased presence of PK-resistant PrP^{Sc} or whether the discrepancy between titre of infectivity and PrP^{Sc} remains. This requires further investigation. Moreover, if the absence of PK-resistant PrP^{Sc} remained consistent upon passage of one 263K/101LL isolate, this would be an ideal model to dissect the strain-specific factors required for infectivity, and to investigate whether PK-resistant PrP^{Sc} was primarily the neurotoxic agent of TSE in this model.

It is not clear where in the cell the $PrP^{C} \rightarrow PrP^{Sc}$ conversion process occurs or where the infectious molecule/complex interacts with PrP. There are several likely scenarios, however. It may be that:

- PrP^{C} interacts with an exogenous infectious molecule on the cell surface and internalises it during the normal recycling process, therefore allowing the infectious molecule access to any PrP already undergoing conversion within the cell. It is possible that this binding/internalisation phase may itself trigger the conversion of PrP.

- Conversion of PrP takes place on the cell surface, making all conformations of PrP readily available to interact with an exogenous infectious molecule.

- The infectious agent is an endogenous molecule or complex and that the interaction between this molecule and PrP^{Sc} occurs within the cell. PrP^{C} and PrP^{Sc} have been shown to react with many molecules including the laminin receptor protein (Rieger et al., 1999), Grb2 and synapsin 1b (Spielhaupter & Schatzl, 2001), and RNA (Adler et al., 2003; Weiss et al., 1997), and probably many more.

Whilst these possibilities do not rule out a form of PrP as the infectious agent, they also suggest that an as yet unidentified molecule may be the infectious agent of TSE, and that this may associate with PrP during TSE disease.

8.4. Infectivity associated with PK-resistant PrP^{Sc}

One infectious unit of TSE is defined as containing 10^5 to 10^6 molecules of PrP^{Sc} (Beekes et al., 1996; Hilmert & Diringer, 1984; McKinley et al., 1991; Meyer et al., 1986). According to the prion hypothesis, PrP^{Sc} is derived from PrP^{C}. If PrP^{C} can give rise to any form of PrP that is infectious the number of PrP molecules per infectious unit would remain constant in this model since all forms of PrP have a molecular weight of approximately 30,000Da. However, since this data has only been published in the hamster TSE model it was not known whether the number of PK-resistant PrP^{Sc} molecules per ifu differs for different models. In the studies performed here, there were $<10^5$ molecules of PrP^{Sc} associated with one infectious unit in brain from the 263K/101LL model. In the ME7-infected models however, there were 10^5 to 10^6 molecules of PrP associated with one infectious unit. This data therefore suggests that one unit of infectivity in different models of TSE is comprised of a different number of PrP^{Sc} molecules. These data may indicate that in the 263K/101LL model either one molecule of PK-resistant PrP^{Sc} from 263K/101LL is more "infectious" than one PK-resistant PrP^{Sc} molecule from the ME7 models, or there is a strain-associated

molecule/complex that is more prevalent in 263K/101LL than in the ME7 models (chapter 6). In the context of the discussion above (section 8.3) it may be the strain-associated complex rather than the PrP that is the infectious agent in the 263K/101LL model.

8.5. Strain specificity of PrP^{Sc}

The demonstration that there was no absolute correlation between PK-resistant PrP^{Sc} and infectivity in brain across the models studied here may suggest intrinsic differences in the PrP^{Sc} in each model. Each of the TSE models studied in this thesis exhibited different disease incubation times, titres of infectivity and vacuolation profiles consistent with different strains of TSE agent (chapter 1.7). It is not clear whether a TSE strain is defined via the conformation of PrP (Safar, 1996) or whether another, perhaps genetic, element is involved (Dickinson & Outram, 1988; Kimberlin, 1976a). It may be that the conformational dependant immunoassay (CDI) could identify different conformations of PrP in the 263K/101LL model compared to the ME7-infected models used in this thesis. This would indicate whether the PK-sensitive, detergent soluble PrP found in the 263K/101LL model had a different conformation compared to PrP^{Sc} found in the ME7 models. If so, this may indicate that this infectious PrP was an intermediate form of the infectious agent. This would also strengthen the experimental evidence to suggest that PrP conformation encodes the unique strain-specificity of each TSE agent.

However, if the infectious agent is not a form of PrP but is associated with PrP then TSE-strain specificity may be conferred by this other molecule or complex of molecules. This is consistent with the strain-specific element of TSE discussed at length both by Dickinson and by Kimberlin (Dickinson & Outram, 1988; Kimberlin, 1976a) where it is proposed that the TSE agent is partially composed of genetic material that can encode the properties of each TSE strain. The alternative infectious agent may be composed partially or entirely of nucleic acids, however studies to find a strain-specific DNA or RNA association with PrP have not been successful (Somerville, 1991). Recent *in vitro* studies have shown that the addition of RNA in cell-

free conversion assays assists in converting PrP-sen to PrP-res (Deleault et al., 2003) and indicates that a nucleic acid component may be required for infectivity in TSE disease. This nucleic acid component may have a strong association with PrP^{Sc} and may encode for the strain specificity of TSE agents, however it is not clear whether this is a host-encoded or exogenous component.

The unique strain-specific component in each TSE model may explain the different disease incubation times for each model. Within the 263K/101LL model, each isolate, 263K/101LL (1), (2) and (3), transmitted disease with distinct incubation times and displayed different abilities to transmit infectivity to 101PP mice. Upon subsequent passage through 101LL mice, each isolate may become a distinct strain of TSE agent. Since it is not known how infectivity is acquired, it would be interesting to follow each 263K/101LL isolate through subsequent passage in 101LL mice and study the correlation between PrP^{Sc} and infectivity at each passage. A faster disease course in the 263K/101LL model may indicate that there are more of the strain specific factors present in this model compared with the other models investigated. Alternatively, upon passage, 101LL mice may select specific TSE isolates, which have short disease incubation times.

8.6. PK-resistant PrP^{Sc} as a marker for infectivity

The important finding of these studies is the demonstration of a model of TSE in which substantial titres of infectivity are present in the absence of detectable PK-resistant PrP^{Sc}. Diagnostic assays that rely on the presence of PK-resistant PrP^{Sc} as an indicator of TSE assume that there is a strong correlation between infectivity and PrP^{Sc}. This includes the ELISA and immunoblot assays that have been approved for use by the EU to screen for BSE and scrapie in Europe (Biffiger et al., 2002; Deslys et al., 2001; Grassi, 2003; Madec et al., 1998; Schaller et al., 1999). As discussed at length in this thesis, there are now several examples of human and animal cases as well as experimental TSE models that dispute this correlation (chapter 8.1). More recently abnormal forms of scrapie and BSE have been described in which PK-resistant PrP^{Sc} was either not detected using the EU-approved

assays (Buschmann et al., 2004) or differed in electrophoretic pattern from that seen previously (Biacabe et al., 2004). Sub-clinical cases of TSE have been described in which clinical symptoms are not evident yet infectivity is present (Hill & Collinge, 2003) and infectivity has been reported in the spleen of 263K-infected hamsters before the appearance of PK-resistant PrP^{Sc} (Czub et al., 1986a). The absence of detectable PK-resistant PrP^{Sc} therefore does not indicate the absence of infectivity and demonstrates the potential for carriers of TSE to be present in the normal population. Such carrier status in humans could result in the transmission of disease to an individual by surgery or transfusion. Furthermore, atypical forms of ruminant TSE could result in TSE-infected foodstuffs inadvertently entering the food chain.

Whilst some diagnostic assays claim to detect the amount of PrP^{Sc} that would be present in one infectious unit (Deslys et al., 2001; Safar et al., 2002) none of these techniques directly measure infectivity. Bioassay remains the most reliable method for detecting infectivity however this is a time consuming and expensive process, not suitable for large-scale diagnostic purposes.

Efforts have been made to find a surrogate marker for infectivity. In cerebrospinal fluid (CSF) the presence of the proteins 14-3-3 and tau have been reported to correlate with CJD (Baxter et al., 2002; Van Everbroeck et al., 2003), however the levels of these proteins were low at disease onset and end-point. CSF samples taken at early onset or pre-clinically therefore are not likely to indicate the presence of TSE. Erythroid differentiation-related factor (EDRF) has also been proposed as a surrogate marker for TSE (Miele et al., 2001). The levels of expression of this protein were found to be significantly reduced in experimentally infected hamsters and mice and in natural BSE and scrapie cases. EDRF is expressed in bone marrow and in blood thus may provide a simple diagnostic assay that could be used to monitor the development of TSE in susceptible individual humans and animals.

The studies performed in this thesis are the first to describe the presence of high titres of infectivity in the absence of PK-resistant PrP^{Sc} in a murine model. These studies, the findings of atypical cases of BSE and scrapie, and the recent report of the possible transfer of infectivity via blood transfusion in humans highlight the need for a more suitable marker of TSE infectivity to be identified and utilised in a rapid and preferably inexpensive diagnostic assay.

8.7. Non-pathogenic PrP^{Sc}

It is not clear whether PrP deposition in the brain is neurotoxic. *In vitro* studies have identified a neurotoxic fragment of PrP from amino acid residues 106-126 (Brown, 2002) therefore full-length PrP itself may have a neurotoxic characteristic. It has been suggested that the deposition of PrP^{Sc} in TSE-infected brain may cause other TSE-associated pathology such as spongiosis and neuronal loss (De Armond et al., 1989; Jeffrey et al., 2001). However this may be misleading. Spongiosis and neuronal loss can occur in infected brains in the absence of PK-resistant PrP^{Sc} (Dorandeu et al., 1998; Foster et al., 2001a), and although outwith the wider remit of this thesis, studies performed here also demonstrated the presence of TSE-associated pathology in the 263K/101LL and GSS/101LL models in the absence of PK-resistant PrP^{Sc} (chapter 4). This may indicate that something other than PK-resistant PrP^{Sc} (perhaps an elusive infectious molecule/complex?) causes TSE pathology. The pro-apoptotic proteins, Fas and caspase-3 have been described in TSE-infected brain (Jamieson et al., 2001) and it may be that the presence of the infectious complex/molecule may trigger apoptosis, microglial activation and contribute to neuronal loss. Equally, these pathological characteristics of TSE may be triggered by the $PrP^{C} \rightarrow PrP^{Sc}$ conversion process itself, or by another unidentified mechanism. Many time-course studies have been performed to identify the causal pathology of TSE (chapter 4) and further pathological studies using the 263K/101LL or GSS/101LL models may help to elucidate the exact cause of TSE pathology. The studies performed in this thesis indicate that these models would provide a PrP^{Sc}-free *in vivo* environment to study the neurodegenerative and pathological aspects of these diseases.

8.8. Is TSE a viral disease?

In the studies performed here individual 263K/101LL and GSS/101LL mice were identified that do not exhibit PrP^{Sc} deposition in areas of the brain where spongiosis is evident. This is similar to the finding that CasBrE, a murine retrovirus, causes spongiosis in infected animals yet virus is not detected in infected animals (Portis, 2001). It is thought that pathogenesis in CasBrE infected animals may be a consequence of indirect effects of viral infection. Similarly, the spongiosis observed in TSE-infected animals may be caused via an indirect effect of the infectious agent of TSE. The presence of this agent may additionally trigger the conversion of $PrP^{C} \rightarrow PrP^{Sc}$. Alternatively if the infectious agent of TSE is a latent endogenous virus, the conversion of $PrP^{C} \rightarrow PrP^{Sc}$ itself may trigger replication of the infectious virus. As yet no viral component has been described in the TSE-infected host, however the virus may be composed of host derived components or may be endogenous.

In CasBrE infected mice, the associated envelope protein has been found to be misfolded. This appeared to up-regulate proteins associated with ER stress such as CHOP, BiP and Grp58, which may in turn account for the observed up-regulation of pro-apoptotic proteins DP5, p21 and GADD45 and the down-regulation of the anti-apoptotic protein IAP2. In TSE, ER stress has also been shown to increase misfolded forms of PrP such as cyPrP (chapter 1.12), which have been proposed to cause neurodegeneration (Ma et al., 2002; Stewart & Harris, 2003). Furthermore, the ER chaperone, BiP, has been found to bind to mutant PrP (Jin et al., 2000) and pro-apoptotic proteins (Fas and caspase-3) have been found in murine models of TSE (Jamieson et al., 2001). Such data indicates that viral and TSE infections may share common neuropathological characteristics. Moreover, it has been proposed that retroviruses are involved in TSE pathogenesis (Dimcheff et al., 2003a) and may be the infectious agent (Manuelidis, 2003). The TSE models studied in this thesis display the spongiosis associated with murine retroviral disease and are therefore ideal to search for a disease-associated virus or nucleic acid.

8.9. Future work

Studies here have demonstrated high titres of infectivity in brain homogenate that further transmitted TSE yet contained non-detectable levels of PK-resistant PrP^{Sc}. A form of PK-sensitive PrP appears to be the infectious agent in these brains, however the true nature of infectivity in such tissue remains to be fully elucidated.

8.9.1. Increased detection of PK-resistant PrP^{Sc}

In brain where PK-resistant PrP^{Sc} levels were low/non-detectable, PrP^{Sc} levels may be concentrated using sodium phosphotungstic acid (NaPTA). Sodium phosphotungstate (NaPTA), has been shown to selectively precipitate extremely low levels of PrP^{Sc}, increasing detection by 1000-fold (Wadsworth et al., 2001) and has also been used in combination with a mild PK treatment on mouse brain samples to detect $sPrP^{Sc}$ (Tremblay et al., 2004). Such treatment may reveal small amounts of PK-resistant PrP^{Sc} and/or $sPrP^{Sc}$ in 263K/101LL and GSS/101LL brain.

The PMCA technique has also been used to amplify low concentrations of PrP^{Sc} in infected brain (Saborio et al., 2001). Amplification of PK-sensitive PrP in 101LL brain may result in the formation of PrP^{Sc} and indicate that PK-sensitive PrP is an intermediate in the $PrP^{C} \rightarrow PrP^{Sc}$ conversion process. Using PMCA an increase in infectivity has not been identified alongside increasing PrP^{Sc} levels. Titration experiments may indicate whether the resultant PrP was infectious.

8.9.2. Further characterisation of PK-sensitive, infectious PrP

Conformational antibodies that can distinguish PrP^{Sc} from PrP^{C} have been described (Korth et al., 1997; Paramithiotis et al., 2003; Zou et al., 2004) (chapter 1.9.3) thus may be useful in further identifying PK-sensitive forms of PrP^{Sc}. Immunoprecipitation of 263K/101LL or GSS/101LL brain homogenate using these antibodies would identify both PK-resistant and PK-sensitive PrP^{Sc}. However these could be separated using different GndHCl concentrations.

The CDI assay may identify $sPrP^{Sc}$ in infected and uninfected 101LL mice, however a suitable antibody (that recognised an epitope exposed in denatured PrP but which is buried in the native conformation) must be found to analyse the samples here. Immunoprecipitation of PrP using the antibodies devised by Sy *et al*, 8H4, 8B4, 7A12 etc (Zanusso et al., 1998) (appendix B) may indicate whether these are useful for the CDI detection of PrP in the samples described here. These antibodies should be primarily assessed by the guanidine melt curve to identify whether antibody epitopes are exposed in denatured PrP but hidden in native PrP (Safar et al., 1998).

Bioassay of PK-treated and non-PK treated fractions of 263K/101LL brain may give an indication of whether $sPrP^{Sc}$ is capable of transmitting infectivity, however, this would not rule out the presence of other transmissible molecules. If PK-resistant PrP^{Sc} alone was the infectious agent, PK-treated brain homogenate should have the same titre of infectivity as untreated homogenate, however if titres are lower in PK-treated compared to untreated fractions, this may indicate that PK-sen PrP is infectious. However, this experiment would not rule out the presence of other molecules that may associate with infectivity.

8.9.3. Cellular localisation of PK-sensitive, infectious PrP

Simple fractionation studies have indicated both a correlation and a separation of PrP^{Sc} and infectivity (Bolton et al., 1982; Manuelidis et al., 1987; Somerville & Dunn, 1996). Sucrose gradient fractionation of brain taken from the models described in this thesis may indicate whether $rPrP^{Sc}$ and $sPrP^{Sc}$ are present in similar cellular compartments or whether they exist in different areas of the cell. Again, after isolating these forms of PrP from sucrose gradients, bioassay would identify whether they associated with infectivity, as indicated by Prusiner, or if they separate, as indicated by Manuelidis and Somerville.

8.10. Concluding remarks

In the studies presented in this thesis, high infectivity titres were found in brain in which PK-resistant PrP^{Sc} could not be detected. The titre of

infectivity did not correlate with the amount of PK-resistant PrP^{Sc} found across all models and was contradictory to the prion hypothesis. Current diagnostic assays rely on the presence of PK-resistant PrP^{Sc} to diagnose TSE and assume that the absence of this form of PrP indicates the absence of infectivity. However, the findings here seriously question the suitability of PK-resistant PrP^{Sc} as a surrogate marker for TSE and indicate that, in the absence of alternative methods, transmission studies remain the only definitive method for identifying infectivity in TSE-affected tissues.

In addition to other studies (Hill et al., 1999a; Shaked et al., 1999), investigations here dissociated the PK-resistant characteristic of PrP from infectivity. The PK-sensitive, infectious form of PrP identified here may represent an intermediate PrP molecule, formed during $PrP^{C} \rightarrow PrP^{Sc}$ conversion, which is the infectious agent. PrP is obviously central to TSE since PrP null mice cannot support disease, however it is not clear whether disease is mediated through a PrP molecule, or whether another molecule (or complex of molecules) is required to associate with PrP. It is entirely possible that the infectious agent of TSE is not PrP but may be a complex of many molecules, including nucleic acids, some of which may be TSE strain specific. This study cannot rule out the possibility that a viral or virino particle may be the infectious agent. Given that the function of PrP^{C} has yet to be elucidated, it is possible that this protein is a cellular receptor for the infectious agent thus facilitating entry of the infectious agent into the cell. The 263K/101LL TSE model investigated here is a paradox to the prion hypothesis but it is an elegant model to further dissect the true nature of the infectious agent and the role of PK-resistant PrP^{Sc} in TSE pathology.

Appendix A

Mouse PrP sequence

"MANLGYWLLALFVTMWTDVGLCKKRPKPGGWNTGGSRYPGQGSPGGNRYPP
QGGTWGQPHGGGWGQPHGGSWGQPHGGSWGQPHGGGWGQGGGTHNQW
NK*P*SKPKTNLKHVAGAAAAGAVVGGLGGYMLGSAMSRPMIHFGNDWEDRYYR
ENMYRYPNQVYYRPVDQYSNQNNFVHDCVNITIKQHTVTTTTKGENFTETDVK
MMERVVEQMCVTQYQKESQAYYDGRRSSSTVLFSSPPVILLISFLIFLIVG"

Mouse *Prnp* sequence

Accession number M18070

```
1     ttgacgccat gactttcata catttgcttt gtagatagat gtcaaggacc ttcagcctaa
61    atactgggca ctgatacctt gttcctcatt ttgcagatca gtcatcatgg cgaaccttgg
121   ctactggctg ctggccctct ttgtgactat gtggactgat gtcggcctct gcaaaaagcg
181   gccaaagcct ggagggtgga acaccggtgg aagccggtat cccgggcagg gaagccctgg
241   aagcaaccgt tacccacctc aggtggcac ctgggggcag ccccacggtg gtggctgggg
301   acaaccccat gggggcagct ggggacaacc tcatggtggt agttggggtc agccccatgg
361   cggtggatgg ggccaaggag ggggtaccca taatcagtgg aacaagccca gcaaaccaaa
421   aaccaacctc aagcatgtgg caggggctgc ggcagctggg gcagtagtgg ggggccttgg
481   tggctacatg ctggggagcg ccatgagcag gcccatgatc cattttggca acgactggga
541   ggaccgctac taccgtgaaa acatgtaccg ctaccctaac caagtgtact acaggccagt
601   ggatcagtac agcaaccaga acaacttcgt gcacgactgc gtcaatatca ccatcaagca
661   gcacacggtc accaccacca ccaaggggga gaacttcacc gagaccgatg tgaagatgat
721   ggagcgcgtg gtggagcaga tgtgcgtcac ccagtaccag aaggagtccc aggcctatta
781   cgacgggaga agatccagca gcaccgtgct tttctcctcc cctcctgtca tcctcctcat
841   ctccttcctc atcttcctga tcgtgggatg agggaggcct tcctgcttgt tccttcgcat
901   ttctcgtggt ctaggctggg ggaggggtta tcc
```

ATG start codon
101P, site of the P to L mutation
Dde1 recognition site

Appendix B

PrP antibody epitopes

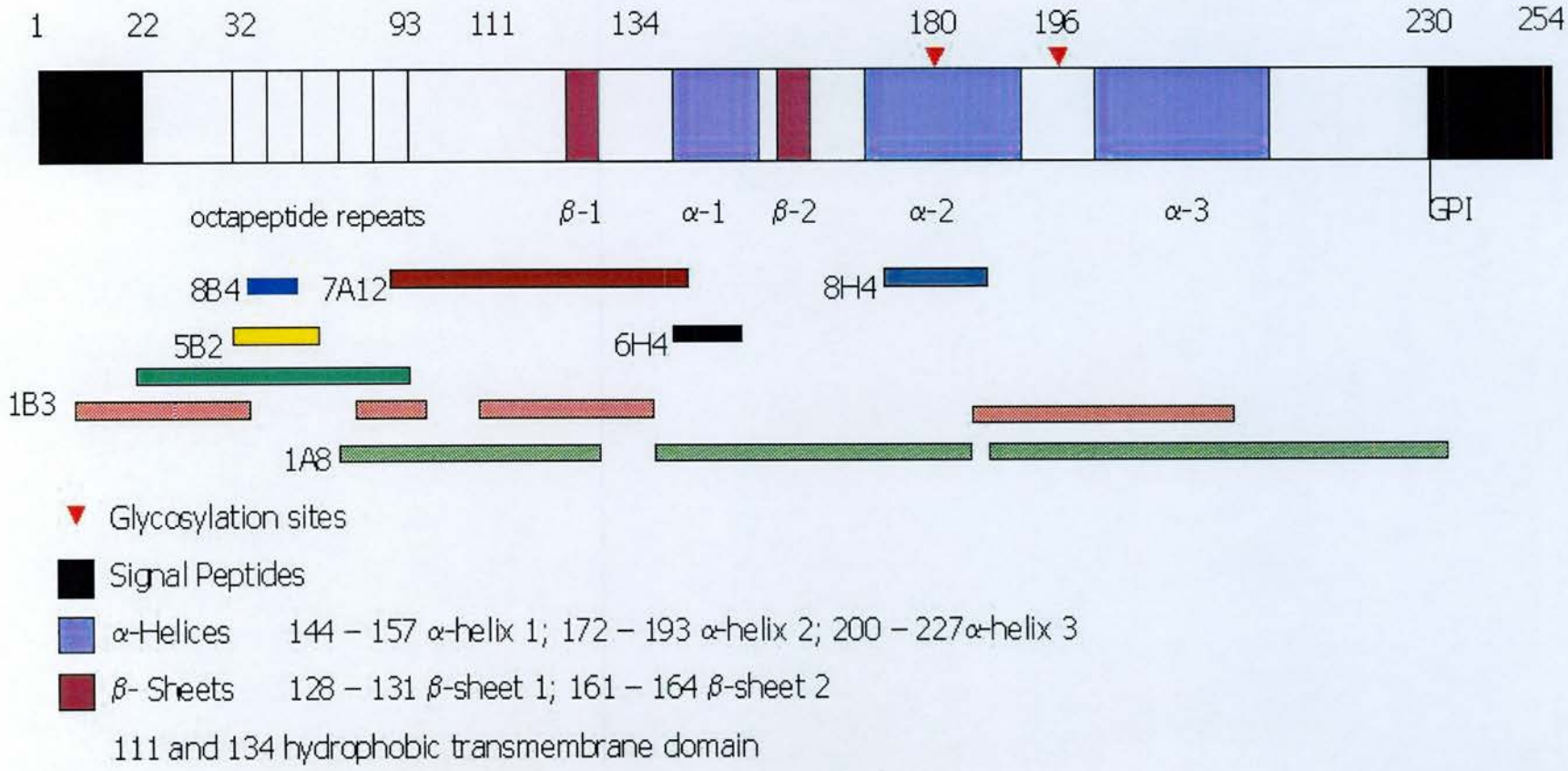

Figure A 1 Schematic representation of epitopes recognised by anti-PrP antibodies

Appendix C

Clinical symptoms of TSE in 129/Ola mice

The clinical symptoms of TSE in mice include ataxia, a weakness of the hind limbs, hunched appearance, general lethargy and a lack of grooming leading to a ruffled coat. 129/Ola mice live to approximately 600 days and upon ageing exhibit the ruffled coat and lethargy see in TSE-affected mice. They also suffer from scratched eyes and ears as they age and are humanely culled when these symptoms of ageing appear therefore, it can be difficult to assess 129/Ola mice infected with TSE, especially as they age. However, personnel at NPU are extremely experienced in observing these animals throughout the course of TSE disease and the course of ageing, and are experienced in assessing clinical symptoms of TSE according to the scoring regime (table AI). TSE-inoculated animals were observed on a daily basis and scored weekly. Animals given three consecutive "+" (or above) scores were culled as clinically positive. Animals that died unexpectedly were given a clinical score based upon the score given in the previous two weeks.

Score	Criteria
1	Not affected by TSE
2	Likely to be affected
+	Definitely affected
g	"2" plus ataxia (gait affected)
G	"+" plus ataxia
..	Scratched back (depends on TSE agent/Mouse strain combination)
X	Scratched eyes (not a clinical disease but at the end of clinical phase some TSE/Mouse combinations (esp. 129/0la) have scratched eyes)
0	Wet around anal region

Table A 1 Clinical symptoms of TSE

Appendix D

Karber calculation data

Titration	Karber Calculation
ME7/101PP	-6-[(1+ 0.167 + 0.091) -0.5]
ME7/101LL	-4-[(1+ 0.875 + 0.583) -0.5]
263K/101LL (1)	-5-[(1+ 0.9167+ 0.417+ 0.091) -0.5]
263K/101LL (2)	-4-[(1+ 0.667 + 0. 143 + 0 + 0.083) -0.5]
263K/101LL (3)	-2-[(1 + 0.5 + 0.857+ 0.875 + 0.182) -0.5]
GSS/101LL	-2-[(1 + 0.86 + 0.75 + 0.6)-0.5]

ME7/101PP brain titrated in 101PP mice
ME7/101LL and 263K/101LL brains titrated in 101LL mice
ID_{50} value for inoculated brain tissue (= 20mg)
ID_{50} value per g brain tissue ([a] x50)
GSS/101LLbrain titrated in 101LL mice (R.Barron, unpublished data

Table A 2 Karber calculation of titre of infectivity in models of TSE

Appendix E

Dose response curve data

Dilution (10^x)	Normalising Factor	ME7/101PP ($10^{8.5}$ ifu/g) Normalised titre	Incubation time (days)	ME7/101LL($10^{7.7}$ ifu/g) Normalised titre	Incubation time (days)	GSS/101LL($10^{6.4}$ ifu/g) Normalised titre	Incubation time (days)
-2	2	$10^{6.5}$	159	$10^{5.7}$	220	$10^{4.4}$	134
-3	3	$10^{5.5}$	170	$10^{4.7}$	249	$10^{3.4}$	156
-4	4	$10^{4.5}$	177	$10^{3.7}$	277	$10^{2.4}$	255
-5	5	$10^{3.5}$	201	$10^{2.7}$	313	$10^{1.4}$	344
-6	6	$10^{2.5}$	269	$10^{1.7}$	409		
-7	7	$10^{1.5}$	291				
-8	8	$10^{0.5}$	244				
-9	9						
-10	10						
-11	11						

Dilution (10^x)	Normalising Factor	263K/101LL (1) ($10^{8.6}$ ifu/g) Normalised titre	Incubation time (days)	263K/101LL (2) ($10^{87.1}$ ifu/g) Normalised titre	Incubation time (days)	263K/101LL (3) ($10^{6.6}$ ifu/g) Normalised titre	Incubation time (days)
-2	2	$10^{6.6}$	109	$10^{5.1}$	129	$10^{4.6}$	262
-3	3	$10^{5.6}$	114	$10^{4.1}$	134	$10^{3.6}$	308
-4	4	$10^{4.6}$	125	$10^{3.1}$	159	$10^{2.6}$	399
-5	5	$10^{3.6}$	144	$10^{2.1}$	193	$10^{1.6}$	398
-6	6	$10^{2.6}$	189	$10^{1.1}$	266	$10^{0.6}$	401
-7	7	$10^{1.6}$	203				
-8	8	$10^{0.6}$	228				
-9	9						
-10	10						
-11	11						

Normalising factor * infectivity titre calculates an infectivity titre for each dilution of agent. Plot this alongside incubation time for dose response curve.

Table A 3 Normalisation of titre of infectivity for each titration experiment

Appendix F

Titration of brain homogenate from the GSS/101LL model

Dilution Group	GSS/101LL	
	n+/nT[a]	Inc Time[b]
10^{-2}	5/5	134±4
10^{-3}	12/14	156±5
10^{-4}	3/4	255±38
10^{-5}	3/5	441±93
10^{-6}	0/7	n/a
10^{-7}	0/6	n/a
10^{-8}	0/4	n/a
10^{-9}	0/7	n/a
10^{-10}	nd	nd
10^{-11}	nd	nd
10^{-2} 101PP	5/5	265±9
ID_{50}	**$10^{4.71}$**	
ID_{50}/g	**$10^{6.4}$**	

[a] n+= number TSE positive animals (assessed by clinical and pathological examination); nT= total number of animals per group.
[b] Mean incubation time (days) of animals scored pathologically positive ± standard error
n/a not applicable
nd not determined
ID_{50} value for inoculated brain tissue (= 20mg) – calculated using the Karber method (chapter 2). For additional data see appendix E.
ID_{50} value per g brain tissue ([a] x50)

Table A 4 Titration data of previously unpublished GSS/101LL brain (R.Barron, NPU, Edinburgh)

Appendix G

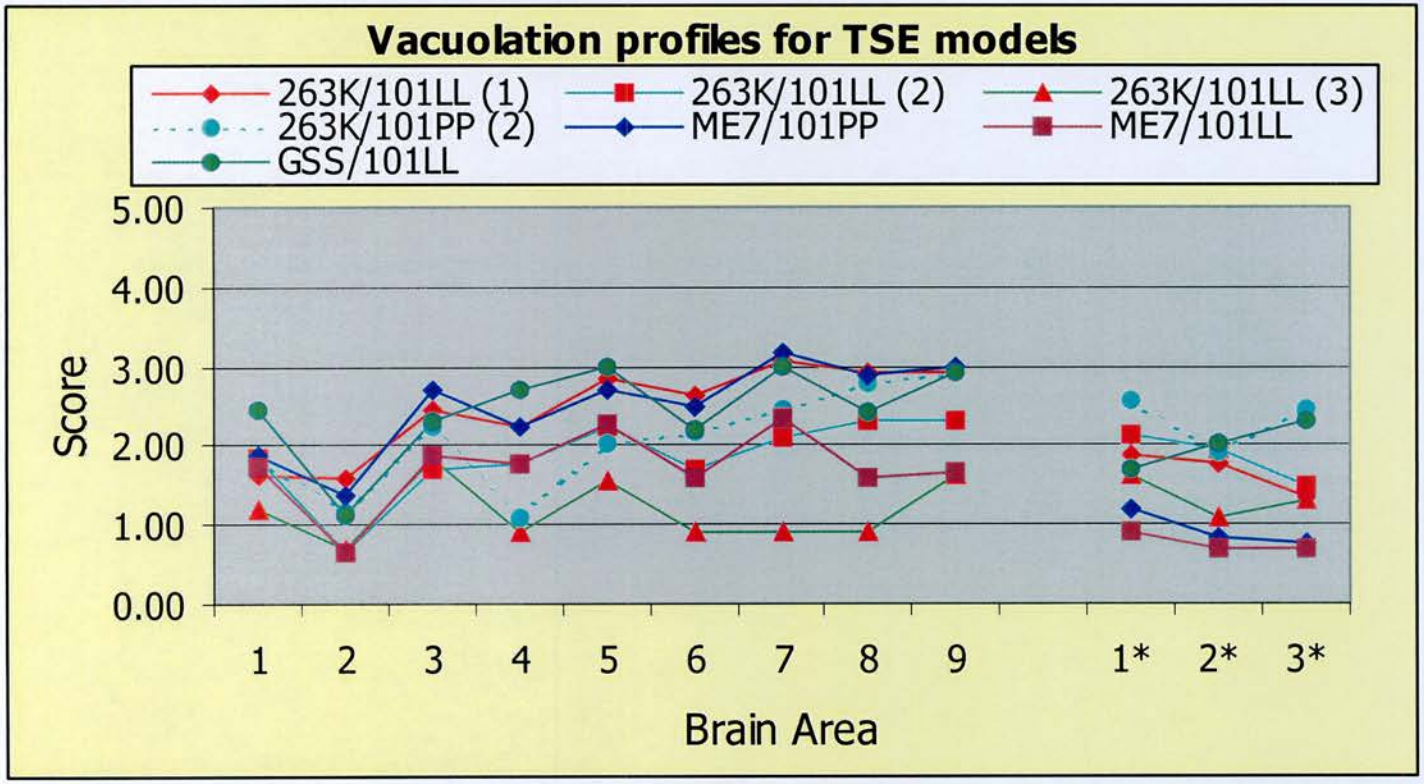

Figure A 2 Vacuolation profile at secondary passage of all TSE models

Comparison of vacuolation profiles for titrated brain from all models studied. ME7/101PP titrated in 101PP mice-blue line, ME7/101LL titrated in 101LL mice-maroon line, 263K/101LL (1) titrated in 101LL mice–red line, 263K/101LL (2) titrated in 101LL mice-turquoise line/red square, 263K/101LL (2) titrated in 101PP mice (263K/101PP)-turquoise dotted line, 263K/101LL (3) titrated in 101LL mice -green line/red triangle, GSS/101LL transmitted to but not titrated in 101LL mice–green line/circles. See chapter 4 for specific brain areas.

Appendix H

Quantification of PK-resistant PrP^{Sc} from TSE-infected brain homogenate

% homogenate loaded	Intensity of detection (Pixels)					
	ME7/101PP			ME7/101LL		
	Blot A	Blot B	Blot C	Blot A	Blot B	Blot C
2	-	-	-	-	-	-
1	434748	103670	763072	887315	1476490	161006
0.5	334445	85249	340217	400801	956700	74282
0.25	149986	24443	192508	266882	319222	46785
0.125	65739	10108	129269	172986	163362	6115
0.0625	63595	729	15100	48391	65331	2938
0.0313	26476	0	9803	18412	39568	1038
0.0156	5304	0	0	0	0	388
0.0078	0	0	0	0	0	55
0.0039	0	0	0	0	0	0
0.0020	0	0	0	0	0	0
50ng recombinant PrP	58506	14872	103933	92713	555238	73778

% homogenate loaded	Intensity of detection (Pixels)					
	263K/101LL (1)		263K/101LL (2)			263K/101LL (3)
	Blot A	Blot B	Blot A	Blot B	Blot C	Blot A
2	-	-	-	-	-	
1	30461	20763	0	0	0	0
0.5	28656	19250	0	0	0	0
0.25	6865	18727	0	0	0	0
0.125	4659	0	0	0	0	0
0.0625	0	0	0	0	0	0
0.0313	0	0	0	0	0	0
0.0156	0	0	0	0	0	0
0.0078	0	0	0	0	0	0
0.0039	0	0	0	0	0	0
0.0020	0	0	0	0	0	0
50ng recombinant PrP	34710	14043	3563	240084	418043	3208

Quantification of PK-resistant PrP^{Sc} from triplicate, duplicate or single immunoblots for each model investigated. Expressed as the number of pixels making up the PrP^{Sc} image as detected using the Kodak Imager Software (chapter 6.2.2). Pixel intensity was converted to ng PrP^{Sc} by comparing number of pixels detected in each sample with those detected in 50ng rPrP (chapter 6.2.2). Refer to chapter 6 for images of each immunoblot.

Table A 5 Quantification of PK-resistant PrP^{Sc}

Appendix I

Quantification of Total PrP from uninfected and TSE-infected brain homogenate

% homogenate loaded	Intensity of detection (Pixels)					
	Uninfected 101PP			Uninfected 101LL		
	Blot A	Blot B	Blot E	Blot C	Blot D	Blot E
2	-		-	-	-	-
1	86672	549487	-	2096164	152526	-
0.5	93563	169394	305850	1315813	59952	227654
0.25	62927	31595	134803	638391	17789	126094
0.125	13958	6261	76623	150034	4434	34877
0.0625	8752	924	65421	78112	3863	104721
0.0313	3633	828	50615	35529	2245	43709
0.0156	40249		-	-		-
0.0078	-		-	-		-
0.0039	-		-	-		-
0.0020	-		-	-		-
50ng recombinant PrP	40249	24319	78413	232376	16171	78413

% homogenate loaded	Intensity of detection (Pixels)							
	ME7/101PP		ME7/101LL		263K/101LL (1)		263K/101LL (3)	
	Blot A	Blot B	Blot A	Blot B	Blot A	Blot B	Blot A	Blot B
2	-	-	-	-	303773	598542	263241	113892
1	499303	87745	92333	22602	357316	686109	219437	112481
0.5	171352	32352	32126	5901	176804	371008	87744	72751
0.25	91329	5923	21154	274	135566	274007	24299	60122
0.125	81014	1023	14833	0	28684	135740	8804	23409
0.0625	11437	528	3745	0	27399	31725	12266	37151
0.0313	2322	563	0	0	0	30495	2931	4875
0.0156	423	23	0	0	0	3541	0	1768
0.0078	0	0	0	0	0	0	0	0
0.0039	0	0	0	0	0	0	0	0
0.0020	0	0	0	0	0	0	0	0
50ng recombinant PrP	20840	3018	11550	3739	18488	89189	9499	57320

Quantification of Total PrP from triplicate, duplicate or single immunoblots for each model investigated, including uninfected 101PP and 101LL mice. Expressed as the number of pixels making up the PrP^{Sc} image as detected using the Kodak Imager Software (chapter 6.2.2). Pixel intensity was converted to ng PrP^{Sc} by comparing number of pixels detected in each sample with those detected in 50ng rPrP (chapter 6.2.2). Refer to chapter 6 for images of each immunoblot.

Table A 6 Quantification of Total PrP

Appendix J

Preparation of Lyophilised Proteinase K (PK)

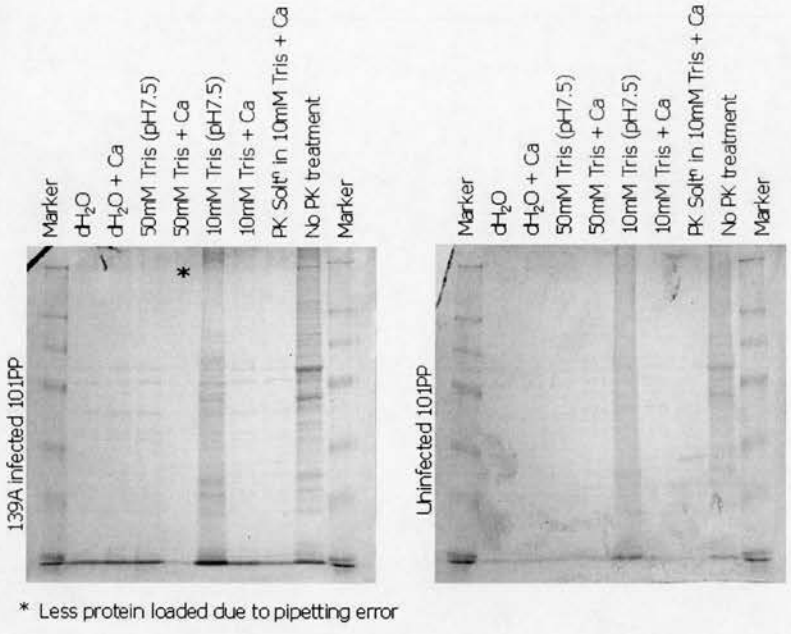

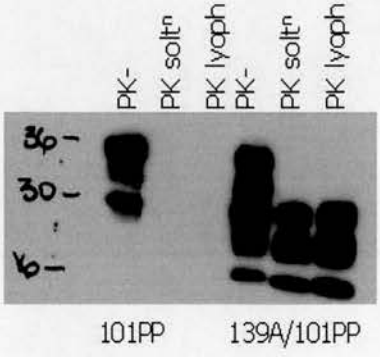

Figure A 3 Reconstituted lyophilised PK solution

Lyophilised PK reconstituted in different buffers; dH_2O ± 1mM calcium, 50mM Tris solution ± 1mM calcium, 10mM Tris solution ± 1mM calcium. Brain homogenate from (A) 139A-infected or (B) uninfected 101PP mice treated with 20µg/ml (final concentration) of each reconstituted PK solution or a commercial, pre-made solution. 2% homogenate reactions analysed using 12% tris/glycine SDS-PAGE and stained with Coomassie Blue solution (0.25%). * Less than 2% homogenate loaded in this well due to pipetting error. (C) PK reconstituted in 10mM Tris pH7.5, 1mM calcium buffer used to treat 139A/101LL and uninfected 101LL brain tissue as before. Immunoblot detection using 8H4 and POD substrate. Markers are indicated at kDa sizes.

Bibliography

Adler, V., Zeiler, B., Kryukov, V., Kascsak, R., Rubenstein, R., Grossman, A. (2003). Small, highly structured RNAs participate in the conversion of human recombinant PrP(Sen) to PrP(Res) in vitro. *Journal of Molecular Biology* **332**:47-57

Aguzzi, A. (1998). Protein conformation dictates prion strain. *Nature Medicine* **4**:1125-6

Armstrong, R.A., Lantos, P.L., Cairns, N.J. (2001). Spatial correlations between the vacuolation, prion protein deposits, and surviving neurons in the cerebral cortex in sporadic Creutzfeldt-Jakob disease. *Neuropathology* **21**:266-71

Barnard, G., Helmick, B., Madden, S., Gilbourne, C., Patel, R. (2000). The measurement of prion protein in bovine brain tissue using differential extraction and DELFIA as a diagnostic test for BSE. *Luminescence* **15**:357-62

Baron, T.G., Madec, J.Y., Calavas, D., Richard, Y., Barillet, F. (2000). Comparison of French natural scrapie isolates with bovine spongiform encephalopathy and experimental scrapie infected sheep. *Neuroscience Letters* **284**:175-8

Barron, R.M., Thomson, V., Jamieson, E., Melton, D.W., Ironside, J., Will, R., Manson, J.C. (2001). Changing a single amino acid in the N-terminus of murine PrP alters TSE incubation time across three species barriers. *EMBO Journal* **20**:5070-8

Barron, R.M., Thomson, V., King, D., Shaw, J., Melton, D.W., Manson, J.C. (2003). Transmission of murine scrapie to P101L transgenic mice. *Journal of General Virology* **84**:3165-72

Bartz, J.C., Aiken, J.M., Bessen, R.A. (2004). Delay in onset of prion disease for the HY strain of transmissible mink encephalopathy as a result of prior peripheral inoculation with the replication-deficient DY strain. *Journal of General Virology* **85**:265-73

Baskakov, I.V., Legname, G., Baldwin, M.A., Prusiner, S.B., Cohen, F.E. (2002). Pathway complexity of prion protein assembly into amyloid. *Journal of Biological Chemistry* **277**:21140-8

Baxter, H.C., Fraser, J.R., Liu, W.G., Forster, J.L., Clokie, S., Steinacker, P., Otto, M., Bahn, E., Wiltfang, J., Aitken, A. 2002. Specific 14-3-3 isoform detection and immunolocalization in prion diseases. *In:* Biochemical Society Transactions. pp. 387-391

Baylis, M., Houston, F., Kao, R.R., McLean, A.R., Hunter, N., Gravenor, M.B. (2002). BSE - a wolf in sheep's clothing? *Trends in Microbiology* **10**:563-70

Beekes, M., Baldauf, E., Diringer, H. (1996). Sequential appearance and accumulation of pathognomonic markers in the central nervous system of

hamsters orally infected with scrapie. *Journal of General Virology* **77** (Pt 8):1925-34

Beekes, M., McBride, P.A., Baldauf, E. (1998). Cerebral targeting indicates vagal spread of infection in hamsters fed with scrapie. *Journal of General Virology* **79** (Pt 3):601-7

Bellinger-Kawahara, C., Cleaver, J.E., Diener, T.O., Prusiner, S.B. (1987). Purified scrapie prions resist inactivation by UV irradiation. *Journal of Virology* **61**:159-66

Bendheim, P.E., Brown, H.R., Rudelli, R.D., Scala, L.J., Goller, N.L., Wen, G.Y., Kascsak, R.J., Cashman, N.R., Bolton, D.C. (1992). Nearly ubiquitous tissue distribution of the scrapie agent precursor protein. *Neurology* **42**:149-56

Bessen, R.A., Kocisko, D.A., Raymond, G.J., Nandan, S., Lansbury, P.T., Caughey, B. (1995). Non-genetic propagation of strain-specific properties of scrapie prion protein. *Nature* **375**:698-700

Bessen, R.A., Marsh, R.F. (1992). Identification of two biologically distinct strains of transmissible mink encephalopathy in hamsters. *Journal of General Virology* **73** (Pt 2):329-34

Biacabe, A.G., Laplanche, J.L., Ryder, S., Baron, T. (2004). Distinct molecular phenotypes in bovine prion diseases. *EMBO* ***Rep*** **5**:110-5

Bieschke, J., Giese, A., Schulz-Schaeffer, W., Zerr, I., Poser, S., Eigen, M., Kretzschmar, H. (2000). Ultrasensitive detection of pathological prion protein aggregates by dual-color scanning for intensely fluorescent targets. *Proceedings of the National Academy of Sciences of the United States of America* **97**:5468-73

Biffiger, K., Zwald, D., Kaufmann, L., Briner, A., Nayki, I., Purro, M., Bottcher, S., Struckmeyer, T., Schaller, O., Meyer, R., Fatzer, R., Zurbriggen, A., Stack, M., Moser, M., Oesch, B., Kubler, E. (2002). Validation of a luminescence immunoassay for the detection of PrP(Sc) in brain homogenate. *Journal of Virological Methods* **101**:79-84

Billeter, M., Riek, R., Wider, G., Hornemann, S., Glockshuber, R., Wuthrich, K. (1997). Prion protein NMR structure and species barrier for prion diseases. *Proceedings of the National Academy of Sciences of the United States of America* **94**:7281-7285

Bolton, D.C., Bendheim, P.E., Marmorstein, A.D., Potempska, A. (1987). Isolation and structural studies of the intact scrapie agent protein. *Archives of Biochemistry and Biophysics* **258**:579-90

Bolton, D.C., McKinley, M.P., Prusiner, S.B. (1982). Identification of a protein that purifies with the scrapie prion. *Science* **218**:1309-1311

Brandner, S., Isenmann, S., Raeber, A., Fischer, M., Sailer, A., Kobayashi, Y., Marino, S., Weissmann, C., Aguzzi, A. (1996). Normal host prion protein necessary for scrapie-induced neurotoxicity. *Nature* **379**:339-43

Brown, D., Hafiz, F., Glasssmith, L., Wong, B., Jones, I., Clive, C., Haswell, S. (2000). Consequences of manganese replacement of copper for prion protein function and proteinase resistance. *EMBO* **19**:1180-1186

Brown, D., Wong, B., Hafiz, F., Clive, C., Haswell, S., Jones, I. (1999). Normal prion protein has an activity like that of superoxide dismutase. *Biochemistry Journal* **344**:1-5

Brown, D.R. (2002). Mayhem of the multiple mechanisms: modelling neurodegeneration in prion disease. *Journal of Neurochemistry* **82**:209-15

Bruce. (1985a). Strain typing studies of scrapie and BSE. *In:* Methods in Molecular Medicine: Prion Diseases. H.B.a.R. Ridley, editor. Humana Press Inc., Totowa, NJ

Bruce, M. (1985b). Agent replication dynamics in a long incubation period model of mouse scrapie. *Journal of General Virology* **66**:2517-2522

Bruce, M., Brown, K., Mabbott, N., Farquhar, C., Jeffrey, M. (2000). Follicular dendritic cells in TSE pathogenesis. *Immunology Today* **21**:442-446

Bruce, M., McBride, P., Farquhar, C. (1989). Precise targeting of the pathology of the sialoglycoprotein, PrP, and vacuolar degeneration in mouse scrapie. *Neuroscience Letters* **102**:1-6

Bruce, M., McBride, P., Jeffrey, M., Scott, J. (1994). PrP in pathology and pathogenesis in scrapie-infected mice. *Molecular Neurobiology* **8**:105-112

Bruce, M.E. (1981). Serial studies on the development of cerebral amyloidosis and vacuolar degeneration in murine scrapie. *Journal of Comparative Pathology* **91**:589-97

Bruce, M.E., Boyle, A., Cousens, S., McConnell, I., Foster, J., Goldmann, W., Fraser, H. (2002). Strain characterization of natural sheep scrapie and comparison with BSE. *Journal of General Virology* **83**:695-704

Bruce, M.E., Dickinson, A.G. (1985). Genetic control of amyloid plaque production and incubation period in scrapie-infected mice. *Journal of Neuropathology and Experimental Neurology* **44**:285-294

Bruce, M.E., Dickinson, A.G. (1987). Biological evidence that scrapie agent has an independent genome. *Journal of General Virology* **68** (Pt 1):79-89

Bruce, M.E., Fraser, H. (1981). Effect of route of infection on the frequency and distribution of cerebral amyloid plaques in scrapie mice. *Neuropathology and Applied Neurobiology* **7**:289-98

Bruce, M.E., Will, R.G., Ironside, J.W., McConnell, I., Drummond, D., Suttie, A., McCardle, L., Chree, A., Hope, J., Birkett, C., Cousens, S., Fraser, H., Bostock, C.J. (1997). Transmissions to mice indicate that 'new variant' CJD is caused by the BSE agent. *Nature* **389**:498-501

Bueler, H., Aguzzi, A., Sailer, A., Greiner, R.A., Autenried, P., Aguet, M., Weissmann, C. (1993). Mice devoid of PrP are resistant to scrapie. *Cell* **73**:1339-1347

Bueler, H., Fischer, M., Lang, Y., Bluethmann, H., Lipp, H.P., DeArmond, S.J., Prusiner, S.B., Aguet, M., Weissmann, C. (1992). Normal development and behaviour of mice lacking the neuronal cell-surface PrP protein. *Nature* **356**:577-82

Buschmann, A., Biacabe, A.G., Ziegler, U., Bencsik, A., Madec, J.Y., Erhardt, G., Luhken, G., Baron, T., Groschup, M.H. (2004). Atypical scrapie

cases in Germany and France are identified by discrepant reaction patterns in BSE rapid tests. *Journal of Virological Methods* **117**:27-36

Buschmann, A., Kuczius, T., Bodemer, W., Groschup, M.H. (1998). Cellular prion proteins of mammalian species display an intrinsic partial proteinase K resistance. *Biochemical and Biophysical Research Communications* **253**:693-702

Cappai, R., Stewart, L., Jobling, M., Thyer, J., White, A., Beyreuther, K., Collins, S., Masters, C., Barrow, C. (1999). Familial prion disease mutation alters the secondary structure of recombinant mouse prion protein: implications for the mechanism of prion formation. *Biochemistry* **38**:3280-4

Carlson, G.A., Kingsbury, D.T., Goodman, P.A., Coleman, S., Marshall, S.T., DeArmond, S., Westaway, D., Prusiner, S.B. (1986). Linkage of prion protein and scrapie incubation time genes. *Cell* **46**:503-511

Carp, R.I., Callahan, S.M. (1986). Scrapie incubation periods and end-point titers in mouse strains differing at the H-2D locus. *Intervirology* **26**:85-92

Caughey, B., Chesebro, B. (1997). Prion protein and the transmissible spongiform encephalopathies. *Trends in Cell Biology* **7**:56-62

Chiesa, R., Harris, D.A. (2001). Prion diseases: what is the neurotoxic molecule? *Neurobiology of Disease* **8**:743-63

Chiesa, R., Piccardo, P., Ghetti, B., Harris, D.A. (1998). Neurological illness in transgenic mice expressing a prion protein with an insertional mutation. *Neuron* **21**:1339-1351

Collinge, J., Sidle, K., Meads, J., Ironside, J., Hill, A. (1996). Molecular Analysis Of Prion Strain Variation and the Etiology Of New Variant CJD. *Nature* **383**:685-690

Collinge, J., Whittington, M.A., Sidle, K.C.L., Smith, C.J., Palmer, M.S., Clarke, A.R., Jefferys, J.G.R. (1994). Prion protein is necessary for normal synaptic function. *Nature* **370**:295-297

Czub, M., Braig, H.R., Blode, H., Diringer, H. (1986a). The major protein of SAF is absent from spleen and thus not an essential part of the scrapie agent. *Archives of Virology* **91**:383-6

Czub, M., Braig, H.R., Diringer, H. (1986b). Pathogenesis of scrapie: study of the temporal development of clinical symptoms, of infectivity titres and scrapie-associated fibrils in brains of hamsters infected intraperitoneally. *Journal of General Virology* **67** (Pt 9):2005-9

Czub, M., Braig, H.R., Diringer, H. (1988). Replication of the scrapie agent in hamsters infected intracerebrally confirms the pathogenesis of an amyloid-inducing virosis. *Journal of General Virology* **69** (Pt 7):1753-6

De Armond, S.J., Gonzales, M., Mobley, W.C., Kon, A.A., Stern, A., Prusiner, H., Prusiner, S.B. (1989). PrPSc in scrapie-infected hamster brain is spatially and temporally related to histopathology and infectivity titer. *Progress in Clinical and Biological Research* **317**:601-18

DeArmond, S. 1988. Prion protein and scrapie pathology. *In:* Alzheimer's disease and related disorders: proceedings of the first international

conference on Alzheimer's disease and related disorders. W.H.M. Iqbal K., Winblad B., editor. pp. 601-618. Alan R Liss, New York, Las Vegas, Nevada

DeArmond, S.J., Mobley, W.C., DeMott, D.L., Barry, R.A., Beckstead, J.H., Prusiner, S.B. (1987). Changes in the localization of brain prion proteins during scrapie infection. *Neurology* **37**:1271-80

Deleault, N.R., Lucassen, R.W., Supattapone, S. (2003). RNA molecules stimulate prion protein conversion. *Nature* **425**:717-20

Deslys, J.P., Comoy, E., Hawkins, S., Simon, S., Schimmel, H., Wells, G., Grassi, J., Moynagh, J. (2001). Screening slaughtered cattle for BSE. *Nature* **409**:476-8

Dickinson, A., Meikle, V. (1969). A comparison of some biological characteristics of the mouse-passaged scrapie agents, 22A and ME7. *Genetic Research* **13**:213-225

Dickinson, A.G., Fraser, H., Meikle, V.M., Outram, G.W. (1972). Competition between different scrapie agents in mice. *Nature New Biology* **237**:244-5

Dickinson, A.G., Meikle, V.M., Fraser, H. (1968). Identification of a gene which controls the incubation period of some strains of scrapie agent in mice. *Journal of Comparative Pathology* **78**:293-9

Dickinson, A.G., Outram, G.W. 1988. Genetic aspects of unconventional virus infections: the basis of the virino hypothesis. *In:* Ciba Foundation Symposium: Novel infectous agents and the central nervous system. G. Bock and J. Marsh, editors. pp. 63-83. John Wiley & Sons, London, UK

Dimcheff, D.E., Askovic, S., Baker, A.H., Johnson-Fowler, C., Portis, J.L. (2003a). Endoplasmic reticulum stress is a determinant of retrovirus-induced spongiform neurodegeneration. *Journal of Virology* **77**:12617-29

Dimcheff, D.E., Portis, J.L., Caughey, B. (2003b). Prion proteins meet protein quality control. *Trends in Cell Biology* **13**:337-40

Diringer, H., Beekes, M., Oberdieck, U. (1994). The nature of the scrapie agent: the virus theory. *Annals of the New York Academy of Sciences* **724**:246-58

Diringer, H., Gelderblom, H., Hilmert, H., Ozel, M., Edelbluth, C., Kimberlin, R.H. (1983). Scrapie infectivity, fibrils and low molecular weight protein. *Nature* **306**:476-8

Dorandeu, A., Wingertsmann, L., Chretien, F., Delisle, M.B., Vital, C., Parchi, P., Montagna, P., Lugaresi, E., Ironside, J.W., Budka, H., Gambetti, P., Gray, F. (1998). Neuronal apoptosis in fatal familial insomnia. *Brain Pathology* **8**:531-7

Drisaldi, B., Stewart, R.S., Adles, C., Stewart, L.R., Quaglio, E., Biasini, E., Fioriti, L., Chiesa, R., Harris, D.A. (2003). Mutant PrP is delayed in its exit from the endoplasmic reticulum, but neither wild-type nor mutant PrP undergoes retrotranslocation prior to proteasomal degradation. *Journal of Biological Chemistry* **278**:21732-43

Duchen, L.W., Poulter, M., Harding, A.E. (1993). Dementia associated with a 216 base pair insertion in the prion protein gene. Clinical and neuropathological features. *Brain* **116** (Pt 3):555-67

Edskes, H.K., Wickner, R.B. (2000). A protein required for prion generation: [URE3] induction requires the Ras-regulated Mks1 protein. *Proceedings of the National Academy of Sciences of the United States of America* **97**:6625-9

Eng, L.F., Ghirnikar, R.S., Lee, Y.L. (2000). Glial fibrillary acidic protein: GFAP-thirty-one years (1969-2000). *Neurochemical Research* **25**:1439-51

Farquhar, C., Dornan, J., Moore, R., Somerville, R., Tunstall, A., Hope, J. (1996). Protease-resistant PrP deposition in brain and non-central nervous system tissues of a murine model of bovine spongiform encephalopathy. *Journal of General Virology* **77**:1941-1946

Farquhar, C., Dornan, J., Somerville, R., Tunstall, A., Hope, J. (1994). Effect of S*inc* genotype, agent isolate and route of infection on the accumulation of protease-resistant PrP in non-central nervous system tissues during the development of murine scrapie. *Journal of General Virology* **75**:495-504

Farquhar, C.F., Somerville, R.A., Ritchie, L.A. (1989). Post-mortem immunodiagnosis of scrapie and bovine spongiform encephalopathy. *Journal of Virological Methods* **24**:215-221

Fischer, M., Rulicke, T., Raeber, A., Sailer, A., Moser, M., Oesch, B., Brandner, S., Aguzzi, A., Weissmann, C. (1996). Prion protein (PrP) with amino-proximal deletions restoring susceptibility of PrP knockout mice to scrapie. *EMBO Journal* 15:1255-64

Flechsig, E., Shmerling, D., Hegyi, I., Raeber, A.J., Fischer, M., Cozzio, A., von Mering, C., Aguzzi, A., Weissmann, C. (2000). Prion protein devoid of the octapeptide repeat region restores susceptibility to scrapie in PrP knockout mice. *Neuron* **27**:399-408

Foster, J.D., Parnham, D., Chong, A., Goldmann, W., Hunter, N. (2001a). Clinical signs, histopathology and genetics of experimental transmission of BSE and natural scrapie to sheep and goats. *Veterinary Record* **148**:165-71

Foster, J.D., Parnham, D.W., Hunter, N., Bruce, M. (2001b). Distribution of the prion protein in sheep terminally affected with BSE following experimental oral transmission. *Journal of General Virology* **82**:2319-26

Fraser, H., Bruce, M., McBride, P., Scott, J. (1989). The molecular pathology of scrapie and the biological basis of lesion targeting. *Progress in Clinical and Biological Research* **317** 637-644

Fraser, H., Dickinson, A.G. (1968). The sequential development of the brain lesion of scrapie in three strains of mice. *Journal of Comparative Pathology* **78**:301-11

Fraser, J., Jeffrey, M., Halliday, W., Fowler, N., Goodsir, C., Brown, D. (1995). Early loss of neurons and axon terminals in scrapie-affected mice revealed by morphometry and immunocytochemistry. *Molecular and Chemical Neuropathology* **24**:245-9

Fraser, J.R. (1996). Infectivity in extraneural tissues following intraocular scrapie infection. *Journal of General Virology* **77** (Pt 10):2663-8

Gabizon, R., McKinley, M.P., Groth, D., Prusiner, S.B. (1988). Immunoaffinity purification and neutralization of scrapie prion infectivity. *Proceedings of the National Academy of Sciences of the United States of America* **85**:6617-21

Gajdusek, D.C., Gibbs, C.J., Alpers, M. (1967). Transmission and passage of experimental "kuru" to chimpanzees. *Science* **155**:212-214

Gambetti, P., Parchi, P., Chen, S.G. (2003). Hereditary Creutzfeldt-Jakob disease and fatal familial insomnia. *Clinics in Laboratory Medicine* **23**:43-64

Gibson, P.H., Somerville, R.A., Fraser, H., Foster, J.D., Kimberlin, R.H. (1987). Scrapie associated fibrils in the diagnosis of scrapie in sheep. *Veterinary Record* **120**:125-7

Gill, A.C., Ritchie, M.A., Hunt, L.G., Steane, S.E., Davies, K.G., Bocking, S.P., Rhie, A.G., Bennett, A.D., Hope, J. (2000). Post-translational hydroxylation at the N-terminus of the prion protein reveals presence of PPII structure in vivo. *EMBO Journal* **19**:5324-31

Gonzalez, L., Martin, S., Jeffrey, M. (2003). Distinct profiles of PrP(d) immunoreactivity in the brain of scrapie- and BSE-infected sheep: implications for differential cell targeting and PrP processing. *Journal of General Virology* **84**:1339-50

Grassi, J. (2003). Pre-clinical diagnosis of transmissible spongiform encephalopathies using rapid tests. *Transfusion Clinique et Biologique* **10**:19-22

Grassi, J., Creminon, C., Frobert, Y., Fretier, P., Turbica, I., Rezaei, H., Hunsmann, G., Comoy, E., Deslys, J.P. (2000). Specific determination of the proteinase K-resistant form of the prion protein using two-site immunometric assays. Application to the post-mortem diagnosis of BSE. *Archives of Virology. Supplementum*:197-205

Groschup, M.H., Weiland, F., Straub, O.C., Pfaff, E. (1996). Detection of scrapie agent in the peripheral nervous system of a diseased sheep. *Neurobiology of Disease* **3**:191-5

Haik, S., Peyrin, J., Lins, L., Rosseneu, M., Brasseur, R., Langeveld, J., Tagliavini, F., Deslys, J., Lasmezas, C., Dormont, D. (2000). Neurotoxicity of the putative transmembrane domain of the prion protein. *Neurobiology of Disease* **7**:644-656

Haire, L.F., Whyte, S.M., Vasisht, N., Gill, A.C., Verma, C., Dodson, E.J., Dodson, G.G., Bayley, P.M. 2004. The crystal structure of the globular domain of sheep prion protein. *Journal of Molecular Biology.* **336** 1175-1183

Harris, D.A. (1999). Cellular biology of prion diseases. *Clinical Microbiology Reviews* **12**:429-44

Hay, B., Barry, R., Lieberburg, I., Prusiner, S., Lingappa, V. (1987). Biogenesis and transmembrane orientation of the cellular isoform of the scrapie prion protein. *Molecular and Cellular Biology* **7**:914-920

Head, M.W., Bunn, T.J., Bishop, M.T., McLoughlin, V., Lowrie, S., McKimmie, C.S., Williams, M.C., McCardle, L., MacKenzie, J., Knight, R., Will, R.G., Ironside, J.W. (2004). Prion protein heterogeneity in sporadic but not variant Creutzfeldt-Jakob disease: U.K. cases 1991-2002. *Annals of Neurology* **55**:851-9

Head, M.W., Tissingh, G., Uitdehaag, B.M., Barkhof, F., Bunn, T.J., Ironside, J.W., Kamphorst, W., Scheltens, P. (2001). Sporadic Creutzfeldt-Jakob disease in a young Dutch valine homozygote: atypical molecular phenotype. *Annals of Neurology* **50**:258-61

Hegde, R.S., Mastrianni, J.A., Scott, M.R., DeFea, K.A., Tremblay, P., Torchia, M., DeArmond, S.J., Prusiner, S.B., Lingappa, V.R. (1998). A transmembrane form of the prion protein in neurodegenerative disease. *Science* **279**:827-34

Hegde, R.S., Tremblay, P., Groth, D., DeArmond, S.J., Prusiner, S.B., Lingappa, V.R. (1999). Transmissible and genetic prion diseases share a common pathway of neurodegeneration. *Nature* **402**:822-6

Herzog, C., Sales, N., Etchegaray, N., Charbonnier, A., Freire, S., Dormont, D., Deslys, J.P., Lasmezas, C.I. (2004). Tissue distribution of bovine spongiform encephalopathy agent in primates after intravenous or oral infection. *Lancet* **363**:422-8

Hill, A.F., Antoniou, M., Collinge, J. (1999a). Protease-resistant prion protein produced in vitro lacks detectable infectivity. *Journal of General Virology* **80** (Pt 1):11-4

Hill, A.F., Butterworth, R.J., Joiner, S., Jackson, G., Rossor, M.N., Thomas, D.J., Frosh, A., Tolley, N., Bell, J.E., Spencer, M., King, A., Al-Sarraj, S., Ironside, J.W., Lantos, P.L., Collinge, J. (1999b). Investigation of variant Creutzfeldt-Jakob disease and other human prion diseases with tonsil biopsy samples. *Lancet* **353**:183-9

Hill, A.F., Collinge, J. (2003). Subclinical prion infection. *Trends in Microbiology* **11**:578-84

Hilmert, H., Diringer, H. (1984). A rapid and efficient method to enrich SAF-protein from scrapie brains of hamsters. *Bioscience Reports* **4**:165-70

Hope, J., Manson, J. (1991). The scrapie fibril protein and its cellular form. *In:* Transmissible spongiform Encephalopathies: Scrapie, BSE and Related Disorders. B. Chesebro, editor. pp. 57-71. Springer-Verlag, Berlin

Hope, J., Wood, S.C., Birkett, C.R., Chong, A., Bruce, M.E., Cairns, D., Goldmann, W., Hunter, N., Bostock, C.J. (1999). Molecular analysis of ovine prion protein identifies similarities between BSE and an experimental isolate of natural scrapie, CH1641. *Journal of General Virology* **80** (Pt 1):1-4

Horiuchi, M., Baron, G.S., Xiong, L.W., Caughey, B. (2001). Inhibition of interactions and interconversions of prion protein isoforms by peptide fragments from the C-terminal folded domain. *Journal of Biological Chemistry* **276**:15489-97

Horiuchi, M., Caughey, B. (1999). Specific binding of normal prion protein to the scrapie form via a localized domain initiates its conversion to the protease-resistant state. *EMBO Journal* **18**:3193-3203

Horiuchi, M., Priola, S.A., Chabry, J., Caughey, B. (2000). Interactions between heterologous forms of prion protein: binding, inhibition of conversion, and species barriers. *Proceedings of the National Academy of Sciences of the United States of America* **97**:5836-41

Houston, F., Foster, J.D., Chong, A., Hunter, N., Bostock, C.J. (2000). Transmission of BSE by blood transfusion in sheep. *Lancet* **356**:999-1000

Hsiao, K.K., Groth, D., Scott, M., Yang, S.L., Serban, H., Rapp, D., Foster, D., Torchia, M., Dearmond, S.J., Prusiner, S.B. (1994). Serial transmission in rodents of neurodegeneration from transgenic mice expressing mutant prion protein. *Proceedings of the National Academy of Sciences of the United States of America* **91**:9126-30

Hsiao, K.K., Scott, M., Foster, D., Groth, D.F., DeArmond, S.J., Prusiner, S.B. (1990). Spontaneous neurodegeneration in transgenic mice with mutant prion protein. *Science* **250**:1587-1590

Hunter, G.D. (1972). Scrapie: a prototype slow infection. *Journal of Infectious Diseases* **125**:427-40

Hunter, N., Foster, J., Chong, A., McCutcheon, S., Parnham, D., Eaton, S., MacKenzie, C., Houston, F. (2002). Transmission of prion diseases by blood transfusion. *Journal of General Virology* **83**:2897-905

Jackson, G.S., Hill, A.F., Joseph, C., Hosszu, L., Power, A., Waltho, J.P., Clarke, A.R., Collinge, J. (1999). Multiple folding pathways for heterologously expressed human prion protein. *Biochimica et Biophysica Acta* **1431**:1-13

Jamieson, E., Jeffrey, M., Ironside, J.W., Fraser, J.R. (2001). Activation of Fas and caspase 3 precedes PrP accumulation in 87V scrapie. *Neuroreport* **12**:3567-72

Jeffrey, M., Goodsir, C.M., Bruce, M.E., McBride, P.A., Fraser, J.R. (1997). In vivo toxicity of prion protein in murine scrapie: ultrastructural and immunogold studies. *Neuropathology and Applied Neurobiology* **23**:93-101

Jeffrey, M., Halliday, W.G., Bell, J., Johnston, A.R., MacLeod, N.K., Ingham, C., Sayers, A.R., Brown, D.A., Fraser, J.R. (2000). Synapse loss associated with abnormal PrP precedes neuronal degeneration in the scrapie-infected murine hippocampus. *Neuropathology and Applied Neurobiology* **26**:41-54

Jeffrey, M., Martin, S., Barr, J., Chong, A., Fraser, J.R. (2001). Onset of accumulation of PrPres in murine ME7 scrapie in relation to pathological and PrP immunohistochemical changes. *Journal of Comparative Pathology* **124**:20-8

Jin, T., Gu, Y., Zanusso, G., Sy, M., Kumar, A., Cohen, M., Gambetti, P., Singh, N. (2000). The chaperone protein BiP binds to a mutant prion protein and mediates its degradation by the proteasome. *Journal of Biological Chemistry* **275**:38699-704

Joiner, S., Linehan, J., Brandner, S., Wadsworth, J.D., Collinge, J. (2002). Irregular presence of abnormal prion protein in appendix in variant Creutzfeldt-Jakob disease. *Journal of Neurology, Neurosurgery and Psychiatry* **73**:597-8

Kaneko, K., Ball, H.L., Wille, H., Zhang, H., Groth, D., Torchia, M., Tremblay, P., Safar, J., Prusiner, S.B., DeArmond, S.J., Baldwin, M.A., Cohen, F.E. (2000). A synthetic peptide initiates Gerstmann-Straussler-Scheinker (GSS) disease in transgenic mice. *Journal of Molecular Biology* **295**:997-1007

Kanyo, Z.F., Pan, K.M., Williamson, R.A., Burton, D.R., Prusiner, S.B., Fletterick, R.J., Cohen, F.E. (1999). Antibody binding defines a structure for an epitope that participates in the PrPC-->PrPSc conformational change. *Journal of Molecular Biology* **293**:855-63

Karber, G. (1931). Beitrag zur kollektiven Behandlung pharmakologischer Reihenversuche. *Archive fur Experimentelle Pathologie und Pharmakologie; Archives in Experimental Pathology* **162**:480-483

Kascsak, R.J., Rubenstein, R., Merz, P.A., Carp, R.I., Wisniewski, H.M., Diringer, H. (1985). Biochemical differences among scrapie-associated fibrils support the biological diversity of scrapie agents. *Journal of General Virology* **66** (Pt 8):1715-22

Kascsak, R.J., Rubenstein, R., Merz, P.A., Tonna-DeMasi, M., Fersko, R., Carp, R.I., Wisniewski, H.M., Diringer, H. (1987). Mouse polyclonal and monoclonal antibody to scrapie-associated fibril proteins. *Journal of Virology* **61**:3688-93

Kimberlin, R.H. (1976a). Experimental scrapie in the mouse: a review of an important model disease. *Science Progress* **63**:461-81

Kimberlin, R.H. (1976b). Slow Virus Diseases. *In:* Slow Virus Diseases of Animals and Man. R.H. Kimberlin, editor. pp. 3-13. North-Holland publishing Co., Amsterdam

Kimberlin, R.H. (1982). Scrapie agent - prions or virinos. *Nature* **297**:107-108

Kimberlin, R.H., Walker, C.A. (1978). Pathogenesis of mouse scrapie: effect of route of inoculation on infectivity titres and dose-response curves. *Journal of Comparative Pathology* **88**:39-47

Kimberlin, R.H., Walker, C.A. (1979). Pathogenesis of mouse scrapie: dynamics of agent replication in spleen, spinal cord and brain after infection by different routes. *Journal of Comparative Pathology* **89**:551-62

Kimberlin, R.H., Walker, C.A. (1988). Pathogenesis of experimental scrapie. *In:* Novel infectious agents and the central nervous system (Ciba Foundation symposium 135). G. Bock and J. Marsh, editors. pp. 37-62. John Wiley & Sons, Chichester, UK

Kimberlin, R.H., Walker, C.A., Fraser, H. (1989). The genomic identity of different strains of mouse scrapie is expressed in hamsters and preserved on reisolation in mice. *Journal of General Virology* **70**:2017-2025

King, C.Y., Diaz-Avalos, R. (2004). Protein-only transmission of three yeast prion strains. *Nature* **428**:319-23

Kirby, L., Birkett, C.R., Rudyk, H., Gilbert, I.H., Hope, J. (2003). In vitro cell-free conversion of bacterial recombinant PrP to PrPres as a model for conversion. *Journal of General Virology* **84**:1013-20

Klohn, P.C., Stoltze, L., Flechsig, E., Enari, M., Weissmann, C. (2003). A quantitative, highly sensitive cell-based infectivity assay for mouse scrapie prions. *Proceedings of the National Academy of Sciences of the United States of America* **100**:11666-71

Kocisko, D.A., Come, J.H., Priola, S.A., Chesebro, B., Raymond, G.J., Lansbury, P.T., Caughey, B. (1994). Cell-free formation of protease-resistant prion protein. *Nature* **370**:471-4

Kocisko, D.A., Priola, S.A., Raymond, G.J., Chesebro, B., Lansbury, P.T., Jr., Caughey, B. (1995). Species specificity in the cell-free conversion of prion protein to protease-resistant forms: a model for the scrapie species barrier. *Proceedings of the National Academy of Sciences of the United States of America* **92**:3923-7

Korth, C., Stierli, B., Streit, P., Moser, M., Schaller, O., Fischer, R., Schulz-Schaeffer, W., Kretzschmar, H., Raeber, A., Braun, U., Ehrensperger, F., Hornemann, S., Glockshuber, R., Riek, R., Billeter, M., Wuthrich, K., Oesch, B. (1997). Prion (PrPSc)-specific epitope defined by a monoclonal antibody. *Nature* **390**:74-7

Kuczius, T., Groschup, M.H. (1999). Differences in proteinase K resistance and neuronal deposition of abnormal prion proteins characterize bovine spongiform encephalopathy (BSE) and scrapie strains. *Molecular Medicine* **5**:406-18

Kurschner, C., Morgan, J.I. (1995). The cellular prion protein (prp) selectively binds to bcl-2 in the yeast 2-hybrid system. *Molecular Brain Research* **30**:165-168

Langeveld, J., Farquhar, C., Pocchiari, M., Birkett, C., Bostock, C., Meloen, R. 1993. Antigenic sites of bovine prion protein. *In:* Transmissible Spongiform Encephalopathies. R. Bradley and B. Marchant, editors. pp. 315-321. Commission of the European Communities, Brussels, Belgium

Lasmezas, C.I., Deslys, J.P., Robain, O., Jaegly, A., Beringue, V., Peyrin, J.M., Fournier, J.G., Hauw, J.J., Rossier, J., Dormont, D. (1997). Transmission of the BSE agent to mice in the absence of detectable abnormal prion protein. *Science* **275**:402-5

Lawson, V.A., Priola, S.A., Wehrly, K., Chesebro, B. (2001). N-terminal truncation of prion protein affects both formation and conformation of abnormal protease-resistant prion protein generated in vitro. *Journal of Biological Chemistry* **276**:35265-71

Lee, D.C., Stenland, C.J., Hartwell, R.C., Ford, E.K., Cai, K., Miller, J.L., Gilligan, K.J., Rubenstein, R., Fournel, M., Petteway, S.R., Jr. (2000). Monitoring plasma processing steps with a sensitive Western blot assay for the detection of the prion protein. *Journal of Virological Methods* **84**:77-89

Li, R., Lui, T., Wong, B.-S., Pan, T., Morallis, M., Swietnicki, W., O'Rourke, K., Gambetti, P., Surewicz, W., Sy, M.-S. (2000). Identification of an Epitope in the C terminus of Normal Prion Protein whose Expression is modulated by Binding Events in the N terminus. *Journal of Molecular Biology* **301**:567-573

Liebman, S.W. (2002). Progress toward an ultimate proof of the prion hypothesis. *Proceedings of the National Academy of Sciences of the United States of America* **99**:9098-100

Liu, T., Li, R., Wong, B.S., Liu, D., Pan, T., Petersen, R.B., Gambetti, P., Sy, M.S. (2001). Normal cellular prion protein is preferentially expressed on subpopulations of murine hemopoietic cells. *Journal of Immunology* **166**:3733-42

Llewelyn, C.A., Hewitt, P.E., Knight, R.S., Amar, K., Cousens, S., Mackenzie, J., Will, R.G. (2004). Possible transmission of variant Creutzfeldt-Jakob disease by blood transfusion. *Lancet* **363**:417-21

Lloyd, S., Onwuazor, O., Beck, J., Mallinson, G., Farrall, M., Targonski, P., Collinge, J., Fisher, E. (2001). Identification of multiple quantitative trait loci linked to prion disease incubation period in mice. *Proceedings of the National Academy of Sciences of the United States of America* **98**:6279-83

Ma, J., Lindquist, S. (2002). Conversion of PrP to a self-perpetuating PrPSc-like conformation in the cytosol. *Science* **298**:1785-8

Ma, J., Wollmann, R., Lindquist, S. (2002). Neurotoxicity and neurodegeneration when PrP accumulates in the cytosol. *Science* **298**:1781-5

MacDonald, S.T., Sutherland, K., Ironside, J.W. (1996). Prion protein genotype and pathological phenotype studies in sporadic Creutzfeldt-Jakob disease. *Neuropathology and Applied Neurobiology* **22**:285-92

MacGregor, I. (2001). Prion protein and developments in its detection. *Transfusion Medicine* **11**:3-14

MacGregor, I., Hope, J., Barnard, G., Kirby, L., Drummond, O., Pepper, D., Hornsey, V., Barclay, R., Bessos, H., Turner, M., Prowse, C. (1999). Application of a time-resolved fluoroimmunoassay for the analysis of normal prion protein in human blood and its components. *Vox Sanguinis* **77**:88-96

Madec, J.Y., Groschup, M.H., Buschmann, A., Belli, P., Calavas, D., Baron, T. (1998). Sensitivity of the Western blot detection of prion protein PrPres in natural sheep scrapie. *Journal of Virological Methods* **75**:169-77

Manolakou, K., Beaton, J., McConnell, I., Farquar, C., Manson, J., Hastie, N.D., Bruce, M., Jackson, I.J. (2001). Genetic and environmental factors modify bovine spongiform encephalopathy incubation period in mice. *Proceedings of the National Academy of Sciences of the United States of America* **98**:7402-7

Manson, J., Jamieson, E., Baybutt, H., Tuzi, N., Barron, R., McConnell, I., Somerville, R., Ironside, J., Will, R., Sy, M.-S., Melton, D., Hope, J., Bostock, C. (1999). A single amino acid alteration (101L) introduced into murine PrP dramatically alters incubation time of transmissible spongiform encephalopathy. *EMBO* **18**:6855-6864

Manson, J., West, J.D., Thomson, V., McBride, P., Kaufman, M.H., Hope, J. (1992). The prion protein gene: a role in mouse embryogenesis? *Development* **115**:117-22

Manson, J.C., Clarke, A.R., Hooper, M.L., Aitchison, L., McConnell, I., Hope, J. (1994a). 129/Ola mice carrying a null mutation in PrP that abolishes messenger-RNA production are developmentally normal. *Molecular Neurobiology* **8**:121-127

Manson, J.C., Clarke, A.R., McBride, P.A., McConnell, I., Hope, J. (1994b). PrP gene dosage determines the timing but not the final intensity or distribution of lesions in scrapie pathology. *Neurodegeneration* **3**:331-40

Manuelidis, L. (2003). Transmissible encephalopathies: speculations and realities. *Viral Immunology* **16**:123-39

Manuelidis, L., Lu, Z.Y. (2003). Virus-like interference in the latency and prevention of Creutzfeldt-Jakob disease. *Proceedings of the National Academy of Sciences of the United States of America* **100**:5360-5

Manuelidis, L., Sklaviadis, T., Manuelidis, E.E. (1987). Evidence suggesting that PrP is not the infectious agent in Creutzfeldt-Jakob disease. *EMBO Journal* **6**:341-7

McBride, P., Bruce, M., Fraser, H. (1988). Immunostaining of scrapie cerebral amyloid plaques with antisera raised to scrapie-associated fibrils (SAF). *Neuropathology and Applied Neurobiology* **14**:325-336

McBride, P.A., Eikelenboom, P., Kraal, G., Fraser, H., Bruce, M.E. (1992). PrP protein is associated with follicular dendritic cells of spleens and lymph nodes in uninfected and scrapie-infected mice. *Journal of Pathology* **168**:413-418

McBride, P.A., Schulz-Schaeffer, W.J., Donaldson, M., Bruce, M., Diringer, H., Kretzschmar, H.A., Beekes, M. (2001). Early spread of scrapie from the gastrointestinal tract to the central nervous system involves autonomic fibers of the splanchnic and vagus nerves. *Journal of Virology* **75**:9320-7

McKinley, M.P., Bolton, D.C., Prusiner, S.B. (1983). A protease-resistant protein is a structural component of the scrapie prion. *Cell* **35**:57-62

McKinley, M.P., Meyer, R.K., Kenaga, L., Rahbar, F., Cotter, R., Serban, A., Prusiner, S.B. (1991). Scrapie prion rod formation in vitro requires both detergent extraction and limited proteolysis. *Journal of Virology* **65**:1340-51

Merz, P.A., Somerville, R.A., Wisniewski, H.M., Iqbal, K. (1981). Abnormal fibrils from scrapie-infected brain. *Acta Neuropathologica* **54**:63-74

Meyer, R.K., McKinley, M.P., Bowman, K.A., Braunfeld, M.B., Barry, R.A., Prusiner, S.B. (1986). Separation and properties of cellular and scrapie prion proteins. *Proceedings of the National Academy of Sciences of the United States of America* **83**:2310-4

Miele, G., Manson, J., Clinton, M. (2001). A novel erythroid-specific marker of transmissible spongiform encephalopathies. *Nature Medicine* **7**:361-4

Millson, G.C., Hunter, G.D., Kimberlin, R.H. (1976). The physio-chemical nature of the scrapie agent. *In:* Slow Virus Diseases of Animals and Man. R.H. Kimberlin, editor. pp. 243-266. North-Holland Publishing Co., Amsterdam

Mishra, R.S., Gu, Y., Bose, S., Verghese, S., Kalepu, S., Singh, N. (2002). Cell surface accumulation of a truncated transmembrane prion protein in

Gerstmann-Straussler-Scheinker disease P102L. *Journal of Biological Chemistry* **277**:24554-61

Monari, L., Chen, S., Brown, P., P, Petersen, R., Mikol, J., Gray, F., Cortelli, P., Montagna, P., Ghetti, B., al, e. (1994). Fatal familial insomnia and familial Creutzfeldt-Jakob disease: different prion proteins determined by a DNA polymorphism. *Proceedings of the National Academy of Sciences of the United States of America* **91**:2839-42

Moore, R.C., Hope, J., McBride, P.A., McConnell, I., Selfridge, J., Melton, D.W., Manson, J.C. (1998). Mice with gene targetted prion protein alterations show that Prnp, Sinc and Prni are congruent. *Nature Genetics* **18**:118-125

Moore, R.C., Lee, I.Y., Silverman, G.L., Harrison, P.M., Strome, R., Heinrich, C., Karunaratne, A., Pasternak, S.H., Chishti, M.A., Liang, Y., Mastrangelo, P., Wang, K., Smit, A.F., Katamine, S., Carlson, G.A., Cohen, F.E., Prusiner, S.B., Melton, D.W., Tremblay, P., Hood, L.E., Westaway, D. (1999). Ataxia in prion protein (PrP)-deficient mice is associated with upregulation of the novel PrP-like protein doppel. *Journal of Molecular Biology* **292**:797-817

Onodera, T., Ikeda, T., Muramatsu, Y., Shinagawa, M. (1993). Isolation of scrapie agent from the placenta of sheep with natural scrapie in Japan. *Microbiology and Immunology* **37**:311-6

Pan, K.M., Baldwin, M., Nguyen, J., Gasset, M., Serban, A., Groth, D., Mehlhorn, I., Huang, Z., Fletterick, R.J., Cohen, F.E., et al. (1993). Conversion of alpha-helices into beta-sheets features in the formation of the scrapie prion proteins. *Proceedings of the National Academy of Sciences of the United States of America* **90**:10962-6

Paramithiotis, E., Pinard, M., Lawton, T., LaBoissiere, S., Leathers, V.L., Zou, W.Q., Estey, L.A., Lamontagne, J., Lehto, M.T., Kondejewski, L.H., Francoeur, G.P., Papadopoulos, M., Haghighat, A., Spatz, S.J., Head, M., Will, R., Ironside, J., O'Rourke, K., Tonelli, Q., Ledebur, H.C., Chakrabartty, A., Cashman, N.R. (2003). A prion protein epitope selective for the pathologically misfolded conformation. *Nature Medicine* **9**:893-9

Parchi, P., Chen, S., Brown, P., Zou, W., Capellari, S., Budka, H., Hainfellner, J., Reyes, P., Golden, G., Hauw, J., Gajdusek, D., Gambetti, P. (1998). Different patterns of truncated prion protein fragments correlate with distinct phenotypes in P102L Gerstmann-Straussler-Scheinker disease. *Proceedings of the National Academy of Sciences of the United States of America* **95**:8322-7

Parchi, P., Zou, W., Wang, W., Brown, P., Capellari, S., Ghetti, B., Kopp, N., Schulz-Schaeffer, W.J., Kretzschmar, H.A., Head, M.W., Ironside, J.W., Gambetti, P., Chen, S.G. (2000). Genetic influence on the structural variations of the abnormal prion protein. *Proceedings of the National Academy of Sciences of the United States of America* **97**:10168-72

Peretz, D., Scott, M.R., Groth, D., Williamson, R.A., Burton, D.R., Cohen, F.E., Prusiner, S.B. (2001). Strain-specified relative conformational stability of the scrapie prion protein. *Protein Science* **10**:854-63

Polymenidou, M., Verghese-Nikolakaki, S., Groschup, M., Chaplin, M.J., Stack, M.J., Plaitakis, A., Sklaviadis, T. (2002). A short purification process

for quantitative isolation of PrPSc from naturally occurring and experimental transmissible spongiform encephalopathies. *BMC Infectious Diseases* **2**:23

Portis, J.L. (2001). Genetic determinants of neurovirulence of murine oncornaviruses. *In:* Neurovirology - Viruses and the Brain. M.J. Buchmeier and I.L. Campbell, editors. pp. 3-29. Adademic Press, San Diago

Priola, S. (1999). Prion protein and species barriers in the transmissible spongiform encephalopathies. *Biomedicine and Pharmacotherapy* **53**:27-33

Priola, S.A., Chabry, J., Chan, K. (2001). Efficient conversion of normal prion protein (PrP) by abnormal hamster PrP is determined by homology at amino acid residue 155. *Journal of Virology* **75**:4673-80

Prusiner, S.B. (1982). Novel proteinaceous infectious particles cause scrapie. *Science* **216**:136-144

Prusiner, S.B., Bolton, D.C., Groth, D.F., Bowman, K.A., Cochran, S.P., McKinley, M.P. (1982a). Further purification and characterization of scrapie prions. *Biochemistry* **21**:6942-50

Prusiner, S.B., Cochran, S.P., Groth, D.F., Downey, D.E., Bowman, K.A., Martinez, H.M. (1982b). Measurement of the scrapie agent using an incubation time interval assay. *Annals of Neurology* **11**:353-8

Raeber, A.J., Klein, M.A., Frigg, R., Flechsig, E., Aguzzi, A., Weissmann, C. (1999). PrP-dependent association of prions with splenic but not circulating lymphocytes of scrapie-infected mice. *EMBO* **18**:2702-2706

Rieger, R., Lasmezas, C.I., Weiss, S. (1999). Role of the 37 kDa laminin receptor precursor in the life cycle of prions. *Transfusion Clinique et Biologique* **6**:7-16

Rohwer, R.G. (1991). The scrapie agent: "a virus by any other name". [Review]. *Currrent.Topics in.Microbiology and.Immunology.* **172**:195-232

Roucou, X., Guo, Q., Zhang, Y., Goodyer, C.G., LeBlanc, A.C. (2003). Cytosolic prion protein is not toxic and protects against Bax-mediated cell death in human primary neurons. *Journal of Biological Chemistry* **278**:40877-81

Rubenstein, R., Merz, P.A., Kascsak, R.J., Carp, R.I., Scalici, C.L., Fama, C.L., Wisniewski, H.M. (1987). Detection of scrapie-associated fibrils (SAF) and SAF proteins from scrapie-affected sheep. *Journal of Infectious Diseases* **156**:36-42

Saborio, G.P., Permanne, B., Soto, C. (2001). Sensitive detection of pathological prion protein by cyclic amplification of protein misfolding. *Nature* **411**:810-3

Saborio, G.P., Soto, C., Kascsak, R.J., Levy, E., Kascsak, R., Harris, D.A., Frangione, B. (1999). Cell-lysate conversion of prion protein into its protease-resistant isoform suggests the participation of a cellular chaperone. *Biochemical and Biophysical Research Communications* **258**:470-5

Safar, J. (1996). The folding intermediate concept of prion protein formation and conformational links to infectivity. *Current Topics in Microbiology and Immunology* **207**:69-76

Safar, J., Wille, H., Itri, V., Groth, D., Serban, H., Torchia, M., Cohen, F., Prusiner, S. (1998). Eight prion strains have PrP^{Sc} molecules with different conformations. *Nature Medicine* **4**:1157-1165

Safar, J.G., Scott, M., Monaghan, J., Deering, C., Didorenko, S., Vergara, J., Ball, H., Legname, G., Leclerc, E., Solforosi, L., Serban, H., Groth, D., Burton, D.R., Prusiner, S.B., Williamson, R.A. (2002). Measuring prions causing bovine spongiform encephalopathy or chronic wasting disease by immunoassays and transgenic mice. *Nature Biotechnology* **20**:1147-50

Sambrook, J., Russell, D.W. (2003). Molecular Cloning: A laboratory manual. Cold Spring Harbour, New York

Schaller, O., Fatzer, R., Stack, M., Clark, J., Cooley, W., Biffiger, K., Egli, S., Doherr, M., Vandevelde, M., Heim, D., Oesch, B., Moser, M. (1999). Validation of a western immunoblotting procedure for bovine PrP(Sc) detection and its use as a rapid surveillance method for the diagnosis of bovine spongiform encephalopathy (BSE). *Acta Neuropathologica* **98**:437-43

Scott, J.R., Fraser, H. (1984). Degenerative hippocampal pathology in mice infected with scrapie. *Acta Neuropathologica* **65**:62-8

Shaked, G.M., Fridlander, G., Meiner, Z., Taraboulos, A., Gabizon, R. (1999). Protease-resistant and detergent-insoluble prion protein is not necessarily associated with prion infectivity. *Journal of Biological Chemistry* **274**:17981-6

Shaked, G.M., Shaked, Y., Kariv-Inbal, Z., Halimi, M., Avraham, I., Gabizon, R. (2001). A protease-resistant prion protein isoform is present in urine of animals and humans affected with prion diseases. *Journal of Biological Chemistry* **276**:31479-82

Somerville, R.A. (1991). The transmissible agent causing scrapie must contain more than protein. *Reviews in Medical. Virology.* **1**:131-139

Somerville, R.A. (1999). Host and transmissible spongiform encephalopathy agent strain control glycosylation of PrP. *Journal of General Virology* **80** (Pt 7):1865-72

Somerville, R.A., Dunn, A.J. (1996). The association between PrP and infectivity in scrapie and BSE infected mouse brain. *Archives of Virology* **141**:275-89

Somerville, R.A., Oberthur, R.C., Havekost, U., MacDonald, F., Taylor, D.M., Dickinson, A.G. (2002). Characterization of thermodynamic diversity between transmissible spongiform encephalopathy agent strains and its theoretical implications. *Journal of Biological Chemistry* **277**:11084-9

Soto, C., Saborio, G.P., Anderes, L. (2002). Cyclic amplification of protein misfolding: application to prion-related disorders and beyond. *Trends in Neurosciences* **25**:390-4

Spielhaupter, C., Schatzl, H.M. (2001). PrPC directly interacts with proteins involved in signaling pathways. *Journal of Biological Chemistry* **276**:44604-12

Stewart, R.S., Drisaldi, B., Harris, D.A. (2001). A transmembrane form of the prion protein contains an uncleaved signal peptide and is retained in the endoplasmic Reticulum. *Molecular Biology of the Cell* **12**:881-9

Stewart, R.S., Harris, D.A. (2001). Most pathogenic mutations do not alter the membrane topology of the prion protein. *Journal of Biological Chemistry* **276**:2212-20

Stewart, R.S., Harris, D.A. (2003). Mutational analysis of topological determinants in prion protein (PrP) and measurement of transmembrane and cytosolic PrP during prion infection. *Journal of Biological Chemistry* **278**:45960-8

Takekida, K., Y, K., Yamazaki, T., Horiuchi, M., Kakeya, T., Shinagawa, M., Takatori, K., Tanimura, A., Tanamoto, K., Sawada, J. (2002). Quantitative analysis of Prion Protein by immunoblotting. *Journal of Health Science* **48**:288-291

Tanaka, M., Chien, P., Naber, N., Cooke, R., Weissman, J.S. (2004). Conformational variations in an infectious protein determine prion strain differences. *Nature* **428**:323-8

Tateishi, J., Kitamoto, T. (1995). Inherited prion diseases and transmission to rodents. *Brain Pathology* **5**:53-59

Tateishi, J., Kitamoto, T., Doh-ura, K., Sakaki, Y., Steinmetz, G., Tranchant, C., Warter, J.M., Heldt, N. (1990). Immunochemical, molecular genetic, and transmission studies on a case of Gerstmann-Straussler-Scheinker syndrome. *Neurology* **40**:1578-81

Taylor, D.M., Brown, J.M., Fernie, K., McConnell, I. (1997). The effect of formic acid on BSE and scrapie infectivity in fixed and unfixed brain-tissue. *Veterinary Microbiology* **58**:167-74

Taylor, D.M., Fernie, K., Steele, P.J., McConnell, I., Somerville, R.A. (2002). Thermostability of mouse-passaged BSE and scrapie is independent of host PrP genotype: implications for the nature of the causal agents. *Journal of General Virology* **83**:3199-204

Taylor, D.M., McConnell, I., Ferguson, C.E. (2000). Closely similar values obtained when the ME7 strain of scrapie agent was titrated in parallel by two individuals in separate laboratories using two sublines of C57BL mice. *Journal of Virological Methods* **86**:35-40

Telling, G.C., Haga, T., Torchia, M., Tremblay, P., DeArmond, S.J., Prusiner, S.B. (1996). Interactions between wild-type and mutant prion proteins modulate neurodegeneration in transgenic mice. *Genes and Development* **10**:1736-50

Telling, G.C., Scott, M., Mastrianni, J., Gabizon, R., Torchia, M., Cohen, F.E., Dearmond, S.J., Prusiner, S.B. (1995). Prion propagation in mice expressing human and chimeric prp transgenes implicates the interaction of cellular PrP with another protein. *Cell* **83**:79-90

Tobler, I., Gaus, S.E., Deboer, T., Achermann, P., Fischer, M., Rulicke, T., Moser, M., Oesch, B., McBride, P.A., Manson, J.C. (1996). Altered Circadian Activity Rhythms and Sleep In Mice Devoid Of Prion Protein. *Nature* **380**:639-642

Tremblay, P., Ball, H.L., Kaneko, K., Groth, D., Hegde, R.S., Cohen, F.E., DeArmond, S.J., Prusiner, S.B., Safar, J.G. (2004). Mutant PrP(Sc) Conformers Induced by a Synthetic Peptide and Several Prion Strains. *Journal of Virology* **78**:2088-99

Tuite, M.F. (2000). Yeast prions and their prion-forming domain. *Cell* 100:289-92

Turk, E., Teplow, D.B., Hood, L.E., Prusiner, S.B. (1988). Purification and properties of the cellular and scrapie hamster prion proteins. *European Journal of Biochemistry* **176**:21-30

Tzaban, S., Friedlander, G., Schonberger, O., Horonchik, L., Yedidia, Y., Shaked, G., Gabizon, R., Taraboulos, A. (2002). Protease-sensitive scrapie prion protein in aggregates of heterogeneous sizes. *Biochemistry* **41**:12868-75

Van Everbroeck, B., Quoilin, S., Boons, J., Martin, J.J., Cras, P. (2003). A prospective study of CSF markers in 250 patients with possible Creutzfeldt-Jakob disease. *Journal of Neurology, Neurosurgery and Psychiatry* **74**:1210-4

Viles, J.H., Cohen, F.E., Prusiner, S.B., Goodin, D.B., Wright, P.E., Dyson, H.J. (1999). Copper binding to the prion protein: Structural implications of four identical cooperative binding sites. *Proceedings of the National Academy of Sciences of the United States of America* **96**:2042-2047

Vorberg, I., Priola, S.A. (2002). Molecular basis of scrapie strain glycoform variation. *Journal of Biological Chemistry* **277**:36775-81

Wadsworth, J., Joiner, S., Hill, A., Campbell, T., Desbruslais, M., Luthert, P., Collinge, J. (2001). Tissue distribution of protease resistant prion protein in variant Creutzfeldt-Jakob disease using a highly sensitive immunoblotting assay. *Lancet* **358**:171-80

Wadsworth, J.D., Hill, A.F., Joiner, S., Jackson, G., Clarke, A.R., Collinge, J. (1999a). Strain-specific prion-protein conformation determined by metal ions. *Nature Cell Biology* **00**:1-5

Wadsworth, J.D.F., Jackson, G.S., Hill, A.F., Collinge, J. (1999b). Molecular biology of prion propagation. *Current Opinion in Genetics & Development* **9**:338-345

Weiss, S., Proske, D., Neumann, M., Groschup, M.H., Kretzschmar, H.A., Famulok, M., Winnacker, E.L. (1997). RNA aptamers specifically interact with the prion protein PrP. *Journal of Virology* **71**:8790-8797

Weissmann, C. (1991). Spongiform encephalopathies. The prion's progress. *Nature* **349**:569-71

Wells, G.A., McGill, I.S. (1992). Recently described scrapie-like encephalopathies of animals: case definitions. *Research in Veterinary Science* **53**:1-10

Wells, G.A., Scott, A.C., Wilesmith, J.W., Simmons, M.M., Matthews, D. (1994). Correlation between the results of a histopathological examination and the detection of abnormal brain fibrils in the diagnosis of bovine spongiform encephalopathy. *Research in Veterinary Science* **56**:346-51

Westaway, D., Dearmond, S.J., Cayetanocanlas, J., Groth, D., Foster, D., Yang, S.L., Torchia, M., Carlson, G.A., Prusiner, S.B. (1994). Degeneration of skeletal-muscle, peripheral-nerves, and the central-nervous-system in transgenic mice overexpressing wild-type prion prot ins. *Cell* **76**:117-129

Wille, H., Zhang, G.F., Baldwin, M.A., Cohen, F.E., Prusiner, S.B. (1996). Separation of scrapie prion infectivity from PrP amyloid polymers. *Journal of Molecular Biology* **259**:608-21

Wong, B., Venien-Bryan, C., Williamson, R., Burton, D., Gambetti, P., MS, S., Brown, D., IM, J. (2000). Copper refolding of prion protein. *Biochemistry and Biophysical Research Communication* **276**:1217-1224

Wurthrich, K., Riek, R. (2001). Three dimentional structures of Prion proteins. *In:* Advances in Protein Chemistry. B. Caughey, editor. pp. xiii, 405p, London Academic Press

Young, K. (1999). The Hunan Genetic Prion Diseases. *In:* Prions: Molecuar and Cellular Biology. D.A. Harris, editor. pp. 139-175. Horizon Scientific Press, Wymondham

Zahn, R., Liu, A., Luhrs, T., Riek, R., von Schroetter, C., Lopez, F., Billeter, M., Calzolai, L., Wider, G., Wuthrich, K. (2000). NMR solution structure of the human prion protein. *Proceedings of the National Academy of Sciences of the United States of America* **97**:145-150

Zanusso, G., Liu, D., Ferrari, S., Hegyi, I., Yin, X., Aguzzi, A., Hornemann, S., Liemann, S., Glockshuber, R., Manson, J., Brown, P., Petersen, R., Gambetti, P., Sy, M. (1998). Prion protein expression in different species: analysis with a panel of new mAbs. *Proceedings of the National Academy of Sciences of the United States of America* **95**:8812-6

Zou, W.Q., Capellari, S., Parchi, P., Sy, M.S., Gambetti, P., Chen, S.G. (2003). Identification of novel proteinase K-resistant C-terminal fragments of PrP in Creutzfeldt-Jakob disease. *Journal of Biological Chemistry* **278**:40429-36

Zou, W.Q., Zheng, J., Gray, D.M., Gambetti, P., Chen, S.G. (2004). Antibody to DNA detects scrapie but not normal prion protein. *Proceedings of the National Academy of Sciences of the United States of America* **101**:1380-5